Targeted anti-angiogenic therapy in metastatic renal cell carcinoma and methodological improvements in assessment of therapeutic response with imaging biomarkers

Submitted to the University of Hertfordshire in partial fulfilment of the requirements of the degree of doctorate in medicine which may be awarded under schedule J

By

Dr. Anup Vinayan

June 2017

Acknowledgements

There have been a lot of people who I came to contact during this tenure who supported me remarkably. First of all, I would like to thank the patients who have agreed to participate in the clinical trial and invested a critical time in their life to help the study. Research nurses and radiographers involved with the study need to special mentioning.

I have reserved my whole-hearted acknowledgements for my family to the last. I would like to thank my parents whose support, both financial and emotional, has helped me through my (many) student years. My wife Anju deserves an enormous acknowledgement. You have provided with relentless support through this rollercoaster of life and work. We have had our difficult times with our research degrees, training and busy and often challenging work schedules. I am so delighted that we never gave up despite the tough times. Without your support, I would never have completed this thesis. I cannot forget my daughter Devu who always waited patiently without complaining when her dad continued to work through evening and weekends. Above all, I would like to thank god for guiding me on the right path. I hope that the experience I have gained will help me in completing future academic endeavors on time and successfully.

Attenuation of neo-angiogenesis with targeted therapy in metastatic renal cell carcinoma may account for its therapeutic effect and could be measured radiologically. The prediction of therapeutic response to anti-angiogenic agents may be improved by methodological changes in interpretation of standard tumour imaging.

(Anup Vinayan 2017)

Abstract

Background

Drugs targeting angiogenic pathway remain the mainstay of treatment for metastatic renal cell carcinoma (mRCC). Tyrosine Kinase Inhibitors (TKI) as Sunitinib, Pazopanib as single agents and humanised monoclonal antibody bevacizumab (Bev) in combination with Interferon- α2a (IFN) have established as the first-line therapy for mRCC. Despite improvements in treatment, there are multiple questions which remain unanswered. In the combination of Bev and IFN, the respective role of each drug and whether any additional anti-angiogenic activity is gained by adding IFN to Bev remains unknown. As the clinical benefit obtained with these cytostatic agents does not always correlate with the conventional response assessment techniques as RECIST, it is necessary to reconsider the methods by which we assess benefit from these therapies. In this thesis, I report three studies aiming to answer these questions.

Methods

With the clinical trial reported here, I explore whether Bev induced changes in vascular parameters measured by Dynamic Contrast Enhanced MRI (DCE-MRI) is significantly enhanced by the addition of IFN. In a phase II, randomised, open labelled, multicentre trial, treatment naïve mRCC patients were randomised to receive Bev on its own or in combination with a low dose (3MU) or standard dose (9MU) IFN. DCE-MRI was used to assess the changes in vascularity with the primary endpoint being, changes in transfer coefficient (Ktrans) after six weeks of treatment.

Abstract
_____

I also report two retrospective imaging-based studies, using contrast-enhanced CT scans, performed to improve the methodology of response assessment for these antiangiogenic therapeutics. Here I explore the use of a) combining changes in size and arterial phase contrast enhancement measured using CT scan and b) changes in CT texture as methods of therapeutic response assessment in mRCC patients treated with TKI.

Results

With the phase 2 clinical trial, we faced significant difficulty in recruitment as a result of restrictions in access to treatment in NHS, other competing studies and restrictions proposed by the DCE-MRI inclusion criteria. With slow recruitment, an unplanned analysis was performed after 21 patients were recruited. Analysis of primary endpoint showed no trend in the difference between arms with no correlation found between change in Ktrans and addition of IFN to bevacizumab. Effect size analysis performed due to the small numbers recruited failed to show any significance in the observed difference in Ktrans. Change in Ktrans and Kep may identify a group of patients likely to have PFS > 6 months, but this observation needs to evaluation in a larger sample size.

Measuring size and change in arterial phase enhancement retrospectively using CT, a new criterion "modified" Choi, which prerequisite a combination of a decrease in arterial phase density by 15% and a decrease in size by 10% for response was

proposed. Response assessment was measured with RECIST, Choi and modified Choi individually in 20 evaluable patients retrospectively and clinical benefit compared with Kaplan-Meier statistics and Log-Rank test. Response assessment as defined by the modified Choi criteria successfully identified patients who received clinical benefit from the treatment. Time to progression (TTP) was 448 days for the partial response and 89 days for stable disease as per the new criteria which were statistically significant with a p-value of 0.002.

The second retrospective analysis explored the textural changes in enhanced CT scan. Performed in collaboration with researchers from Brighton University who developed the software algorithm used to assess changes in entropy and uniformity, 87 metastases from 39 patients with mRCC were analysed at baseline and after two cycles of TKI treatment. Textural parameters and response assessment criteria were correlated with TTP. After two cycles of TKI, the decrease in tumour entropy was 3%-45%, and increase in uniformity was 5%-21%. At a threshold change of -2% with uniformity, on a coarse scale of 2.5, the textural change was able to separate responders from non-responders. With Kaplan-Meier analysis comparing all four criteria, the percentage change in uniformity was statistically more significant than for RECIST, Choi, and Modified Choi criteria. Cox regression analysis showed that texture uniformity was an independent predictor of time to progression.

<u>Discussion</u>

With the studies reported here, I was able to demonstrate the importance of improving the methodology in assessment of therapeutic response to targeted anti-angiogenic therapy in metastatic renal cell carcinoma. Even though the clinical trial, terminated early due to slow recruitment, did not reach its primary endpoint, changes in other vascular parameters as Kep combined with changes Ktrans showed tendency towards identifying a group of patients who derived clinical benefit of >6months with these therapies. This is particularly exciting as given the vascular stabilisation effect proposed for bevacizumab, the effusion parameter Kep may be a better tool in assessing response rather than Ktrans and warrants further assessment in a larger cohort. Modified choi criterion and textural analysis are two important methodological improvements in response assessment of cytostatic anti-angiogenic therapy. In the analyses reported here, both techniques have shown superiority over RECIST in response assessment and differentiating mRCC patients who is likely to gain clinical benefit by TKI therapy. Validation of these criteria on a larger patient cohort is important. As these criterions are assessed on standard enhanced CT scans, incorporating these criteria, especially modified choi criterion, as part of standard CT assessment could be performed and will provide a real world validation. Retrospective assessment using larger cohort of patients from previous phase 3 trials or inclusion of these parameters prospectively in phase 3 trials would also help us in evaluating these modalities further.

Table of contents

Table of contents

Table of contents

Table of contents

List of Figures

List of Tables

List of publications and posters

Publications

P.Nathan, A.Vinayan, D.Stott, J.Juttla, V.Goh; " CT response assessment combining reduction in both size and arterial phase density correlates with time to progression in metastatic renal cancer patients treated with targeted therapies" Cancer Biology & Therapy 9(1); 15-19; January, 2010; © 2010 Landes Bioscience.

V.Goh, B.Ganeshan, P.Nathan, A.Vinayan, K.Miles "Assessment of response to tyrosine kinase inhibitors in metastatic renal cell cancer: CT texture as a predictive biomarker" Radiology: 2011 Oct;26(1): 165-71

Nathan.PD, A.Vinayan; "Imaging techniques as predictive and prognostic biomarkers in renal cell carcinoma"; Ther Adv Med Oncol. 2013 Mar;5(2):119-31.

Abstracts / Poster presentations

Dr. B.ganeshan, Dr.M.Rajpopat, Dr. A.Vinayan, Dr.P.Nathan, Dr.V.Goh, Prof K.Miles; "CT texture and enhancement: potential predictive biomarkers of response to treatment in metastatic renal cancer". – Abstract - European Congress of Radiology 2010.

Juttla.J, Vinayan.A, Nathan.P, Goh.V; "Size and enhancement response criteria for TKIs in metastatic renal cell cancer: Does arterial or portal

venous phase imaging alter respone categorization?" RSNA 2010; abstract no:9007274.

P.Nathan, A.Vinayan, D.Stott, V.Goh; "CT response assessment combining reduction in size and arterial enhancement correlates with the time to progression in metastatic renal cell cancer patients treated with TKIs." ECCO 15/ESMO34–2009– Poster/poster discussion (abs number 7.112)

Glossary

ADC	Apparent Diffusion Co-efficient
AE	Adverse Event
AJCC	American Joint Committee on Cancer
ALP	Alkaline phosphatase
ALT (SGPT)	Alanine aminotransferase
ANC	Absolute neutrophil count
ANOVA	Analysis of variance
ASL	Arterial Spin Labelling
AST (SGOT)	Aspartate aminotransferase
AUC	Area under the plasma concentration-time curve
b.i.d.	Twice Daily
BOLD	Blood Oxygen Level Dependent
BP	Blood pressure
CALGB	Cancer and Leukaemia Group B
ccRCC	clear cell Renal cell Carcinoma
CD	Cyclin Dependent Kinase
CEA	Carcinoembryonic Antigen
CEC	Ciculating Endothelial Cells
CEPC	Ciculating Endothelial Progenitor Cells
CHF	Congestive heart failure
CI	Confidence interval
C_{max}	Maximum plasma concentration
CMP	Cortico Medullary Phase
CNS	Central Nervous System
CPU	Clinical Pharmacology Unit
CR	Complete Response
CRF	Case Report Form[s]
CT	Computer Tomography
CTC	Common Toxicity Criteria
CVAD	Central Venous Access Device
CXR	Chest X-Ray
DCE	Dynamic Contrast Enhanced
DLT	Dose Limiting Toxicity
DWI	Diffusion Weighted Imaging
EC_{50}	plasma concentration associated with half-maximal effect
ECG	Electrocardiogram
ECOG	Eastern Cooperative Oncology Group
EDTA	Ethylene diamine tetra acetic acid
EGF	Epidermal Growth Factor
EGFR	Epidermal Growth Factor Receptor

EMEA	European Agency for the Evaluation of Medicinal Products
EP	Excretory Phase
ESF	eligibility screening form
EU	European Union
FA	Flip Angle
FBC	Full Blood Count
FDA	Food and Drug Administration
FDG	Flourodeoxyglucose
FID	Free Induction Decay
FISH	Fluorescence in situ hybridization
FLIM	Fluorescence lifetime Imaging
FOV	Field of View
FRET	Fluorescence Resonance Energy Transfer
FSE	Fast Spin Echo
FT	Fourier Transfomration
GCP	Good Clinical Practice
Gd	Gadolinium
GdDOTA	Gadolinium Dotaric acid
GE	Gradient Echo
GIST	Gastro Intestinal Stromal Tumour
H_0	Null hypothesis
H_1	Alternative hypothesis
Hep	Hepatitis
HIF	Hypoxia Inducible Factor
HIV	Human Immunodeficiency Virus
HPLC	High performance liquid chromatography
HR	Hazard Ratio
HRE	Hypoxia Response Element
HU	Hounsfield Unit
ICH	International Conference on Harmonization
IFN	Interferon
IHC	Immunohistochemistry
IL-2	Interleukin-2
IMP	Investigational Medicinal Product
INR	International Normalisation Ratio
IRB/IEC	Institutional Review Board/Independent Ethics Committee
ITT	intent to treat
iv	Intravenous
k_{eo}	Equilibration rate constant
K_{ep}	Effusion co-efficient
K^{trans}	Transfer co-efficient
kV	Kilo Voltage

LoG	Laplacaian of Gaussian
mA	milli Ampere
MAPK	Mitogen Associated Protein Kinase
MIU	Million International Units
mRCC	metastatic Renal Cell Carcinoma
MRI	Magnetic Resonance Image
MTD	Maximum Tolerated Dose
mTOR	mammalian Target of Rapamicin
MU	Million Units
MVD	Mean Vessel Density
NCCN	National Comprehensive Cancer Network
NCDB	National Cancer Data Base
NCI	National Cancer Institute
NCI-CTC	National Cancer Institute-Common Toxicity Criteria
NYHA	New York Heart Association
ORR	Objective response rate
OS	Overall survival
p.o.	Oral administration
PD	Progressive disease
PD-1	Programmed Death - 1
PET	Positro Emission Tomography
PFS	Progression free survival
PI3	Phosphatidyl Insoitol 3-OH
PK	Pharmacokinetic
PR	Pulse rate
PR	Partial Response
PS	Performance Status
PT	Prothrombin Time
q.d.	Once daily administration
q.w.	Once a week
Q3W	Every 3 weeks
RCC	Renal Cell Carcinoma
RECIST	Response Evaluation Criteria in Solid Tumours
RF	Radiofrequency
ROC	Reciever Operating Characteristic
ROI	Region of Interest
SAE	Serious Adverse Event
SD	Stable Disease
SNR	Signal to Noise Ratio
SUVmax	Standardised Uptake Value maximum
T	Tesla
t.b.d.	to be determined

Glossary

$T_{1/2}$	half-life
TE	Echo Time
Tiw	Three times a week
TR	Repetition Time
TTP	Time to Tumour Progression
ULN	Upper Limit of Normal
USS	Ultra Sound Scan
Ve	Extracellular Volume
VEGF	Vascular Endothelial Growth Factor
VHL	Von-Hippel Lindau
WBC	White Blood Count
WBMRI	Whole Body Magnetic Resonance Imaging

Chapter 1.

General Introduction

1.1. Renal Cell Carcinoma (RCC)

1.1.1. Background

Renal cell cancer (RCC) accounts for approximately 3% of adult malignancy incidence worldwide. The annual incidence in the UK in 2013 was 11,873 (CRUK 2013). Increasing trends of incidence have been noted since 1970 (CRUK 2013, ONS.GOV.UK 2015). RCC is strongly related to age with more than half of the patients presenting are above the age of 70. Cigarette smoking is shown to be a significant risk factor for the development of RCC (Ferlay, Autier et al. 2007). The disease is also associated with obesity shown by case-control and cohort studies and industrial exposure to cadmium exposure is also suggested as a potential risk factor (Chris Protzel 2012). 40-50% of these cancers present while the disease is still confined within kidneys, a significant proportion of which is detected as an incidental finding. Despite having curative nephrectomy, 30 – 50% of these patients recur with metastatic disease while another 1/3rd patients present with metastatic disease de novo (CRUK 2013). Prognosis of metastatic kidney cancer remains very poor with the majority of patients with metastatic disease dying within two years of diagnosis. Five-year survival in patients presenting with metastatic disease is around 5-6%. Management of advanced RCC has always been a challenge as these group of disease never showed a clinically relevant response to traditional cytotoxic chemotherapeutic drugs (Hartmann and Bokemeyer 1999). With increased knowledge of pathogenesis of these tumours, the treatment landscape of this disease has undergone significant change over the last decade.

1.1.2. Pathophysiology of renal cell carcinoma

Renal cell carcinoma includes a heterogeneous group of cancer with different genetic and molecular alterations. Major histological subtypes in this group of disease include clear cell, papillary (type 1 and 2) and chromophobe RCC. These 3 groups form approximately 90% of the renal malignancies (Lopez-Beltran, Scarpelli et al. 2006). Other less common histological subtypes include medullary, collecting duct, multilocular cystic, unclassified etc. The International Society of Urological Pathology (2012) has further described new distinct epithelial tumours. These include tubulocystic, acquired cystic disease associated, clear cell tubulo papillary, MiT family translocation associated and hereditary leiomyomatosis associated RCC.

In most cases of clear cell renal cell carcinoma (ccRCC), whether sporadic or hereditary, structural alterations of the short arm of chromosome 3 have been noted. Significantly, Von Hippel-Lindau protein (VHL) is coded at short arm of chromosome 3 (3p25). VHL is a tumour suppressor gene and 80% of clear cell renal cell carcinoma harbour somatic or epigenetic alterations in this gene resulting in inactivation of the gene (Gnarra, Tory et al. 1994, Brugarolas 2014).

VHL tumour suppressor gene has a significant role in cellular oxygen sensing which materializes through its interaction with hypoxia inducible factor (HIF) in the cells. HIF plays a pivotal role in renal tumorigenesis as it acts as a transcription factor for genes involved in angiogenesis, proliferation, cell survival, apoptosis etc (Turner, Moore et

al. 2002, Semenza 2003). Preclinical studies suggest a causal role in deregulation of

HIF subunit, HIF2α, in RCC pathogenesis (Kondo, Kim et al. 2003).

<u>Hypoxia inducible factor (HIF)</u>

HIF has α (HIF-1α, HIF-2α, HIF-3α) and β (HIF-1β/ARNT) subunits. The α subunit is

generally unstable except under hypoxic conditions. HIF-α subunits acts as a

transcription factor for a variety of proteins including vascular endothelial growth

factor (VEGF).

Under normoxic conditions, VHL protein (pVHL) stimulates degradation of HIF-α and

thus resulting in inactivation of its transcription. In the state of normoxia, HIF-α is

hydroxylated with proline hydroxylases. pVHL recognises and binds to HIF-α with the

help of two other proteins (elongins). This complex undergoes poly-ubiquitination and

degradation through proteasomes.

In conditions of cellular hypoxia, proline hydroxylase fails to hydroxylate HIF-α, this

results in little or no ubiquitination of HIF-α. Excess HIF-α in cell, translocate to the

nucleus and heterodimerises with the β subunit of HIF. The complex stabilizes the α

subunit. HIF-α/ HIF-β complex binds to hypoxia response elements (HRE) on nuclear

DNA and stimulates the transcription of genes involved in growth, angiogenesis,

survival/apoptosis etc. including VEFG. This interaction is represented schematically

in figure 1.1.

Figure 1.1   HIF-1 and its regulation by VHL
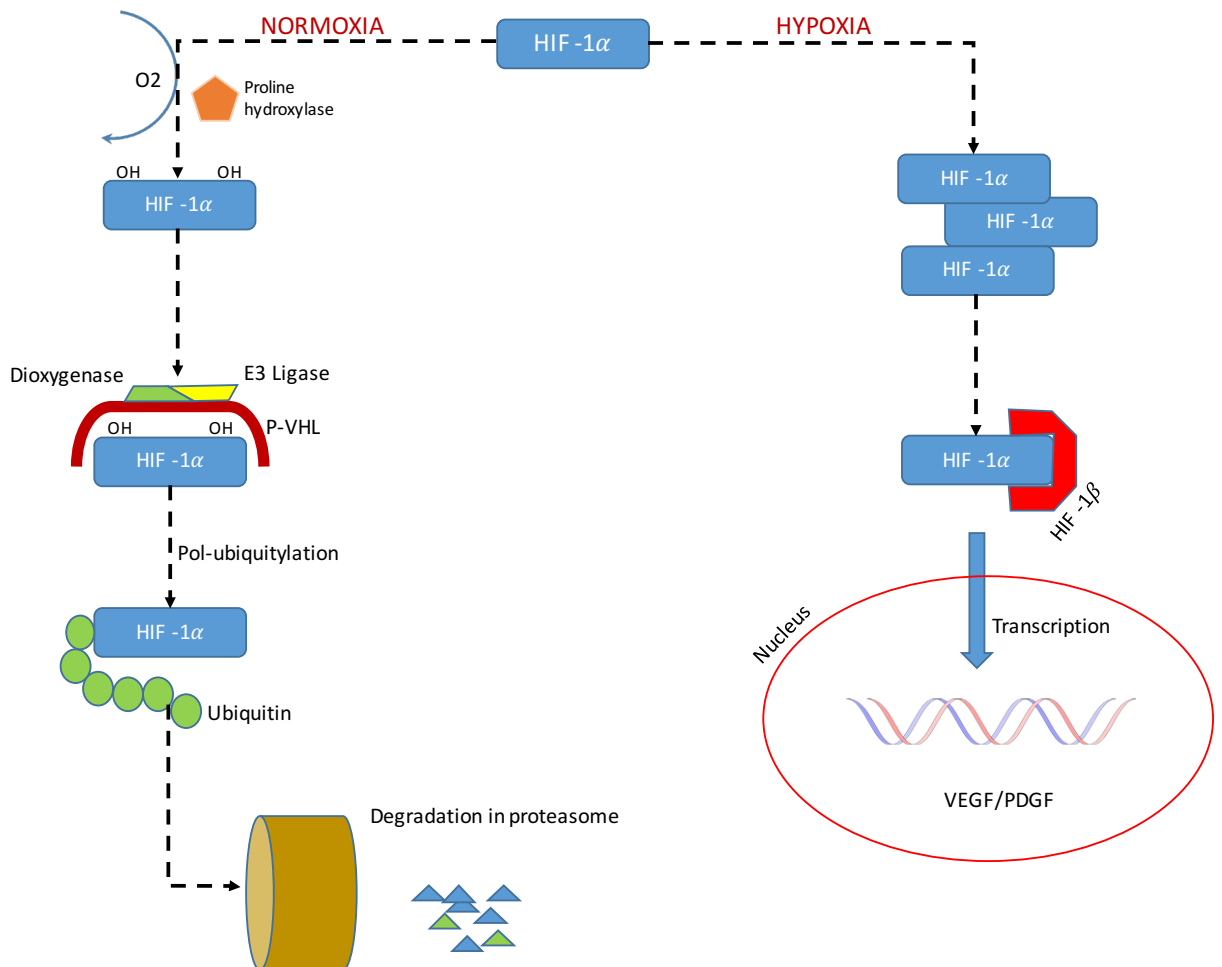
Most sporadic ccRCC harbor changes in the VHL gene which render them inactive resulting in constitutive activation of HIF-1α/2α (Banks, Tirukonda et al. 2006, Kaelin 2007). Further studies have shown that HIF-2α activation significantly impacts development of renal cell carcinoma (Kondo, Kim et al. 2003).

Stabilisation of α subunits of HIF can also happen through other oncogenic pathways as phosphatidylinositol 3-OH kinase (PI3K/AKT) and MAPK (mitogen associated protein kinase) pathways. Activation of PI3K pathway produces mTOR dependent translation of HIFα (Rochlitz, Peter et al. 1992, Hay 2005, Brugarolas 2014).

Several other driver genes have been noted to be active in pathogenesis of renal cell carcinoma. These include PBRM1, BAP1, SETD2, TCEB1 and KDM5C. The effects of these mutations are still not fully understood (Ibragimova, Maradeo et al. 2013, Brugarolas 2014).

Multiple hereditary forms of RCC are also known with its associated specific sites of mutations (Pavlovich and Schmidt 2004).

a) Von Hippel-Lindau associated – VHL3p25-26

b) Hereditary papillary RCC – MET7q31-34

c) Birt-Hogg-Dubé syndrome – FLCN 17p11

d) Hereditary leiomyomatosis associated (HLRCC) – FH1q42-43

e) Tuberous sclerosis associated – TSC1 9q34 / TSC2 16p13

1.1.3. Staging of renal cell carcinoma

Renal cell carcinoma is classified using TNM staging. TNM classification is based on primary tumour character (T), Nodal status (N) and Metastatis (M). Since its introduction, TNM staging is one of the widely accepted methods of tumour staging. Current TNM staging 7.0 classifies RCC as below (Edge and Compton 2010).

T staging

T1: Confined to Kidney <7cm

T1a: confined to kidney <4cm

T1b: confined to kidney >4cm<7cm

T2: Confined to Kidney >7cm

T2a: confined to kidney >7cm<10cm

T2b: confined to kidney >10cm

T3: Tumour or tumour thrombus extension to major veins or perinephric tissue

T3a: Spread to renal vein.

T3b: extension to infra diaphragmatic IVC

T3c: Spreads to supra diaphragmatic IVC or invades vessel walls.

T4: Involvement of Ipsilateral adrenal gland/involvement of Gerota's fascia

N – Nodal staging

N0: No nodal involvement

N1: metastatic involvement of regional nodes.

M – Metastasis

M0: No distant metastasis

M1: Distant metastasis.

Table 1.1   Staging of RCC

Staging	TNM character
Stage1	T1N0M0
Stage2	T2N0M0
Stage 3	T3 or N1
Stage 4	T4 or M1

1.1.4. Systemic therapy of metastatic renal cell carcinoma

Renal cell carcinoma has traditionally been thought of as a chemotherapy-resistant and radiotherapy-resistant disease. Immunotherapy with interferon-α (IFN-α) and interleukin-2 (IL-2) have been the treatment of advanced RCC with the treatment benefiting only a small minority (8%) with significant associated toxicities (A Ritchie 1999, Coppin, Porzsolt et al. 2000) . With improved knowledge of pathophysiology of RCC, targeted treatment with agents that target angiogenesis and growth factor signaling have become the standard of treatment for this disease.

Several targeted therapeutic drugs have been approved by regulatory bodies for management of advanced renal cell carcinoma. These include multi-targeted tyrosine kinase inhibitors as sunitinib (Motzer, Hutson et al. 2007), sorafenib (Escudier, Eisen et al. 2009), pazopanib (Motzer, Hutson et al. 2013), axitinib (Hutson, Lesovoy et al. 2013), mTOR inhibitors as temsirolimus (Motzer, Hudes et al. 2007), everolimus (Motzer, Escudier et al. 2008) and recombinant monoclonal antibody against VEGF – bevacizumab (Escudier, Bellmunt et al. 2010).

Sunitinib, pazopanib, temsirolimus and Avastin (bevacizumab) were licensed for first line systemic therapy, while sorafenib and axitinib were approved for use post progression on other treatment lines.

Sunintib was assessed in comparison with interferonα (Motzer, Hutson et al. 2007). A phase 3 trial with 750 patients showed a progression free survival (PFS) of 11 months' vs 5 months in favour of sunitinib.

Pazopanib was trialled in three different phase 3 trials; against placebo, against sunitinib in first line metastatic setting and against placebo in cytokine-refractory RCC (Sternberg, Davis et al. 2010, Motzer, Hutson et al. 2013, Sternberg, Hawkins et al. 2013). PFS advantage was noted for the trial against placebo (11.1months Vs 2.8months) with no overall survival benefit likely due to early cross over from placebo to treatment arm. Similar efficacy was noted for pazopanib and sunitinib with different toxicity profile. Quality of life was noted to be better in patients who received pazopanib (Motzer, Hutson et al. 2013).

Sorafenib and axitinib were approved as second line therapy and a PFS advantage of 2.4months was observed against placebo for sorafenib while axitinib showed a 2.0months PFS advantage over sorafenib in patients previously exposed to anti-angiogenic therapy (Escudier, Eisen et al. 2007, Hutson, Lesovoy et al. 2013).

Bevacizumab a recombinant humanised monoclonal antibody against VEGF was assessed in combination with interferon-α2a against interferon-α2a in two phase 3 trials. AVOREN trial (Escudier, Bellmunt et al. 2010) demonstrated an improvement in median PFS from 5.4months in the interferon only arm to 10.2 months in the combination arm with a hazard ratio of 0.63 in favour of the combination. CALBG trial with a similar design of AVOREN study also showed a similar outcome with a hazard

ratio of 0.71 in favour of bevacizumab. Overall response rate in these study was around 25% (Rini, Halabi et al. 2008). Again no overall survival benefit was shown by any of these trials. AVOREN trial was un-blinded as an interim analysis showed clinical benefit and patients were crossed over to the treatment arm. The confounding effect of this crossover and availability and use of other targeted therapy as salvage is likely to have influenced the overall survival assessment of these cohort of patients. Phase 3 registration trials of these drugs and their out-come are listed here table 1.2.

More recently, anti-CTLA4 antibody ipilimumab and check point inhibitor drugs such as nivolumab have shown promising benefits in treatment of metastatic RCC which has progressed through other lines of therapy. In a phase 3 study comparing against everolimus in metastatic RCC patients who have progressed on previous line of treatment nivolumab showed an improvement in overall survival 25.0 months Vs 19.6 months with a hazard ratio of 0.71. Nivolumab has since been granted license for use in metastatic RCC as a second or later line therapy (Motzer, Escudier et al. 2015).

Table 1.2   Phase 3 trials of targeted therapy approved for management in metastatic renal cell carcinoma

Drug	Type	Line of therapy	Treatment	PFS (HR)	OS
Bevacizumab	Recombinant humanised monoclonal antibody against VEGF	1st line	Bevacizumab+interferon vs interferon	10.2 vs 5.4 (0.63)	23.3 vs 21.3
		1st line	Bevacizumab+interferon vs interferon	8.5. vs 5.2 (0.72)	18.3 vs 17.4
Sunitinib	VEGFR/PDGF inhibitor	1st line	Sunitinib vs interferonα	11.0 vs 5.0 (0.42)	---
Pazopanib	VEGF/PDGF/c-kit inhibitor	1st line	Pazopanib vs placebo	11.1 vs 2.8 (0.40)	22.0 vs 23.5
			Pazopanib vs sunitinib	8.4 vs 9.5	28.3 vs 29.1
		Post cytokine	Pazopanib vs placebo	7.4 vs 4.2 (0.54)	22.7 vs 18.7
Sorafenib	VEGFR2/PDGF/MAPK/MEK inhibitor	2nd line	Sorafenib vs placebo	5.5 vs 2.8 (0.44)	17.8 vs 15.2
Axitinib	VEGF1-3,PDGF, c-kit inhibitor	2nd line	Axitinib vs sorafenib	6.7 Vs 4.7 (0.66)	
		1st line	Temsirolimus vs interferon	3.8 vs 1.9	10.9 vs 7.3
Temsirolimus	mTOR inhibitor	1st line	Temsirolimus +bevacizumab vs interferon + bevacizumab	9.1 vs 9.3	25.8 vs 25.5
		2nd line	Temsirolimus vs sorafenib	4.3 vs 3.9 (0.87)	12.3 vs 16.6
Everolimus	mTOR inhibitor	2nd line	Everolimus vs placebo	4.0 vs 1.9 (0.30)	-
Nivolumab	Anti PD-1 antibody	2nd line	Nivlumab vs everolimus		25.0 vs 19.6

- PFS=progression free survival in months, HR = hazard ratio, OS= overall survival in months.

1.1.5. Treatment response assessment

Accurate therapeutic response assessment is a significant part of any treatment. Critical decisions are made whether to continue a particular treatment or change to another regime based on these assessments. Methods of treatment response assessment need to be validated and accepted. Identification of non-responders earlier than any clinical symptoms avoid unnecessary side effects and allow the patient and clinician to decide on switching to a potentially beneficial treatment. Along with clinical benefit in day to day treatment, this has an important role the development of new drugs. Identification of potential responders or non-responders and identification of at risk population for side effects would identify patients who will have maximum benefit from a specific intervention.

Current method of standard treatment assessment for most of anti-cancer treatment is based on imaging defined response assessment criteria called RECIST (Response Evaluation Criteria in Solid Tumours). This continues to be the case for response assessment of treatment in advanced renal cell carcinoma. RECIST response assessments are based solely on changes in size of the target lesions (NCI 2000, Patrick Therasse, Richard S. Kaplan et al. 2000). The treatment paradigm of different malignancies has changed significantly over the years. Cytostatic targeted agents are now being used as standard. It is also common that these drugs are now being used continuously as a maintenance treatment. With the changes that are ongoing, it is important that we rethink whether the response assessment tools that we use are fit for purpose.

Over the last decade, since proposal of Choi criteria in 2006 for assessment of imatinib response in Gastro Intestinal Stromal Tumours (Choi, Charnsangavej et al. 2007), different research groups have assessed options of using patterns of changes noted in standard imaging modalities (e.g.: contrast enhancement changes, volumetric changes etc.) and newer imaging defined criteria as response assessment tools. This is discussed further in this thesis in chapter 5 where I explore the option of combining size and change in arterial density in treatment response assessment of solid tumours. Along with CT based imaging criteria, ^{18}FDG PET-CT (Fluorodeoxyglucose positron emission tomography), functional MRI scans as Dynamic Contrast Enhanced MRI (DCE-MRI), Diffusion-Weighted Imaging MRI (DWI-MRI), perfusion imaging etc. are being used more and more for response assessment calculation. In Chapter 4.0 of this thesis, I detail a study where DCE-MRI was used in measuring antiangiogenic effects of bevacizumab and interferon in mRCC patients.

1.2. Tumour Vasculature

1.2.1. Angiogenesis

Angiogenesis is the process of new blood vessel formation from pre-existing vasculature. Angiogenesis is a physiological process and is involved in normal growth, physiologically in placenta, endometrium and is also involved in pathological conditions such as wound healing. The concept of angiogenesis as a fundamental step of tumour growth and metastasis was proposed by Dr. Judah Folkman in 1971. Folkman proposed that beyond the diffusion limit of oxygen (1-2mm), tumour cell growth required angiogenesis (Folkman, Merler et al. 1971, Folkman and Shing 1992).

The process of angiogenesis is monitored and regulated by a complex mechanism of interaction involving a growing number of proangiogenic and antiangiogenic factors (Poon, Fan et al. 2001, Clamp and Jayson 2005). The intricate communication between these factors are responsible for stimulation, inhibition and control of angiogenesis and vascular remodelling (Risau 1997, Carmeliet and Jain 2000).

RCC is a highly vascular tumour which is not surprising, given its pathogenesis involving the VHL-HIF-angiogenic pathway as described earlier. Vascular Endothelial Growth Factor A (VEGF-A) or simply VEGF, is a key mediator of angiogenesis and is known to be significantly over expressed in ccRCC (Minardi, Santoni et al. 2015, Zeng, Zeng et al. 2016). Expression of tumour VEGF is also noted to correlate with tumour stage and surrogate for prognosis in ccRCC. The VEGF family consists of five glycoproteins: VEGF-A, VEGF-B, VEGF-C, VEGF-D and placental growth factor (PGF) of

which the best characterised is VEGF-A. The actions of VEGF-A are mediated

principally via the VEGF receptors 1 and 2 (Rosen 2002). VEGF is a potent stimulator

of neovascularisation leading to the development of a structurally and functionally

abnormal vasculature which may impair the effective delivery of chemotherapy. The

presence of VEGF promotes the survival of these new vessels by upregulating the

expression of anti-apoptotic proteins bcl-2 and XIAP (Gerber, Dixit et al. 1998, Gerber,

McMurtrey et al. 1998). Multiple mechanisms of VEGF action have been proposed

including endothelial cell proliferation and survival, increased migration and invasion

of endothelial cells, increased permeability of existing vasculature, homing of

endothelial cell precursors as well as autocrine effects on tumour cell function (Ellis

and Hicklin 2008).

1.2.2. Tumour blood flow

According to Poiseuille's law, blood flow through a single rigid cylindrical vessel is proportional to the pressure difference between the ends of the tube and inversely proportional to the fourth power of vessel radius. Blood vessels in newly formed tumours are usually immature and chaotic (Benjamin, Golijanin et al. 1999). With a network of complex immature and leaky vessels, calculation of blood flow is complicated as it is also dependent on vascular morphology, vessel number, branching pattern and interstitial pressure.

It has been shown that interstitial pressure in solid tumours is high in both experimental condition and *in vivo* conditions (Less, Posner et al. 1992, Griffon-Etienne, Boucher et al. 1999). Increase in interstitial pressure is likely due to increased leakiness of tumour vasculature and absence of any lymphatic vessels in the tumour. Increased proliferation of tumour cells and change in viscosity could also contribute to the changes in interstitial pressure (Griffon-Etienne, Boucher et al. 1999).

Perfusion pressure in tumours will depend on the feeding arteriolar and venous pressures and could be hence significantly different depending on the site of metastasis. All of the above factors hence would contribute to significant heterogeneity in tumour blood flow.

Jain et.al in 2005 hypothesised that anti-angiogenic treatment results in vascular normalisation of tumour blood vessels (Jain 2005). Even though this effect is probably short lived, resulting in a normalisation window, it is suggested that maturing of these blood vessels would lead to a homogenous blood flow and result in reduction of hypoxia and increased delivery and possible efficacy of systemic therapeutic drugs (Goel, Wong et al. 2012). The precise effect of anti-VEGF related normalisation on tumour control remains controversial.

1.2.3. Methods to measure tumour blood flow

Measurement of blood flow through a tumour tissue is complex. Several methods exist which can be used to assess the blood flow rate in tissue. These include direct and indirect measurements. Indirect measurement of tumour blood flow can be made by using three principles: 1) Measuring the mean transit time of a tracer through a tissue, 2) modelling the uptake kinetics of a tracer or 3) measuring fractional distribution of the cardiac output.

1.2.4. Kety model

Kety suggested a model of tissue uptake of a freely diffusible tracer based on the Fick

principle and adapted it for determination of regional blood flow rate by measuring

local clearance of a radioactive tracer (Kety 1949). The model was further developed

to allow quantification of blood flow rate using an intravenous bolus injection of an

inert, freely diffusible tracer iodoantipyrine. The relation between tissue

concentration (C_t) , blood flow rate (F), arterial concentration (C_a) is shown by the

following equation called Kety equation (Kety.S 1960(a), Kety.S 1960(b), Tozer, Shaffi

et al. 1994).

Kety Equation:

$$C_t(T) = EF \int_0^T C_a e^{\frac{-EF}{\lambda}(T-t)} dt$$

E =Extraction fraction (fractional loss from blood to tissue in a single passage)

F is blood flow rate (ml whole blood per g of tissue per minute)

λ is the tissue-blood partition coefficient of the substance

C_a is the arterial blood concentration

C_t is the tissue concentration

T is the time factor for measurement of C_t

t is the time of onset

Dynamic Contrast Enhanced Magnetic Resonance Imaging (DCE-MRI) uses models based on the Kety equation (Tofts 1997, Tofts, Brix et al. 1999). The gadolinium-based tracers used in MRI scans such as gadopentetate dimeglumine (Gd-DTPA) brings about another degree of complexity in the calculation as they do not have the character of free diffusibility and are also not purely intravascular. In such situations, the result will be influenced by the permeability of tissue vessels and vascular surface area. DCE-MRI and its contrast kinetic parameters are discussed later in this chapter (section 1.4.2) and also in chapter 4.0 where DCE-MRI parameters are used to assess vascular changes in response to therapy.

1.3. Biomarkers

1.3.1. Definition

In 1998, the National Institutes of Health (NIH) Biomarkers definitions working group defined a biomarker as a "a characteristic that is objectively measured and evaluated as an indicator of normal biological processes, pathogenic processes, or pharmacologic responses to a therapeutic intervention." (Biomarkers_Definitions_Working_Group 2001, Strimbu and Tavel 2010). Biomarkers should be accurately measurable and also reproducible. These should be evaluated and validated for use as a surrogate indicator that would represent a clinical outcome.

1.3.2. Predictive and Prognostic biomarkers

A predictive biomarker is a biomarker which can identify a subpopulation of patients who are likely to respond to a therapeutic intervention. In contrast, prognostic biomarkers provide information on the likely course of the disease without treatment. Validated tools which could identify the likely course of the disease or clinical benefit from a therapy are invaluable and would lead to significant improvement in clinical management. Early identification of the group of patients who would derive little or no benefit from the treatment is beneficial as we could avoid them being exposed to these medications and thus their potential side effects.

Biomarkers have a significant role in drug development where the target population for a new drug could be defined more accurately to assess the clinical effectiveness. This has importance as significant number of molecules which have proven its efficacy

clinically have failed to pass the health-economic assessment of reimbursement authorities. Identifying the sub-population of patients who would derive most benefit from the drug would alter the cost-effectiveness analyses of regulatory authorities.

1.3.3. Imaging techniques as biomarkers

Imaging techniques used as a biomarkers are appealing as they are often non-invasive and could be repeated at intervals to assess disease status or response to a therapy. Imaging defined RECIST criteria has been the gold standard for treatment response assessment since its introduction in 2000 (Patrick Therasse, Richard S. Kaplan et al. 2000). Various imaging techniques have been researched exhaustively to evaluate as possible biomarker in a variety of malignancies. These involve further exploration of elements of standard imaging techniques like CT or USS (e.g. contrast enhancement, volumetric assessment) or use of newer and functional imaging as DCE-MRI, Diffusion Weighted Imaging (DWI) MRI, DCE-CT/USS etc. DCE-MRI has been studied in this setting, providing proof of mechanism of action of antiangiogenic therapy on tumour vasculature with reductions in K^{trans} observed (Flaherty, Rosen et al. 2008). DCE-MRI derived vascular parameters also hold promise as predictive biomarkers for VEGF inhibition in other solid tumours such as glioblastoma (Batchelor, Sorensen et al. 2007) colorectal cancer (Morgan, Thomas et al. 2003) and RCC. With pathogenesis involving the angiogenesis pathway, high vascularity noted in the tumour and use of anti-angiogenic agents as standard therapy, RCC is an ideal tumour where these techniques could be evaluated. A review of the published literature which uses imaging as a biomarker in RCC is comprehensively described in chapter 2.0.

1.4.   MRI methods

1.4.1. Overview of MRI Principles

MRI is based on the principle of directional magnetic field associated with movement of charged particles. Each nucleus, with different number of protons or neutrons is thought to have its characteristic spinning motion (precession). Any moving charged particle will have an associated magnetic field. In human body, up to 70% is constituted by water molecules. The single proton in a hydrogen atom of a water molecule is positively charged and is spinning continuously. As these molecules are exposed to an external magnetic field, the protons move around depending on the direction of the magnetic field. Frequency of the precession movement for these protons (resonance, or Larmor frequency: ω_0) for a given magnetic strength B_0, can be calculated by the equation below.

Equation 1.1

$$\omega_0 = \gamma B_0$$

γ= gyromagnetic ratio, B0 magnetic strength, ω_0 = lamor frequency

The net magnetic moment adding up all the vectors of all the precessing protons align along B_0 and is the net magnetic moment vector (M). On using radiofrequency (RF) pulses, proton alignment in any object can be temporarily altered and pushes the net magnetic moment (M) away from the direction of the external magnetic field. When RF signal is removed, nuclei realign themselves back to equilibrium. This is called relaxation. The relaxivity of a tissue can be described as longitudinal relaxation time (T1) and transverse relaxation time (T2). During relaxation, nuclei lose energy which

is emitted as an RF signal called Free Induction Decay(FID). By using magnetic field

gradients in different planes, FID from all planes can be calculated and spatial

information and construction of the 2D or 3D images of signal intensity measured. The

pattern and duration of RF pulses and field gradients can be adjusted to give different

signal intensities for a single tissue. Even though it is possible to use intrinsic contrast,

use of external paramagnetic contrast will result in improvement of soft tissue

contrast.

1.4.2. DCE-MRI

DCE-MRI involves the rapid acquisition of sets of T_1-weighted images through a tissue or tumour as an intravenous bolus of gadolinium-based contrast agent is injected. This low molecular weighted extrinsic paramagnetic contrast agent has a small local magnetic field that induces a shortening of relaxation times of surrounding protons resulting in a change in signal intensity of tissues. Signal intensity changes over time are converted into contrast agent concentration data and with pharmacokinetic modeling of contrast agent uptake, allow for the quantitative estimation of vascular characteristics (Hayes, Padhani et al. 2002).

Quantitative kinetic parameters can be derived for whole tumour regions of interest and on a pixel-by-pixel basis. K^{trans} (transfer constant; units: min^{-1}) is a parameter which describes the rate of trans-endothelial flow of contrast medium from plasma into the interstitium. k_{ep} (washout rate constant; units: min^{-1}) describes the diffusion of contrast agent back into the vasculature from where it is excreted, usually by the kidneys. Other derived quantitative kinetic parameters include the fractional plasma volume (v_p; units: %) and the fractional extravascular, extracellular space (v_e, units %). Mathematical relation of these parameters are as detailed by equations 1.3 and 1.4 which are explained later in this chapter.

Another useful parameter in assessment of tumour permeability and leakage space is the initial area under the gadolinium concentration curve (IAUGC). IAUGC is

standardly calculated in our department in the first 60s post contrast injection IAUGC$_{60}$.

With the help of the kinetic parameters, Dynamic contrast-enhanced MRI (DCE-MRI) is able to provide information on tumour perfusion and permeability. Thus the technique yields detailed insights into tumour vascular function by assessing the kinetics of extracellular contrast agents.

Based on the tissue, its vasculature structure, perfusion and permeability of vessels and extracellular space, the observed kinetics of the paramagnetic contrast agent varies. Different curves of enhancement pattern have been identified based on this.

Type 1 curve – Slow progressive enhancement pattern typically seen in benign tissue. Low-grade malignancies can also show this type of enhancement.

Type 2 curve – Rapid enhancement followed by a plateau phase. These tissue enhancement pattern can be suspicious but could not be definitive of malignancy. Some benign tissue could also show this enhancement pattern.

Type 3 curve – Rapid onset of enhancement followed by a rapid washout. This is characteristic of tumour tissue with high vascularity but with premature vessels with high permeability. mRCC tissue are highly vascular and immature irregular vascular supply and would expect to show type 3 enhancement characteristics.
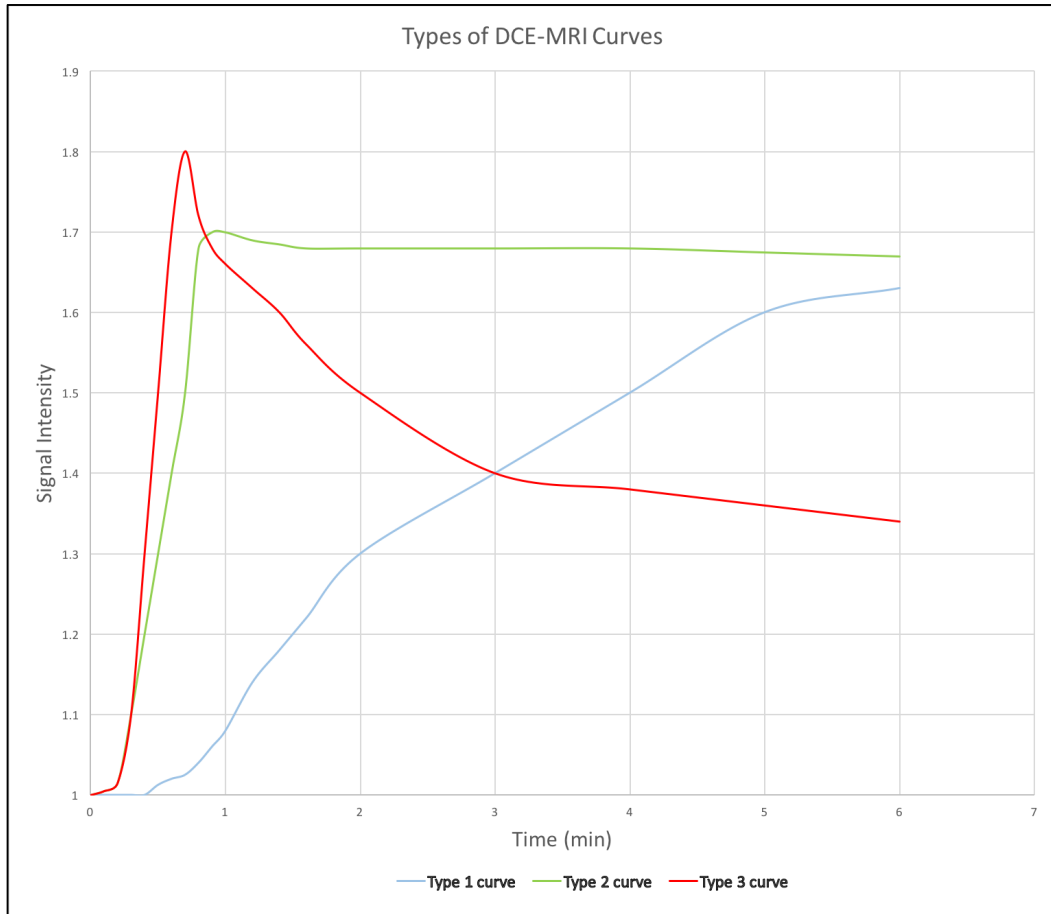
Figure 1.2   Types of DCE-MRI Curves

1.4.2.1.   Theory of DCE-MRI

The Kety equation (equation 1.2) for a freely-diffusible tracer forms the basis of the theory underlying the use of DCE-MRI to measure physiological parameters as tissue blood flow and permeability (Kety.S 1960(b), Tofts and Kermode 1991, Tofts, Brix et al. 1999)

Equation 1.2

$$Ct(T) = EF \int_0^T C_a e^{\frac{-EF}{\lambda}(T-t)} dt$$

E is the extraction fraction (fractional loss from blood to tissue in a single passage)

F is blood flow rate (ml whole blood per g of tissue per minute)

λ is the tissue-blood partition coefficient of the substance

C_a is the arterial blood concentration

C_t is the tissue concentration

T is the time factor for measurement of C_t

t is the time of onset

DCE-MRI provides information of tumour vascular function including information on tumour perfusion and permeability. To incorporate the use of extracellular tracer material, this equation can be further adapted as equation 1.3

Equation 1.3

$$Ct(T) = K^{trans} \int_0^T C_p(t) e^{-K_{ep}(T-t)} dt$$

C_p is arterial plasma concentration of Gd-DTPA, K^{trans} is the volume constant for the transfer of Gd-DTPA from the vessel into the extracellular extravascular space (EES) and k_{ep} is the rate constant for the transfer of Gd-DTPA from the EES back into the plasma (Tofts and Kermode 1991, Tofts, Brix et al. 1999).

Vessel permeability will be heterogeneous in tumours. In this situation, K^{trans} could be determined by a combination of flow, permeability and vessel surface area. The ratio of K^{trans} to k_{ep} gives the volume of EES per unit volume of tissue, v_e, otherwise known as the leakage space. Mathematically this can be represented with the equation (1.4) below.

Equation 1.4

$$Ve = \frac{K^{trans}}{k_{ep}}$$

This model assumes an instantaneous bolus, instant mixing of gadolinium-based contrast within the blood and within the leakage space after transfer from the vessel, and ignores the contribution of intravascular tracer to the tissue concentration.

1.4.2.2.　　　DCE-MRI for monitoring vascular targeting therapy

DCE-MRI is one of the most validated MRI technique in assessing vascular changes. The studies include direct correlative assessment with traditional measures of angiogenesis as mean vascular density (MVD) of blood vessels assessed via immunohistochemistry or tissue expression of proangiogenic factors as VEGF (Buckley, Drew et al. 1997, Su, Cheung et al. 2003). Broad correlation has been noted between DCE-MRI estimates and MVD in these studies.

Several studies have assessed use of DCE-MRI in assessment of response to anti-vascular therapy (Galbraith, Maxwell et al. 2003, Nathan, Zweifel et al. 2012). In 2008 in a pilot study, DCE-MRI assessment in metastatic RCC patients treated with sorafenib showed that reduction in K^{trans} was associated with improved progression free survival (PFS) (Flaherty, Rosen et al. 2008). A second phase 2 study published around the similar time showed good correlation of high baseline K^{trans} with better PFS (Hahn, Yang et al. 2008).

1.5.   Aims of the thesis

Therapeutic agents which target antiangiogenic pathway are now well established as treatment of metastatic RCC. These include multi-targeted tyrosine kinase inhibitors (sunitinib, pazopanib etc) and recombinant humanized monoclonal antibody bevacizumab in combination with interferon-α2a. Therapeutic response assessment on use of these newer "targeted" treatments have always been a challenge with RECIST assessment not successful in identifying all groups of patients who derive clinical benefit from the treatment. The high vascularity of RCC makes it an ideal target to use arterial enhancement imaging and to assess potential changes in vascularity in response to therapy. With the projects included in this thesis I intend to explore the use of three imaging based techniques in assessing effects of treatment in metastatic RCC with drugs that target anti-angiogenic pathway.

1. To use DCE-MRI to assess whether addition of interferonα2a to bevacizumab would add to the antiangiogenic effect of bevacizumab in metastatic RCC.

2. To assess if change in DCE-MRI parameters correlates with treatment response in metastatic RCC.

3. To assess efficacy of combining size and arterial phase contrast enhancement in prediction of treatment response to tyrosine kinase inhibitors in metastatic RCC.

4. To assess the use and efficacy of contrast enhanced CT texture in prediction of treatment response to tyrosine kinase inhibitors in metastatic RCC.

Chapter 2.

Literature search –

Imaging biomarkers in renal

cell carcinoma

2.1.   Introduction

Based on the theme of this dissertation, a literature review was performed to assess the research available where imaging techniques have been used as possible biomarkers in RCC. This literature search was performed using online resources Medline/Pubmed and supplemented by hand searching of abstracts from American Society of Clinical Oncology and European Society of Medical Oncology meetings. The search strategy included terms such as renal cell carcinoma, RCC, functional imaging, dynamic imaging, biomarker, response assessment, prognostic, predictive. Only studies published in English language were selected. The results were then separated as possible predictive biomarkers which predicts benefit from a therapy and prognostic biomarker which could provide an insight into the natural course of the disease according to the modality used. The review was published in a peer reviewed journal Therapeutic Advances in Medical Oncology as "Imaging techniques as predictive and prognostic biomarkers in renal cell carcinoma"; Ther Adv Med Oncol.2013 Mar;5(2):119-31. This review forms the basis of this chapter.

2.2.   Predictive and prognostic biomarker

The National Institute of Health definition of a biomarker is discussed in the last chapter (section 1.3.1). RCC is a heterogeneous group of disease with differing natural history. Reliable identification of the subtypes and assessment of extent / stage of the disease is of utmost importance and would guide therapy options. With introduction of multiple therapies which work through varying mechanisms, it is becoming more and more important to match the therapy and subgroup of patients who would derive maximal benefit or avoid the group that would not gain any clinical benefit. Validated tools which predict the clinical benefit or identify risk of toxicity would help to personalise treatment and avoid exposing patients to unnecessary side effects from a treatment that offers marginal benefits.

Biomarkers also have significant importance in drug discovery and development where evidence of drug activity can help in selecting the functional dose of a drug.

At present, we can name multiple examples where treatments with evidence of clinical benefit being declined for use by regulatory authorities on the grounds of cost effectiveness. By identifying the patient group who is likely to benefit from the treatment, biomarkers will improve the cost-effectiveness analyses and thus impact on decisions made by regulatory authorities. This will lead to a higher chance of new treatments being available to the patients for whom it matters.

Imaging as biomarker is an attractive and indispensable option due to the minimal invasiveness in this approach. This would mean that a significant number of imaging modalities could be repeated at intervals to monitor the progress in a patient with minimal chance of harm.

Imaging based response assessment criteria (RECIST) have been the cornerstone in treatment response assessment in oncology. RECIST criteria is discussed in chapter 1 and in chapter 5.0 (section 5.1.1). Unidimensional size based assessment with RECIST criteria have been useful in therapy assessment with cytotoxic chemotherapy. With the introduction of cytostatic targeted therapy where response in size may not correlate with the clinical benefit obtained, use of RECIST assessment on its own may not be adequate. A retrospective analysis of 39 patients published by Teo et.al suggested that some patients continue to derive clinical benefit despite showing progressive disease according to RECIST criteria (MinYuen Teo and incorporating the National Children's Hospital 2012). RCC is a highly vascular tumour which makes it an attractive target to assess change in vascularity or change in contrast enhancement. Since the proposal of Choi criteria in Gastrointestinal stromal tumours (GIST), which takes into account changes in contrast enhancement along with changes in size, researchers have been trying different imaging based criteria which could act as potential biomarker in response to targeted therapy.

2.3.   Biomarkers based on CT imaging

2.3.1. Multi-slice CT to assess RCC histological subtypes

Sher and colleagues retrospectively assessed 87 patients and compared CT images with histopathology. Images were acquired during unenhanced, cortico-medullary phase (CMP) and excretory phase (EP) (30 and 300 s after contrast injection respectively). Degree of enhancement in the CMP and EP was noted to be the most valuable parameter in attempting to differentiate between histological subtypes ($p < 0.001$). Histological subtypes showed different mean CT attenuation (+2 standard deviations) in CMP. For clear cell RCC this was 138.2 ± 38.0 HU while for papillary and chromophobe tumours this was 89.2 ± 31.4 HU and 55.17 ± 24.0 HU respectively. Enhancement in excretory phase also showed significant difference between histological subtypes with clear cell carcinoma showing an enhancement of 73.0 ± 17.6 HU while papillary and chromophobe had an enhancement of 70.0 ± 10.4 and 33.9 ± 12.1 HU respectively. The cut-off value for highest accuracy for diagnosis of clear cell carcinoma was 83.5 HU for CMP and 64.5 HU for EP (Sheir, El-Azab et al. 2005).

Intra-tumoural necrosis noted on CT scan was shown to be an independent predictor of high Fuhrman grade by Oh et.al in 2016. A retrospective review of 169 patients showed that presence of intra-tumoural necrosis was associated with high odds for high Fuhrman grade (p <0.03) (Oh, Sung et al. 2016)

2.3.2. New criteria for response assessment

2.3.2.1.   Choi criteria

Choi et.al proposed an alternate criterion which takes into account either a change in size or change in contrast enhancement has been shown to be better in predicting response to imatinib in GIST (Choi 2008). In RCC, Vander Veldt (2010) showed that Choi criteria correlated to time to progression better than RECIST (van der Veldt, Meijerink et al. 2010). In a 55 patient retrospective analysis of metastatic RCC patients treated with sunitinib, responders according to Choi criteria had significantly better predictive value for PFS and OS ($p < 0.001$ for both) than RECIST ($p = 0.689$ and 0.191 respectively) at the initial assessment on treatment. The predictive value of RECIST rose to a statistically significant level only when best response during treatment was taken into account. Hittinger et.al (2011) compared Choi and RECIST in a 22 patient cohort treated with sorafenib where Choi criteria was able to differentiate patients who had increased PFS or OS (Hittinger, Staehler et al. 2011).

2.3.2.2.   Modified Choi criteria

Based on combination of change in size and arterial based enhancement, we have proposed a modification of the Choi criteria and assessed whether this could reliably identify responders (Nathan, Vinayan et al. 2010). The results of this study which forms part of this thesis is described in chapter 5.0.

2.3.2.3.   SACT criteria

Proposed by Smith et.al (Smith, Lieber et al. 2010) SACT criteria used CT based volumetric attenuation along with size for response assessment. According to SACT criteria, favourable response is defined as any of the following:

- Decrease in tumour size of at least 20%

- Decrease in tumour size of at least 10% and at least half of non-lung target lesions with decreased mean attenuation of at least 20 Hounsfield units (HU)

- One or more lung lesions with decreased mean attenuation by at least 40 HU.

Un-favourable response was defined as

- Increase in tumour size of at least 20%;

- New metastasis

- Marked central fill in of a target lesion

- New enhancement in a homogenously hypo-attenuating non-enhancing mass.

The study compared SACT criteria with RECIST and a volumetric attenuation data in predicting a PFS greater than 250days. Favourable response as per SACT criteria had a sensitivity of 75% and specificity of 100% in identifying the group of patients with PFS >250 days. Sensitivity and specificity for RECIST was 16% and 100% and 93% and 44% for this volumetric analysis.

2.3.2.4.   MASS criteria

MASS criteria (Morphology, Attenuation, Size and Structure) was proposed by the

same group who proposed SACT criteria (Smith, Shah et al. 2010). MASS criteria

defines

favourable response as

- No new lesion and

- Any of

   o   Decrease in tumour size by 20%

   o   One or more predominantly enhancing solid enhancing lesions with

       marked central necrosis

   o   Marked decrease in attenuation ($\geq$40HU)

-

Unfavourable response according to MASS criteria were defined as

- Increase in tumour size of at least 20% in the absence of marked necrosis or

   marked decreased attenuation

- New metastasis

- Marked central fill-in

- New increased enhancement.

The MASS criteria showed an increased sensitivity of 86% and specificity of 100% in

recognizing good responders (TTP and improved disease specific survival $p < 0.0001$).

2.3.2.5.   Tumour burden and growth rate

In 69 patients with metastatic RCC treated with VEGF-targeted therapy, Bassapa and colleagues assessed the tumour burden (TB). With multivariate analysis, total number of metastases (<10) and TB above the diaphragm (<6.5 cm) at baseline were independent positive predictors of OS [Basappa et $al.$ 2011]. TB (p = 0.003) and total metastases (≤12) were noted as predictors of OS at the time of disease progression (Basappa, Elson et al. 2011).

Predictive effect of the initial tumour size and the rate of size reduction in response to targeted therapy was also reported by Yuasa and colleagues (Yuasa, Urakami et al. 2011). A linear, moderate to strong association was noted between pre-treatment tumour size and reduction in growth rate on therapy (correlation coefficient –0.441, $p < 0.001$) in a 139 patient retrospective analysis. When a threshold value of 23.9 mm was applied, it was noted that smaller tumours showed a better rate of shrinkage ($p < 0.001$).

2.3.3. DCE-CT in assessing vascularity and treatment response

DCE-CT to assess tumour vascularity was performed by Wang et.al (2006). They showed that enhancement characteristics in DCE-CT correlated well to the tumour micro vascular density (MVD) (Wang, Min et al. 2006). This technique does hold promise as concentration kinetics of CT contrast are related directly and linearly to the visualised enhancement and analysis is therefore relatively straight forward (Miles 2002). A Danish renal cancer group study published in 2014 showed that a high baseline blood flow (BF) and reduction in BF and blood volume early in treatment corresponded to improved treatment outcome to bevacizumab and interferon-α2a treatment (Mains, Donskov et al. 2014).

Potential guidelines for DCE-CT image acquisition and analysis has been published by Miles et.al in 2012 (Miles, Lee et al. 2012) but there still remains little general agreement about the techniques to use for modelling and further quantitative analysis.

2.4. Biomarkers based on US imaging

2.4.1. DCE-US as a predictive marker

Use of DCE-US as a predictive tool in treatment response assessment in metastatic renal cell carcinoma was investigated by Lamuraglia and colleagues. In a randomised control trial comparing sorafenib and placebo, DCE-US was performed at baseline, week 3 and week6. Responders defined by stable or decrease in tumour size along with decrease in contrast uptake >10% at week3 showed a statistically significant improvement in PFS (p<0.0004) and OS (p<0.0004) (Lamuraglia, Escudier et al. 2006). Lassau et.al (2012) in a large multi-centric trial investigated the use of DCE-US as predictive biomarker in patients treated with anti-angiogenic agents (Nathalie Lassau, Louis Chapotot et al. 2012). 157 RCC patients were included in this study, recruited from 19 centres in France. DCE-US was performed at baseline, day7, day14, day30, day60 and 2 monthly thereafter. Study suggested that a decrease in area under curve (AUC) by >40% at one month was predictive of time to progression.

A third study assessing DCE-US performed by Williams and colleagues (2011) showed a decrease in median tumour blood volume by 73.2% at 2 week of treatment (Williams, Hudson et al. 2011). But these changes did not show any correlation to PFS.

2.5.   Biomarkers based on PET imaging

2.5.1. FDG-PET in RCC diagnosis and staging

Different studies have reported wide variation in sensitivity of FDG-PET CT scan in RCC diagnosis and staging (32% - 100%) (Montravers, Grahek et al. 2000, Nakatani, Nakamoto et al. 2011). The largest of these series, published by Kang and colleagues, included 66 patients with RCC and showed a sensitivity of 60% (Kang, White et al. 2004). Nakatani et.al suggested a higher FDG sensitivity for RCC metastasis but this is yet to be validated (Nakatani, Nakamoto et al. 2009). Even though PET-CT is used currently as a standard technique in multiple tumour types to assess metastasis (eg: upper GI, Lung), it has been found to be inferior than whole body MRI scan in assessing RCC metastasis. This could be due to the frequency of metastatic spread to the bone, liver etc from RCC (Antoch, Vogt et al. 2003, Schmidt, Baur-Melnyk et al. 2005).

2.5.2. FDG-PET as a prognostic biomarker

Baseline SUVmax from pretreatment FDG-PET as a prognostic marker was evaluated by Nakaigawa in 2012. With 67 enrolled patients, wide variation of SUVmax was noted in renal cell carcinoma with increasing levels of SUVmax showing a trend towards poorer survival (p<0.0001). Stratified SUVmax, (<7.0, 7.0 – 12 and >12) showed a median PFS 1229 days, 446 and 95 days representatively. High baseline SUV was again noted as a poor prognostic factor in a separate study of 35 patients with metastatic RCC treated with TKI (Ueno, Yao et al. 2012).

2.5.3. FDG-PET in treatment response assessment

Le Moulec and colleagues assessed the role of baseline enhancement and change in enhancement of FDG-PET with clinical outcome (S. Le Moulec 2010). The group reported that negative PET-CT at baseline showed a better outcome with clinical benefit of increased median survival (p=0.05). Patients with baseline SUVmax >5.7 had a short PFS (3months vs 9 months p=0.03) and OS (9.1months vs 23months).

Ueno et.al (2012) assessed FDG-PET scan as a predictive biomarker and suggested that change in SUVmax at one month after treatment initiation with tyrosine kinase inhibitors can be predictive of PFS and OS (Ueno, Yao et al. 2012). In 35 patients with metastatic RCC treated with TKI, they noted that good responders defined as no increase in tumour size (sum of all target lesions) with decrease in SUVmax of ≥20% showed statistically significant improvement in PFS and OS than non-responders (Ueno, Yao et al. 2012).

Sequential FDG-PET in response assessment of Sunitinib was reported by Powles et.al in 2011. They assessed this with 3 FDG-PET CT at baseline, week 4 and week 16 on treatment. In this phase 2 study with 44 metastatic RCC patients, though metabolic response was noted in 57% of patients in 4 weeks, no significant correlation was noted between change in SUVmax at 4weeks and PFS or OS. The study showed correlation between poor OS and progressive disease diagnosed with FDG-PET at 16weeks on treatment (Kayani, Avril et al. 2011).

## 2.6.	Biomarkers based on MR imaging

2.6.1. MRI to assess RCC histological subtypes

Pedrosa and colleagues assessed the possibility of diagnosing histological subtypes of RCC using MRI. MRI scans were sub-grouped into 8 groups based on size, location, necrosis, signal intensity type and extent of fat and contrast enhancement, peri-renal far invasion etc. On comparing with histopathology, MRI classification had 93% sensitivity, and 75% specificity in diagnosing ccRCC. Sensitivity and specificity was 80% and 94% respectively in assessing papillary subtype (Pedrosa, Chou et al. 2008).

DCE-MRI scan as tool for differentiation of histological subtypes was assessed by Sun and colleagues (Sun, Ngo et al. 2009). Analysing the contrast enhancement both in cortico-medullary (CMP) and nephrographic phase, these researchers were able to distinguish between clear cell and papillary subtypes. Signal intensity change at CMP was noted to be the most significant tool in this with a sensitivity of 93% and specificity of 96%.

Palmowski also reported that DCE-MRI could predict nuclear grade of RCC. High perfusion values noted in the entire tumour and most vascular area corresponded to high grade tumours ($p < 0.05$) (Palmowski, Schifferdecker et al. 2009).

Diffusion weighted (DW)-MRI was also shown to be a useful non-invasive tool to predict RCC nuclear grade (Goyal, Sharma et al. 2012) . Similar results were shown by Mirka and colleagues. In a 139 patient cohort, DW-MRI on a 3.0T (Tesla) scan, ADC maps were able to differentiate between low and high grades of RCC and also differentiate between clear cell and other histological subtypes (p=0.002 for papillary, p=0.048 for chromophobe) (Mirka, Korcakova et al. 2015)

2.6.2. Whole body MRI in assessment of skeletal metastasis

With development in MRI technology, we are now able to perform whole body MRI (WBMRI) imaging. Use of WBMRI in assessment of skeletal metastasis has been investigated (Chan, Chan et al. 1997, Tamada, Nagai et al. 2000). In RCC, Shohaib and colleagues assessed the usefulness of whole body MRI in comparison with standard 99Tc nuclear medicine based whole body bone scan in assessing skeletal metastasis. 47patients were analysed in this prospective study. Both MRI and bone scan showed high specificity (97% vs 94%) but MRI scan was noted to be significantly superior with regard to sensitivity (94% vs 62% p=0.0007) in skeletal metastasis detection. Using MRI scan also has advantage of being able to assess soft tissue disease simultaneously (Sohaib, Cook et al. 2009).

In comparison with CT scan, reported by Platzek and colleagues, WBMRI showed higher accuracy in diagnosing metastasis especially in the musculoskeletal system (97% vs 82% p<0.000) (Platzek, Zastrow et al. 2010).

2.6.3. DCE-MRI as a predictive biomarker

Use of DCE-MRI as a biomarker of angiogenesis and vascularity has been researched and validated over the last decade in multiple tumour types. This includes direct correlation of vascularity using immuno-histochemical assessment of micro vascular density (MVD) (Buckley, Drew et al. 1997). Varying results have been shown on attempting to correlate imaging with tissue expression of proangiogenic growth factors including VEGF (Padhani and Dzik-Jurasz 2004, Schlemmer HP 2004).

Unlike DCE-CT, where relationship of image enhancement and contrast kinetics is linear and depends directly on concentration and timing of contrast, contrast kinetics with change in signal intensity in DCE-MRI scan is non-linear and and hence complex (Kiessling, Jugold et al. 2007). In DCE-MRI, this relationship also depends on imaging sequence, machine setup, heterogeneity of the tumour and inherent relaxation rate of the tissue (Padhani 2003). Imaging dependent vascular parameters as K^{trans} (transfer co-efficient – influx of contrast from plasma to interstitial space), K_{ep} (efflux back to vasculature), V_e (volume of distribution), rBF (relative blood flow), rBV (relative blood volume) and IAUGC (Initial area under gadolinium curve) need to be assessed and fitted with known statistical model for reliable assessment of contrast kinetics.

DCE-MRI was used for assessment of metastatic RCC patients treated with sorafenib in a pilot study published by Flaherty and colleagues in 2008 (Flaherty, Rosen et al. 2008). With this study the researchers showed a statistically significant correlation between reduction of K^{trans} and improved PFS (p=0.01). High baseline Ktrans was also noted as a predictive marker for good treatment response (p<0.002).

Relation of high K^{trans} at baseline with improved PFS was also noted by Stadler and colleagues again with sorafenib treatment in metastatic RCC (p<0.027). No correlation of change between K^{trans} and PFS was noted in this study (Hahn, Yang et al. 2008).

2.6.4. Role of functional MRI with no external contrast

2.6.4.1. Arterial Spin labelled (ASL)- MRI

This technique utilises the inherent nuclear spin of protons in water to magnetically label arterial blood. As labelled blood flows through the tissue of interest, its kinetics could be quantitatively measured. Capability of this technique to predict anti-angiogenic therapy response was investigated by de Bzelaire and colleagues (De Bazelaire, Rofsky et al. 2005). In a feasibility study of 10 patients both ASL-MRI and DCE-MRI were used to assess treatment response to antiangiogenic agent (PTK787/ZK222584) in metastatic RCC. This study demonstrated correlation of blood flow changes as measured by ASL-MRI at 1 month with change in tumour size at 4 months or at disease progression (de Bazelaire, Alsop et al. 2008). Given the non-contrast dependent imaging, ASL-MRI could be a good addition in imaging biomarker if validated.

2.6.4.2. Blood oxygen level dependent (BOLD)-MRI

BOLD-MRI utilises the difference in magnetic property of oxy-haemoglobin and deoxy-haemoglobin and hence can be related to tumour hypoxia. In a multi-parametric MRI assessment study by Notohamiprodjo it was noted that perfusion parameters shown by DCE-MRI correlated broadly to R2* maps of BOLD MRI (Notohamiprodjo, Staehler et al. 2013). A histogram analysis of BOLD MRI based R2* and ADC mapping with DW-MRI was also found to be of use in differentiating high grade from low grade tumours (Zhang, Wu et al. 2015).

2.6.4.3.   Diffusion weighted (DW)-MRI.

This non-contrast dependent MRI technique exploits the Brownian motion of the water molecule in the tissue to acquire functional images.

DW-MRI as a predictive biomarker of antiangiogenic therapy response was assessed by Desar and colleagues. They reported the capability of this technique to detect anti-angiogenic effects of sunitinib in RCC as early as 3-10days from treatment initiation (Desar, ter Voert et al. 2011).

Bharwani et.al in 2012 showed that in mRCC patients treated with sunitinib, 47% showed significant changes in whole tumour ADC (Apparent Diffusion Co-efficient). Even though changes in ADC did not correlate with outcome, high baseline and greater than median increase in AUC (defined as the proportion of the tumour with ADC values below the 25th percentile of ADC histogram) showed reduced overall survival (Bharwani, Miquel et al. 2014).

Goyal and colleagues investigated the role of DW-MRI as a non-invasive prognostic biomarker. They aimed to compare the DW-MRI parameters and histology and concluded that lower mean ADC on DW-MRI correlates with high nuclear grade of RCC (Goyal, Sharma et al. 2012).

Chapter 3.

Materials and Methods

3.1.   Introduction

In this chapter I detail the methods used in the three studies described as part of this dissertation. Three projects were carried out based on different imaging-based techniques to assess the effects induced and also to assess the effectiveness of these techniques in assessing treatment related response in metastatic RCC patients when treated with targeted treatment which acts through the anti-angiogenic pathway.

In the first study described, Dynamic Contrast-Enhanced (DCE) MRI scans were used to assess whether addition of interferonα2a to bevacizumab would add to the anti-angiogenic effect of bevacizumab in metastatic RCC. This was a prospective, multi-centric, randomised, open-labelled clinical trial which I co-ordinated. Along with assessing the anti-angiogenic effect by measuring DCE-MRI vascular parameters, we also explored whether these vascular changes could correlate with response to treatment or clinical effectiveness and thus whether they could act as an early predictive biomarker. In the first section of this chapter (3.2), I explain this study in detail; "DCE-MRI associated vascular changes with bevacizumab with or without interferon-α 2a in advanced RCC". Results of the study are discussed in chapter 4.0 of this thesis.

In the second and third part of this chapter (sections 3.3 and 3.4), I detail two retrospective studies which were performed to assess CT defined criteria in assessing response to treatment in metastatic RCC patients treated with tyrosine kinase inhibitors which affect the anti-angiogenic pathway. In the study described in section 3.3, I assessed the role of change in arterial enhancement along with change in tumour size as a predictive biomarker in metastatic RCC patients treated with tyrosine kinase inhibitors and propose a new criterion named as "modified" Choi criterion. The background, outcome and discussion of this study is described in chapter 5.0 of this thesis.

The third study in this thesis assesses the role of CT-defined textural analysis in prediction of treatment response in metastatic RCC. This was a collaborative project with a group of researchers from University of Sussex and Brighton who developed the algorithm for textural analysis. Textural analysis study used retrospective approach where metastatic RCC patients treated with tyrosine kinase inhibitors were studied and their baseline and treatment response scans analysed with the textural analysis. Background and results of this study is discussed in detail in chapter 6.0 of this thesis.

3.2. DCE-MRI assessment of vascular changes induced with bevacizumab with or without interferon-α2a in advanced renal cell carcinoma

3.2.1. Introduction

3.2.2. Study design and assessments

This clinical trial was designed as a three-arm randomised multi-centric open-labelled phase 2 study. Metastatic (stage IV) or locally advanced (inoperable stage III) RCC with good or intermediate prognosis by Motzer score (Motzer, Bander et al. 1996, Motzer, Bacik et al. 2002) who were systemic treatment naïve in metastatic setting formed the subjects of this trial (Appendix 9.2).

Recruitment was planned from three UK centres - Mount Vernon Hospital, The Royal Marsden Hospital, Addenbrooke's Hospital. Eligible patients were randomised to one of the three treatment arms (10 patients per arm), with treatment regimens as below:

- Arm A: Bevacizumab 10mg/kg every 2 weeks

- Arm B: Bevacizumab 10mg/kg every 2 weeks plus low-dose IFN-α2a 3MU Three times in a week (t.i.w), commencing on Day 0.

- Arm C: Bevacizumab 10mg/kg every 2 weeks plus standard dose IFN-α2a 9 MU t.i.w. Patients will commence on IFN-α 3MU t.i.w on Day 0, and escalate dose to 9MU t.i.w on Day 14.

All patients continued on their randomised treatment regimen until the first tumour assessment at week 8. At this point the decision to introduce or modify the interferon-α2a dosage was made at the discretion of the treating physician. Bevacizumab dosing remained unchanged unless clinically indicated as explained in section (3.2.5).

Treatment with both study drugs continued until disease progression, unacceptable toxicity, or consent was withdrawn. In the event of interferon-α2a-related toxicity, dose reduction was allowed. In case of withdrawal of interferon-α2a, bevacizumab was continued until disease progression.

Patients in all arms underwent two baseline DCE-MRI scans in the week pre-treatment and then further scans at weeks 2 (prior to IFN dose escalation in Arm C), and 6 post-commencement of bevacizumab. Two baseline DCE-MRI were performed to assess the reproducibility of these imaging parameters. This is explained in detail in this chapter in section 3.2.7.4.

Patients also underwent CT scans of the chest, abdomen and pelvis performed at baseline, at week 8 and three-monthly thereafter. This is standard practice in our institution and hence patients were not exposed to extra CT scans and unnecessary radiation. Tumour response was to be assessed by RECIST criteria as per standard practice.

Patients all had the required haematological and biochemistry tests analysed as standardly required for TKI therapy. In addition, patients had peripheral blood and serum samples taken to be analysed for surrogate biomarkers. The samples required and their handling are explained in section 3.2.4.8 of this chapter and in Appendix 9.7.

A total of thirty subjects were to be recruited to the study over a planned recruitment period of 9 months (please refer to section 3.2.9 for the statistical details). Patients were randomised to one of the three arms as described before. An online software randomization.com (www.randomization.com) was used to randomise patients. This software uses a pseudo-random number generator of Winchmann and Hill (1982) as modified by McLeod (1985). The randomisation list was produced from the software and individual patient allocation performed with the seed generated from the primary randomisation. Study sites contacted the study coordinator at Mount Vernon site for allocation of treatment for individual patients and their trial-specific number.

Figure 3.1   Overview of trial scheme.

Systemic treatment naïve metastatic RCC (n=30)

Bev* 10mg/kg 2qw monotherapy (n=10)

Bev* 10mg/kg 2qw + IFN 3MiU q3w (n=10)

Bev* 10mg/kg 2qw + IFN 3MiU q3w (n=10)

Bev* 10mg/kg 2qw + IFN increased to 9MiU q3w

Continue Bev* ± IFN[$][#]

PD

PD

PD

Time scale

Day 0   Wk 2   Wk 6   Wk 8   PD

Screening phase:
DCE-MRI X 2
CT Scan

- DCE MRI

- Dose escalation for arm C

1^0 end point Vascular change – DCE MRI

2^0 end point Response rate - CT-Scan

2^0 end point PFS.

-    = Bevacizumab (Avastin®)
- $ = Interferon - α
- #   = Bevacizumab + IFN will be continued on all patients after 8Wk CT to PD; dosing at Investigator discretion

3.2.2.1.   Inclusion and exclusion criteria

Pre-defined inclusion and exclusion criteria were stipulated with the trial protocol. Eligibility of potential patients were initially assessed by the treating investigator at individual sites according to the protocol. This was reassessed by the co-ordinating investigator at the sponsor site prior to recruitment. The inclusion and exclusion criteria used for patient selection are as below.

3.2.2.2.   Inclusion criteria

1. Written informed consent

2. Male or female subjects ≥ 18 years

3. Patients with previously untreated metastatic (stage IV) or locally advanced (inoperable stage III) RCC

4. Histologically and/or cytologically confirmed, advanced RCC, for whom a majority component of conventional clear-cell type is mandatory.

5. Good or intermediate prognosis disease as defined by Motzer score.

6. RECIST measurable lesion(s), which is amenable to DCE-MRI scanning

7. Life expectancy of at least 12 weeks

8. Eastern Co-operative Oncology Group (ECOG) performance status 0-2

9. Adequate haematological function – absolute neutrophil count (ANC) ≥1.5 x 10^9/L, Platelet count ≥100 x 10^9/L and haemoglobin ≥8 g/dL (may be transfused to maintain or exceed this level)

10. Adequate liver function:

11. Total bilirubin <1.5 x upper limit of normal (ULN) AND

12. Asparagine aminotransferase (AST), alanine aminotransferase (ALT) <2.5 x ULN (without liver metastases); <5 x ULN (liver metastases).

13. Adequate renal function:

14. Serum creatinine ≤1.5 x ULN

15. Urine dipstick for proteinuria <2+. If ≥2+ proteinuria on dipstick urinalysis at baseline, 24hour urine collection must show protein <1 g/24hrs.

Requirement for renal function was amended in a substantial amendment so as to include creatinine clearance measurement either by direct calculation of glomerular filtration using ethylenediaminetetraacetic acid test (^{51}Cr-EDTA) or by using calculated creatinine clearance using Cockcroft-Gault method (see Appendix 9.4). Changes in substantial amendment are detailed in the next section of this chapter.

16. International normalised ratio (INR) ≤1.5 within 7 days prior to enrolment if not on anticoagulants. Patients on anticoagulants should have stable INR with a target range less than 3.0.

Women of childbearing age must have a negative pregnancy test and must use adequate contraception during the treatment phase of the study and for 9 months afterwards. Women who wish to breastfeed are not eligible for the study.

3.2.2.3. Exclusion criteria

17. Diagnosis of brain metastasis. CT or MRI brain scan was to be performed to exclude brain metastases if there was a clinical suspicion

18. Major surgery (incl. open biopsy) or radiation therapy within 28 days prior to enrolment (palliative radiotherapy to painful bone lesions was allowed within 14 days prior to enrolment)

19. Core biopsy or other minor surgical procedure, excluding placement of a vascular access device, within 7 days prior to enrolment

20. Congestive heart failure (NYHA Class II, II, or IV), unstable angina pectoris, or myocardial infarction within 6 months prior to enrolment

21. Inadequately controlled hypertension (defined as a blood pressure of > 150 mmHg systolic and/or > 100 mmHg diastolic on medication), or any prior history of hypertensive crisis or hypertensive encephalopathy

22. CVA or transient ischemic attack within 6 months of enrolment

23. Significant vascular disease (e.g., aortic aneurysm, aortic dissection), or symptomatic peripheral vascular disease

24. Evidence or history of recurrent thromboembolism (>1 episode of DVT/PE) during the past 6 months, bleeding diathesis or coagulopathy

25. Chronic daily intake of aspirin >325 mg/day or clopidogrel >75 mg/day, or steroids (prednisone > 12.5 mg/day or dexamethasone > 2 mg/day).

26. History of abdominal or tracheo-oesophageal fistula, gastrointestinal perforation, or intra-abdominal abscess within 6 months prior to study enrolment

27. Serious, non-healing wound, ulcer, or bone fracture

28. Pregnant or breast-feeding mothers

29. No contraindication to MRI scanning

30. Current active second malignancy

31. Patients with a history of allergic reactions to contrast agents

32. Patients with gross ascites

33. Seizure disorder requiring medication

34. HIV/Hep B/Hep C/ other infection >CTC 2;

35. Other investigational drug during trial or within 30 days

36. Adjuvant anti-angiogenic therapy within 6 months of enrolment

37. Any significant medical illness or significant abnormal laboratory finding that would, in the investigator's judgment, make the patient inappropriate for this study, or would increase the risk associated with the patients' participation in the study.

3.2.2.4.   Amendments

Initial trial protocol was amended to increase safety and aimed at avoiding any confounding treatment with anti-angiogenics. The amendments included:

1. Change of renal function inclusion criteria from serum creatinine <1.5 times upper limit of normal to calculated creatinine clearance or ^{51}Cr-EDTA (GFR) ≥ 50ml/min. Calculated creatinine clearance calculation was to be performed by Cockcroft-Gault formula (see appendix 9.4); ^{51}Cr-EDTA test could also be used by the investigator to measure the renal function if calculated creatinine clearance is <50ml/min and if the investigator felt that this was not an accurate representation of patient's renal function. We felt that calculated creatinine clearance and ^{51}Cr-EDTA GFR are better markers of renal functions than absolute value of creatinine in plasma and thus increasing the safety of patients. The Cockcroft-Gault formula is the most commonly used standardised technique for the calculation of creatinine clearance.

2. To exclude patients who have had anti-angiogenics in the last 6 months prior to enrolment in trial. Prior recent usage of anti-angiogenic therapy may affect the vascularity of a metastatic lesion. A 6 month wash-out period is believed to reduce effects of such therapy, to avoid any confounding of the primary endpoint analysis.

3.2.3. Randomisation

Patients were randomised into 3 arms using an online software (www.randomization.com). The software utilises a pseudo-random number generator of Winchmann and Hill (1982) as modified by McLeod (1985). A randomisation list was produced from this software and individual patient allocation performed with the seed generated from the primary randomisation. The randomisation list was controlled by the trial co-ordinator at Mount Vernon and was unavailable to any of the investigators with any patient contact. Study sites contacted the study co-ordinator at Mount Vernon for allocation of patients to the trial arms. The contact number of the trial co-ordinator was easily available to the investigators and sites and was provided in the trial protocol and site files.

3.2.4. Schedule of clinical assessments and procedures

3.2.4.1.   Patient identification

Patients were identified by the investigators in individual recruiting centres and approached regarding potential participation in the clinical trial. The patient information leaflet, approved by National and Local Research Ethics Committees, was provided to all patients and the trial was explained. Patients were reviewed in clinic usually in a week after they had had a chance to review the trial information and other treatment options and had a chance to discuss any questions regarding this.

All subjects were asked to provide written informed consent before any study specific assessments or procedures were performed. The written informed consent form used was a version controlled document approved by the Ethics Committee (Appendix 9.5). All assessments and trial procedures were performed in compliance with the most up to date version of the protocol, including principles of ICH-GCP, any relevant research governance and other regulatory requirements as appropriate.

Patients who fulfilled all inclusion and none of the exclusion criteria were accepted into the study. Inclusion of any subject who did not meet these criteria was only considered after discussion with the Chief Investigator who could grant a waiver. Investigators or site coordinators contacted the trial co-ordinator at Mount Vernon for a temporary registration to consider patient for screening. This allowed us to capture the number of patients who were considered for trial but failed screening.

3.2.4.2. Clinical assessment

Patients were continually assessed as per trial protocol. The procedures that were to be performed varied according to the trial period of individual patients. This is detailed further in this section.

3.2.4.3. Screening and enrollment period

Following investigations and procedures were performed within 28 days prior to starting treatment;

1. Written informed consent.

2. Histological confirmation of RCC with majority clear cell element.

3. Whole body CT scans (chest, abdomen and pelvis) with RECIST measurement of target lesions.

4. Medical history was noted to rule out any significant comorbidities.

5. Demographic data: age, sex, height, weight, ethnicity were also collected.

Investigations and procedures performed within 14 days prior to start of treatment;

1. Urine or serum pregnancy test for women of childbearing age

2. Full Physical Examination, including 12 lead ECG

3. Vital Signs (BP, pulse, respiration rate)

4. ECOG performance status

5. Record of all concomitant medications

6. Full blood count(FBC): Haemoglobin, differential WBC and platelet count

7. Urea, electrolytes & biochemistry panel (LFT, LDH, glucose, Calcium)

8. Dipstick urinalysis

9. Coagulation panel (prothrombin time or INR)

Following completion of screening: Randomisation was performed followed by the research MRI Scans. Research MRI - 2 baseline scans (DCE-MRI along with Diffusion and BOLD imaging). Blood for biomarkers was collected simultaneously with the treatment, and urine for proteomics was performed once during the period.

3.2.4.4.   Treatment period

Visits in the treatment phase occurred on Days 0, 14 and at Week 6. Assessments at these visits included the following:

1. Investigations 7-14 as per screening/enrolment period

2. Recording of dosing of bevacizumab and interferon.

3. Recording of all adverse events. CTC grading and causality recorded as per protocol

4. Blood samples for biomarker analysis at week 2, 6 and 8

5. MRI at Week 2 and Week 6 (In Arm C, MRI was performed prior to dose escalation.

3.2.4.5. Follow-up period

Visits in the follow-up phase were performed every 12 weeks after completion of primary end point at week 8. This continued until disease progression. Assessments at these visits included all the tests as in treatment phase (section 3.2.4.4) except for MRI and peripheral blood biomarker analysis. Treatment response assessment continued with whole body CT scan (chest, abdomen, pelvis) as per the local rules.

3.2.4.6. Final visit at discontinuation

A final visit was performed at either 30 days after last dose of drug or at study discontinuation. All assessments as per section 3.2.4.4 along with blood sample for biomarker assessment were performed at that visit. Once treatment had ceased due to disease progression, follow-up occurred by routine follow-up visits according to local policy, or by telephone.

3.2.4.7. Radiological assessment

Patients underwent two baseline research MRI scans in the week pre-treatment followed by further scans at weeks 2 and 6 (assessment of primary endpoint).

The main requirement in these MRI scans were the acquisition of DCE-MRI images. Use of DCE-MRI in assessing change in vasculature has been discussed earlier. DCE-MRI scan acquisition involved imaging pre- and post-administration of intravenous contrast agent - intravenous gadoteric acid formed with gadolinium oxide and DOTA (2.5mmol/kg body weight Gd-DOTA, Guerbet). In addition, we planned to perform a Blood Oxygenation Level-Dependent (BOLD) scan (prior to administration of the contrast agent) to assess the oxygenation status of red blood cells in perfused regions, and a Diffusion-Weighted (DW) MRI scan to assess cellularity along with the DCE-MRI. With these scans we aimed to characterise the spatial patterns of angiogenesis across the full extent of the tumour, to quantify the perfusion characteristics of the tumour (in terms of flows and permeability), and to assess any drug-induced changes in tissue oxygenation and cellularity. Details of image acquisition and processing can be found in section 3.2.7.2.

Additionally, CT scans of chest, abdomen and pelvis were performed at baseline and at 8 weeks. This allowed a formal assessment of the comparison between change in tumour size and DCE-MRI-defined changes in K^{trans}. Further imaging with CT scans in follow up phase was performed every 12 weeks or as per local policy as long as the patient continued on trial i.e. until disease progression.

3.2.4.8. Laboratory assessment

Laboratory assessments included regular samples and assessments required for safe delivery of anti-angiogenic medication and samples required for biomarker assessment for the clinical trial. Regular samples for haematology, clinical chemistry and coagulation were collected as per study sites standard procedure in management of patients on bevacizumab and or interferon.

Additional samples for biomarker assessment were taken as per the trial protocol (please refer to Table 3.1 and Appendix 9.7). A total of 25ml of blood was collected at each time point twice during screening, week 2, week 6, week 8 and finally at drug discontinuation.

Samples for biomarker analyses were collected in 2x 10ml samples in EDTA vials and 1x 5ml sample in a lithium heparin vial. We also collected 15ml of urine once during the screening phase. A sample handling manual was available for all recruiting sites to process the sample according to protocol (Appendix 9.7).

The planned biomarker assay included:

1. Circulating endothelial cells, peripheral blood analysis of angiogenic and hypoxia regulated markers.

2. Peripheral blood analysis for microRNA

3. Proteomics

Biomarker assay was performed at Oxford under the general overview of Prof Adrian Harris and Dr. John Smythe. The 10ml EDTA sample for circulating endothelial cell assessment was transferred on the day of collection at room temperature to the National Blood Service and Stem cell research at John Radcliffe Hospital for circulating endothelial cell assay.

The rest of the samples (1x10ml of blood in EDTA and 1x5ml of blood in Lithium heparin vacutainers) were processed at site and stored at -80°C. These samples were planned to be transferred as a batch (once all time points from each individual patient were reached) to Oxford for proteomics and microRNA assessment. The sample handling manual detailed all of the procedures that the sites required for sample processing (see Appendix 9.7). In addition, all site teams involved in sample handling were provided with face-to-face training by the co-ordinating investigator from Mount Vernon.

A multi-parameter flow cytometric assay was used in measuring CEC (circulating endothelial cells) and CEPC (circulating endothelial progenitor cells) on the day of collection. Endothelial cell populations were quantified by flow cytometry with a BD LSRII machine (Beckton Dickinson). Antibodies recognising CD34, CD45, CD133, CD144 and Tie2 were used in characterisation and measurement of endothelial cells. CEC was defined as CD45$^-$/dim, CD34+, CD144+ and CEPC was defined as CD45$^-$/dim, CD133+ and tie2+. Quantification of the target population in relation to haemopoetic progenitor cells was quantified by numbers gated in relation to the total mononuclear

cell gate cross referenced by the mononuclear cell concentration in the original blood sample. Immunofluorescence using CalceinAM were used in assessing total and viable CEC cells. Variation of these cellular parameters during treatment has been calculated in individual patients and statistical significance of the changes assessed.

3.2.4.9.   Histopathological specimen

Paraffin-embedded blocks were requested to be sent to the sponsor site at Mount Vernon Hospital. These specimens were to be transferred to the John Radcliffe Hospital, Oxford for further analysis after anonymizing appropriately. It was planned that immunohistochemical analysis (IHC), fluorescence resonance energy transfer (FRET) and fluorescence lifetime imaging (FLIM) will be performed on these samples.

Table 3.1   Schedule of assessment

	Screening/Baseline		Treatment Phase				Follow-up
Day	-28 to -1	-14 to -1	Day 0	Day 14	Week 6	Week 8 / every 3 months	Final Visit at Discontinuation
						Visit until progression	
Informed consent	X						
Demographics	X						
Medical and disease history	X						
Serum or urine pregnancy test [b]		X					
Physical examination [c]		X		X	X	X	X
Weight		X		X	X	X	X
Blood pressure		X		X	X	X	X
ECOG PS				X	X	X	X
Haematology [d]	X	X		X	X	X	X
Coagulation [e]		X		X	X	X	X
Biochemistry [f]		X		X	X	X	X
Urinalysis [g]		X		X	X	X	X
DCE-MRI assessment		X (twice)		X [h]	X		
Concomitant meds		X	X	X	X	X	X

Table 3.1 cont.

	Screening/Baseline		Treatment Phase				Follow-up
Day	-28 to -1	-14 to -1	Day 0	Day 14	Week 6	*Visit until progression* Week 8 / 3 monthly	*Final Visit at Discontinuation*
Adverse events[j]			X	X	X	X	X
CT assessment		X[k]				X	X
Blood sample for biomarkers[l]		X (twice)	X	X	X	X[m]	X
Urine sample for proteomics		X	X	X	X	X	X

b Serum or urine, for women of childbearing potential. To be performed within 14 days before inclusion. If not performed within 7 days prior to the first infusion, a confirmatory urine test will be required.

c As per standard of care

d Includes white blood cell count (WBC) with differential, platelet count, red blood cell count (RBC) and hemoglobin (Hgb) at baseline.

e Includes prothrombin time (PT), and partial thromboplastin time (PTT) within 14 days before inclusion. Patients commenced on anticoagulant therapy should have anticoagulation checked regularly

f To include creatinine (if dipsticks≥ 2+ proteinuria) AST, ALT, LDH at baseline.

g Subjects discovered to have a ≥ 2+ proteinuria on dipstick urinalysis at baseline should undergo 24-hour urine collection and must demonstrate ≤ 1g of protein in 24 hours to be eligible. Thereafter, urine dipstick or 24 hour-protein determination performed prior to each bevacizumab dose. In case of 2+ or greater dipstick proteinuria, a 24 hour-urine collection is mandatory.

h For patients in Arm C, DCE-MRI assessment must be performed prior to escalation of IFN dose

i Subjects in Arm B will receive IFN 3 MU tiw; Subjects in Arm C will commence on IFN 3 MU tiw on Day 0 and escalated to 9MU tiw on Day 14.

j Serious and non-serious adverse events to be collected up to 28 days after the last bevacizumab infusion. Serious adverse events (SAEs) related to bevacizumab should be reported for the duration of the study.

k Baseline CT tumour assessment may be based on the original diagnostic CT if performed within 28 days of starting treatment only at 8 week visit. [l] Blood sampling for biomarker assessment will include a single baseline sample for preparation of genomic DNA, and samples of peripheral blood and blood serum will be collected at each visit indicated

m only at 8 week visit.

3.2.5. Investigational medicinal product

Bevacizumab and Interferon alpha 2a were considered as Investigational Medical Product (IMP) for this study. Even though both these drugs are individually approved for use with multiple indications and the combination of bevacizumab and interferon-α2a is approved for use in management of advanced RCC, with the use of different doses of interferon-α2a and a bevacizumab-only arm used in the trial, these were classified as IMP. Both bevacizumab and interferon-α2a were supplied by Roche Products Ltd ®, referred to as Roche.

3.2.5.1.   Bevacizumab

Bevacizumab was supplied by Roche, appropriately labelled as IMP, to the pharmacy departments at participating investigational sites. Bevacizumab was supplied as a clear to slightly opalescent, colourless to pale brown, sterile liquid for intravenous infusion in single-use glass vials (25mg/mL), which are preservative-free. Shelf life and handling instructions were provided by Roche. Bevacizumab was provided as single use 400mg and 100mg vials and the dose required was drawn up at individual site as per pharmacy protocols.

3.2.5.2.   Interferon-α2a

Interferon-α2a was supplied by Roche, in its commercial presentation to the site pharmacies. Appropriate labelling as IMP was performed at the individual sites. Interferon-α2a was supplied as 0.5ml prefilled syringes with 3, 6 or 9 MIU for subcutaneous administration only. Shelf life and handling instructions were provided by Roche.

3.2.5.3.   Dose and schedule

Patients were randomised to three arms as explained before. All patients received bevacizumab 10mg/kg every two weeks. Patients in Arm B and C had subcutaneous injections of interferon-α2a administered three times a week.

Patients in Arm B had interferon-α2a at the dose of 3MIU/dose while patients in Arm C had interferon-α2a at the dose of 3MIU/dose for the first 2 weeks prior to dose escalation to 9MIU/dose. All patients continued on their randomised treatment for

the first 8 weeks until response assessment. The decision to introduce or modify interferon-α2a was made at the investigator's discretion. The bevacizumab dose continued unchanged.

All patients continued on their respective treatment until progression, unacceptable toxicity or if consent was withdrawn. In the event of IFN-related toxicity, dose reduction was allowed; in case of withdrawal of IFN, bevacizumab was allowed to be continued until disease progression.

3.2.5.4. Adverse event monitoring

Any adverse event, clinical or lab abnormality was noted on every clinical review. These were recorded and reported through the CRF forms. Common Toxicity Criterion 3.0 was used to assess toxicities. Intensity of all adverse events were graded according to the NCI Common Terminology Criteria for Adverse Events v 3.0 (CTCAE) on a five-point scale (Grade 1 to 5) and reported in detail on the CRF. Only the highest grade of each toxicity in an individual patient was reported in the study.

The causality of each toxicity to the IMPs were documented as a Yes or No. If there was a reasonable suspected causal relationship to the study medication i.e. there was evidence or arguments to suggest a causal relationship, drug-event relationship was assessed as Yes.

3.2.5.5.   Serious adverse event monitoring

Any serious adverse events (SAE) affecting the participant patients were immediately reported as per MHRA regulations. SAE, SAR (Serious Adverse Reactions) and SUSAR (Suspected Unexpected Serious Adverse Reactions) were defined according to ICH GCP definitions and reported with an initial report being filed within 24h of knowledge of the event. SAE reports were sent to Roche by the investigating team with a copy to the sponsor site. Reporting of these events to the regulatory body was done via Roche.

3.2.5.6.   Dose modification and delays

Dose modifications were specified in the trial protocol (see Appendix 9.8). This was planned according to the observed toxicity grade and causality of the toxicity. Patients with grade 4 toxicity /unacceptable grade 3 toxicity came of the IMP permanently. With any grade 3 toxicity attributed to interferon-α2a, the drug was withheld and restarted once the toxicity resolved to ≤grade 1. Dose reduction was mandated if there had been > 2weeks of delay due to toxicity. Dose reductions were predefined in the protocol.

With bevacizumab-related toxicity, dose reduction was not allowed. It was mandated that any patients permanently discontinued bevacizumab if they developed gastrointestinal perforation, arterial thromboembolic event, Grade 3/4 haemorrhagic events, grade 4 hypertension or grade 4 proteinuria. Management of bevacizumab-specific hypertension and proteinuria is detailed in the protocol and attached here as an appendix (9.8).

3.2.6. Independent safety monitoring

Safety of the treatment provided was evaluated as a planned interim analysis. A safety analysis was performed after 15 patients completed their primary trial endpoint. The safety analysis population included all subjects who received at least one dose/infusion and had a safety assessment performed at baseline. All safety parameters are summarised and presented in the Chapter 4.0 (section 4.5.2). In patients who were considered for safety analysis, all adverse events including clinical and laboratory events were collected and graded according to CTCAE version 3.0. Causality of adverse events and relation to IMP's were assessed as explained earlier in this chapter (section 3.2.5.4). Data obtained was analysed by an expert experienced in managing RCC patients and was independent of the management of the clinical trial.

Adverse event data was to be reported according to overall and intensity of the adverse events. Subjects who experienced the same event on more than one occasion were counted only once in the calculation of the event frequency.

3.2.7. DCE-MRI data collection and analysis

3.2.7.1.   Lesion suitability criteria for DCE-MRI

Along with the clinical and laboratory inclusion exclusion criteria, we had to make sure that the target lesions used were analysable using DCE-MRI. Patients with lesions unsuitable for DCE-MRI analysis were excluded from trial.

- Tumour mass had to be ≥ 3cm in size. Ideally 4-12 cm lesions were preferred.

- Cystic and largely necrotic tissues ideally avoided.

- Lesions had to be away from pulsatility artefacts.

- Lesions of the lungs were in general excluded. Large lesions in lung ≥4cm were permitted provided they were away from large vessels and heart.

- Bony metastases were excluded unless they had a sizeable and clearly-defined soft tissue component.

- Liver lesions had to be > 3 cm and well defined. Liver lesions had preferably to be in the right hepatic lobe (the left lobe suffers from transmitted cardiac pulsations).

- Previously irradiated lesions could not be used as targets for DCE-MRI assessment.

Patient-specific factors made them ineligible for DCE-MRI assessment.

- Allergic reaction to MRI / CT contrast agents

- Patients with gross ascites as the dose calculation of contrast becomes difficult

- Medications which could potentially change vascular permeability or blood flow were kept at a constant level during until the primary end point.

3.2.7.2.   MRI image acquisition

MRI examinations were performed on either a 1.5T (tesla) Siemens Symphony scanner (©Siemens Medical System, Erlangen Germany) – MVCC or 1.5T Toshiba vantage Elan scanner (©Toshiba Medical Systems Europe) – Addenbrooke's. Target lesions to be assessed were predetermined from baseline CT imaging according to the suitability criteria as explained earlier in this chapter. Care was taken to position the patient in exactly the same position for subsequent scans.

Dedicated coils BO1-2 SP1-4 were used to obtain the images. Initial localiser and diagnostic T1- and T2-weighted were obtained through the tumour in coronal and axial planes followed by DWI and T2* images. Pre-bolus proton density–weighted and T1 gradient-echo sequences (TR 139ms, TE 4.76ms and flip angle of 70°) were then collected in the coronal – sagittal plane along the aorta followed by T2* weighted images collected along the same axis. Volume-interpolated breath-hold examination (VIBE) sequences were then acquired with dynamic T1-weighted images (TR 4.50ms, TE 1.42ms and flip angle of 3° and 21°) matched to the plane of proton density scans every 5 seconds (60 scans) for the purpose of T1 mapping (Parker, Suckling et al. 1997, Galbraith S M 2002) Intravenous gadoteric acid formed with gadolinium oxide and DOTA (2.5mmol/kg body weight Gd-DOTA, Guerbet) was injected at 4ml/s during the fifth acquisition point followed by a 20ml saline flush at 4ml/s. Post contrast T1 fat saturated images were collected with TR 227ms, TE 4.76ms and flip angle 70°. MR image acquisition sequence factors are detailed in table 4.2.

DOTAREM®

Gd-DOTA Meglumine (DOTAREM®) was used as the contrast agent for DCE-MRI scans. DOTAREM is a well-researched macrocyclic gadolinium based contrast agent with gadoteric acid as the active ingredient (MHRA 2002). DOTA has paramagnetic properties which increase the contrast enhancement in MRI. Distribution of gadoteric acid is within extracellular fluids of the body and does not bind to plasma albumin. This accounts for the use of DOTA in imaging of blood vessels. DOTA has been compared to the more established Gd-DTPA (Magnevist®) in mouse models. This has shown that DOTA is as safe and efficacious as Magnevist (Oudkerk, Sijens et al. 1995).

DOTAREM® has a good safety profile. The main side effect of concern is allergic reaction to the agent. Nephrogenic systemic fibrosis is a rare but a recognised complication of the contrast agent with higher risk associated with poor renal function. Hence renal function monitoring is of significant importance with use of Gd-DOTA.

Table 3.2   MR image acquisition sequences

Sequence	Imaging Plane	Breath Hold	TR (ms)	TE (ms)	Flip Angle (degrees)	Turbo / EPI factor	Averages	B values (s/mm2)	No. of Slices	Slice Thickness (mm)	Time of acquisition (Minutes)
T2 FSE	axial	Yes	3500	111		29	1		13	8	0.18
T1 GE	axial	Yes	139	4.76	70		1		13	8	0.14
T1 GE	Coronal	Yes	139	4.76	70		1		13	8	0.15
T2 FSE	Coronal	Yes	3220	111		29	1		13	8	0.17
T2 FSE	Coronal	Yes	2000	99		29	1		4	5	0.11
T1 GE	Coronal	Yes	138	4.76	70		1		4	5	0.15
T2 FSE	Coronal	Yes	2200	107		29	1		8	5	0.12
T1 GE (Dixon)	Coronal	Yes	170	4.92 / 2.22	70		1		8	5	0.14
Diffusion (epi)	Coronal	No	3100	60		192	6	0,25,50,100,250, 500,750	20	5	6.04
Diffusion (epi)	Coronal	No	2900	66		108	6	0,800	20	5	3.19
ISWI	Coronal	Yes(x8)	100	5,10,30, 45,60	25		1		8	5	1.08
3 degree VIBE	Coronal	Yes	4.5	1.42	3		3		14	5	0.12
21 degree VIBE	Coronal	Yes (x95)	4.5	1.42	21		1		14	5	10.32
T1 GE + fs	Coronal	Yes	227	4.76	70		1		14	5	0.19

GE–gradient echo sequence,

FSE–fast spin echo,

VIBE–volume interpolated breath-hold examination,

TR–repetition time,

TE–Echo

3.2.7.3. MRI data analysis

Quantitative parameter calculation from DCE-MRI images was performed using specialist MRI software (MRIW version 4.3, Institute of Cancer Research, London, UK) (James A D'Arcy, David Collins et al. 2006). The software is used under a research agreement between ICR and Paul Strickland Scanner Centre (at Mount Vernon).

Quantitative analysis required conversion of MR signal intensities to contrast concentration changes (Parker, Suckling et al. 1997). Individual DCE-MRI images were imported into MRIW® software and regions of interest (ROI) drawn on the T1-weighted subtraction images. ROI were drawn around the tumour by a single investigator and this was reviewed by a consultant radiologist experienced in analysing MR images. Images acquired in the coronal plane was used for delineation of ROI. Peripheral slices were discarded so as to avoid uncertainty of the MR parameters at the edge of the imaging fields. Up to eight central slices from the tumour were selected and ROI contoured. If movement artefact was noted, motion correction with the software was performed prior to ROI delineation.

Patient weight, volume of contrast infused and reference flip angles were all reviewed at this stage of image analysis. The reference flip angle was assessed by reviewing a known T1 value of fat which at 1.5T should be 300ms (Galbraith S M 2002). The Arterial Input Function (AIF) was assumed using the population mean (Parker, Roberts et al. 2006)

and extended Kety model was used in this assessment (Tofts 1997). Modelling- based quantitative analysis is discussed in chapter 1.0 (section 1.2.4) and calculations are discussed in the next section (3.2.7.4). Contrast concentration - time data obtained from the resultant calculation was reviewed to assess fitness to the model. Results from individual image slices were saved as .txt and .xml files for post processing. Post-processing of these .txt and .xml files was performed by Dr. N.J. Taylor to obtain the quantified values of the DCE – MRI imaging parameters.

3.2.7.4. Statistical consideration of DCE-MRI

3.2.7.4.1. Repeatability and reproducibility

Repeatability (of results of measurements): NIST definition for repeatability is as follows: "Closeness of the agreement between the results of successive measurements of the same measure and carried out under the same conditions of measurement" (nist.gov 1994). Conditions suggested by the definition are called repeatability conditions. These include:

1) Identical procedure being measured

2) Measurement done by the same instrument and conditions

3) Performed by the same observer at the same location

4) It also requires that the procedure is performed within a short time period

Quantitative expression of repeatability could be seen in the dispersion characteristic of the data. Data showing smaller dispersion is likely to increase the repeatability of the data. Methods to assess repeatability were developed by Bland and Altman (Altman DG 1983, Bland and Altman 1986, Bland and Altman 1996). The coefficient of repeatability (r) represents the value below which the absolute difference between two repeated test results may be expected to lie within a probability of 95%.

Reproducibility (of results of measurements):

Reproducibility of the tests describes the agreement between the same test results carried out under different conditions. This shows the ability of the test results to be replicated by another person or group working independently from the initial reporter (nist.gov 1994).

3.2.7.4.2. Calculation of repeatability with DCE-MRI

Classic repeatability is almost impossible to achieve with the definition above. We were unable to repeat the DCE-MRI scan on the same day due to the contrast injection which is required to collect the necessary data. Repeating the contrast on the same day risks affecting the renal function and hence must be avoided. A minimum of 24 h was needed for the contrast to be cleared from the system, hence DCE-MRI scan repeatability was performed on separate days, attempting to keep the other variables the same.

For each patient, the difference "d" between the two measurements of the parameter measured was calculated. The Shapiro-Wilk test is used to test "d" for normality. Kendall's tau is then calculated to test for a correlation of the absolute difference of "d" with the mean of the measurements. If the Shapiro-Wilk test indicates non-normal data, then the data was transformed using natural logarithms before the statistics were calculated. This returns the distribution to normal.

Once the data has been tested and transformed (if necessary), the following statistical

measures of reproducibility can be obtained from a one-way analysis of variance

(ANOVA): 95% confidence interval (CI) for change is calculated by equation 3.1:

Equation 3.1

$$CI = \pm \left[\frac{1.96 dSD}{\sqrt{n}} \right]$$

n= number of patients.

dSD = Mean squared difference in a group of n $dSD = \left(\frac{\Sigma d^2}{n} \right)$

Any change in a group of n greater than this value would be significant at the 5% level,

and is presented as a percentage of the overall mean.

The within patient standard deviation (wSD) is derived from the dSD using equation

3.2:

Equation 3.2:

$$wSD = \frac{dSD}{\sqrt{2}}$$

Within patient coefficient of variation wCV using equation 3.3.

Equation 3.3

$$wCV = \frac{wSD}{\text{overall mean of the parameter}}$$

The repeatability of a parameter, r for an individual patient is given by equation 3.4.

Equation 3.4

$$r = 2.77wSD$$

or

$$r = 1.96dSD$$

The r value, and more usefully, r as a % of the mean value, was used to define the 95% confidence intervals for a real change. Excel Spreadsheets were used for calculating all the individual patients' percentage changes.

Cohort data

Patients were grouped into three treatment cohorts. These cohorts are a subset of the study patients, and to work out if the mean change for all the patients in a cohort is significant, 95% confidence intervals for the relevant number of patients in the cohort were used. With the reproducibility spreadsheet, required values were calculated by changing the number of patients.

3.2.8. Statistical consideration and analytical plan

3.2.8.1.   Primary variable

The primary efficacy endpoint for a subject was DCE-MRI-defined changes in K^{trans} from baseline to after 6 weeks of bevacizumab monotherapy or bevacizumab and low or standard dose interferon-α2a combination therapy.

3.2.8.2.   Secondary variables

3.2.8.2.1.   Vascular endpoint

- Change in vascular permeability (K^{trans}) from baseline to 2, and 6 weeks post commencement of bevacizumab

- Correlation of DCE-MRI defined changes in K^{trans} with clinical benefit and symptoms

- Correlation of DCE-MRI defined changes in K^{trans} with surrogate biomarkers

3.2.8.2.2.   Efficacy endpoints

- Progression-free survival (PFS)

- Comparison of PFS with MRI parameters

- Overall response

Progression-free survival: was defined as the time in days from the date of randomization to the date of the first event. Progression events considered were:

−   progression during or after treatment for subjects who had stable disease or no response

−   progression during or after treatment for subjects with partial response

−   relapse for subjects with a complete response (CR)

−   death from any cause

Subjects who had not experienced an event at the data cut-off date were censored at the last date of disease assessment. For composite endpoints, the earliest date of all available individual censoring times was used.

Comparison of PFS was performed between the treatment arms and also with the MRI-derived vascular parameters.

3.2.8.2.3. Safety endpoints

Safety end points reviewed were as below. These were assessed, reviewed independently and reported with descriptive statistics:

- Treatment duration of bevacizumab and IFN

- treatment withdrawal

- dose modification

- Incidence of adverse events (worst grade)

3.2.8.2.4. Exploratory endpoints

Exploratory end points included measurement of other surrogate biomarker analysis from peripheral blood analysis of circulating endothelial cells (CEC), circulating endothelial progenitors (CEPC), and pro-angiogenic monocytic cells.

Diffusion MRI and BOLD MRI images were also acquired during screening, treatment phase and follow-up phase.

3.2.9. Statistical model

3.2.9.1.　　　Sample size and power calculation

Effective analysis of a randomised control trial prerequisites careful determination of

the power function and determination of the sample size and effect size. Components

required for a sample size calculation includes

1. Type 1 error (α) – which denotes the chance of a false positive result

2. Type 2 error (β) – which denotes the chance of a false negative result

3. Power (1- β) – assesses the probability of detecting a statistically significant

   difference when a specified difference between group exist

4. Effect size – minimal difference between groups that is clinically plausible

5. Variance – Variability of outcome measures expressed as standard deviation

   of a continuous outcome.

Certain variables are assumed in the statistical consideration of a randomised control

trial based on general acceptance for calculation of sample size/effect size. Type 1

error (α) is usually fixed at 0.05 which limits the chance of a false positive conclusion

to <5%. It is also possible that the outcomes draw a false negative conclusion (β).

Conventionally this is set to 20%. The Power (1- β) of a study is set to reflect the ability

to identify 80% chance a true effect that is present in the sample. General variance in

the population for a given variable is expressed as its standard deviation. This is usually

an unknown quantity and hence could be estimated from a previous pilot study.

Finally, effect of interest is regarded as the minimal difference which is likely to be

clinically significant and be reliably detected. In a given randomised control trial, if the

sample size is already fixed based on availability, the effect size that would determine

a real effect could be determined by power calculation.

In this trial, decisions regarding power calculations were based on a trial design in

which there are 3 arms; A) Bevacizumab, B) Bevacizumab + 3MU Interferon, C)

Bevacizumab + 3mu rising to +9mu after 2/52 Interferon. Sample size was restricted

to a total of n=30 according to the IMP availability for the trial. It was hence decided

that there will be 10 patients in each arm of the study. Patients are scanned 2x pre-

treatment, 1x at 2/52, and 1x at 6/52. The primary aim of the study is to determine

the extent to which changes in K^{trans} differ between the arms of the study. In order to

assess the statistical significance of the outcome, previously collected DCE-MRI data

from Paul Strickland Scanner Centre for change in K^{trans} was used.

To assess changes in K^{trans} from before to after treatment: We assumed a two-sided

paired test, with α=0.05. From previously-collected data at the Paul Strickland

Scanner Centre, we estimated that the standard deviation of the change in K^{trans} from

before to after treatment to be 0.128. For 1-β=0.80, a change in K^{trans} of 0.128 will be

reliably detectable. The power function is provided in figure 3.2.

Figure 3.2   Power function Ktrans before and after treatment

For two-sided paired test, assuming α=0.05, 1-β=0.80, and the standard deviation of

the change to be 0.128.
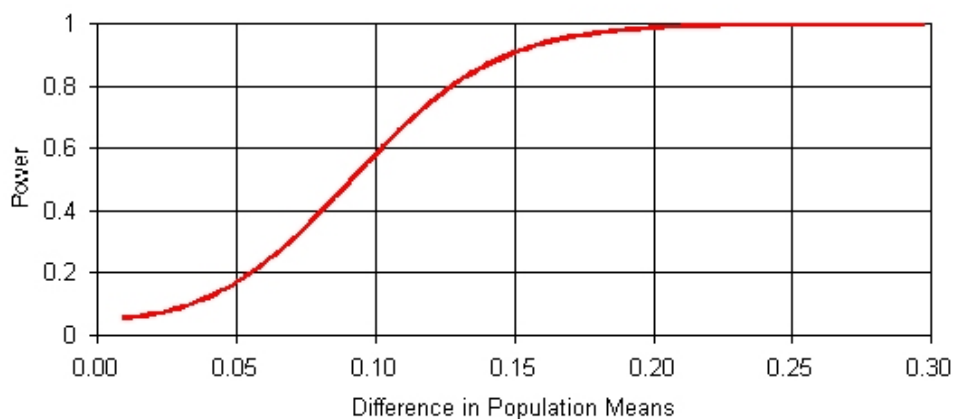
Comparisons between treatment arms:

 Comparisons were made between the treatment arms at week 2 and week 6. At week

2, the two interferon arms have been treated the same, giving an allocation ratio of

2:1. Assuming two-sided independent test with α=0.05 and 1-β=0.80, a difference in

K^{trans} of 0.144 will be reliably detectable. Similarly, at the third follow-up where

treatment allocation is equal, a difference in K^{trans} of 0.170 will be reliably detectable.

The power functions can be observed in Figures 3.3 and 3.4.

Observation of changes in K^{trans} between these treatment groups has not been

observed before, so the size of the effects to be observed was unknown. The data

collected hence should provide a robust estimate of the effect size, providing valuable

data upon which to base future studies.

Figure 3.3   Power function - K^{trans} between treatment arms at week2
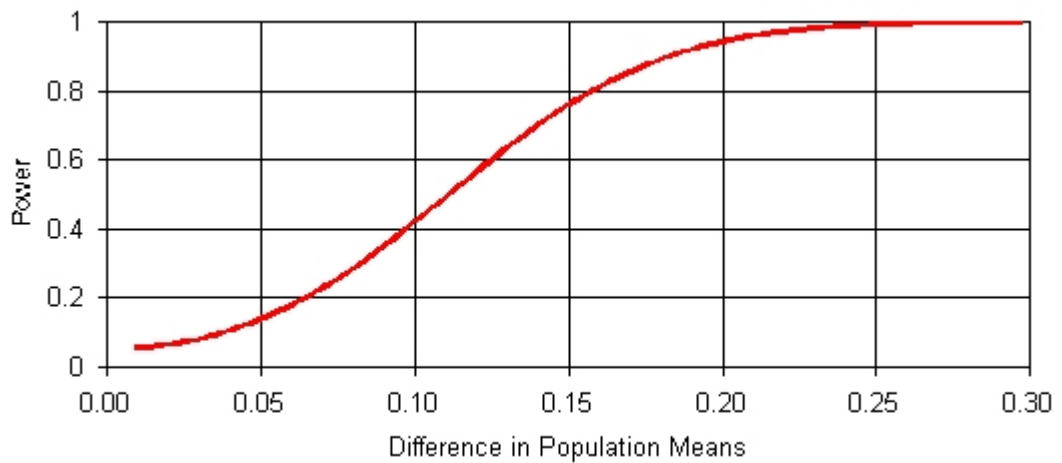
At week 2, Arm B and C are considered together giving a randomisation of 2:1

For a two sided independent test,

Total n=30 with an allocation of 2:1 between two groups

α = 0.05 and Power (1- β) = 0.8

Standard Deviation of variance = 0.128

Detectable change in K^{trans} = 0.144

Figure 3.4   Power function - K^{trans} between treatment arms at week6
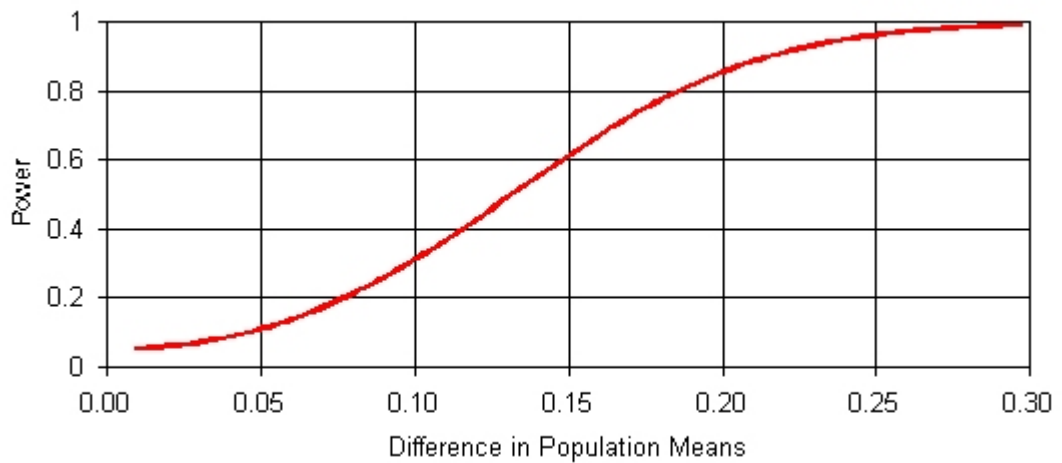
At week 6, we have equal randomisation for all 3 arms.

For a two sided independent test

n = 10 in each group with a 1:1:1 randomisation

α = 0.05 (<5% chance of the results to be false positive)

Power (1- β) = 0.8 (80% chance that the effect is true)

Standard Deviation of variance = 0.128

Detectable change in K^{trans} = 0.170

3.2.9.2. Analysis of DCE-MRI vascular endpoint

The primary objective of the study was to characterise bevacizumab-induced changes in K^{trans}, and any IFN dose response in potentiating bevacizumab induced changes in this vascular parameter. Given the limited sample size the analyses focuses on estimating the magnitude of changes in K^{trans} in each arm of the study. There are two sets of analyses, the first comparing the bevacizumab only arm to the other two arms at 2 weeks follow up (where the INF treated patients have had the same dose), and the second comparing changes in K^{trans} between all three arms of the study specifically to determine if an IFN dose response exists (e.g. between the IFN treated arms). Before-to-after comparisons within each arm were evaluated using paired comparisons (either a paired t-test or a non-parametric test where appropriate), and aimed to characterise the magnitude of the change in each arm with confidence intervals. Comparison between the groups focuses on determining whether the change in K^{trans} differs between the arms was evaluated using independent group tests (either an independent t-test or a non-parametric test where appropriate) and the magnitude of the changes in K^{trans} in each arm estimated with confidence intervals.

3.2.9.3.   Efficacy analysis

Efficacy analysis was based on the intent-to-treat population defined as all randomized subjects who receive at least one dose of bevacizumab. The end points are defined as:

Progression-free survival (PFS)

Comparison of PFS with MRI parameters.

Response rate

As the sample size is relatively small, power is limited for these analyses and interpretation of the outcomes of the analysis will focus on defining confidence intervals.

PFS (as defined in section 3.2.8.2.2) was determined for each patient in days, allowing the survival functions to be estimated from continuous time. Analysis for end point, progression-free survival, followed the same scheme. The survival function for patients in each of the three arms were estimated using the Kaplan-Meier method, and comparison of survival evaluated using the log-rank test.

Spearman correlation was used to ascertain the correlation of PFS to the different MRI parameters K^{trans}, K_{ep}, V_e and $IAUGC_{60}$.

Treatment response of tumours were defined according to the RECIST criteria. The analysis evaluated the extent to which different proportions of patients fall into each response category across different treatment conditions using an appropriate test for proportions (χ^2), which is reported with confidence intervals. As response was determined early after the onset of treatment, comparisons were performed between the bevacizumab arm and the two bevacizumab + interferon-α2a arms.

3.3. CT response assessment combining reduction in size and arterial enhancement in metastatic RCC patients treated with targeted therapy

3.3.1. Materials and methods

3.3.1.1. Patient selection

Patients with metastatic clear cell RCC, who started treatment with multi-targeted tyrosine kinase inhibitors (TKI's), were the target group in this study. All patients selected were enrolled in either one of two clinical trials, a phase II clinical trial (Eudract 2006-002455-33) receiving Cediranib (a mult-targeted tyrosine kinase inhibitor) or an expanded access study (Eudract 2005-002097-30) of Sunitinib (mult-targeted tyrosine kinase inhibitor).

These patients were recruited into the above-mentioned trials between November 2005 and February 2008 at Mount Vernon Cancer Centre. All patients selected had good or intermediate prognosis according to Motzer score (Motzer, Bander et al. 1996, Motzer, Bacik et al. 2002) and had good performance status (PS 0-1) (ECOG-ACRIN 1982, Oken, Creech et al. 1982). Patients from this cohort who continued on study drug until progressive disease, unacceptable toxicity or withdrawal of consent were selected for this retrospective analysis.

3.3.1.2. Inclusion criteria

1. Metastatic RCC with no previous exposure to anti-angiogenic TKI

2. Patients started on anti-angiogenic tyrosine kinase inhibitors

3. Baseline contrast enhanced CT staging scan within 4 weeks of treatment initiation

4. Measurable disease according to RECIST criteria

3.3.1.3. Exclusion criteria

1. Previous exposure to tyrosine kinase inhibitors

2. Non-contrast enhanced CT scan either at baseline or at response assessment

3. Patients who stopped treatment due to toxicities rather than disease progression

Patients with impaired renal function or allergies that precluded a contrast enhanced CT scan were excluded from this study. Patients who stopped treatment because of toxicities rather than progression of their disease were also excluded from analysis as we wished to correlate imaging features with time to progression of disease whilst on treatment.

3.3.1.4. Radiological assessment

All patients had a contrast enhanced staging CT scan at baseline performed within 4 weeks of initiation of treatment and had a response assessment CT scan at twelve weeks after initiation of treatment.

CT scanning was performed with a multi detector CT (Siemens Sensation 16®, Siemens Medical Solutions, Forccheim, Germany). Iodinated contrast agent (Optiray®, Covidien Healthcare, Mansfield, MA, USA) was used as the contrast agent. The contrast agent was injected with a pump injector at the rate of 4ml/sec and followed by saline. A dose of 100ml of the contrast was used (350mg/ml) which is the standard protocol in our institution. Imaging was performed at both arterial and portal venous phase. Arterial phase imaging was acquired with a 25sec delay and images captured from supraclavicular fossa to the iliac crest. Portal venous phase imaging was performed to image abdomen and pelvis from dome of diaphragm to the pubis with a delay of 70sec from injection.

In our institution, this has been the standard imaging protocol. The advantage of this approach is that it enables capture of early enhancement as seen with highly vascular tumours as RCC (Raptopoulos, Blake et al. 2001, Lee, Heiken et al. 2005).

3.3.1.5.   Radiological data analysis

All CTs (baseline and 12-week scan) were analysed. Target lesions were selected in each patient using the baseline scan. The size of the target lesions was recorded in centimetres (cm) and the sum of the target lesion size, where multiple target lesions were present, was calculated as per RECIST criteria. Total change in the sum of the target lesion size before and after treatment in cm and the percentage change compared to the baseline were calculated.

To calculate the change in enhancement, target lesions were delineated from the surrounding tissue by manual assessment and a region of interest (ROI) was identified by the investigator. Care was taken to ensure the ROI included the entire visible tumour (Goh, Halligan et al. 2008). ROI was cross-checked by an experienced radiology consultant. Hounsfield unit (HU) density at the arterial phase of enhancement was recorded in each ROI and mean enhancement at baseline and twelve-week scan and change in enhancement between the scans were calculated. Percentage change in mean enhancement was noted.

3.3.1.6.   Response assessment

Patients were assigned to progressive disease (PD), stable disease (SD) or partial response (PR) using each of the following criteria: RECIST, Choi and "modified Choi"

RECIST criteria - mandates a 30% decrease in the size of sum of longest diameters of the target lesions for a partial response (PR) and a 20% increase in size of sum of longest diameters of the target lesions for progressive disease (PD). Changes less than a 30% reduction in size or a 20% increase in size are assigned as stable disease (SD). Choi criteria require either a 10% reduction in size or a 15% decrease in the density of target tumours for a PR.

With the modified Choi Criteria, it was mandated that both the 10% decrease in size and 15% decrease in enhancement in arterial phase were required to amount for a partial response (PR). If only one factor was present it was categorised as stable disease (SD). Please see Chapter 5.0 section 5.1.3 for further details.

3.3.1.7.   Clinical data

The gold standard method of assessing benefit of cancer drugs is to measure the overall survival (OS) data, where death of patients constitutes the endpoint. As more and more active agents are now available, cancers are being treated with multiple lines of treatment. Serial therapies may potentially confound the benefit derived by a single treatment. This also requires a long period of follow up. The use of time to disease progression (TTP) as a surrogate has been evaluated (Zhuang, Xiu et al. 2009). It has been suggested that TTP and progression free survival (PFS) could be used as an effective surrogate to measure treatment effectiveness. TTP directly measures the treatment effect of the drug and is not confounded by subsequent treatments or non-cancer related deaths.

For the present study, we selected time to disease progression (TTP) as the clinical end point as this clearly demonstrates the duration of therapeutic response. TTP was defined as the time from the time period in days from the start of systemic therapy with the planned tyrosine kinase agent to the date where disease progression was documented radiologically. The clinical records for individual patients were obtained and analysed. The date of the baseline CT scan and initiation of the therapy were noted. All patients had a clinic visit at least every 6 weeks and had CT scans performed for response assessment every 3 months during their follow up. Each of the follow up CT scans was examined and status of the disease was analysed. The date disease progression was reconfirmed.

The date of stopping the systemic therapy was also reviewed analysed to confirm that

therapy was stopped due to disease progression or lack of clinical benefit rather than

due to toxicity.

TTP was defined as the number of days measured from the start of therapy to the day

in which progression was confirmed by standard RECIST radiological criteria. In order

to compare the three response criteria, individual patients were assigned to either the

SD or PR groups defined by each of the three response criteria. The clinical data was

then correlated with each of the criteria in further statistical analysis described here

with results detailed in chapter 5.0.

3.3.2. Statistical analysis

Post categorisation to PR and SD groups with each of the criteria, SPSS software was used in the statistical analysis (SPSS v 16.0 copyright © SPSS inc1989-2007). In analysing time to progression data for PR and SD groups of different criterion and in calculating the statistical significance, the options were to calculate the mean time to progression and use a non-parametric test as Mann-Whitney U test to analyse the significance of difference between groups. We also considered plotting the Kaplan-Meier curve for TTP data, calculating median TTP from the curve and using log rank test to determine the significance (p-value). As the study involved analysing time to event data, the second method was chosen in analysis. Kaplan-Meier survival curves were plotted for PR and SD groups for each response criteria. Median TTP with 95% confidence intervals was calculated from the Kaplan-Meier curves. Median TTP was correlated with the SD and PR classifications for the three response assessment criteria. Log rank test was used to assess the significance of differences obtained in the analysis. Additionally, a scatter plot was created plotting size change against density change with data grouped into TTP <100 days, 100-199 days, 200-399 days and >400 days. The scatter plot enabled an exploratory analysis of alternative thresholds for response other than those defined by the response criteria discussed above.

3.4. CT texture as a potential biomarker of response

This section describes the methods used for a retrospective analysis where response assessment for metastatic RCC treated with anti-angiogenic tyrosine kinase inhibitors was correlated to textural analysis based on contrast enhanced CT scan. The study background and its results are explained in chapter 6.0 of this thesis.

3.4.1. Materials and methods

3.4.1.1. Clinical assessments

Patients with metastatic RCC treated with TKIs at our institution (Mount Vernon Cancer Centre) from 2005 to 2009 were identified retrospectively from the clinical database. Institutional review board waiver was obtained for this retrospective analysis. Patients were selected from the database for the analysis based on a pre-planned inclusion and exclusion criteria.

3.4.1.1.1. Inclusion criteria

1. TKI naïve patients receiving TKI as first or second line treatment for metastatic renal cell carcinoma.

2. Baseline contrast enhanced CT within 4 weeks of treatment commencement.

3. Contrast enhanced CT following treatment to assess response.

3.4.1.1.2. Exclusion criteria

1. Contraindications to contrast enhanced CT. These included:

    a. Hypersensitivity reaction to iodinated contrast.

    b. Renal impairment - Serum creatinine >120 µmol.

2. Failure of intravenous cannulation resulting in non-contrast CT scan.

3. Suboptimal contrast enhancement (aortic enhancement <200 HU at 25s).

Individual patient notes and pathological reports were analysed in detail to collect clinical details. Histological details of the tumour including histological variants, Fuhrman grade, and presence of necrosis or sarcomatoid elements were noted from the pathology report. Clinical characteristic at diagnosis, details of treatment and follow up were collected from patient's clinical notes and clinic letters. Details collected included:

1. Patient demographics

2. Date of diagnosis

3. Risk criteria according to Motzer criteria (Motzer, Mazumdar et al. 1999)

4. Previous treatment details if applicable

5. Current treatment regime

6. Start date of current treatment regime

7. Stop date where current treatment regime was discontinued

8. Best response obtained with the current treatment regime

9. Time to progression

Time to progression of the disease (TTP) was calculated as the number of days from beginning of current systemic treatment to the time progression of disease was noted, either by radiology according to RECIST criteria, or if there was definite clinical evidence of disease progression.

3.4.1.2.   Radiological assessments

All patients had contrast enhanced CT scans prior to initiation of treatment. This is the standard policy of our institution. A mandatory cut off of 4 weeks has been used to make sure that all patients have had a recent imaging done. Patients who did not have baseline imaging within 4 weeks prior to initiation of treatment were excluded from this study. This created a quality control where treatment response can be effectively analyzed. Follow up CT scans were performed after 2 cycles of treatment, which was performed between week 10 and 12 of initiation of treatment.

All patients had contrast enhanced multi detector CT scans (Somatom Definition or Sensation 16, Seimens Healthcare, Forchheim Germany). Iodinated contrast agent (Optiray 350, Covedien Healthcare, Mansfield, MA, USA) was used as the contrast agent.

100ml of 350mg/ml concentration agent was injected followed by a 50ml saline flush injected via a pump at 4ml/sec. Arterial phase enhancement imaging were collected for thorax and upper abdomen (supraclavicular fossa to top of iliac crest) and porto-venous phase enhancement imaging was used further to image abdomen and pelvis (dome of diaphragm to pubis). Arterial phase enhancement images were collected at 25sec delay and porto-venous phase images were collected at 70 sec delay. This is the standard imaging protocol for our institution.

Acquisition parameters for the CT scan included:

- 120kV

- Effective mAs 150 – thorax

- Effective mAs 200 – abdomen and pelvis

- Dose modulation positive

- Pitch - 1.2

- Detector configuration - 24x1.2mm

- Slice collimation – 3mm

- Scan field of view – 300-450mm

- Matrix – 512mm

Target lesions were identified and defined on baseline scan as per RECIST criteria 1.1 (5 target lesions with maximum 2 per organ)(Patrick Therasse, Richard S. Kaplan et al. 2000, Eisenhauer, Therasse et al. 2009). Target lesions were delineated by drawing ROI around the target lesion to encompass the lesion completely. Once ROI was drawn, this was cross checked by a consultant oncology radiologist with more than 10 years of experience in treatment response assessment of cancer patients.

Size of each target lesions were calculated separately as the largest unidimensional measurement and total sum of the size of target lesions calculated. Enhancement in aorta was calculated initially to make sure that there is optimal enahcement. Aortic enhancement of <200 HU was defined as suboptimal. Enhancement in each pixel inside the ROI is calculated by the standard CT imaging software and average enhancement was calculated. Post treatment contrast enhanced CT scan, was reviewed to assess treatment response. ROI was drawn around the same target lesions used in baseline scan. The largest unidimensional diameter noted for all target lesions and mean density in HU is calculated for all lesions. Treatment response was evaluated by RECIST, Choi and modified Choi criteria. Patients are classified according to the response obtained as stable disease (SD), partial response (PR) and progressive disease (PD) by each criteria separately. Images from pre and post treatment scans were anonymysed before it was transferred for textural analysis.

3.4.2. Textural analysis

Textural analysis was performed with a software TexRad® assessing arterial phase images. TexRAD® is a computer program that has been developed by researchers of the University of Sussex and Brighton (Ganeshan.B, Miles.K). Algorithm for TexRAD® was

Initially formed and developed in MATLAB (technical computing language, Mathworks Inc, Natick, USA) as a research prototype. This was further developed as a standalone prototype for clinical analysis and assessed in different tumour types. Founders of TexRAD® eventually entered into a partnership with Miles Medical Pt Limited and Cambridge Computing Imaging Limited and Imaging equipment limited to form TexRAD limited. This technique comprised of an initial filtration step using Laplacian of Gaussian (LoG) spatial band-pass filter to selectively extract features of different sizes and intensity.

Textural analysis comprises of two main stages:

1. Image filtration

2. Quantification of texture

3.4.2.1. Image filtration

The first step of analysis is image filtration. Filtration technique with Laplacian of Gaussian (LoG) spatial band-pass filter was chosen to selectively extract features with different sizes and intensity. Laplacian of Gaussian technique is one of the first and also most common methods to detect regions in a digital image that differ in properties. At first second order (2 dimensional) Gaussian distribution (G) of the image was calculated. The following equation (3.5) was used for this calculation:

Equation 3.5:

$$G(x, y) = \mathrm{e}^{-\frac{x^2 + y^2}{2\sigma^2}}$$

"G" – Gaussian distribution
"x" and *"y" are co-ordinates of the image matrix.*
"σ" - Standard deviation of the Gaussian distribution.

Calculation of two-dimensional Gaussian distribution of the image results in selection of parts of the image according to the sigma of Gaussian distribution. Areas of image which are smaller than the sigma of Gaussian distribution are effectively blurred and wiped out. Thus the Gaussian distribution consistent with a particular σ value allows to accent textural features of a particular scale on contrast agent-enhanced CT images. This filtration technique was used in this study to filter out textural features of varying scale: fine scale enhances parenchyma, while medium or coarse scale enhances blood vessels.

Use of Laplacian (∇^2) of Gaussian was selected as it provides one of the most isotropic output with less burden on the computational resources. Laplacian is useful in assessing areas of rapid intensity changes in the image. These areas could represent zero crossing of the filter. After filtration, negative value pixels are given a value of zero. Equation 3.6 is used to compute the Laplacian of Gaussian filter (∇^2G).

Equation 3.6:

$$\nabla^2 G(x, y) = \frac{-1}{\pi\sigma^4}\left(1 - \frac{x^2 + y^2}{2\sigma^2}\right)e^{\left(\frac{x^2+y^2}{2\sigma^2}\right)}$$

Assessing the above-described equation with different σ values can give a measure of the width of the filter in pixel values. This represents the diametric opposite areas where zero is crossed in this circularly symmetric filter. Sigma σ value seems to be directly proportional to the bandwidth of the filter in the spatial domain and inversely proportional to the pass-band region of the filter in the frequency domain. Thus smaller σ sigma value results in a smaller filter width of the cancer and thus highlighting finer details. Conversely, a higher sigma value will result in higher σ, which will be used to assess coarse features in the image.

Though filtration can be performed either in spatial domain or in frequency domain, we selected to apply filter in the frequency domain for this study. This is due to the fact that filtration in spatial domain, involves intense computation. Quantization errors are also known to be more when using filtration in spatial domain. This is more

so in using small σ values. It is hence more efficacious to use the frequency domain

and image in spatial domain can be achieved with inverse Fourier transformation of

the filtered spectrum (Chen, Crownover et al. 1999).

3.4.2.2.   Quantification of texture

For quantification of texture, ROIs were initially delineated around the target lesions by an investigator. Once ROI of all target lesions were defined, this was assessed by a consultant oncological radiologist with more than 10-year experience in assessing treatment response in oncology patients. ROI was further refined by exclusion of areas with air. This was performed with a thresholding procedure that removed any pixels with attenuation values less than -50HU.

Same patient specific ROI was used for texture analysis of different σ values. For this study we selected filter parameters between 1.0 and 2.5. 1.0 will hence indicate fine texture and 2.5 indicating coarse texture. Values between 1.0 and 2.5 (1.5, 1.8 and 2.0) will represent medium texture. Any pixels with a negative value were given a value of zero. By using mathematical equations, heterogeneity within this ROI was quantified. Heterogeneity was calculated with and without image filtration by estimating the entropy (irregularity, e) as per equation 3.7 and uniformity (distribution of gray level, u) as according to equation 3.8. Both equations are described below.

Equation 3.7:

$$e = -\sum_{l=1}^{k}[p(l)\,log_2[p(l)]$$

Equation – 3.8:

$$u = \sum_{l=1}^{k}[p(l)]^2$$

e = entropy
u = uniformity
l is the pixel value (between *l* =1 to *k*) in the the ROI and
p(l) the probability of the occurrence of that pixel value.

Heterogeneity is represented by values of higher entropy and lower uniformity (Ng, Kozarski et al. 2013). Entropy and uniformity were recorded for absolute scale values for each patient's tumor on the baseline CT and CT following 2 cycles of treatment. Percentage change in image entropy and uniformity were also recorded.

3.4.3. Statistical analysis.

Individual patient data from baseline and treatment response scan were assessed to ascertain the average textural measurements. Percentage change from baseline was used here for statistical analysis. Statistical analysis was performed using (SPSS version 17.0. 2008, SPSS Statistics for Windows Chicago: SPSS Inc. and also MedCalc for Windows, version 9.2.0.0; Medcalc, Mariakerke, Belgium). The ability of texture parameters to predict for TTP was assessed by Kaplan-Meier analysis. The relationship between textural analysis, RECIST, Choi and modified Choi criteria was assessed. Receiver Operating Characteristic (ROC) curve was used to analyse the threshold values of the textural analysis. The area under the ROC curve was recorded and the point on the ROC curve furthest from the line of discrimination was considered as the optimum threshold. Non-parametric log rank test was utilized to evaluate the differences between Kaplan Meier curves for PR, SD, and PD. Statistical significance was set at 5%. In order to determine independent predictors of time to progression, Cox regression analysis was performed with all significant parameters.

Chapter 4.

DCE-MRI assessment of Vascular changes induced with bevacizumab with or without interferon-α2a in advanced renal cell carcinoma

4.1.   Introduction

In this chapter, I discuss the background and results of a prospective clinical trial to explore whether addition of interferon enhances the anti-angiogenic effect of bevacizumab in advanced RCC patients measured by changes in vascular parameters of dynamic contrast enhanced MRI scan (DCE-MRI). The methods employed in this study is detailed previously in Chapter 3 Section 3.2. This was a prospective open labelled randomised multi-centric clinical trial. I was the co-ordinating investigator of the trial involved in the set-up, day to day running and analysis of the study.

Treatment of advanced RCC has changed significantly since the introduction of agents that target angiogenesis and growth factor signalling. With the improved knowledge of the pathophysiology of RCC as explained in Chapter 1 Section 1.1, multiple agents have been found to have efficacy in controlling RCC and has received regulatory body approval. These include multi-targeted tyrosine kinase inhibitors as sunitinib (Motzer, Hutson et al. 2007), sorafenib (Escudier, Eisen et al. 2009), pazopanib (Motzer, Hutson et al. 2013) and recombinant humanized monoclonal antibody bevacizumab in combination with interferon-α2a (Escudier, Pluzanska et al. 2007).

4.1.1. Bevacizumab +IFN in treatment of advanced renal cell carcinoma.

Role of bevacizumab and interferon-α2a in management of advanced RCC is discussed in chapter 1.0 of this thesis. Interferon-α2a is known to have therapeutic benefit in treatment of RCC with modest survival advantage benefitting a small proportion of patients exposed to it.

A three-arm randomised-phase II study in RCC with bevacizumab at a dose of 3 or 10mg/kg every 2 weeks vs. placebo demonstrated a 10% response rate and a statistically significant improvement in progression-free survival (2.5 months to 4.8 months) in patients who received high-dose bevacizumab (Yang, Haworth et al. 2003).

The interim results of the AVOREN study, a double blind, placebo-controlled randomised study of bevacizumab + IFN versus IFN, demonstrated an improvement in median PFS from 5.4 months in the IFN alone arm to 10.2 months in the combination arm (HR 0.63, p<0.0001) (Escudier, Pluzanska et al. 2007). In addition, an interim analysis from a North American study with a similar design to AVOREN showed a benefit of bevacizumab in combination with IFN over IFN alone for both progression free-survival (HR= 0.71, p<0.0001), and overall response rates (25.5% vs. 13%, respectively, p<0.0001) (Rini, Halabi et al. 2008).

Based upon the results of the AVOREN study, the EMEA granted the following licence in December 2007: "Avastin in combination with interferon alfa-2a is indicated for first line treatment of patients with advanced and/or metastatic renal cell cancer."

As there was no single agent bevacizumab arm in the AVOREN study, it is unknown what degree of additional antiangiogenic activity is provided by the addition of IFN to bevacizumab. IFN has anti-angiogenic activity (von Marschall, Scholz et al. 2003) and it is therefore possible that there is an additive or synergistic effect of IFN and bevacizumab on tumour vasculature. It is also unknown what dose of IFN is required to do so.

Data from two independent studies suggest that the combination of an angiogenesis inhibitor and lower dose IFN may be as effective as standard dosing of IFN. As part of the AVOREN study, the protocol allowed dose reduction in the event of grade 3 IFN-attributable adverse events (AEs). A retrospective sub-group analysis of patients who received reduced doses of IFN in combination with bevacizumab compared to those patients that had no dose reduction was equivalent for both progression-free survival and response rates (Melichar, Koralewski et al. 2008). Prospective data from a randomised phase II study comparing sorafenib in combination with either standard dose (9MiU tiw) or low dose (3MiU tiw) IFN, demonstrated similar outcomes in terms of progression free survival and overall clinical benefit (Bracarda, Porta et al. 2013).

This study aims to address the important question whether IFN confers an additional anti-vascular effect to that seen with bevacizumab and if so, to identify the dose of IFN required.

4.1.2. DCE-MRI in monitoring anti-angiogenic therapy in humans

DCE-MRI is one of the most researched and validated MRI-based techniques targeted to use as a biomarker for angiogenesis. Several studies involving the use of DCE-MRI to assess anti-vascular therapies have been reported, including three Phase I studies involving combretastatin A4 phosphate (CA4P) (Dowlati, Robertson et al. 2002, Galbraith, Maxwell et al. 2003, Stevenson, Rosen et al. 2003, Nathan, Zweifel et al. 2012). These results revealed variability in DCE-MRI measured tumour response to differing doses of CA4P and furthermore also revealed marked intra-tumoural heterogeneity of vascular response. Another study investigating the effect of dose escalation of PTK787 on metastatic colorectal cancer reported that the authors were able to generate a dose response curve comparing the drug area under the curve exposure to the vascular inhibitory effect (Morgan, Thomas et al. 2003). Use of DCE-MRI in monitoring physiological responses for dose findings could be a potentially important aspect when evaluating agents with minimal systemic toxicities.

DCE-MRI has also been used in studies to assess effectively the antiangiogenic effects of bevacizumab, in combination with other agents, in a variety of malignancies

including locally advanced breast cancer, ovarian cancer and glioblastoma (Wedam, Low et al. 2006, Hsu, Ferl et al. 2013).

As discussed in chapter 2.0, there is limited published data on the use of DCE-MRI in assessing responses to vascular targeted therapies in RCC. In a Phase II study involving sorafenib, patients from one institution underwent DCE-MRI before and after the start of therapy. Interestingly in this group, not only were large reductions seen in the K^{trans} values but also an association was observed between initial tumour K^{trans} and time to tumour progression. A second phase 2 study published at about the same time showed good correlation of high baseline K^{trans} with better PFS (Flaherty, Rosen et al. 2008) (Hahn, Yang et al. 2008).

4.2. Ethics committee and MHRA approval

The planned study was submitted for approval of both National Research Ethics Committee, and Medicines and Health Regulatory Authority (MHRA). Version-controlled documents of Protocol, Patient information sheet (Appendix - 9.5), Informed consent form (Appendix – 9.6.), GP letter, patient diary card, peer review reports were reviewed by the ethics committee and favourable approval was received after minor amendment of the Patient information sheet. Local research and ethics committee, and Research and Development approval were also needed at individual sites prior to recruitment of patients at that Centre. As the trial included use of bevacizumab and interferon-α2a, approval from MHRA was also obtained.

4.3. Objectives

4.3.1. Primary Objective

The primary objectives of the study are:

1. To establish whether bevacizumab-induced changes in DCE-MRI vascular parameters are significantly enhanced by the addition of interferon-α2a. And if so:

2. To establish whether there is an interferon-α2a dose response in potentiating bevacizumab induced changes in DCE-MRI vascular parameters.

4.3.2. Secondary Objectives

1. To correlate changes in DCE-MRI vascular parameters for each treatment group with the following:

    a. Progression-free survival

    b. Tumour response and changes in tumour size

    c. Other surrogate biomarkers

2. To assess the degree of change in baseline K^{trans} within each arm of treatment.

3. To investigate changes in diffusion and BOLD MRI and their correlation with other pharmaco-dynamic endpoints.

4. To assess the efficacy and safety profile of bevacizumab monotherapy or in combination with low or standard doses of IFN

4.4. Study design and assessments

This was a prospective multi-centric randomised open labelled phase 2 clinical trial.

The trial schema is as follows. The methods including planned analysis and statistical

consideration is detailed in Chapter 3.0 Section 3.2

Figure 4.1   Flow chart of trial protocol
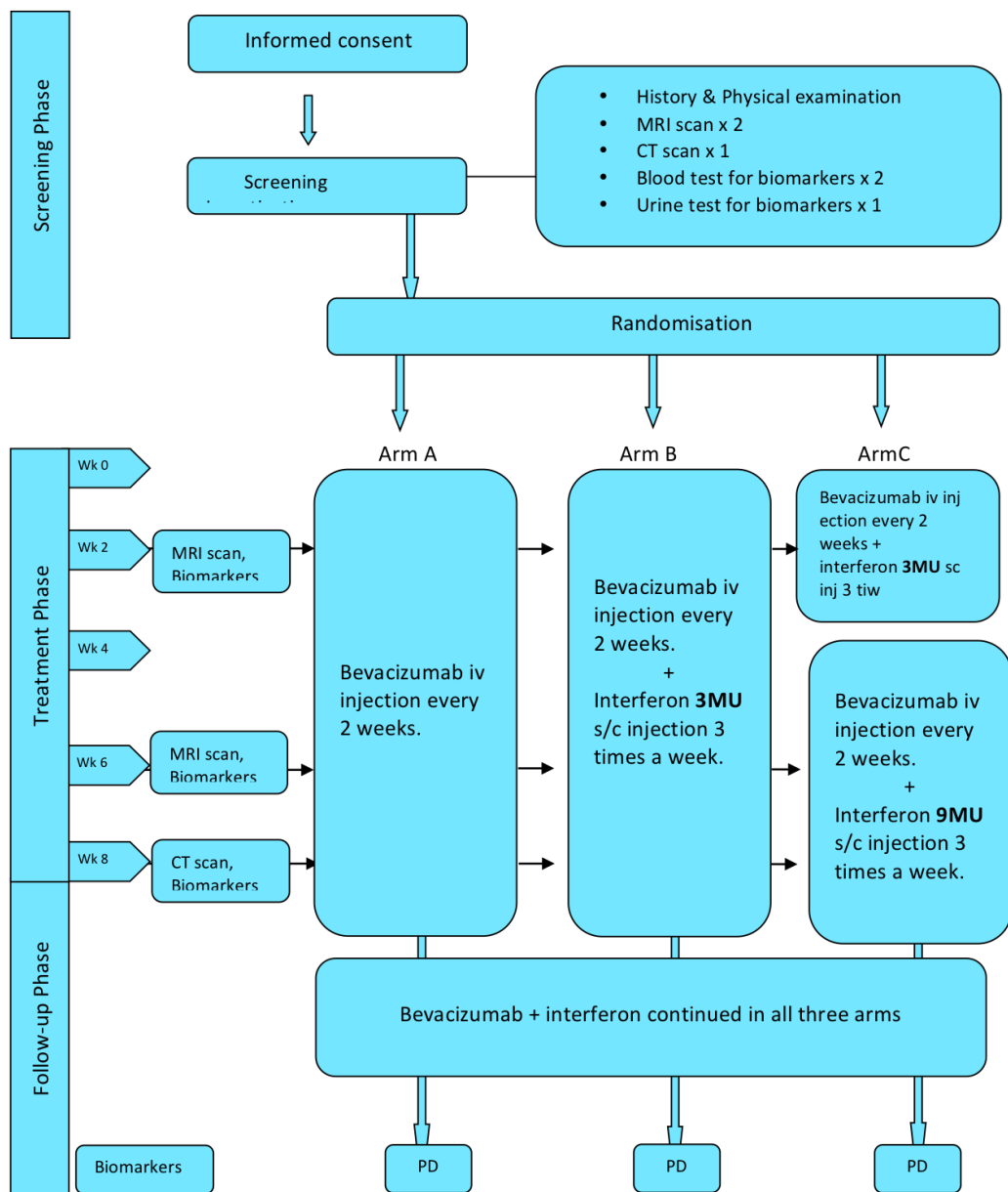
4.5.   Results

4.5.1. Recruitment and randomisation to arms

Of the three sites open for recruitment, only two sites recruited patients for the trial. The first Centre was opened for recruitment in September 2009, and the first patient recruited in December 2009. 25 patients were screened for the study between December 2009 and February 2012. As the recruitment was very slow, the steering committee decided to perform an un-planned interim analysis after 24 months of recruitment to assess for any trends to justify continued recruitment in the trial. At this point, excluding the 4 screen failures, 21 patients were randomised into three arms. Analysis of the primary endpoint data (change in K^{trans}) showed no trend in difference between the arms and the decision was taken that it would be futile to complete the planned accrual of a further 10 patients.

6 patients received bevacizumab only, 6 patients had bevacizumab in combination with standard dose (9MU) IFN and 9 patients were randomised to bevacizumab and low dose IFN (3MU). One patient in the bevacizumab monotherapy arm was taken off the trial before the week 8 primary end point analyses and hence was replaced as per protocol. All remaining 20 patients completed the primary end point. All patients had metastatic disease with no prior systemic treatment. 6 patients had the primary renal tumour in-situ. Lesions used as targets for analysis with DCE-MRI are listed in Table 4.1

Table 4.1   Lesions used for DCE-MRI analysis

Primary renal tumour	6
Abdominal LN	3
Mediastinal LN	3
Lung metastasis/chest wall	2
Peritoneal metastasis	2
Adrenal metastasis	3
Renal bed recurrence	1

At the time of data collection, all 20 patients had progressed on treatment and had been taken off-study. A total of 5 patients had to be excluded from the primary DCE-MRI analysis due to technical reasons. These included movement and cardiac artefacts, technical failure of MRI to load, breath-hold failure and one where the lesion in the chest wall was too small to characterise with DCE-MRI. 15 evaluable patients and hence 60MRI (2 pre-treatments and two on treatment per patient) scans were thus analysed: Four patients in the bevacizumab monotherapy arm, four receiving bevacizumab and standard dose IFN (9MU) and 7 patients treated with bevacizumab and 3MU IFN.

4.5.2. Safety analysis

A planned independent safety analysis was performed after 15 patients completed their primary end point on the study. All adverse events including clinical and laboratory AE were collected and graded according to CTCAE version 3.0. Causality of the AE were determined as per Section 3.2.5.2. The data obtained was analysed by an independent expert. The methods are detailed earlier in the section 3.2.6. Assessment of adverse events (AE) in this cohort is explained here.

G1-G2 Adverse Events

With bevacizumab monotherapy (Arm A), 4 patients (80%) developed AEs. 14 adverse events were reported in this group with an average of 2.8 AEs per patient. In Arm B, where patients had bevacizumab and 3MU of interferon-α2a, all 5 patients (100%) had low grade adverse events. This group had 45 adverse events reported so on average each patient developed 9 AEs. All 5 patients in Arm C (100%) developed AE with 41 adverse events in total. On average each patient developed 8.2 AEs.

G3-G4 Adverse Events

High-grade side effect detection is of paramount importance. Grade 3/4 AE were noted in 1 of the 5 patients treated with bevacizumab monotherapy (20%). On addition of low dose of IFN, 3 of the 5 patients (60%) developed high-grade side effects with a total of 4 high grade AEs.

When high dose interferon-α2a was used (Arm C), interestingly only 20% i.e. 1 of the 5 patients developed a higher grade AE.

SAEs

Six (40%) of the 15 patients had a SAE. Only 1 of the 6 SAE reported was treatment-related which required intervention. No deaths due to adverse events were reported.

Drug discontinuations: Treatment was discontinued only in one patient (arm A) due to an unrelated SAE. Dose reduction and delays have not been reported.

G3-G4 adverse events were seen in 5 (30%) of the 15 patients, one patient developed two G3-G4 adverse events. Given the small number of G3-G4 AEs it was difficult to remark with confidence on the difference in incidence of AEs between the 3 treatment arms. The percentage of with G3-G4 adverse events is noted to be smaller than that observed in similar trials. In the AVOREN trial (Escudier, Pluzanska et al. 2007), 60% of the patients treated with Interferon and bevacizumab had G3-G4 adverse events and 80% of the patients who had the same treatment noted G3-G4 toxicities within the CALGB 90206 trial (Rini, Halabi et al. 2008). Such differences could be due to the smaller sample size and to the different treatment doses. No definite trial data exists regarding the overall frequency of G3-G4 AEs in renal cancer patients treated with bevacizumab only.

Apart from one patient in Arm A (Patient 4), all the patients in the study experienced G1 - G2 AEs. The incidence of G1- G2 AEs was smaller in arm A compared with arm B and arm C. An average of 2.8 AEs per patient were seen in arm A compared with 9 and 8.2 AEs per patient in arm B and C respectively. This was not unexpected as most

of the AEs were caused by the interferon. The incidence of G1 – G2 AEs was virtually identical between arm B and arm C although the patients in arm C had a higher dose of interferon. Previous studies have shown that a lower interferon dose is associated with fewer G3 - G4 AEs but no data are available regarding the incidence of G1 - G2 AEs (Melichar, Koralewski et al. 2008, Bracarda, Porta et al. 2013). It is likely that the similar incidence of AEs was due to the small patient number and the fact that low grade adverse events are very common with interferon.

Thus with the safety analysis, no unexpected toxicities were observed in the group. An expected increase of AEs was observed in patients treated with the combination of bevacizumab and interferon although no dose reductions or dose delays have been reported.

4.5.3. Reproducibility of DCE-MRI parameters

Assessment of reproducibility of the DCE-MRI parameters was performed as detailed in Section 3.2.7.4. The difference between two measurements (d) was assessed for normality with Shapiro-Wilk test. Then Kendall's Tau was calculated to test the correlation of "d" with the mean of the measure (Bland and Altman 1996). ANOVA was used to assess the statistical measures. These include,

1) Mean Squared difference $\textbf{dSD} = \left(\frac{\sum \textbf{d}^2}{\textbf{n}}\right)$

2) Group Confidence interval $\textbf{CI} = \pm\left[\frac{\textbf{1.96dSD}}{\sqrt{\textbf{n}}}\right]$

3) Within patient standard deviation $\textbf{wSD} = \frac{\textbf{dSD}}{\sqrt{\textbf{2}}}$

4) Within patient coefficient of variation $\textbf{wCV} = \frac{\textbf{wSD}}{\textbf{oveall mean of the parameter}}$

5) Reproducibility coefficient $\textbf{r} = \textbf{2.77wSD}$

Individual values which fall outside "r" is likely due to be a true effect and hence significant. Group 95% CI in a cohort is calculated by using the relevant n numbers in the cohort.

Values were calculated for K^{trans}, k_{ep}, v_e and $IAUGC_{60}$ individually. The outcome values are summarized in the following Table 4.4.

Table 4.2 Reproducibility statistics for DCE-MRI parameters

Parameter	K^{trans}	K^{trans} (no outliers)	k_{ep}	k_{ep} (no outliers)	v_e	v_e (no outliers)	$IAUGC_{60}$	$IAUGC_{60}$ (no outliers)
dSD	0.0913	0.0715	0.7762	0.1246	0.0401	0.0175	4.4273	2.5064
group CI	0.0447	0.0467	0.3928	0.0677	0.0203	0.0114	2.1694	1.4182
as % mean	12.5128	11.0957	29.3427	5.0294	7.2819	3.7547	7.8399	4.9644
wCV	0.1806	0.1201	0.4100	0.0654	0.1017	0.0406	0.1131	0.0620
wSD	0.0646	0.0506	0.5488	0.0881	0.0283	0.0124	3.1306	1.7723
r	0.1788	0.1401	1.5203	0.2440	0.0785	0.0342	8.6718	4.9093
r as %	50.0177	33.2649	113.5677	18.1215	28.1836	11.2565	31.3385	17.1858
Shapiro-Wilk	normal	normal	normal	normal	normal	normal	normal	normal
F	13.633	22.843	1.764	77.975	39.611	221.841	36.104	75.752
ICC	0.855	0.906	0.244	0.973	0.947	0.990	0.943	0.972
tau	0.283	0.500	0.048	0.103	0.048	0.000	0.200	0.091
p	0.139	0.075	0.846	0.675	0.846	0.920	0.306	0.737

4.5.4. Primary variable analysis (K^{trans})

Aim of the primary analysis was to assess the changes in DCE-MRI defined parameter K^{trans} from baseline to week 6 on treatment between the three arms of the trial. Please refer to Section 3.2.8 and 4.3 where this is described.

Value of K^{trans} over the different time points in the trial is graphically represented here in Figure 4.2 and 4.3.

Figure 4.2   **Box and whisker plot K^{trans} over different trial time points.**
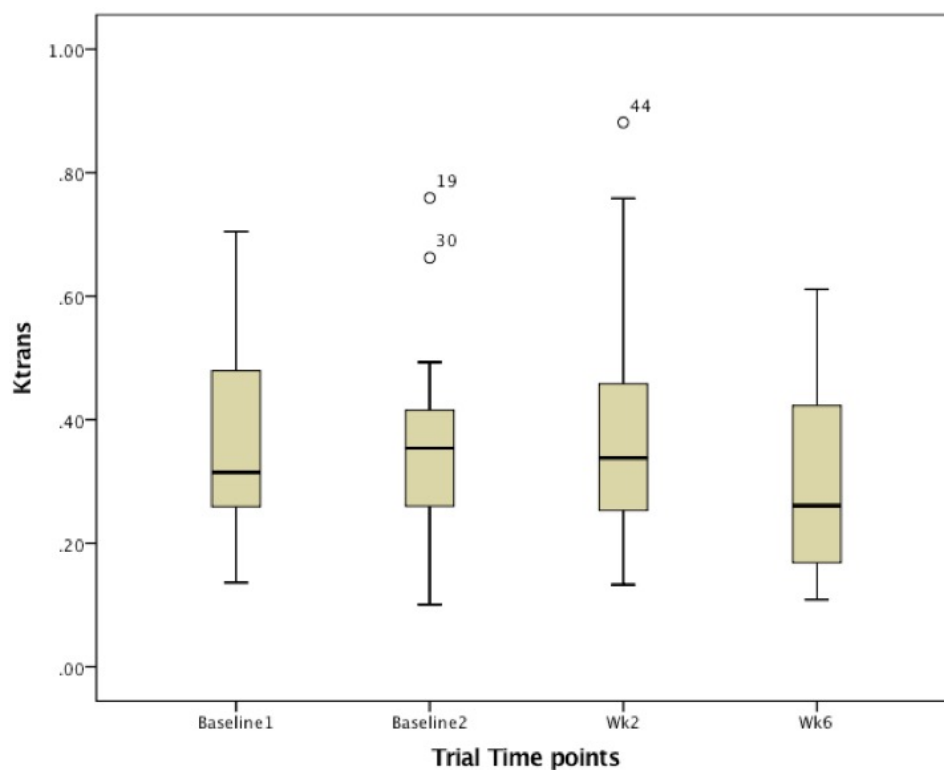
Figure 4.3 **Variation in K^{trans} in individual patient over the trial**
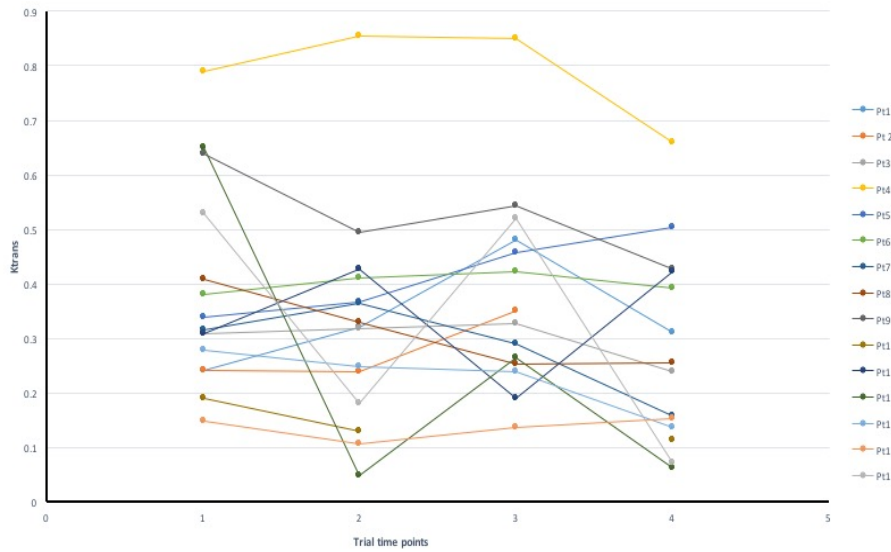
To assess the true change in K^{trans} due to treatment, baseline reproducibility was initially calculated as explained in Section 3.2.7.4. After normalising and excluding any outliers, these values as percentage for individual patients were noted to be 33.26 for K^{trans}, 18.12 for k_{ep}, 11.25 for v_e and 17.18 for $IAUGC_{60}$.

The mean decrease in K^{trans} for all patients was -2.25% at week2 and -11.33% at week 6. Analysing treatment cohorts, between baseline and week 6, Arm A had a decrease in K^{trans} of 26.44% (95%CI -17.42 to -35.46). Changes in K^{trans} in Arm B and C were -4.56% and 32.84% (SD of 35.09) respectively. Changes in K^{trans} at week 6 (compared to baseline) was statistically significant for Arms A and C but not for Arm B. No statistical significance or trend were noted in the observed change between treatment arms. This has been detailed along with the other MRI parameter changes in Table 4.3

4.5.5. Secondary variable analyses

Secondary analyses included assessment of other DCE-MRI associated vascular endpoints, efficacy analyses, safety endpoints and exploratory assessments including laboratory endothelial cells quantification. Please refer to Section 3.2.8.

4.5.5.1.   Secondary MRI variable analyses (Vascular end point)

At week 2 comparison was made in the changes of K^{trans} from baseline between bevacizumab alone group (Arm A) vs bevacizumab + interferon-α2a groups (Arms B + Arm C). Arm A showed a change of -0.03% in K^{trans} from baseline and combined IFN groups showed a change in K^{trans} of -1.360 with a standard deviation of 33.06. These values were also not considered to represent a true i.e. statistically significant change. Similar calculations have been performed for all the other MRI parameters including k^{ep}, v_e and $IAUGC_{60}$. Changes in all MRI parameters from baseline to week 2 and week 6 are reported in Table 4.3

Table 4.3   Change of MRI parameters at different time points in trial.

	baseline (mean)	Week2 (change in %)	Week6 (change in %)
Arm A (bev)			
K^{trans}	0.3445	-0.03	-26.439
k_{ep}	1.022	-2.877	-9.017
v_e	0.319	3.015	-10.559
$IAUGC_{60}$	28.11	9.952	-10.593

Arm B (bev +3MU IFN)			
K^{trans}	0.3997	18.12	-4.56
k_{ep}	1.358	-2.808	-11.947
v_e	0.304	17.684	7.213
$IAUGC_{60}$	34.99	8.506	-6.114

Arm C (bev+9MU IFN)			
K^{trans}	0.3726	-35.45	-32.841
k_{ep}	1.997	-15.111	-20.08
v_e	0.1865	-21.369	-17.181
$IAUGC_{60}$	24.648	-16.043	-29.646

Combined ArmB+C			
K^{trans}	0.3885	-1.36	
k_{ep}	1.59	-7.282	
v_e	0.261	3.482	
$IAUGC_{60}$	31.229	-1.313	

No statistically significant changes in secondary outcome measurements was seen. A trend of decrease of the Kep values was noted between the arms at week 6 was seen (p=0.862 Arm A vs B and p=0.450 Arm A vs C).

4.5.5.2.   Clinical outcome analysis (efficacy end points)

With clinical outcome analysis, median progression-free survival (PFS) of all evaluable patients was 308 days. With cohort analysis comparing the PFS, Kaplan-Meier statistics were used and a log-rank test used to assess the significance. Median PFS for Arm A was 108 days (95% CI 0 -147). PFS was 308 days (95% CI -95.0 - 520.9) for Arm B and 378 days (95% CI 0 – 775) for Arm C. No significance was noted with p value obtained by log-rank test. Kaplan-Meier curve for PFS is shown in Figure 4.4

Figure 4.4   **Kaplan Meier curve comparison of PFS between the treatment arms.**
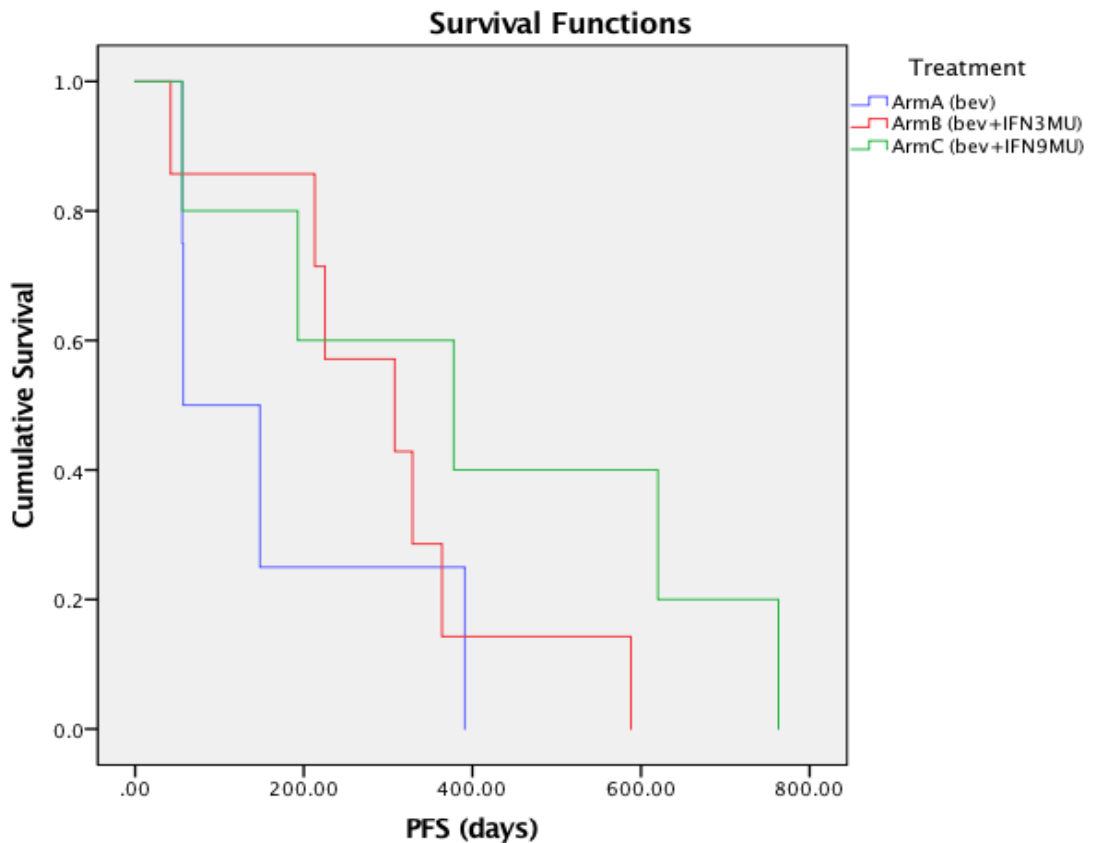
Log-rank test was performed for overall analysis and paired comparison between two arms each. χ^2 test was performed and p value calculated from the log-rank test. This is detailed in Table 4.4. Log-rank test showed no significance between any of the treatment arms in Kaplan-Meier analysis.

Table 4.4   Log-rank test: Significance of PFS difference between treatment arms

Pairwise Comparisons (PFS vs Treatment arms)							
	Treatment	ArmA		ArmB		ArmC	
		χ^2	p-value	χ^2	p-value	χ^2	p-value
Log-rank (Mantel-Cox)	ArmA			.573	.449	1.669	.196
	ArmB	.573	.449			1.589	.208
	ArmC	1.669	.196	1.589	.208		

4.5.5.3.   Comparison of PFS with MRI parameters

PFS was plotted against the vascular parameters of K^{trans}, k_{ep}, v_e and $IAUGC_{60}$ and Spearman Correlation coefficient "r" was calculated to assess if there is any trend for correlation (Table 4.5)

Table 4.5   Spearman correlation coefficient comparing the vascular parameters

and progression-free survival

Spearman correlation coefficient (rho): MRI parameters vs PFS			
	Baseline	Percentage Change of MRI parameter in Week2	Percentage Change of MRI parameter in Week6
K^{trans}	0.165 (0.557)	-0.391 (0.167)	-0.279 (0.313)
k_{ep}	0.287 (0.33)	-0.585* (0.028)	-0.47 (0.077)
$IAUGC_{60}$	-0.165 (0.557)	-0.359 (0.228)	-0.111 (0.693)
v_e	-0.0276 (0.319)	-0.166 (0.572)	0.043 (0.879)

Rho for two tailed test according to Spearman's-coefficient with alpha 0.05. Values in

parenthesis suggests significance of the correlation (Zar 1972).

No significant statistically correlation was noted between PFS and K^{trans} values at

baseline or the changes in K^{trans} during treatment. Subsequent analysis performed

similar analysis for all MRI parameters reviewed here including k_{ep}, v_e and $IAUGC_{60}$

measured at baseline, week 2 and week 6. Correlation was noted with change of kep

at Week 2 and PFS but this was not sustained in the change of kep at week 6.

4.5.5.4. Clinical benefit

The aim of this analysis was to assess whether MRI vascular parameters at baseline, week 2 or week 6 could predict and identify patients who get any meaningful clinical benefit with the treatment. We felt that with the median progression free survival of 10.5 months with the combination treatment of bevacizumab + interferon-α2a as reported by the trials, (Escudier, Bellmunt et al. 2010), the patients could be categorised into two groups with a PFS cut-off of 6 months.

Patients who had PFS $\leq$ 6months and >6months were re-categorised from the trial data. Baseline and mean change in the parameters were assessed and Mann-Whitney U test was used to assess the significance of difference between the groups (table 4.6a and 4.6b)

Table 4.6a   Comparison of vascular parameters (K^{trans}, k_{ep}) with clinical benefit (PFS).

	K^{trans}			k_{ep}		
	Baseline	Change at Wk2	Change at wk6	Baseline	Change at Wk2	Change at wk6
Group 1 PFS <6m	0.349	12.18	0.959	1.302	13.62	9.41
Group2 PFS >6m	0.3802	-3.274	-17.479	1.507	-10.63	-17.21
p value	0.662	0.423	0.582	0.756	0.033	0.197

Table 4.6b   Comparison of vascular parameters (v_e & IAUGC) with clinical benefit (PFS)

	v_e			$IAUGC_{60}$		
Group 1 PFS <6m	0.301	-0.88	-10.88	30.59	2.01	-11.94
Group2 PFS >6m	0.264	5.75	-0.6	30.7	0.97	-14.41
p value	0.6672	0.596	0.756	0.857	*	0.952

There was no statistically significant difference in MRI vascular parameters between the groups of patients who derived clinical benefit of >6months compared to those who did not. Greater changes in K^{trans} and k_{ep} were seen in patients with PFS > 6 months however due to the small sample size these changes were not statistically significant. Even though changes in k_{ep} value from baseline to week 2 showed a p value of 0.033 between the two groups suggesting a statistical significance, this was not sustained in the changes noted at week 6 and with the small sample size (n=5, group 1) this is unlikely to represent a true change.

4.5.5.5. Circulating endothelial cell quantification

Exploratory analysis assessing circulatory endothelial cell quantification was performed to assess effects of treatment on circulating endothelial cells (CEC) in peripheral blood at similar time points as DCE-MRI. The assay was performed with multi-parametric flow cytometer analysis using a BD LSRII machine (Beckton Dickinson). The technique of assessment is explained in the methods Section 3.2.4.8. Baseline and variation of WBC and MNC showed that for most patients, WBC counts appear to decrease between baseline and week 2, but generally no change in WBC counts were noted over the course of treatment. WBC and MNC count are mainly within normal range at baseline and on treatment for majority of patients Figure4.5a & b.
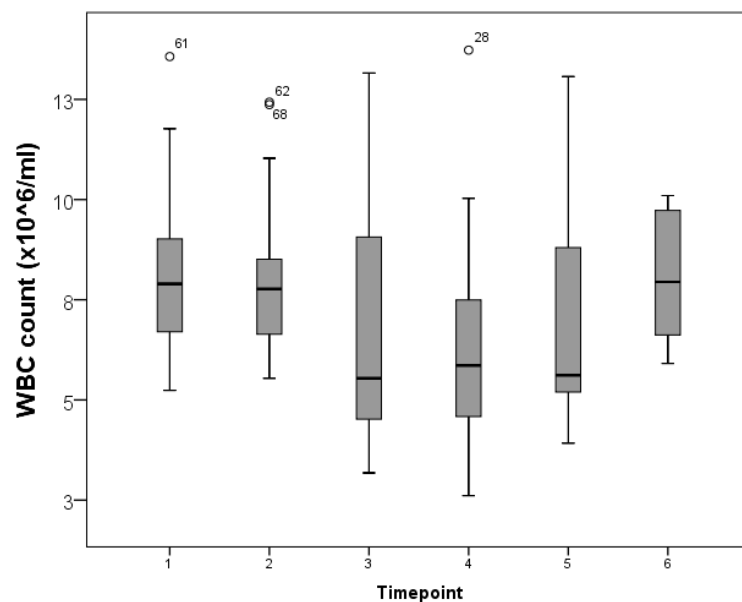
Figure 4.5(a)   Box plot - WBC count at different time points in trial.
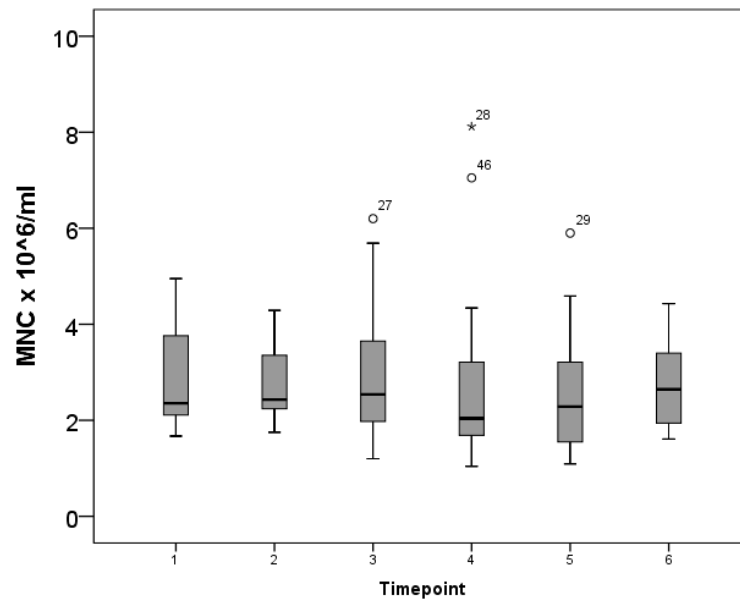
Figure 4.5(b)   Box plot - MNC count at different time points in trial.

Boxes represent Inter-Quartile Range (25-75%); 'whiskers' represent 95% confidence (2.5-97.5%); middle line represents median. Outliers are shown as circles or stars labelled with patient number. Circle = between 1.5 and 3 IQR (inter-quartile range) from the end of the box (ends of box denote 25th and 75th percentile)

CD34 counts appear to lie within the normal range and experience little variation during treatment with baseline values falling between ±0.02 and ±0.65 x10^3/ml. One patient had high CD34 at the baseline which increased at week 2 but dropped to normal range by week 6. Representing the CD34 as percentage of MNC, variation in CD34 over the course of treatment for individual patients have been plotted - see Figure 4.6.

Figure 4.6   Variation of CD34 as percentage of MNC in individual patient
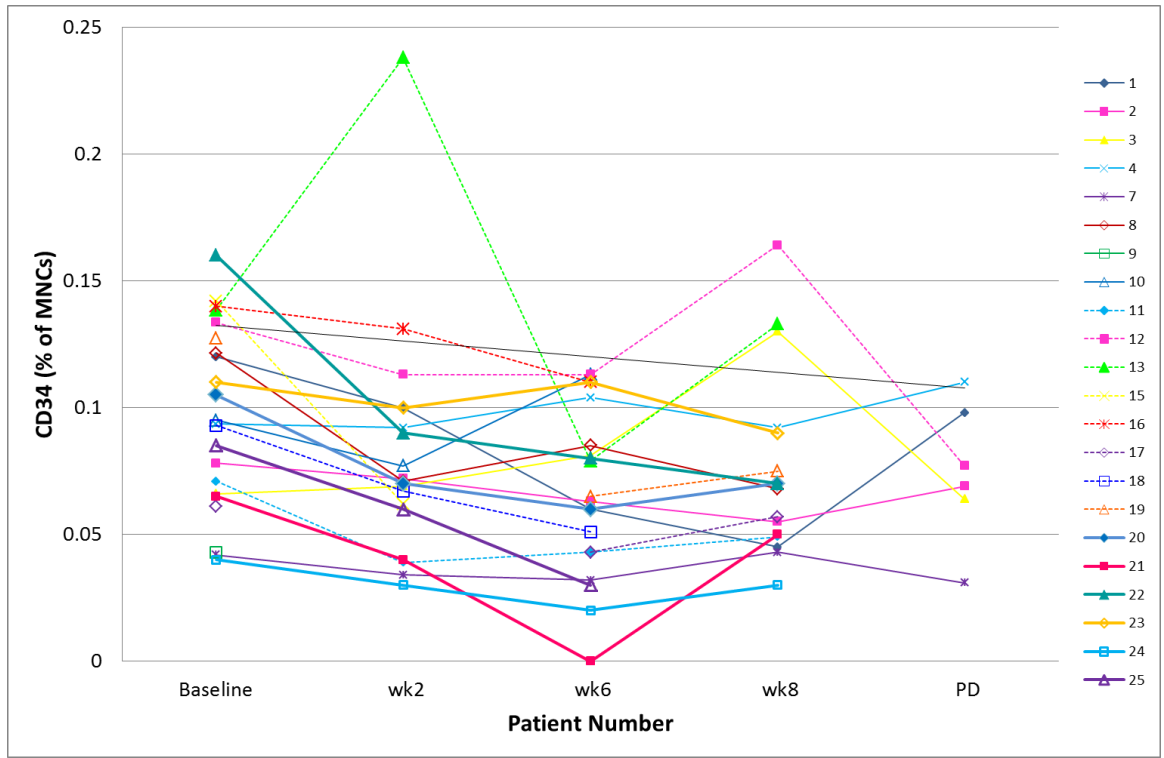
Total and viable CEC were assessed with the fluorescine dye CalceinM. Total and viable

CEC showed large variation between the two baseline samples. This persists when

looking at CD45dim/neg, CD34+, CD144+ or Tie2+ve cells. These are showed in Figures

4.7 a&b and 4.8a&b.

Figure 4.7(a)   Total CEC over the trial – Box and whisker plot with outliers.
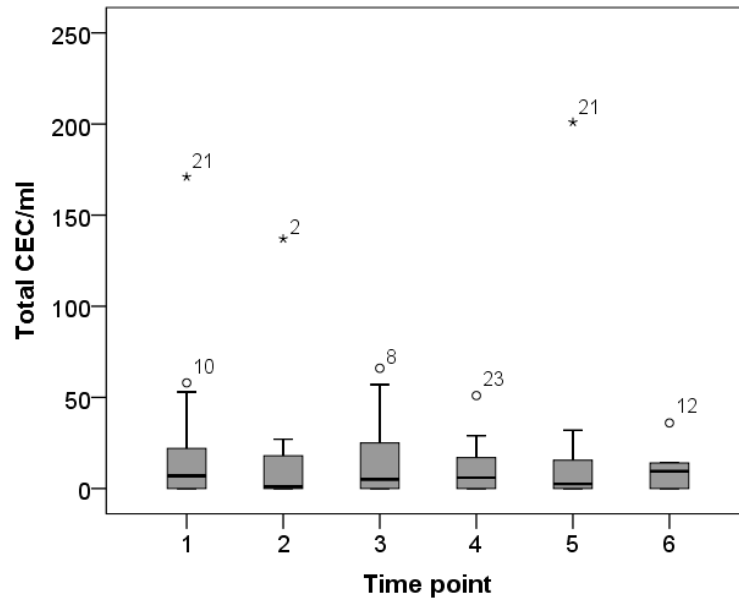
Figure 4.7(b)   Viable CEC over the trial – Box and whisker plot with outliers.

170
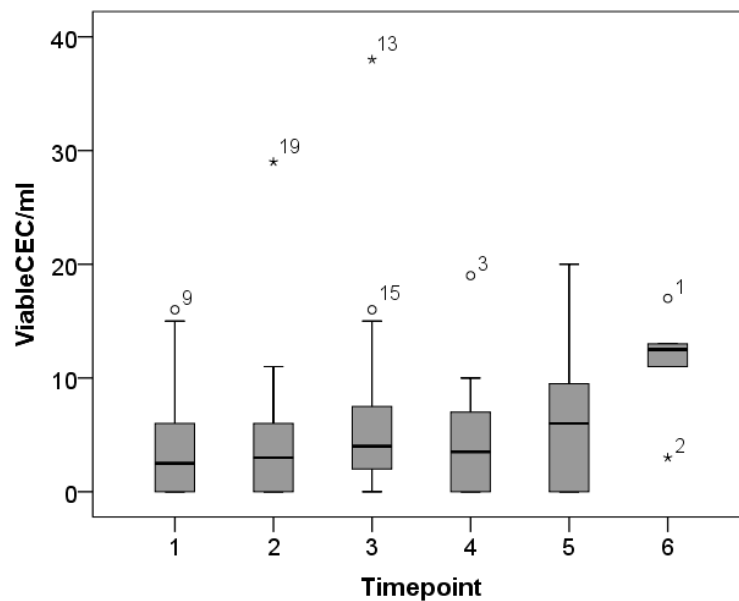
Figure 4.8(a)   Change of Total CEC over the trial period in individual patients.
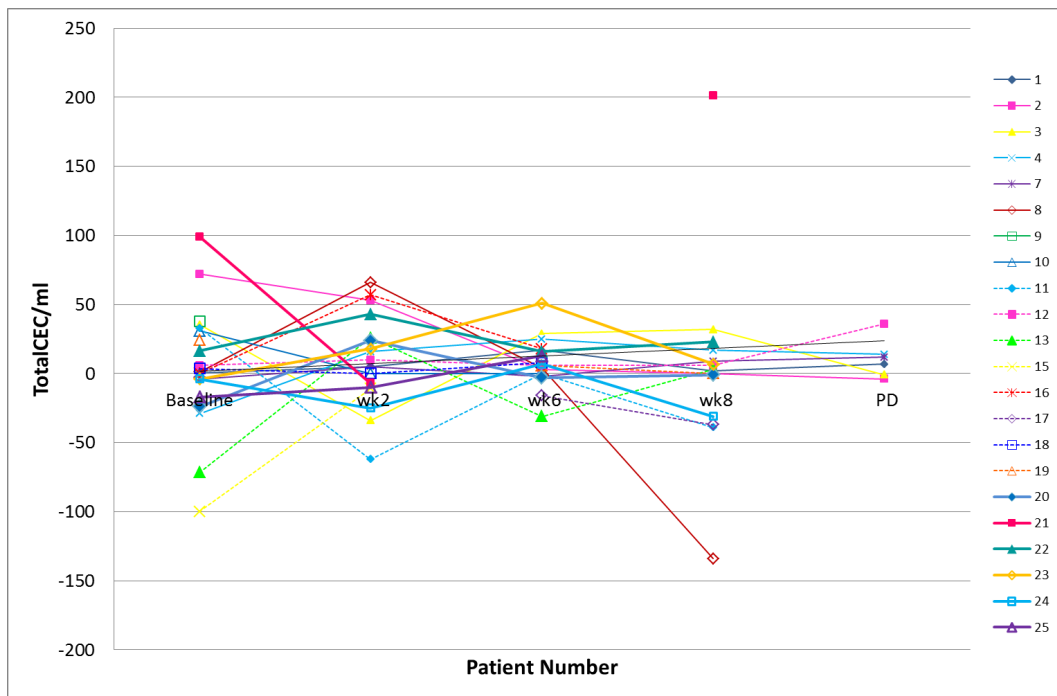
Figure 4.8(b)   Change of Viable CEC over the trial period in individual patients.
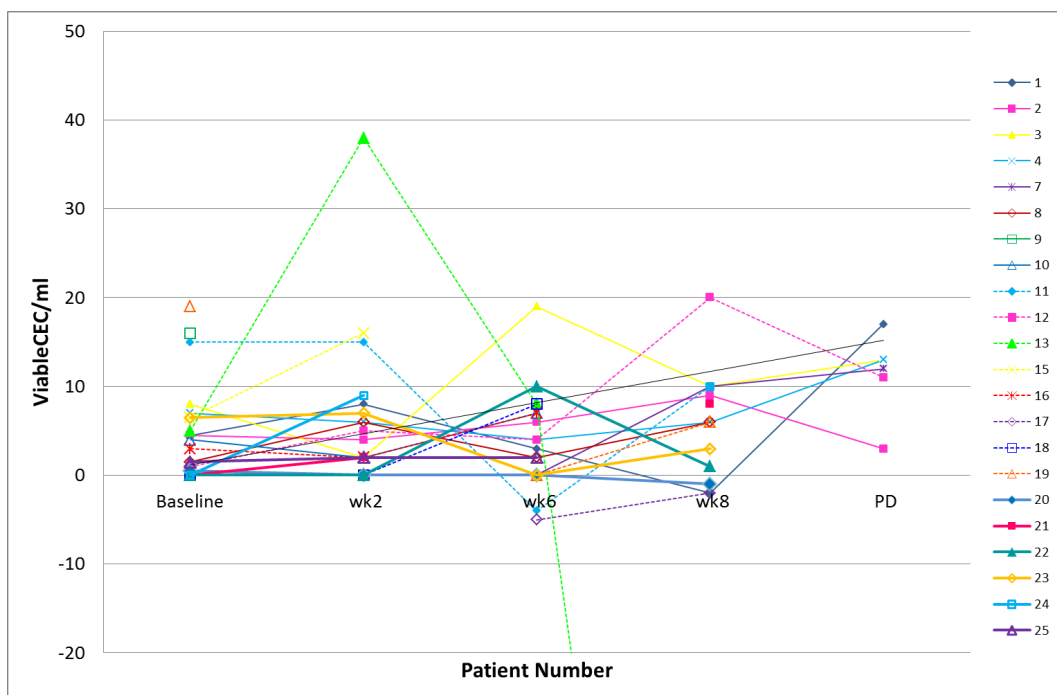
No obvious overall changes were noted in the CEC numbers with treatment. Some

patients appear to exhibit an increase in CEC numbers at 2 weeks. It is unclear whether

171

this represents a real change. Along with the CD34, CD45 and CD144, Tie2 was used

as these cells are likely to represent proangiogenic mononuclear cells. There does not

appear to be any obvious change in Tie2 positive cell concentration for any patients.

This is represented in Figure 4.9.

Figure 4.9 **Change ofCD45- Tie2+ MNC over the trial period in individual**

patients.
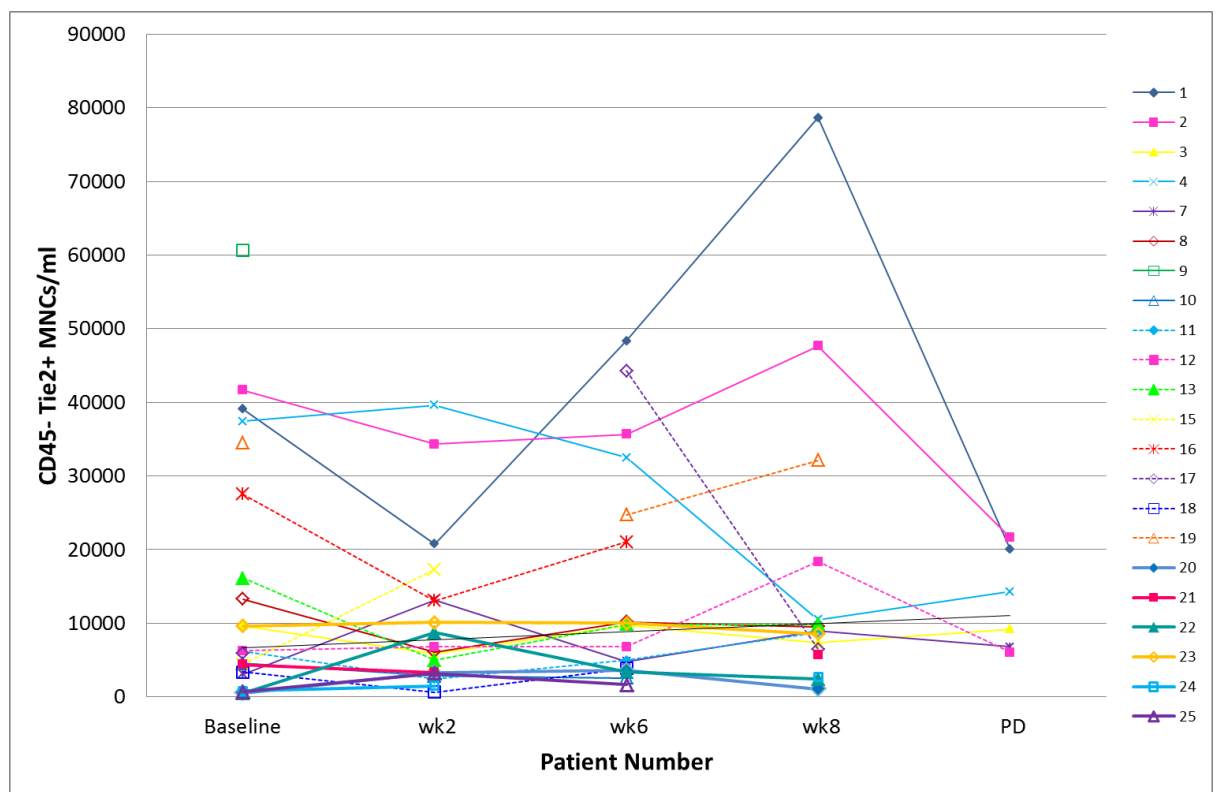
4.6.   Discussion.

This trial attempts to address whether IFN measurably adds to the anti-angiogenic effect of bevacizumab.

The AVOREN and CALBG 90206 trials (Escudier, Pluzanska et al. 2007), (Rini, Halabi et al. 2008) both compared combination bevacizumab and interferon with single agent interferon. Both studies lacked a single agent bevacizumab arm. Data regarding the efficacy of single agent bevacizumab treatment in metastatic RCC is therefore limited to that available from small phase 2 trials. The additional benefit conferred to bevacizumab treatment by IFN is therefore unknown, as is whether any benefit is mediated by anti-angiogenic effects.

The trial accrued very slowly. Many patients with metastatic RCC did not have lesions of a size or location that enabled DCE-MRI analysis. Additionally, competing first line studies and the inability to access sunitinib in the NHS at some Centres after patients had been treated with bevacizumab on trial resulted in the very slow recruitment and one centre being unable to recruit any patients.

As evident from the MRI analysis, even among patients with lesions suggested to be suitable for analysis, 5 (25%) patients were unable to be analysed due to technical issues including movement artefacts despite attempts to correct motion, cardiac artefacts, technical failure of MRI to load and breath hold failure.

Among the patients analysed, no correlation was found between change in K^{trans} and addition of IFN to bevacizumab. Effect size analysis was performed due to the smaller sample size recruited and the change in K^{trans} was still not noted to be significant.

Change in K^{trans} and k_{ep} may identify a group of patients likely to have PFS > 6 months (p 0.03), but this observation needs to be tested in a larger sample size. The small sample size makes it difficult in this case to analyse the significance of this change.

Although K^{trans} is the best-studied DCE-MRI parameter, the importance of k_{ep} or rate constant, which measures the efflux of the contrast from the extravascular extracellular space is increasingly recognised. Pre-clinical studies in a mouse xenograft model have suggested that k_{ep} might be a better parameter in assessing response to anti-angiogenic agents (Song, Cho et al. 2013). This need to be evaluated in a larger cohort.

In summary, in this small study we were unable to demonstrate significant differences in vascular parameter change between RCC patients receiving single agent bevacizumab or combination bevacizumab and IFN. The study was technically demanding and patients were difficult to accrue. Change in K^{trans} and k_{ep} may identify patients likely to have more durable benefit from anti-angiogenic treatment but this observation needs to be replicated in a larger sample size.

Chapter 5.

CT response assessment combining reduction in size and arterial enhancement in metastatic RCC patients treated with targeted therapy

5.1.   Introduction

In this chapter I compare the use of existing standard imaging guided methods for therapeutic response assessment in metastatic RCC patients treated with tyrosine kinase inhibitors and propose a new criterion, the "modified Choi" criterion, as an enhanced method for this purpose, with the help of a retrospective clinical study. This study has been published in the Journal of Cancer Biology & Therapy 9(1); 15-19; January, 2010 (see list of abstracts and publications).

As discussed in previous chapters, accurate therapeutic response assessment is of paramount importance in a clinical setting where decisions need to be taken about whether to continue or change a treatment regime. Validated methods of therapeutic response assessment may identify potential responders or non-responders and identify the *at risk* population for side effects. This would distinguish the patient who will obtain maximum benefit from a specific intervention and avoid exposing patients to unnecessary side effects and allow an early change to a more potentially beneficial therapy

Imaging as a tool for response assessment has the advantage of being non-invasive and can be performed repeatedly at intervals. CT scanning is the most common imaging technique used in oncology for treatment response assessment. Using this technique has the advantage of wide availability of equipment and interpretational skills and less inter-observer reporting variability.

Current methods of response assessment

Current accepted standard for treatment assessment for many anticancer treatment is based on an imaging-defined response assessment criteria called RECIST (Response Evaluation Criteria in Solid Tumours) (Patrick Therasse, Richard S. Kaplan et al. 2000). It is based entirely on the size change of the tumours. While RECIST is clinically relevant in the response assessment of conventional chemotherapeutic agents, this appears not to be the case for the new generation of targeted anti-cancer agents. Many targeted agents have profound anti-tumour effects with resulting clinical benefit yet have low RECIST defined response rates. The first attempt to move away from the framework of using criteria solely based on size was proposed by Choi et.al (Choi 2008). The Choi criteria was proposed to re-evaluate the response assessment in Gastro Intestinal Stromal Tumours (GIST) treated with Imatinib (Glivec®) considering either change in size or tumour enhancement as a response to systemic therapy. Reduction or absence of tracer uptake post therapy has also been proposed as a method of response assessment with FDG-PET scan. Despite these suggestions, RECIST remains the most established and widely used technique to assess treatment response in metastatic RCC.

5.1.1. RECIST (Response Evaluation Criteria in Solid tumours)

RECIST 1.0 was introduced in 2000 as a standardised method to evaluate response to treatment with chemotherapeutic agents (Patrick Therasse, Richard S. Kaplan et al. 2000). This was further updated in 2009 (Eisenhauer, Therasse et al. 2009). Treatment response defined by RECIST is based on the change in size of the sum of uni-dimensional measurements of tumour target lesions performed with a specific imaging modality.

The tumours are classified as measurable (target) and non-measurable (non-target) lesions. Lesions that measure more that 2.0cm by non-helical CT methods and 1.0cm by helical CT and those that can be measured accurately and repeatedly are considered measurable lesions. With RECIST 1.1, the target lesions (maximum five per organ and ten in total) are defined with an imaging technique (eg: CT/MRI/USS etc) performed prior to treatment initiation. The maximum diameters of the target lesions are noted in the axial plane (short axis measurement is used if lymph nodes are used as target lesion) and the sum of the largest diameter of the target lesions is calculated. The follow up scans for response assessment are performed using the same modality with the target lesions measured the same way.

5.1.1.1.   Response categorisation using RECIST criteria

1. Complete response (CR):   Disappearance of all target lesions

2. Partial response (PR):   >30% decrease in sum of longest diameter of target lesions

3. Progressive disease (PD):
   1) >20% increase in sum of longest diameter of target lesions taking as reference the smallest noted since treatment initiation
   2) Appearance of new lesion

4. Stable disease (SD):   Response not fitting with any of the above

5.1.2. Choi criteria

With increasing use of targeted agents in pharmacological management in oncology, it has been noted that the response obtained as defined by RECIST criteria does not correlate with the clinical benefit gained from these agents. Choi et al. (2008) proposed an alternative method (Choi criteria) for response assessment of GIST (Gastro Intestinal Stromal Tumour) treated with Imatinib (a tyrosine kinase inhibitor blocking activated c-kit). It was noted that a significant change in CT assessed density inside the tumour occurred quite early in the treatment of patients who had a good clinical response to treatment. This was despite only a minimal decrease in tumour size thus failing to meet the response criteria (RECIST) (Choi, Charnsangavej et al. 2007, Choi 2008). The criteria took into consideration the change in size or change in enhancement after a contrast enhanced CT scan to define responders to treatment and non-responders. Size was measured as per the RECIST criteria guidelines. The enhancement of tumour in HU (Hounsefield Units) was calculated from CT images. The Choi criteria proposed either a decrease in size of 10% *OR* decrease in enhancement by 15% for a response. 97% of patients with a good response fell into this category thus providing a good prognostic indicator.

5.1.2.1. Response categorisation according to Choi criteria

a) Complete response (CR):   Disappearance of all target lesions

b) Partial response (PR):

     c) ≥10% decrease in sum of longest diameter of target lesions <u>OR</u>

     d) ≥15% decrease of mean contrast enhancement of target lesions

e) Progressive disease (PD):

     a) Increase in tumour size >10% and does not meet criteria of PR by contrast enhancement

     b) New lesion or intra-tumoural nodule

f) Stable disease (SD):   Response not fitting with any of the above

5.1.3. Proposed new criteria - "modified" Choi

Anti-angiogenic targeted treatment as sunitinib, sorafenib and bevacizumab + interferon, have transformed the treatment of RCC. Progression free survival has doubled compared to either standard treatments or placebo. Yet, RECIST defined response rates are relatively low (sunitinib 31%, sorafenib 10% and bevacizumab + interferon 30%) (Motzer, Hutson et al. 2007, Escudier, Bellmunt et al. 2010). Many patients who derive significant clinical benefit from these drugs never attain a RECIST defined response.

As discussed earlier in the thesis, RCC is highly vascular driven in part by the VEGF-HIF pathway (see section1.1.2). RCC and its metastasis enhance effectively with intravenous contrast. With the increased vascularity it has been noted that these tumours enhance well in the arterial phase of the CT image acquisition (Raptopoulos, Blake et al. 2001, Lee, Heiken et al. 2005). In this study, Raptopoulos and colleagues suggested that up to 10% of RCC metastases could be even missed by not acquiring arterial phase images.

With "modified" Choi criteria, we chose to use a CT defined criteria including the change in size and enhancement in arterial phase. Response according to "modified"Choi criteria were defined as below.

5.1.3.1. Response categorIsation according to "modified" Choi Criteria

g)	Complete response (CR):	Disappearance of all target lesions
h)	Partial response (PR):	i) ≥10% decrease in sum of longest diameter of target lesions <u>AND</u>
		j) ≥15% decrease of mean contrast enhancement of target lesions
k)	Progressive disease (PD):	a) Increase in tumour size >10%
		b) New lesion or intra-tumoral nodule
l)	Stable disease (SD):	Response not fitting with any of the above

5.2. Materials and Methods

This was a retrospective analysis on metastatic RCC patients treated with tyrosine kinase inhibitors. Patient selection and exclusion, methods of clinical and radiological assessment, response evaluation and statistical methods used for this study have been previously detailed in chapter 3.0 (section 3.3)

5.3.   Results

5.3.1. Patient recruitment

Data from a total of 32 patients with mRCC who had treatment with tyrosine kinase inhibitors (cediranib/sunitinib) were analysed. These patients received treatment on 2 studies as detailed in section 3.3.1 (Eudract 2006-002455-33 or Eudract 2005-002097-30).

Patients received treatment with sunitinib (n = 18) or cediranib (n = 14). 10 patients were noted to have renal impairment and hence were unable to have contrast enhanced CT scans. These patients were excluded from the study. A further two patients were excluded as these patients discontinued the treatment due to toxicity rather than disease progression. The remaining 20 patients were evaluated for the study. Among the 20 evaluable patients, 11 had treatment with sunitinib and 9 had treatment with cediranib. Of the evaluated patients, 14 patients had disease progression on treatment at the time of analysis. Time to progression in these patients was 260 days (median). Of all the remaining 6 evaluable patients all had more than 1 year follow up with a median of 483 days.

5.3.2. Response assessment analysis

Separate analyses with each of the three response criteria were performed to categorise the partial response (PR) or stable disease (SD) as defined by each of the criteria.

Table 5.1   Response assessment and categorisation using three different criteria

Criteria	Partial response	Stable disease	Progressive disease
RECIST	*5*	*15*	*0*
Choi	*19*	*1*	*0*
"Modified" Choi	*13*	*7*	*0*

5.3.3. Clinical benefit analysis

Clinical benefit analysis was performed by initially assessing the time to progression (TTP) of the disease. TTP was defined as the time in days from the start of systemic therapy with the planned tyrosine kinase agent to the date where disease progression was documented radiologically. Please refer to chapter 3.0 (section 3.3.1.7).

The time to progression of the disease was then correlated with the response assessment categories as defined by the three different criteria separately. This is detailed in table 5.2 and represented in figure 5.1

Table 5.2   Response classification and association with TTP

Classification	Partial response (PR)		Stable disease (SD)		Log rank
	No. of patients	TTP days median (95% CI)	No. of patients	TTP days median (95% CI)	Test *sign.*
RECIST	5	168 (50–286)	15	428 (129–726)	0.643
Choi	19	399 (85–713)	1	*	*
Modified Choi	13	448 (99–797)	7	89 (79–99)	0.002

Table adapted from (Nathan, Vinayan et al. 2010) * single patient in a group hence no

statistical comparison

Figure 5.1   Median TTP (days) for PR and SD groups as defined by three criteria
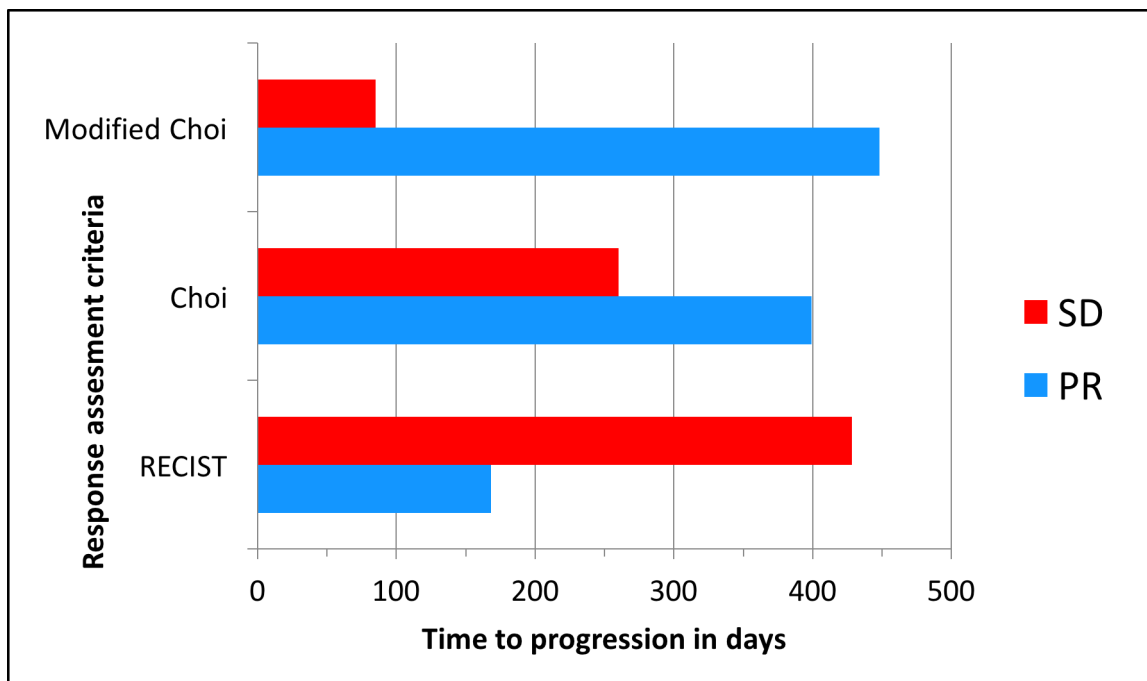
SD - stable disease, PR - partial response

With the response assessment after 2 cycles, none of the patients progressed on treatment with any of the response criteria. When association between response criteria and TTP were analysed, modified Choi criteria showed the greatest association with TTP. According to modified Choi, median TTP for patients who attained partial response (PR) was 448 days (95% CI 99–797) while patients with stable disease (SD) had a median TTP of 89 days (95% CI 79–99). With RECIST criteria, patients who had PR had a median TTP of 168 (95% CI 50–286) days and 428 (95% CI 129–726) days for patients categorised as SD. With the standard Choi criteria, median TTP of the PR group was 399 (95% CI 85–713) days. Only one patient had Choi criteria-defined stable disease. Kaplan-Meier analyses were performed for the groups as shown in Figures 5.2a, 5.2b & 5.2c.

Statistically significant difference was noted in median time to progression between PR and SD groups when defined according to modified Choi criteria (Log Rank test p = 0.002). No significant difference in median TTP was noted with Kaplan-Meier curves for SD & PR groups defined by RECIST criteria (Log Rank test: p values of 0.643). Statistical significance with log rank test was not performed between the two groups with Choi criteria as there was only a single patient defined as having SD according to Choi.

Figure 5.2   Kaplan- Meier survival curve assessment for RECIST 5.2a, Choi 5.2b

and modified Choi (5.2c)
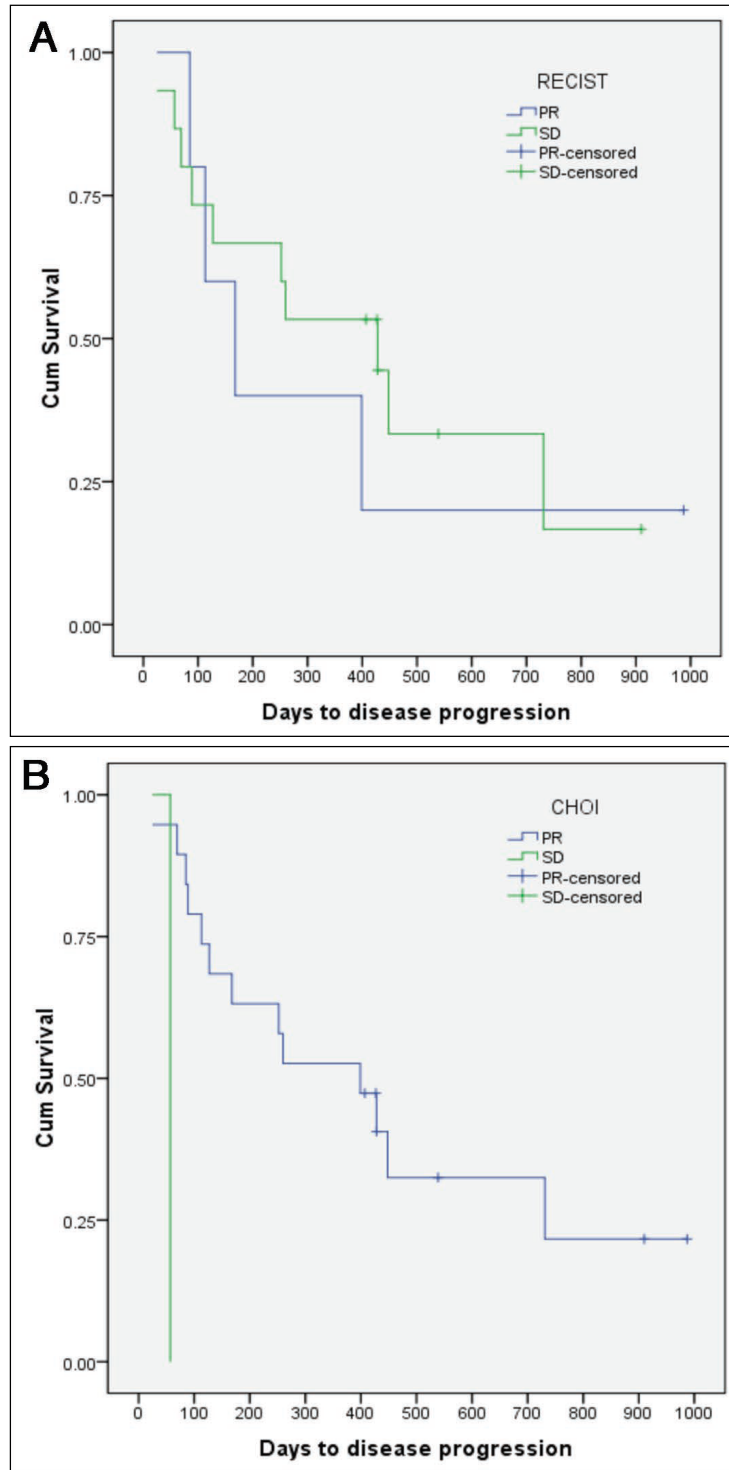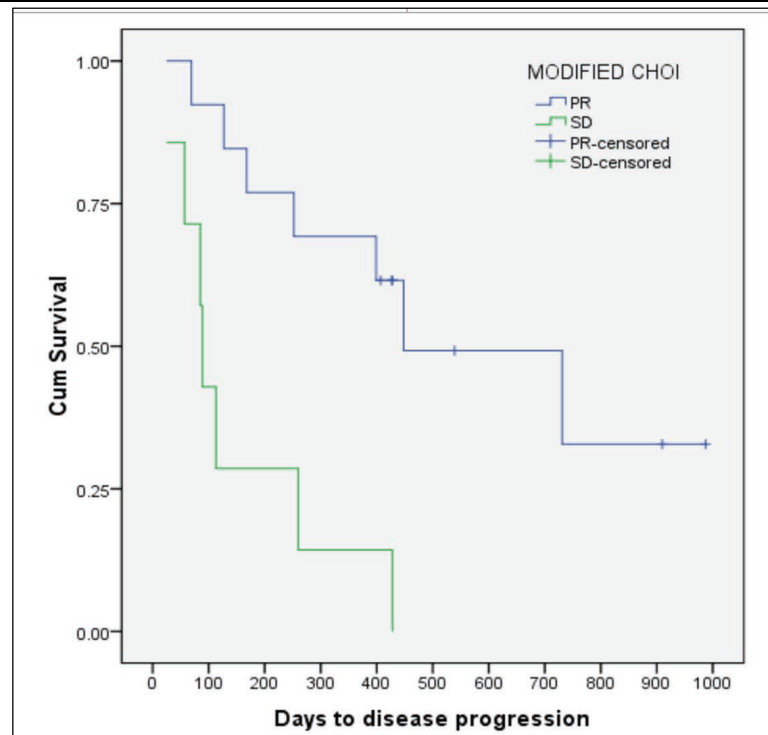
Figures adapted from (Nathan, Vinayan et al. 2010)

a) RECIST estimated median TTP 168 and 428 days for PR and SD group with log rank P value 0.643.

b) Choi criteria estimated median TTP was 399 for the PR group. As only 1 patient had Choi defined SD, no statistical analysis was performed.

c) Modified choi criteria showing a TTP 448 and 95 days for PR and SD groups with a significance of p=0.002 with log rank p test.

5.3.4. Exploratory analysis.

To identify other potential thresholds besides the 15% change in enhancement and 10% change in size, patients were sub-grouped into TTP a <100days, 100-299 days, 200-300 days. A scatter plot was corrected according to these groups against change in size and contrast enhancement.
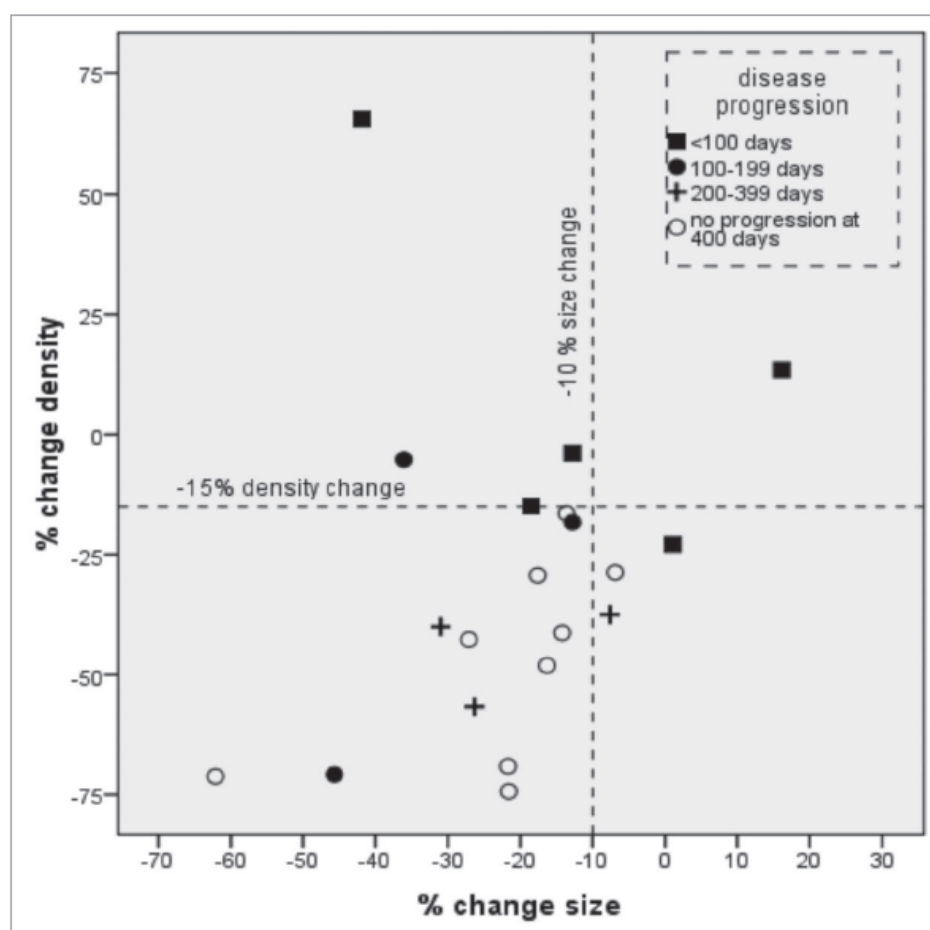
Figure 5.3. Scatter plot of change in density and change in size for all patients.

TTP groups as indicated figure from (Nathan, Vinayan et al. 2010).

5.4.   Discussion

Response assessment based on imaging modalities have been an important and unavoidable part of oncological management. With cytocidal chemotherapies, response assessment using criteria based solely on tumour size change may be entirely appropriate. With use of targeted treatments, it was noted that the RECIST defined respond rate did not correspond to the extent of clinical benefit. Response rate as per RECIST were only in the range of 10-30 % (Escudier, Pluzanska et al. 2007, Motzer, Hutson et al. 2007). Even patients who did not achieve the partial response status experienced significant prolongation of progression free survival. Hence the role of RECIST based response assessment is questionable in the setting of cytostatic targeted treatments.

Arterial based imaging is highly suitable in RCC due to its increased vascularity(Raptopoulos, Blake et al. 2001). This is particularly so, given that anti-angiogenic targeted therapies are significantly active in the treatment of advanced RCC. Arterial based imaging is thought to be a suitable method to assess clinically relevant anti-angiogenic drug induced changes in this disease. Arterial-phase contrast enhanced CT scans has been used here to evaluate standard RECIST, Choi, and modified criteria.

In this retrospective analysis we compared RECIST, Choi and the proposed "modified" Choi criteria in which both a minimum of a 10% reduction in size and a 15% reduction in density were required to define a response in metastatic RCC patients receiving

either sunitinib or cediranib. Response categorisation as defined by each criterion was correlated with RECIST defined time to progression.

With our analysis, "modified" Choi criteria was noted to be superior to RECIST and conventional Choi criteria to successfully identify a group of patients with extended TTP (median 448 days) with non-responders having a significantly shorter TTP (median 89 days).

CT based imaging has a number of advantages over other methods evaluating vascular changes in response to drug therapy such as DCE-MRI and DCE-US. Firstly, CT scanning is widely available. With the advent of CT scanners which acquire images quicker, obtaining arterial phase images will be easily achievable. DCE-MRI is not available at most centres. USS based imaging has the disadvantage that it is not suited for all anatomical sites. also has significant inter observer variation. All target lesions that are currently assessed by RECIST criteria should be amenable to assessment by our modified criteria.

Evaluation of region of interest (ROI) is one area where inter-observer and intra-observer variability could creep through. This applies to all imaging modalities. The best method to perform ROI delineation remains a topic of dispute, whole tumour ROI may be the most reproducible method rather than arbitrary smaller ROI (Goh, Halligan et al. 2008). We used the whole tumour ROI delineation for this study.

This small study requires validation on a larger dataset, ideally with images taken from a variety of scanning centres to demonstrate the broader applicability of this technique. With some of the other centres assessing CT in single portal-venous as standard, it remains to be seen if the modified response criteria could still be used. This is more so as in the portal venous phase, change or reduction in enhancement is less likely to be as distinct as in the arterial phase.

With this study, we have observed that response criteria combining changes in both size and enhancement of arterial perfusion in advanced RCC categorises the responders better. This in turn leads to a better prediction for outcome with TKI based treatment compared to standard RECIST or Choi criteria.

A cross validation of the modified Choi criteria was performed with the dataset used for the textural analysis project where modified choi criteria was tested against RECIST, Choi and textural analysis. This project is explained in chapter 6.0 of this thesis. Even though some of the patients used for the current analysis were included in the textural analysis, this constituted less than 50% of the cohort. The results the textural analysis cohort also showed an advantage for modified choi criteria over RECIST in differentiating responders vs non-responders with a statistical significance $p=0.042$.

If further validation with a larger dataset confirms superiority of modified Choi criteria over RECIST, it may essentially become a more appropriate method for response assessment in therapeutic response assessment in these group of patients.

Chapter 6.

CT texture as a potential biomarker of treatment response to TKI in metastatic renal cell carcinoma

6.1.   Introduction

Post demonstration of the use of CHOI criteria, changes in measurement of CT scan based mean contrast enhancement with treatment have been of significant interest for researchers. Different criteria have been proposed incorporating changes in size and density to measure treatment response and to act as predictive biomarkers for the response. These includes the "modified" Choi criteria proposed by us, explained in the previous chapter 5.0. Other criteria which tried to utilize the difference in CT enhancement includes SACT criteria: favourable response defined by >20% reduction in size, or >10% reduction in size and > 50% of non-lung target lesions with >20HU (House field Unit) reduction in mean attenuation, or one or more target lesions >40HU reduction in mean attenuation (Smith, Lieber et al. 2010) and MASS criteria: favourable response defined by a decrease in tumour size of ≥20% or one or more predominantly solid enhancing lesions with marked central necrosis or marked decreased attenuation (≥ 40 HU) (Smith, Shah et al. 2010).

Heterogeneity in malignant tumours is well recognized with variability between the cancer cells in a single macroscopic tumour. Differences in genetic and epigenetic make up would contribute to this heterogeneity (Beca and Polyak 2016, Gay, Baker et al. 2016). Along with variation in the cancer cells, heterogeneity is seen in the surrounding matrix and tumour blood supply. Variability seen in treatment response could possibly be attributed to these genetic and epigenetic changes.

Primary renal cell carcinoma tumours are very heterogeneous. The heterogeneity has been assessed by deep sequencing and chromosome aberration analysis (Gerlinger ,

Rowan et al. 2012). In this study showing branched evolutionary growth, up to 69% of somatic mutations were not detectable across every tumour region. These intra tumour heterogeneity represents variation in protein function and result in tumour adaptation to its surroundings with resultant significant challenges to the therapeutic effectiveness. Identification and assessment of intra-humoral heterogeneity would be a promising way to optimize biomarkers which is predictive and prognostic.

All the current proposed CT based criteria, including the modified Choi that we discussed in chapter 5.0 does not take into account this heterogeneity. A mean value of density is used in these studies to account for this heterogeneity. It is also uncertain the extent to which this heterogeneity is of clinical importance. The pathological grading of the RCC tumours, using Fuhrman's grading uses the highest grade noted in the tumour sample to grade the tumour (Motzer, Bacik et al. 2002, Beck, Patel et al. 2004, Lebret, Poulain et al. 2007). There is emerging evidence demonstrating that proportion of high-grade tumours and sarcomatoid changes seen in the tumour specimen is associated with poorer prognosis (Delahunt, Bethwaite et al. 2007).

Analysis of CT texture has been of use in differentiating malignant and benign lesions of the lung (Ganeshan, Abaleke et al. 2010). Analysis of CT texture, may describe the heterogeneity in tumour morphology that is not reflected by CT density or size.
A suggestion from computer simulation analysis studies on textural analysis suggested that that the texural analysis may in fact reflect changes in underlying vasculature (Bezy-Wendling, Kretowski et al. 2001). Exploratory studies provided predictive and

prognostic information assesed by the image brightness and coarseness in non-small

cell lung cancer and colorectal cancer (Miles, Ganeshan et al. 2009, Ganeshan, Abaleke

et al. 2010). In this chapter I explain a pilot study that was performed to assess the

use of CT textural analysis as a predictive biomarker in metastatic renal cell carcinoma

patients treated with Tyrosine kinase inhibitors (TKI).

The aim of this pilot study was

1) To assess the changes in tumour CT texture following 2 cycles of TKIs; and

2) To determine if tumour texture predicts time to progression in metastatic renal cell

cancer treated with TKIs.

This project was performed in collaboration with a research team at the University of Sussex (Brighton) who developed the software for textural analysis TexRAD®. I was involved in the clinical part of the project including planning of the study, identification of the patients according to pre-planned inclusion and exclusion criteria, collecting all necessary clinical data of patients analysed, selection and delineation of the target lesions, assessment of response for each patient and calculation of the time to disease progression. Textural analysis was performed Dr. Balaji Ganeshan and reviewed by Prof Ken Miles who were the scientific and clinical director of the TexRAD®. TexRAD® team were unaware of the clinical data and treatment outcome. Once the radiological analyses were complete, statistical analysis comparing the textural analysis and clinical outcome were performed by both team. Results have been published in a peer reviewed journal with all authors having control of the data and information submitted for publication.

V.Goh, B.Ganeshan, P.Nathan, A.Vinayan, K.Miles "Assessment of response to tyrosine kinase inhibitors in metastatic renal cell cancer: CT texture as a predictive biomarker" Radiology: 2011 Oct;26(1): 165-71 (Goh, Ganeshan et al. 2011)

In this Chapter I explain the above mentioned study with due reference to the role of other authors.

6.2. Materials and methods

Methods employed in this retrospective analysis has been detailed earlier in chapter 3.0. This involves methods used for patient selection, predetermined inclusion and exclusion criteria, Theory behind textural analysis and radiological assessment and statistical analysis. Please refer to section 3.4 for details.

6.3. Results

6.3.1. Patient selection

After assessing our institutional database, 68 patients with metastatic renal cell carcinoma treated with tyrosine kinase inhibitors were identified. This cohort of patients was considered as the potential subjects who could be enrolled into the textural analysis study. Inclusion and exclusion criteria have been assessed against these individual patients to assess their eligibility for analysis. Inclusion and exclusion criteria are explained in section 3.4.1. Of the 68 patients identified, 20 had to be excluded as they had non-contrast enhanced CT scans. Main reasons for not proceeding with contrast enhanced CT was low renal function defined as increased creatinine >150μmol/L or low glomerular filtration rate (GFR). No patients in this cohort had previous allergic reactions to iodinated contrast or failure to access intravenous cannula documented as a reason for not having contrast enhanced CT. Another 18 patients had to be excluded as the contrast enhancement in their scans were noted to be suboptimal. A total of 40 patients were selected who had baseline

contrast enhanced CT. 1 more patient had to be excluded as the patient did not

complete 2 cycles of treatment due to toxicities. Remaining 39 patients were selected

for analysis. Flow chart of the study population and selection has been demonstrated

in figure 6.1.

Figure 6.1   CT Texture assessment - Trial flow chart
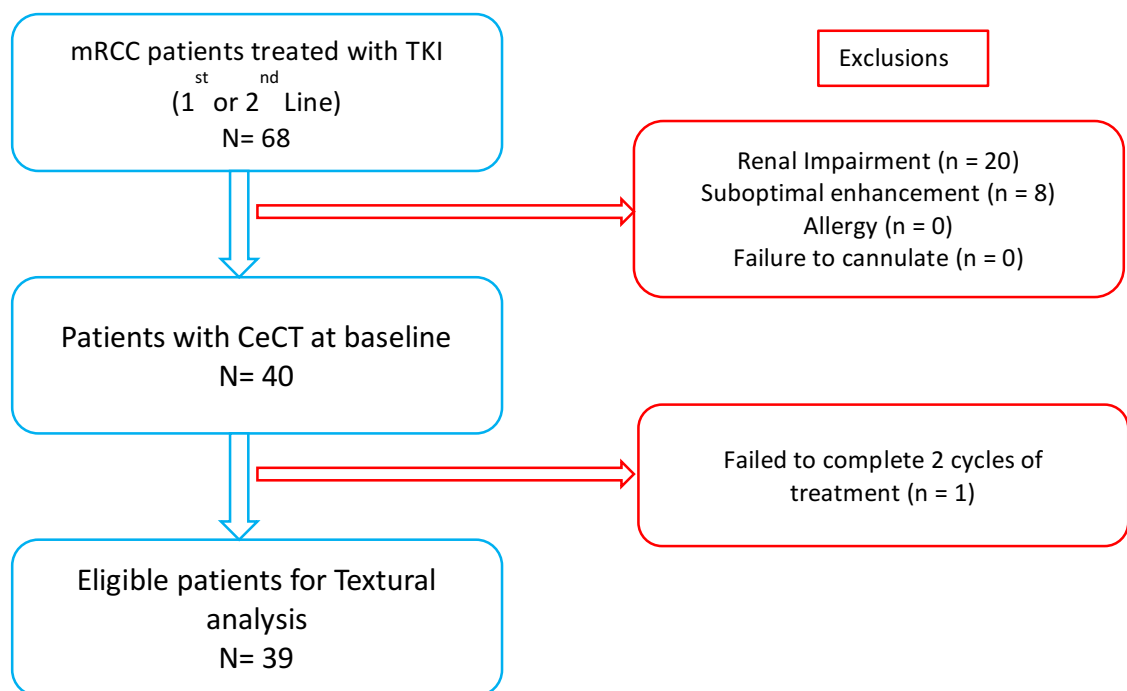
mRCC = metastatic renal cell carcinoma, TKI = Tyrosine Kinase Inhibitors, IV =

intravenous, ceCT = contrast enhanced CT.

Patients selected for textural analysis included 23 males and 16 female patients with a mean age of 61.43 years. Age range was between 38.6 to 75.8 years. Tumours in 37 patients were categorized as clear cell RCC whilst 1 patient had papillary RCC and another had higher percentage of sarcomatoid elements in the RCC histology. A variety of Tyrosine kinase inhibitors (TKI's) were used in treatment of these patients. Patients were treated with sunitinib (n=26), cedirinib (n=6), pazopanib (n=4) and regorafenib (n=3). With the 39 patients, a total of 87 target lesions were analysed with a mean of 2 and a median of 3 lesions per patients.

All patients had CT scans prior to initiation of treatment. All had CT scans done within 4 weeks of treatment and average days of difference between baseline CT scan and treatment initiation was 14.2 days. Follow up CT scans were performed after 2 cycles of treatment, which was done between week 10 and 12 of initiation of treatment. On region of interest selection (ROI), Mean ROI size was 2791 pixels (range, 72-17442 pixels).

6.3.2. Treatment response assessment

Treatment response categorization was performed by RECIST, Choi and modified Choi criteria following two cycles of treatment.

Of the 39 patients, according to RECIST criteria, 6 patients had partial response to treatment (PR) and 32 patients had Stable disease (SD). One patient was noted to have progressed with in the time. Categorization with Choi criteria showed 33 responders with 3 patients each had stable disease and progressive disease. With the modified Choi criteria, the numbers were 22, 14 and 3 for PR, SD and PD respectively (Table 6.1).

Table 6.1   Response Categorization after 2 cycles of treatment with TKI's

Response Criteria	Partial Response	Stable Disease	Progressive Disease
RECIST	6 (15)	32 (82)	1 (3)
Choi	33 (84)	3 (8)	3 (8)
Modified Choi	22 (56)	14 (36)	3 (8)

Data given are in absolute numbers with percentages in parentheses. Table adapted from our publication (Goh, Ganeshan et al. 2011)

6.3.3. Textural analysis

Textural analysis was performed as explained in the materials and methods section 3.4.2. Images underwent a second degree Gaussian filtration followed by application of Laplacian filter as per the equations

Equation 3.5:

$$G(x, y) = e^{-\frac{x^2+y^2}{2\sigma^2}}$$

Equation-3.6:

$$\nabla^2 G(x, y) = \frac{-1}{\pi\sigma^4}\left(1 - \frac{x^2 + y^2}{2\sigma^2}\right)e^{\left(\frac{x^2+y^2}{2\sigma^2}\right)}$$

"∇^2" - Laplacian of Gaussian distribution.

"G" – Gaussian distribution

"x" and "y" are co-ordinates of the image matrix.

"σ" - Standard deviation of the Gaussian distribution.

After filtration, σ values of 1.0, 1.5, 1.8, 2.0 and 2.5 were used in images quantification of texture (described in section 3.4.2.2). This was followed by calculation of entropy "e" and uniformity "u".

Equation 3.7:

$$e = -\sum_{l=1}^{k}[p(l)\,log_2[p(l)]]$$

Equation 3.8:

$$u = \sum_{l=1}^{k}[p(l)]^2$$

l is the pixel value (between *l* =1 to *k*) in the the ROI and

p(l) the probability of the occurrence of that pixel value.

Table 6.2a and 6.2b summarizes the mean absolute scale values of entropy (e) and

uniformity (u) with and without filtration. For filtration, σ values: 1, 1.5, 1.8, 2 and 2.5

were used at baseline and following 2 cycles.

Table 6.2a   Entropy at baseline and after 2cycles with different filter scales

Filter scale value	Baseline	After 2 treatment	Change (%)
No filtration	6.95 (± 0.37)	6.7 (± 0.43)	-3.08 (±4.34)
1.0	3.06 (± 0.55)	2.6 (± 0.84)	-15.20 (± 23.35)
1.5	2.31 (± 0.72)	1.81 (± 0.92)	-21.73 (±39.66)
1.8	1.89 (± 0.81)	1.53 (± 0.92)	-16.96 (± 50.40)
2.0	1.62 (± 0.85)	1.35 (± 0.88)	-9.51 (± 133.76)
2.5	1.23 (± 0.81)	1.08 (± 0.77)	-45.77 (± 139.91)

Table 6.2b   Uniformity at baseline and after 2cycles with different filter scales

Filter scale value	Baseline	After 2 treatment	Change (%)
No filtration	0.012 (± 0.002)	0.012 (± 0.004)	+21.0 (± 28.36)
1.0	0.47 (± 0.07)	0.53 (± 0.13)	+14.72 (± 20.80)
1.5	0.59 (± 0.11)	0.67 (± 0.16)	+14.91 (± 20.21)
1.8	0.66 (± 0.13)	0.72 (± 0.16)	+10.61 (± 19.48)
2.0	0.71 (± 0.15)	0.76 (± 0.15)	+8.15 (± 17.99)
2.5	0.78 (± 0.14)	0.80 (± 0.13)	+ 4.96 (± 17.26)

Table 6.2a and 6.2b showing mean value of entropy and uniformity for baseline and after two cycles of treatment. Change between mean and after two cycles recorded in column 4 as percentage. Values in parentheses are standard deviation. Tables are adapted from our publication (Goh, Ganeshan et al. 2011)

Of the 39 patients included and analysed in the study, 26 patients have had disease progression within the time of data collection. On analysis of time to progression, median time to progression in days was 336 in this cohort with a range 57 to 1364 days.

Ability of textural parameters to identify responders and non-responders to treatment was assessed. Imaging textural characteristics including entropy and uniformity at baseline, post completion of two cycles of treatment and percentage change in the textural characters after two cycles of treatment were analysed to assess if these could correlate with time to progression.

ROC curve and Kaplan-Meier analyses were performed for entropy and uniformity at different scale values. With statistical significance (p) calculated from Kaplan-Meier analyses. This is summarized in Table 6.3

At baseline, significant p values defined as <0.05 were noted for entropy at 2.5 filter scale (p=0.02). With uniformity assessment significant p value were noted at filter scales 1.8 and above (p=0.02). With analysis of change in these parameters (as percentages) from baseline to cycle 2, entropy and uniformity showed significance at different filter values. For percentage entropy change, significance was noted with filter 1.8 (p=0.05) and 2.0 (p=0.03) whilst filters 1.0 (p = 0.02), 2.0 (p=0.02) and 2.5 (p=0.0008) showed significance with percentage change in uniformity.

With a filter scale value of 2.5, both baseline entropy and uniformity and percentage

change of uniformity were significant thus predictors of time to progression.

With the ROC curve analysis, using a threshold change of ≤-2% in uniformity at a scale

value of 2.5, the area under the ROC curve was statistically significant (p=0016) and

AUC=0.71 (95% CI 0.53, 0.85). This is shown in Figure 6.2.
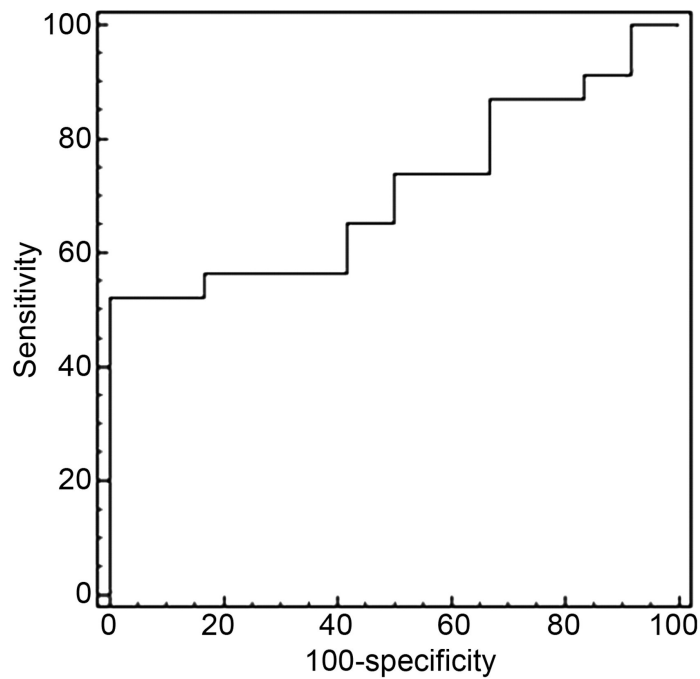
Figure 6.2   ROC curve showing percentage change in uniformity.

Adapted from our publication (Goh, Ganeshan et al. 2011)

Change in uniformity was compared to RECIST, Choi and modified Choi criteria in separating responders from non-responders to treatment. Kaplan-Meier curves analyses was performed for all three criteria and uniformity and difference between these techniques were assessed.

At a threshold change of -2% with uniformity, textural change was able to separate responders from non-responders. With Kaplan-Meier analysis comparing all four criteria, percentage change in uniformity was statistically more significant than for RECIST, Choi, and Modified Choi criteria (p=0.008 versus p=0.267, p=0.053, p=0.042 respectively; see Figure 6.3.

Cox regression analysis indicated that the percentage change in coarse uniformity was an independent predictor (odds ratio, OR =4.02 (95% CI 1.52,10.65); p=0.0053), while Modified Choi criteria were not significant (OR=1.07 (95% CI 0.38,3), p=0.8911). This indicated that there was no interaction between texture uniformity and the enhancement and size change (assessed by the modified Choi criteria).

Figure 6.3   Kaplan Meier curve according to different criteria
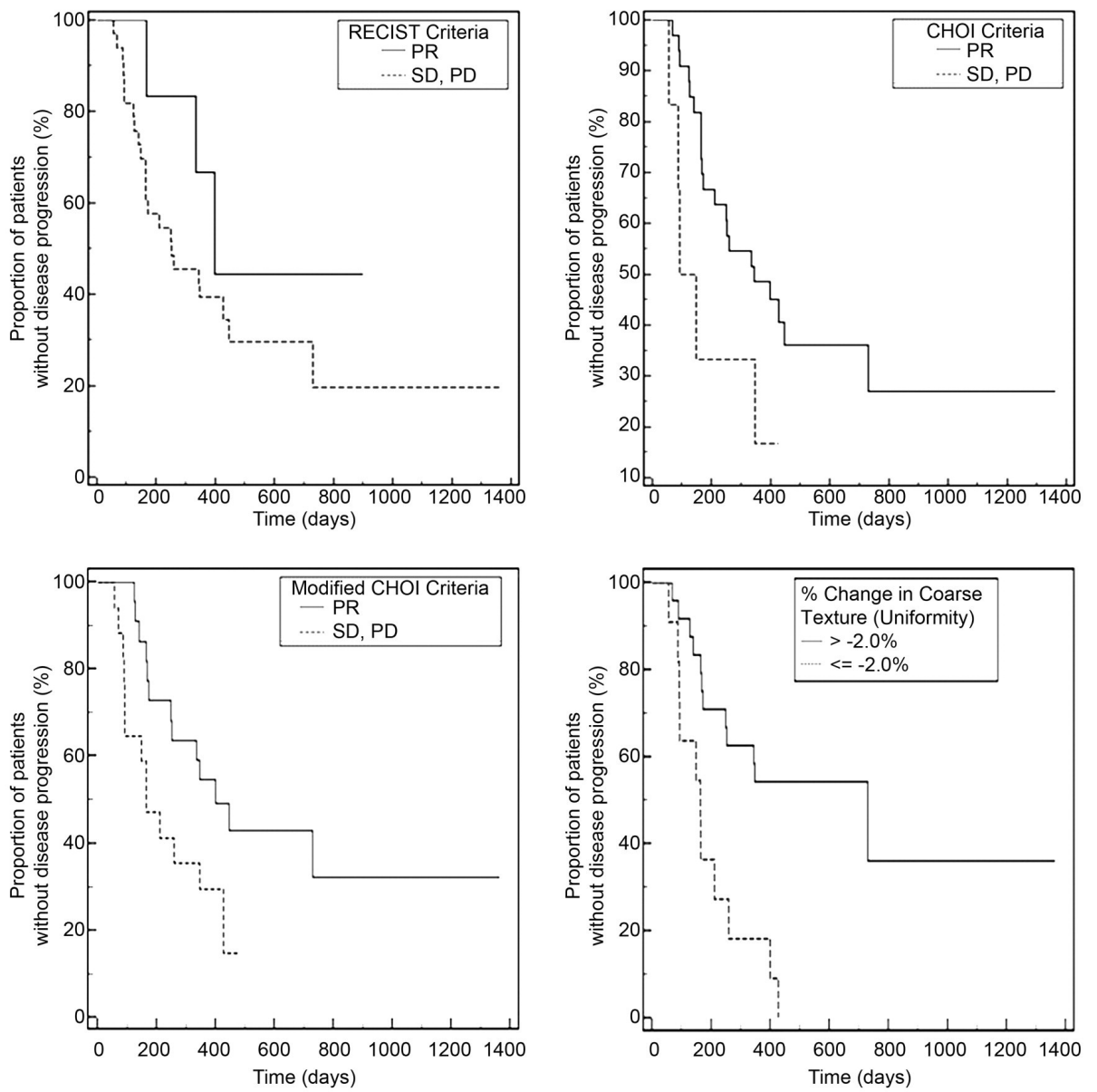
Fig 6.3 Kaplan Meier curve for responder's vs non-responder's with different criteria

RECIST, Choi, modified Choi and percentage change in uniformity.

Table 6.3   Summary of ROC curve and Kaplan-Meier analysis

Filter scale value	Entropy		Uniformity	
	ROC threshold %	P value	ROC threshold %	P value
Baseline				
Unfiltered	>6.33	0.28	<0.01	0.54
1.0	>2.48	0.10	<0.52	0.21
1.5	>1.46	0.09	>0.4	0.17
1.8	>1.07	0.09	>0.48	0.02
2.0	≤2.65	0.07	>0.48	0.02
2.5	≤2.33	0.02	>0.55	0.02
Percentage change				
Unfiltered	<-5.26	0.19	>13.96	0.13
1.0	>-6.66	0.11	≤2.58	0.02
1.5	>-7.80	0.15	<3.14	0.07
1.8	>-13.11	0.05	≤5.23	0.07
2.0	>-5.35	0.03	≤0.49	0.02
2.5	>4.02	0.11	≤2.00	0.0008

Summary of ROC curve and Kaplan-Meier analysis with different filter values at baseline and change of the parameters after treatment. P value is obtained from Kaplan-Meier analysis. Adapted from our publication (Goh, Ganeshan et al. 2011)

6.4.   Discussion

Heterogeneity is a well-recognized feature of malignancy. Heterogeneity in renal cell carcinoma is well documented. Genetic and epigenetic changes contribute to the heterogeneity in cancer cells and in the surrounding matrix. Heterogeneity of the tumour blood supply is suggested to be associated with multiple factors including oxidative stress, promotion of survival factors, and genomic instability (Nelson, Tan et al. 2004). With change in vascularity, cellular fraction of the tumour may be altered and changes in cell behaviour which could impact on the response of these cells to treatment. Poor delivery of chemotherapeutic agents to areas of low vascularity could be a significant problem. It is also well recorded that tumours with hypoxia are more radiation resistant.

Assessing heterogeneity with standard CT scan alone is difficult as much of the visible heterogeneity in CT is due to photon noise. This has no biological significance and could in fact mask any underlying heterogeneity.

CT textural analysis with filters that select for image features can reduce the interference of photon noise and end up enhancing the heterogeneity that is biologically relevant. Quantification of the parameters with entropy and uniformity at relevant scales can thus be of clinical relevance.

In the study described here we found that tumour heterogeneity had reduced after two cycles of treatment. This was evident from the change in entropy (which reflect

irregularity) and increase in uniformity. These changes are consistent with change in

vascularity of the tumour with development of necrosis.

Textural changes in uniformity after two cycles of treatment have been the best

parameters which correlate to clinical effectiveness measured as time to progression.

In our cohort of patients, percentage change in textural uniformity after two cycles of

treatment (above 2.0) was superior than the standard RECIST criteria or the combined

size and enhancement criteria (Choi and modified Choi) in predicting the time to

progression. Percentage change in uniformity, using a threshold of -2% or less at a

coarse scale (filter value 2.5) selected the patients who responded to treatment than

partial response suggested by RECIST, Choi or modified Choi criteria. Hence the

textural analysis provides additional information which could be complementary to

assess and select patients who are unlikely to respond to a treatment thus avoiding

toxicities in those individuals.

Along with the change in uniformity, baseline entropy and uniformity at a coarse scale

also correlated with time to progression, thus indicating that baseline heterogeneity

be potentially useful as a predictive biomarker of treatment response

An advantage of texture analysis is that it imposes no additional burden on a patient,

as it is an additional post processing step of standard CT images that were obtained

for standard response assessment.

One of the limitations with this technique is that it requires contrast enhanced CT scanning. Our study suggested approximately 29% of patients had to be excluded due to renal function abnormality. Thus this test may not be of use in around 1/3rd of patients in this disease (Nathan, Vinayan et al. 2010). Textural analysis may still give some valuable information on underlying heterogeneity without the use of contrast. This has been assessed in non-small cell lung cancer and colorectal cancer but never been assessed in renal cell carcinoma (Miles, Ganeshan et al. 2009, Ganeshan, Abaleke et al. 2010).

Phase of contrast enhancement and acquisition parameters could also affect the textural parameters. However, to date there have been no studies which explore these issues reliably.

Chapter 7.

Discussion

In summary, this thesis incorporates three studies assessing metastatic RCC patients treated with anti-angiogenic therapy. All studies aimed at evaluating imaging based techniques to calculate changes related to antiangiogenic therapy and treatment response.

Vascular parameters of DCE-MRI were used to assess whether addition of interferon-α2a improved the antiangiogenic effect of bevacizumab. Ability of DCE-MRI vascular parameters to act as predictive biomarker of treatment response was also evaluated in this study. With two contrast enhanced CT based studies were aimed at evaluating a) "modified" Choi criteria and b) Textural analysis as possible predictive biomarker of treatment response.

The two major phase-3 trials (AVOREN & CALBG 90206), lacked a single agent bevacizumab arm and the additional benefit supplemented by interferon on bevacizumab is therefore unknown. With a phase-2 clinical trial, we aimed to answer this important scientific question using DCE-MRI as the method of assessment.

The trial designed as a prospective, multi-centric, randomised control trial with 10 patients in each arm. The trial was powered so as to identify the true differences of DCE-MRI parameters with in the treatment arm before and after treatment and to assess the between arms robustly.

Randomisation was performed by an independent person with no clinical input with the patients to avoid any treatment bias. The three arms of randomisation gave us the opportunity to explore the dose response to IFN if a synergistic effect was noted on the anti-vascular effect of bevacizumab. Continued effect of lower dose IFN in response and a better toxicity profile was seen in a previous retrospective analysis published by Melicher et.al (Melichar, Koralewski et al. 2008). Our trial hence also aimed to reaffirm these findings in a prospective phase 2 trial. Furthermore, using two DCE-MRI at the baseline gave us a unique opportunity to assess and account for the natural variation of vascular and perfusion changes to these tumours. These perfusion changes could have otherwise confounded the results of the DCE-MRI vascular parameters calculated in the trial. A statistical calculation of repeatability co-efficient (r) and assessment of r-value individually in each group based on the number of patients (n) was hence used to analyse the results so as to reaffirm that the results obtained are likely to be statistically robust.

Introduction of dose escalation of interferon in Arm-C at two weeks gave us enabled the investigators to assess the toxicity of IFN in all patients at the lower dose prior to escalation. Having a DCE-MRI scan at two weeks prior to dose escalation also gave us an opportunity to directly compare the bev only arm (Arm-A) with bev + IFN arms (Arm B+C) with a larger sample number in order to validate the statistics.

The trial was technically challenging and was difficult to accrue. It portrays the difficulties that an investigator driven phase 2 trial in NHS could face. Competing first line trials and inability to access sunitinib in NHS at some centre's after patient had been treated on bevacizumab on trial resulted in very slow recruitment and one of the three centre being unable to recruit any patients. Many patients even though had metastatic disease did not have lesions which could be reliably assessed with DCE-MRI. Even among patients with lesions thought to be suitable for analysis, 25% were unable to be analysed due to technical issues. This was a major limitation in accrual and hence impacted on the reliable analysis of the trial outcome.

Analysis of DCE-MRI is dependent of the choice of ROI assessment. As performed in the previous studies where DCE-MRI technique have been used, we have opted to use the whole tumour volume in the MRI slice as the region of interest. A possible criticism of this approach could be related to the impact of necrotic tissue, if present in the tumour, to the DCE-MRI derived vascular parameters. One approach in this setting would be to restrict the ROI to the periphery of the tumour. This approach need to be investigated in further studies. We decided against this as it was felt that restricting the ROI to some part of the tumour is likely to introduce sampling bias given the heterogenous nature of RCC tumours. Previous work from Goh et.al assessing different methods of ROI delineation using perfusion CT suggested that whole tumour ROI would be the most reproducible method of assessment (Goh, Halligan et al. 2008).

One of the limitations that we had in this trial is that the ROI assessment was performed by a single investigator. Inter-investigator and even intra-investigator variability have been documented in the assessment of ROI in different trials. It is important that the technique suggested is reproducible in other centres by other investigators and the discordance in assessment of the ROI is minimised. In order to minimise the impact of a single investigator effect, the ROI volumes were cross assessed by a consultant radiologist with more than 15years experience in cancer imaging. ROI discordance were discussed and modified if necessary.

We concentrated on the changes in K^{trans} to the proposed treatment as this was the most studied and associated DCE-MRI variable with changes in vascularity. In our study, considering the limitations of the study, no definite correlation was found between change K^{trans} and addition of interferon to bevacizumab which was the primary endpoint of the study. This was despite the effect size analysis calculation to account for the low recruitment. Exploratory analysis showed that the changes in K^{trans} and K_{ep} with treatment could be potential candidates to be investigated further to act as predictive biomarker to therapy. Patients with a clinical benefit measured as PFS of >6months were noted to have significant reduction in Kep as early as week2 (p=0.03). With the small sample size that was analysed, we were unable to determine whether this represented a true change and hence would warrant assessment in a large cohort for confirmation.

Combining change in size and arterial enhancement, "modified" Choi criterion has been able to identify a group of patients who derived more clinical benefit with extended time to disease progression. By combining decrease in size by 10% with reduction of arterial enhancement by 15% to define responders, "modified" Choi criteria was found to be statistically superior than standard RECIST and Choi criteria in differentiating responders reliably in our cohort of patients. If this effect is to hold to true in a larger cohor, modified choi criterion may become an appropriate tool for assessing these cohort of patients.

Contrast enhanced CT based textural analysis requires post processing with the support of a computer based algorithm. This technique has the advantage that it has the ability to evaluate imaging based heterogeneity in mRCC (calculated by entropy and uniformity) which the other response criteria are unable to account for. Tumour heterogeneity is a well-recognised feature of renal cell carcinoma. Complex heterogeneity seen in the cancer cells, surrounding matrix and the vasculature could result in differential response to a therapy and is likely due to the genetic and epigenetic changes acquired by the tumour during its pathogenesis or as response to therapeutic intervention by natural selection. As discussed earlier in section 6.4, heterogeneity of the tumour blood supply is suggested to be associated with multiple factors including oxidative stress, promotion of survival factors, and genomic instability (Nelson, Tan et al. 2004). With the change in vascularity, the cellular fraction of the tumour and its behaviour varies and this can also impact on the response of

these cells to treatment. This could result in poor delivery of chemotherapeutic agents. Resistance to radiotherapy has also been well documented in areas with significant hypoxia. Previous studies with computer simulation and also human studies have suggested that the textural changes reflect change in vascularization (Bezy-Wendling, Kretowski et al. 2001).

Assessing heterogeneity with standard CT scan alone is difficult as much of the visible heterogeneity in CT is due to photon noise. This has no biological significance and could in fact mask any underlying heterogeneity. CT textural analysis with filters that select for image features can reduce the interference of photon noise and end up enhancing the heterogeneity that is biologically relevant. Quantification of the parameters with entropy and uniformity at relevant scales can thus be of clinical relevance

In our cohort of patients, ability of textural analysis to act as a predictive biomarker was consistently demonstrated. Increase in textural uniformity after two cycles of treatment was recognized to be good surrogate, better than standard RECIST or combined size and enhancement criteria in identifying patient subgroup who is likely to benefit from treatment. Baseline entropy and uniformity at a coarse scale was also noted to have some correlation in predicting the response to therapy. This suggests the possibility of predicting whether a patient is likely to have a good benefit from the proposed therapy even before initiating it.

Advantage of both modified Choi criteria and textural assessment are that they do not impose any additional burden on a patient as it is the standard contrast enhanced CT images which are used for additional processing and analysis. CT scans are currently available in majority of centres in the western world. Clinical expertise to analyse the images and availability of this technique is much more widespread than the DCE-MRI technique. CT scans also have the advantage that this is less operator dependent than techniques as USS.

A significant limitation of both these studies is the small number of patients who underwent analysis. A cross validation was attempted for the modified choi criterion using the cohort used for textural analysis. But even here the sample numbers remain low and it need to be seen if the benefits seen would hold true in a larger cohort. Validation of the technique on a prospective clinical database or use of large cohorts from registration trials of the VEGF TKI's may be options to validate these techniques effectively.

Efficacy of textural analysis is being assessed in different tumour types. There has been studies of this technique in small cell lung cancer, colorectal cancer and brain tumours. With each tumour type showing differing degrees of heterogeneity, it will be curious to see whether the textural changes hold true in different tumour type assessment. There may also be potential to correlate the textural changes as seen with contrast enhanced CT with spatially matched histological results obtained from the surgical resection specimen.

It is well recognised that the phase of intravenous contrast enhancement influences the detection of lesion in RCC (Hollett, Jeffrey et al. 1995, Ascenti, Visalli et al. 2004). RCC metastases are highly vascular and is likely to show early enhancement and rapid washout (Namasivayam, Martin et al. 2007, Muglia and Prando 2015). It is likely that the enhancement changes detected in the portal-venous phase alone will be less prominent and may not be representative in characterising differences post therapy. With some centres assessing the abdomen and pelvis with CT scan in single portal-venous phase as standard and in those conditions, "modified" Choi based categorisation may not be precise in its categorisation.

As a follow up study from the results discussed in chapter 5.0, we have compared difference in treatment response assessment between arterial and portal-venous enhancement in renal cell carcinoma. This study presented as an abstract in RSNA (Juttla.J 2010), demonstrated the importance of the use of the appropriate phase of image enhancement for response categorisation. Results from this analysis shows change in response type for some patients with suggestion that arterial phase imaging may be better in assessing the vascular effects on anti-angiogenic therapy in RCC.

The phase of image capture will be an area to concentrate in future trials and also in assessing to expand these techniques to perform response assessment in other disease types. It may be that the timing of image acquisition could end up being significant in different tumour types or subtypes. With improvement in the CT technology and faster acquisition of images, it is possible that we may be able to

develop specific or combination of imaging sequences according to different disease types or the therapeutic agents that the patients are are being treated with so as to get the maximum clinically significant information out of these imaging techniques.

With the prospective trial reported in this thesis where DCE-MRI technique was utilised, K^{trans} induced response was used as the primary end point as it has been the most researched and validated vascular parameter associated with this technique.

Our study suggests the possibility that effusion constant Kep could be an important parameter that we have to investigate in further studies where effects of anti-angiogenics are monitored. This is supported by early mouse xenograft studies reported by Song and colleagues (Song, Cho et al. 2013). This study described statistical significant association between Kep and tumour volume changes suggesting the use of Kep as a biomarker of anti-angiogenic therapy. Effects that we have observed in these studies need to be validated by observation in a larger sample size.

The land scape of treatment of malignancies including metastatic renal cell carcinoma continues to evolve with new research. Immunotherapy modalities as anti-CTLA4 antibody ipilimumab and check point inhibitor drugs such as nivolumab have now shown benefit in treatment of mRCC (Motzer, Escudier et al. 2015, George, Motzer et al. 2016, Sidaway 2016). This is resulting in a change in treatment paradigm in treatment naive metastatic RCC patients especially with a high risk Motzer score. VEGF-TKI still remains an important treatment modality in metastatic RCC treatment.

Appropriate sequencing or combination of these immune-stimulant drugs and VEGF TKI are still unknown and is a field of ongoing research.

It is also worth to note that the effect of immunotherapeutic drugs and the clinical benefits obtained from these treatment modalities does not correlate to the size change as predicted by RECIST critieria. It has been reported that on treatment with immunotherapeutic agents, the response obtained could follow different patterns including an initial increase in tumour burden which if classified with traditional RECIST criteria would be regarded as progressive disease resulting in recommendation of treatment withdrawal. A new modified iRECIST criteria have been recently proposed for assessment of response to treatment with immunotherapeutic agents (Seymour, Bogaerts et al. 2017).

With any modality of treatment, accurate therapeutic assessment is vital. RECIST continue to be the tool to assess response despite being imperfect and being unable to identify all subgroups who may derive clinical benefit from these targeted therapies. Advanced imaging techniques have the potential to serve as diagnostic, prognostic and predictive biomarkers. Further studies are required to identify the appropriate imaging biomarker for a meaningful response assessment. The studies reported here signifies the opportunity of using imaging modality or combination of imaging modalities to act as prognostic or predictive biomarkers in a therapeutic setting. This would open the way for further studies to improve our understanding for imaging based response assessment of renal cell carcinoma and other malignancies.

Chapter 8.

Reference

A Ritchie, G. G., M Parmar - Medical Research Council Renal Caner Collaborators (1999). "Interferon-alpha and survival in metastatic renal carcinoma: early results of a randomised controlled trial. Medical Research Council Renal Cancer Collaborators." Lancet **353**(9146): 14-17.

Altman DG, B. J. (1983). "Measurement in Medicine: the Analysis of Method Comparison Studies." The Statistician **32**: 307-317.

Antoch, G., F. M. Vogt, L. S. Freudenberg, F. Nazaradeh, S. C. Goehde, J. Barkhausen, G. Dahmen, A. Bockisch, J. F. Debatin and S. G. Ruehm (2003). "Whole-Body Dual-Modality PET/CT and Whole-Body MRI for Tumor Staging in Oncology." JAMA **290**(24): 3199-3206.

Ascenti, G., C. Visalli, A. Genitori, A. Certo, A. Pitrone and S. Mazziotti (2004). "Multiple hypervascular pancreatic metastases from renal cell carcinoma: dynamic MR and spiral CT in three cases." Clin Imaging **28**(5): 349-352.

Banks, R. E., P. Tirukonda, C. Taylor, N. Hornigold, D. Astuti, D. Cohen, E. R. Maher, A. J. Stanley, P. Harnden, A. Joyce, M. Knowles and P. J. Selby (2006). "Genetic and epigenetic analysis of von Hippel-Lindau (VHL) gene alterations and relationship with clinical variables in sporadic renal cancer." Cancer Res **66**(4): 2000-2011.

Basappa, N. S., P. Elson, A.-R. Golshayan, L. Wood, J. A. Garcia, R. Dreicer and B. I. Rini (2011). "The impact of tumor burden characteristics in patients with metastatic renal cell carcinoma treated with sunitinib." Cancer **117**(6): 1183-1189.

Batchelor, T. T., A. G. Sorensen, E. di Tomaso, W. T. Zhang, D. G. Duda, K. S. Cohen, K. R. Kozak, D. P. Cahill, P. J. Chen, M. Zhu, M. Ancukiewicz, M. M. Mrugala, S. Plotkin, J. Drappatz, D. N. Louis, P. Ivy, D. T. Scadden, T. Benner, J. S. Loeffler, P. Y. Wen and R. K. Jain (2007). "AZD2171, a pan-VEGF receptor tyrosine kinase inhibitor, normalizes tumor vasculature and alleviates edema in glioblastoma patients." Cancer Cell **11**(1): 83-95.

Beca, F. and K. Polyak (2016). "Intratumor Heterogeneity in Breast Cancer." Adv Exp Med Biol **882**: 169-189.

Beck, S., M. Patel, M. Snyder, M. Kattan, R. Motzer, V. Reuter and P. Russo (2004). "Effect of papillary and chromophobe cell type on disease-free survival after nephrectomy for renal cell carcinoma." Annals of Surgical Oncology **11**(1): 71-77.

Benjamin, L. E., D. Golijanin, A. Itin, D. Pode and E. Keshet (1999). "Selective ablation of immature blood vessels in established human tumors follows vascular endothelial growth factor withdrawal." J Clin Invest **103**(2): 159-165.

Bezy-Wendling, J., M. Kretowski, Y. Rolland and W. Le Bidon (2001). "Toward a better understanding of texture in vascular CT scan simulated images." IEEE Trans Biomed Eng **48**(1): 120-124.

Bharwani, N., M. E. Miquel, T. Powles, P. Dilks, A. Shawyer, A. Sahdev, P. D. Wilson, S. Chowdhury, D. M. Berney and A. G. Rockall (2014). "Diffusion-weighted and multiphase contrast-enhanced MRI as surrogate markers of response to neoadjuvant sunitinib in metastatic renal cell carcinoma." Br J Cancer **110**(3): 616-624.

Biomarkers_Definitions_Working_Group (2001). "Biomarkers and surrogate endpoints: preferred definitions and conceptual framework." Clin Pharmacol Ther **69**(3): 89-95.

Bland, J. M. and D. G. Altman (1986). "Statistical methods for assessing agreement between two methods of clinical measurement." <u>Lancet</u> **1**(8476): 307-310.

Bland, J. M. and D. G. Altman (1996). "Measurement error proportional to the mean." <u>Bmj</u> **313**(7049): 106.

Bracarda, S., C. Porta, C. Boni, A. Santoro, C. Mucciarini, A. Pazzola, E. Cortesi, D. Gasparro, R. Labianca, F. Di Costanzo, A. Falcone, M. Cinquini, C. Caserta, C. Paglino and V. De Angelis (2013). "Could interferon still play a role in metastatic renal cell carcinoma? A randomized study of two schedules of sorafenib plus interferon-alpha 2a (RAPSODY)." <u>Eur Urol</u> **63**(2): 254-261.

Brugarolas, J. (2014). "Molecular genetics of clear-cell renal cell carcinoma." <u>J Clin Oncol</u> **32**(18): 1968-1976.

Buckley, D. L., P. J. Drew, S. Mussurakis, J. R. Monson and A. Horsman (1997). "Microvessel density of invasive breast cancer assessed by dynamic Gd-DTPA enhanced MRI." <u>J Magn Reson Imaging</u> **7**(3): 461-464.

Carmeliet, P. and R. K. Jain (2000). "Angiogenesis in cancer and other diseases." <u>Nature</u> **407**(6801): 249-257.

Chan, Y., K. Chan, W. Lam and C. Metreweli (1997). "Comparison of whole body MRI and radioisotope bone scintigram for skeletal metastases detection." <u>Chin Med J (Engl)</u> **110**(6): 485-489.

Chen, Q. S., R. Crownover and M. S. Weinhous (1999). "Subunity coordinate translation with Fourier transform to achieve efficient and quality three-dimensional medical image interpolation." <u>Med Phys</u> **26**(9): 1776-1782.

Choi, H. (2008). "Response Evaluation of Gastrointestinal Stromal Tumors." <u>Oncologist</u> **13**(suppl_2): 4-7.

Choi, H., C. Charnsangavej, S. C. Faria, H. A. Macapinlac, M. A. Burgess, S. R. Patel, L. L. Chen, D. A. Podoloff and R. S. Benjamin (2007). "Correlation of Computed Tomography and Positron Emission Tomography in Patients With Metastatic Gastrointestinal Stromal Tumor Treated at a Single Institution With Imatinib Mesylate: Proposal of New Computed Tomography Response Criteria." <u>J Clin Oncol</u> **25**(13): 1753-1759.

Chris Protzel, M. M., Oliver W. Hakenberg (2012). "Epidemiology, Aetiology and Pathogenesis of Renal Cell Carcinoma." <u>European Urology Supplements</u> **11**: 52-59.

Clamp, A. R. and G. C. Jayson (2005). "The clinical potential of antiangiogenic fragments of extracellular matrix proteins." <u>Br J Cancer</u> **93**(9): 967-972.

Cockcroft, D. W. and M. H. Gault (1976). "Prediction of creatinine clearance from serum creatinine." <u>Nephron</u> **16**(1): 31-41.

Coppin, C., F. Porzsolt, J. Kumpf, A. Coldman and T. Wilt (2000). "Immunotherapy for advanced renal cell cancer." <u>Cochrane Database Syst Rev</u>(3): Cd001425.

CRUK. (2013). "KIdney cancer statistics." from http://www.cancerresearchuk.org/health-professional/cancer-statistics/statistics-by-cancer-type/kidney-cancer.

de Bazelaire, C., D. C. Alsop, D. George, I. Pedrosa, Y. Wang, M. D. Michaelson and N. M. Rofsky (2008). "Magnetic Resonance Imaging–Measured Blood Flow Change after Antiangiogenic Therapy

with PTK787/ZK 222584 Correlates with Clinical Outcome in Metastatic Renal Cell Carcinoma." Clinical Cancer Research **14**(17): 5548-5554.

De Bazelaire, C., N. M. Rofsky, G. Duhamel, M. D. Michaelson, D. George and D. C. Alsop (2005). "Arterial spin labeling blood flow magnetic resonance imaging for the characterization of metastatic renal cell carcinoma1." Academic Radiology **12**(3): 347-357.

Delahunt, B., P. B. Bethwaite and J. N. Nacey (2007). "Outcome prediction for renal cell carcinoma: evaluation of prognostic factors for tumours divided according to histological subtype." Pathology **39**(5): 459-465.

Desar, I. M., E. G. ter Voert, T. Hambrock, J. J. van Asten, D. J. van Spronsen, P. F. Mulders, A. Heerschap, W. T. van der Graaf, H. W. van Laarhoven and C. M. van Herpen (2011). "Functional MRI techniques demonstrate early vascular changes in renal cell cancer patients treated with sunitinib: a pilot study." Cancer Imaging **11**: 259-265.

Dowlati, A., K. Robertson, M. Cooney, W. P. Petros, M. Stratford, J. Jesberger, N. Rafie, B. Overmoyer, V. Makkar, B. Stambler, A. Taylor, J. Waas, J. S. Lewin, K. R. McCrae and S. C. Remick (2002). "A phase I pharmacokinetic and translational study of the novel vascular targeting agent combretastatin a-4 phosphate on a single-dose intravenous schedule in patients with advanced cancer." Cancer Res **62**(12): 3408-3416.

ECOG-ACRIN. (1982). from http://ecog-acrin.org/resources/ecog-performance-status.

Edge, S. and C. Compton (2010). "The American Joint Committee on Cancer: the 7th Edition of the AJCC Cancer Staging Manual and the Future of TNM." Annals of Surgical Oncology **17**(6): 1471-1474.
Eisenhauer, E. A., P. Therasse, J. Bogaerts, L. H. Schwartz, D. Sargent, R. Ford, J. Dancey, S. Arbuck, S. Gwyther, M. Mooney, L. Rubinstein, L. Shankar, L. Dodd, R. Kaplan, D. Lacombe and J. Verweij (2009). "New response evaluation criteria in solid tumours: revised RECIST guideline (version 1.1)." Eur J Cancer **45**(2): 228-247.

Ellis, L. M. and D. J. Hicklin (2008). "Pathways mediating resistance to vascular endothelial growth factor-targeted therapy." Clin Cancer Res **14**(20): 6371-6375.

Escudier, B., J. Bellmunt, S. Negrier, E. Bajetta, B. Melichar, S. Bracarda, A. Ravaud, S. Golding, S. Jethwa and V. Sneller (2010). "Phase III trial of bevacizumab plus interferon alfa-2a in patients with metastatic renal cell carcinoma (AVOREN): final analysis of overall survival." J Clin Oncol **28**(13): 2144-2150.

Escudier, B., T. Eisen, W. M. Stadler, C. Szczylik, S. Oudard, M. Siebels, S. Negrier, C. Chevreau, E. Solska, A. A. Desai, F. Rolland, T. Demkow, T. E. Hutson, M. Gore, S. Freeman, B. Schwartz, M. Shan, R. Simantov and R. M. Bukowski (2007). "Sorafenib in advanced clear-cell renal-cell carcinoma." N Engl J Med **356**(2): 125-134.

Escudier, B., T. Eisen, W. M. Stadler, C. Szczylik, S. Oudard, M. Staehler, S. Negrier, C. Chevreau, A. A. Desai, F. Rolland, T. Demkow, T. E. Hutson, M. Gore, S. Anderson, G. Hofilena, M. Shan, C. Pena, C. Lathia and R. M. Bukowski (2009). "Sorafenib for Treatment of Renal Cell Carcinoma: Final Efficacy and Safety Results of the Phase III Treatment Approaches in Renal Cancer Global Evaluation Trial." J Clin Oncol **27**(20): 3312-3318.

Escudier, B., A. Pluzanska, P. Koralewski, A. Ravaud, S. Bracarda, C. Szczylik, C. Chevreau, M. Filipek, B. Melichar, E. Bajetta, V. Gorbunova, J.-O. Bay, I. Bodrogi, A. Jagiello-Gruszfeld and N. Moore (2007). "Bevacizumab plus interferon alfa-2a for treatment of metastatic renal cell carcinoma: a randomised, double-blind phase III trial." The Lancet **370**(9605): 2103-2111.

Ferlay, J., P. Autier, M. Boniol, M. Heanue, M. Colombet and P. Boyle (2007). "Estimates of the cancer incidence and mortality in Europe in 2006." Ann Oncol **18**(3): 581-592.

Flaherty, K. T., M. A. Rosen, D. F. Heitjan, M. L. Gallagher, B. Schwartz, M. D. Schnall and P. J. O'Dwyer (2008). "Pilot study of DCE-MRI to predict progression-free survival with sorafenib therapy in renal cell carcinoma." Cancer Biol Ther **7**(4): 496-501.

Folkman, J., E. Merler, C. Abernathy and G. Williams (1971). "Isolation of a tumor factor responsible for angiogenesis." J Exp Med **133**(2): 275-288.

Folkman, J. and Y. Shing (1992). "Angiogenesis." Journal of Biological Chemistry **267**(16): 10931-10934.

Galbraith S M, L. M. F., Taylor N J, Rustin G J S, Bentzen S, Stirling J, Padhani A R. (2002). "Reproducibility of dynamic contrast-enhanced MRI in human muscle and tumours: comparison of quantitative and semi-quantitative analysis." NMR in Biomedicine 15: 132–42 **15**: 132-142.

Galbraith, S. M., R. J. Maxwell, M. A. Lodge, G. M. Tozer, J. Wilson, N. J. Taylor, J. J. Stirling, L. Sena, A. R. Padhani and G. J. Rustin (2003). "Combretastatin A4 phosphate has tumor antivascular activity in rat and man as demonstrated by dynamic magnetic resonance imaging." J Clin Oncol **21**(15): 2831-2842.

Ganeshan, B., S. Abaleke, R. C. Young, C. R. Chatwin and K. A. Miles (2010). "Texture analysis of non-small cell lung cancer on unenhanced computed tomography: initial evidence for a relationship with tumour glucose metabolism and stage." Cancer Imaging **10**: 137-143.

Gay, L., A.-M. Baker and T. A. Graham (2016). "Tumour Cell Heterogeneity." F1000Research **5**: F1000 Faculty Rev-1238.

George, S., R. J. Motzer, H. J. Hammers, B. G. Redman, T. M. Kuzel, S. S. Tykodi, E. R. Plimack, J. Jiang, I. M. Waxman and B. I. Rini (2016). "Safety and Efficacy of Nivolumab in Patients With Metastatic Renal Cell Carcinoma Treated Beyond Progression: A Subgroup Analysis of a Randomized Clinical Trial." JAMA Oncol.

Gerber, H. P., V. Dixit and N. Ferrara (1998). "Vascular endothelial growth factor induces expression of the antiapoptotic proteins Bcl-2 and A1 in vascular endothelial cells." J Biol Chem **273**(21): 13313-13316.

Gerber, H. P., A. McMurtrey, J. Kowalski, M. Yan, B. A. Keyt, V. Dixit and N. Ferrara (1998). "Vascular endothelial growth factor regulates endothelial cell survival through the phosphatidylinositol 3'-kinase/Akt signal transduction pathway. Requirement for Flk-1/KDR activation." J Biol Chem **273**(46): 30336-30343.

Gerlinger , M., A. J. Rowan , S. Horswell , J. Larkin , D. Endesfelder , E. Gronroos , P. Martinez , N. Matthews , A. Stewart , P. Tarpey , I. Varela , B. Phillimore , S. Begum , N. Q. McDonald , A. Butler , D. Jones , K. Raine , C. Latimer , C. R. Santos , M. Nohadani , A. C. Eklund , B. Spencer-Dene , G. Clark , L. Pickering , G. Stamp , M. Gore , Z. Szallasi , J. Downward , P. A. Futreal and C. Swanton (2012). "Intratumor Heterogeneity and Branched Evolution Revealed by Multiregion Sequencing." New England Journal of Medicine **366**(10): 883-892.

Gnarra, J. R., K. Tory, Y. Weng, L. Schmidt, M. H. Wei, H. Li, F. Latif, S. Liu, F. Chen, F. M. Duh and et al. (1994). "Mutations of the VHL tumour suppressor gene in renal carcinoma." Nat Genet **7**(1): 85-90.

Goel, S., A. H.-K. Wong and R. K. Jain (2012). "Vascular Normalization as a Therapeutic Strategy for Malignant and Nonmalignant Disease." Cold Spring Harbor Perspectives in Medicine **2**(3): a006486.

Goh, V., B. Ganeshan, P. Nathan, J. K. Juttla, A. Vinayan and K. A. Miles (2011). "Assessment of response to tyrosine kinase inhibitors in metastatic renal cell cancer: CT texture as a predictive biomarker." Radiology **261**(1): 165-171.

Goh, V., S. Halligan, A. Gharpuray, D. Wellsted, J. Sundin and C. I. Bartram (2008). "Quantitative assessment of colorectal cancer tumor vascular parameters by using perfusion CT: influence of tumor region of interest." Radiology **247**(3): 726-732.

Goyal, A., R. Sharma, A. S. Bhalla, S. Gamanagatti, A. Seth, V. K. Iyer and P. Das (2012). "Diffusion-weighted MRI in renal cell carcinoma: a surrogate marker for predicting nuclear grade and histological subtype." Acta Radiol **53**(3): 349-358.

Griffon-Etienne, G., Y. Boucher, C. Brekken, H. D. Suit and R. K. Jain (1999). "Taxane-induced apoptosis decompresses blood vessels and lowers interstitial fluid pressure in solid tumors: clinical implications." Cancer Res **59**(15): 3776-3782.

Hahn, O. M., C. Yang, M. Medved, G. Karczmar, E. Kistner, T. Karrison, E. Manchen, M. Mitchell, M. J. Ratain and W. M. Stadler (2008). "Dynamic Contrast-Enhanced Magnetic Resonance Imaging Pharmacodynamic Biomarker Study of Sorafenib in Metastatic Renal Carcinoma." J Clin Oncol **26**(28): 4572-4578.

Hartmann, J. T. and C. Bokemeyer (1999). "Chemotherapy for renal cell carcinoma." Anticancer Res **19**(2c): 1541-1543.

Hay, N. (2005). "The Akt-mTOR tango and its relevance to cancer." Cancer Cell **8**(3): 179-183.
Hayes, C., A. R. Padhani and M. O. Leach (2002). "Assessing changes in tumour vascular function using dynamic contrast-enhanced magnetic resonance imaging." NMR Biomed **15**(2): 154-163.
Hittinger, M., M. Staehler, N. Schramm, C. Übleis, C. Becker, M. Reiser and F. Berger (2011). "Course of size and density of metastatic renal cell carcinoma lesions in the early follow-up of molecular targeted therapy." Urologic oncology.

Hollett, M. D., R. B. Jeffrey, Jr., M. Nino-Murcia, M. J. Jorgensen and D. P. Harris (1995). "Dual-phase helical CT of the liver: value of arterial phase scans in the detection of small (< or = 1.5 cm) malignant hepatic neoplasms." Am. J. Roentgenol. **164**(4): 879-884.

Hsu, Y. H., G. Z. Ferl and C. M. Ng (2013). "GPU-accelerated nonparametric kinetic analysis of DCE-MRI data from glioblastoma patients treated with bevacizumab." Magn Reson Imaging **31**(4): 618-623.

Hutson, T. E., V. Lesovoy, S. Al-Shukri, V. P. Stus, O. N. Lipatov, A. H. Bair, B. Rosbrook, C. Chen, S. Kim and N. J. Vogelzang (2013). "Axitinib versus sorafenib as first-line therapy in patients with metastatic renal-cell carcinoma: a randomised open-label phase 3 trial." Lancet Oncol **14**(13): 1287-1294.

Ibragimova, I., M. E. Maradeo, E. Dulaimi and P. Cairns (2013). "Aberrant promoter hypermethylation of PBRM1, BAP1, SETD2, KDM6A and other chromatin-modifying genes is absent or rare in clear cell RCC." Epigenetics **8**(5): 486-493.

Jain, R. K. (2005). "Normalization of tumor vasculature: an emerging concept in antiangiogenic therapy." Science **307**(5706): 58-62.

James A D'Arcy, David Collins, Anwar Padhani, Simon Walker Samuel, John Suckling and M. Leach (2006). "Magnetic Resonance Imaging Workbench: Analysis and Visualization of Dynamic Contrast-enhanced MR Imaging Data." RadioGraphics **26**(2): 621-632.

Juttla.J, V. A., Nathan.P, Goh.V (2010). Size and enhancement response criteria for TKIs in metastatic renal cell cancer: Does arterial or portal venous phase imaging alter respone categorization? RSNA 2010; abstract no:9007274.

Kaelin, W. G., Jr. (2007). "The von Hippel-Lindau tumor suppressor protein and clear cell renal carcinoma." Clin Cancer Res **13**(2 Pt 2): 680s-684s.

Kang, D. E., R. L. White, Jr., J. H. Zuger, H. C. Sasser and C. M. Teigland (2004). "Clinical use of fluorodeoxyglucose F 18 positron emission tomography for detection of renal cell carcinoma." J Urol **171**(5): 1806-1809.

Kayani, I., N. Avril, J. Bomanji, S. Chowdhury, A. Rockall, A. Sahdev, P. Nathan, P. Wilson, J. Shamash, K. Sharpe, L. Lim, J. Dickson, P. Ell, A. Reynolds and T. Powles (2011). "Sequential FDG-PET/CT as a Biomarker of Response to Sunitinib in Metastatic Clear Cell Renal Cancer." Clinical Cancer Research **17**(18): 6021-6028.

Kety, S. S. (1949). "Measurement of regional circulation by the local clearance of radioactive sodium." Am Heart J **38**(3): 321-328.

Kety.S (1960(a)). "Blood-tissue exchange methods. Theory of blood-tissue exchange and its application to measurement of blood flow." Methods Med Res(8): 223-227.

Kety.S (1960(b)). "Measurement of local blood flow by the exchange of an inert, diffusible substance." Methods Med Res(8): 228-236.

Kiessling, F., M. Jugold, E. Woenne and G. Brix (2007). "Non-invasive assessment of vessel morphology and function in tumors by magnetic resonance imaging." European Radiology **17**(8): 2136-2148.

Kondo, K., W. Y. Kim, M. Lechpammer and W. G. Kaelin, Jr. (2003). "Inhibition of HIF2alpha is sufficient to suppress pVHL-defective tumor growth." PLoS Biol **1**(3): E83.

Lamuraglia, M., B. Escudier, L. Chami, B. Schwartz, J. Leclère, A. Roche and N. Lassau (2006). "To predict progression-free survival and overall survival in metastatic renal cancer treated with sorafenib: Pilot study using dynamic contrast-enhanced Doppler ultrasound." European Journal of Cancer **42**(15): 2472-2479.

Lebret, T., J. E. Poulain, V. Molinie, J. M. Herve, Y. Denoux, A. Guth, A. Scherrer and H. Botto (2007). "Percutaneous Core Biopsy for Renal Masses: Indications, Accuracy and Results." The Journal of Urology **178**(4): 1184-1188.

Lee, E. Y., J. P. Heiken, P. C. Huettner and W. Na-ChiangMai (2005). "Renal Cell Carcinoma Visible Only During the Corticomedullary Phase of Enhancement." Am. J. Roentgenol. **184**(3_supp): S104-106.

Less, J. R., M. C. Posner, Y. Boucher, D. Borochovitz, N. Wolmark and R. K. Jain (1992). "Interstitial hypertension in human breast and colorectal tumors." Cancer Res **52**(22): 6371-6374.
Lopez-Beltran, A., M. Scarpelli, R. Montironi and Z. Kirkali (2006). "2004 WHO classification of the renal tumors of the adults." Eur Urol **49**(5): 798-805.

Mains, J. R., F. Donskov, E. M. Pedersen, H. H. T. Madsen and F. Rasmussen (2014). "Dynamic Contrast-Enhanced Computed Tomography as a Potential Biomarker in Patients With Metastatic Renal Cell Carcinoma: Preliminary Results From the Danish Renal Cancer Group Study-1." Investigative Radiology **49**(9): 601-607.

Melichar, B., P. Koralewski, A. Ravaud, A. Pluzanska, S. Bracarda, C. Szczylik, C. Chevreau, M. Filipek, R. Delva, E. Sevin, S. Negrier, J. McKendrick, A. Santoro, P. Pisa and B. Escudier (2008). "First-line bevacizumab combined with reduced dose interferon-{alpha}2a is active in patients with metastatic renal cell carcinoma." Ann Oncol **19**(8): 1470-1476.

MHRA. (2002). "Dotarem Summary of product characters." from http://www.mhra.gov.uk/home/groups/spcpil/documents/spcpil/con1463719652207.pdf.

Miles, K. A. (2002). "Functional computed tomography in oncology." Eur J Cancer **38**(16): 2079-2084.

Miles, K. A., B. Ganeshan, M. R. Griffiths, R. C. Young and C. R. Chatwin (2009). "Colorectal cancer: texture analysis of portal phase hepatic CT images as a potential marker of survival." Radiology **250**(2): 444-452.

Miles, K. A., T.-Y. Lee, V. Goh, E. Klotz, C. Cuenod, S. Bisdas, A. M. Groves, M. P. Hayball, R. Alonzi and T. Brunner (2012). "Current status and guidelines for the assessment of tumour vascular support with dynamic contrast-enhanced computed tomography." European Radiology **22**(7): 1430-1441.

Minardi, D., M. Santoni, G. Lucarini, R. Mazzucchelli, L. Burattini, A. Conti, M. Bianconi, M. Scartozzi, G. Milanese, R. D. Primio, R. Montironi, S. Cascinu and G. Muzzonigro (2015). "Tumor VEGF expression correlates with tumor stage and identifies prognostically different groups in patients with clear cell renal cell carcinoma." Urol Oncol **33**(3): 113.e111-117.

MinYuen Teo, R. S. M. D. o. M. O., Adelaide and Meath Hospital, and D. incorporating the National Children's Hospital, Ireland (2012). "Does RECIST-defined progression correlate with lack of further sunitinib (SU) benefit in advanced

renal cell carcinoma (aRCC)?" J Clin Oncol 30, 2012 (suppl; abstr e15093).

Mirka, H., E. Korcakova, J. Kastner, M. Hora, O. Hes, P. Hosek and J. Ferda (2015). "Diffusion-weighted imaging using 3.0 T MRI as a possible biomarker of renal tumors." Anticancer Res **35**(4): 2351-2357.

Montravers, F., D. Grahek, K. Kerrou, N. Younsi, J. D. Doublet, B. Gattegno, J. Rossert, M. A. Costa de Beauregard, P. Thibault and J. N. Talbot (2000). "Evaluation of FDG uptake by renal malignancies (primary tumor or metastases) using a coincidence detection gamma camera." J Nucl Med **41**(1): 78-84.

Morgan, B., A. L. Thomas, J. Drevs, J. Hennig, M. Buchert, A. Jivan, M. A. Horsfield, K. Mross, H. A. Ball, L. Lee, W. Mietlowski, S. Fuxuis, C. Unger, K. O'Byrne, A. Henry, G. R. Cherryman, D. Laurent, M. Dugan, D. Marme and W. P. Steward (2003). "Dynamic contrast-enhanced magnetic resonance imaging as a biomarker for the pharmacological response of PTK787/ZK 222584, an inhibitor of the vascular endothelial growth factor receptor tyrosine kinases, in patients with advanced colorectal cancer and liver metastases: results from two phase I studies." J Clin Oncol **21**(21): 3955-3964.

Motzer, R. J., J. Bacik, T. Mariani, P. Russo, M. Mazumdar and V. Reuter (2002). "Treatment Outcome and Survival Associated With Metastatic Renal Cell Carcinoma of Non-Clear-Cell Histology." J Clin Oncol 20(9): 2376-2381.

Motzer, R. J., N. H. Bander and D. M. Nanus (1996). "Renal-Cell Carcinoma." New England Journal of Medicine 335(12): 865-875.

Motzer, R. J., B. Escudier, D. F. McDermott, S. George, H. J. Hammers, S. Srinivas, S. S. Tykodi, J. A. Sosman, G. Procopio, E. R. Plimack, D. Castellano, T. K. Choueiri, H. Gurney, F. Donskov, P. Bono, J. Wagstaff, T. C. Gauler, T. Ueda, Y. Tomita, F. A. Schutz, C. Kollmannsberger, J. Larkin, A. Ravaud, J. S. Simon, L. A. Xu, I. M. Waxman and P. Sharma (2015). "Nivolumab versus Everolimus in Advanced Renal-Cell Carcinoma." N Engl J Med 373(19): 1803-1813.

Motzer, R. J., B. Escudier, S. Oudard, T. E. Hutson, C. Porta, S. Bracarda, V. Grünwald, J. A. Thompson, R. A. Figlin, N. Hollaender, G. Urbanowitz, W. J. Berg, A. Kay, D. Lebwohl and A. Ravaud (2008). "Efficacy of everolimus in advanced renal cell carcinoma: a double-blind, randomised, placebo-controlled phase III trial." The Lancet 372(9637): 449-456.

Motzer, R. J., G. R. Hudes, B. D. Curti, D. F. McDermott, B. J. Escudier, S. Negrier, B. Duclos, L. Moore, T. O'Toole, J. P. Boni and J. P. Dutcher (2007). "Phase I/II Trial of Temsirolimus Combined With Interferon Alfa for Advanced Renal Cell Carcinoma." J Clin Oncol 25(25): 3958-3964.

Motzer, R. J., T. E. Hutson, D. Cella, J. Reeves, R. Hawkins, J. Guo, P. Nathan, M. Staehler, P. de Souza, J. R. Merchan, E. Boleti, K. Fife, J. Jin, R. Jones, H. Uemura, U. De Giorgi, U. Harmenberg, J. Wang, C. N. Sternberg, K. Deen, L. McCann, M. D. Hackshaw, R. Crescenzo, L. N. Pandite and T. K. Choueiri (2013). "Pazopanib versus sunitinib in metastatic renal-cell carcinoma." N Engl J Med 369(8): 722-731.

Motzer, R. J., T. E. Hutson, P. Tomczak, M. D. Michaelson, R. M. Bukowski, O. Rixe, S. Oudard, S. Negrier, C. Szczylik, S. T. Kim, I. Chen, P. W. Bycott, C. M. Baum and R. A. Figlin (2007). "Sunitinib versus Interferon Alfa in Metastatic Renal-Cell Carcinoma." N Engl J Med 356(2): 115-124.

Motzer, R. J., M. Mazumdar, J. Bacik, W. Berg, A. Amsterdam and J. Ferrara (1999). "Survival and Prognostic Stratification of 670 Patients With Advanced Renal Cell Carcinoma." J Clin Oncol 17(8): 2530-.

Muglia, V. F. and A. Prando (2015). "Renal cell carcinoma: histological classification and correlation with imaging findings." Radiologia Brasileira 48(3): 166-174.

Nakatani, K., Y. Nakamoto, T. Saga, T. Higashi and K. Togashi (2009). "The potential clinical value of FDG-PET for recurrent renal cell carcinoma." Eur J Radiol.

Nakatani, K., Y. Nakamoto, T. Saga, T. Higashi and K. Togashi (2011). "The potential clinical value of FDG-PET for recurrent renal cell carcinoma." Eur J Radiol 79(1): 29-35.

Namasivayam, S., D. R. Martin and S. Saini (2007). "Imaging of liver metastases: MRI." Cancer Imaging 7(1): 2-9.

Nathalie Lassau, V. V., Sophie Taieb, Joëlle Lacroix, Richard Aziza, Marie Cuinet, Jean-Charles Soria,, S. K. I. G. R. Louis Chapotot, Villejuif, France; Department of Radiology, Beaujon, C. University Hospital, France; Centre Oscar Lambret, Lille, France; Centre François Baclesse, Caen, France; and T. Centre Claudius Regaud, France; Centre Léon Bérard, Lyon, France (2012). "Evaluation with DCE-US of antiangiogenic treatments in 539 patients allowing the selection of one surrogate marker correlated to overall

survival." J Clin Oncol 30, 2012 (suppl; abstr 4618).

Nathan, P., M. Zweifel, A. R. Padhani, D. M. Koh, M. Ng, D. J. Collins, A. Harris, C. Carden, J. Smythe, N. Fisher, N. J. Taylor, J. J. Stirling, S. P. Lu, M. O. Leach, G. J. Rustin and I. Judson (2012). "Phase I trial of combretastatin A4 phosphate (CA4P) in combination with bevacizumab in patients with advanced cancer." Clin Cancer Res 18(12): 3428-3439.

Nathan, P. D., A. Vinayan, D. Stott, J. Juttla and V. Goh (2010). "CT response assessment combining reduction in both size and arterial phase density correlates with time to progression in metastatic renal cancer patients treated with targeted therapies." Cancer Biol Ther 9(1): 15-19.

NCI, R. g. (2000). "RECIST guidelines." 2000, from http://imaging.cancer.gov/clinicaltrials/imaging.

Nelson, D. A., T. T. Tan, A. B. Rabson, D. Anderson, K. Degenhardt and E. White (2004). "Hypoxia and defective apoptosis drive genomic instability and tumorigenesis." Genes Dev 18(17): 2095-2107.

Ng, F., R. Kozarski, B. Ganeshan and V. Goh (2013). "Assessment of tumor heterogeneity by CT texture analysis: can the largest cross-sectional area be used as an alternative to whole tumor analysis?" Eur J Radiol 82(2): 342-348.

nist.gov. (1994). from http://www.nist.gov/pml/pubs/tn1297/index.cfm.

Notohamiprodjo, M., M. Staehler, N. Steiner, F. Schwab, S. P. Sourbron, H. J. Michaely, A. D. Helck, M. F. Reiser and K. Nikolaou (2013). "Combined diffusion-weighted, blood oxygen level-dependent, and dynamic contrast-enhanced MRI for characterization and differentiation of renal cell carcinoma." Acad Radiol 20(6): 685-693.

Oh, S., D. J. Sung, K. S. Yang, K. C. Sim, N. Y. Han, B. J. Park, M. J. Kim and S. B. Cho (2016). "Correlation of CT imaging features and tumor size with Fuhrman grade of clear cell renal cell carcinoma." Acta Radiol.

Oken, M. M., R. H. Creech, D. C. Tormey, J. Horton, T. E. Davis, E. T. McFadden and P. P. Carbone (1982). "Toxicity and response criteria of the Eastern Cooperative Oncology Group." Am J Clin Oncol 5(6): 649-655.

ONS.GOV.UK. (2015). from http://www.ons.gov.uk/ons/rel/vsob1/cancer-statistics-registrations--england--series-mb1-/index.html.

Oudkerk, M., P. E. Sijens, E. J. Van Beek and T. J. Kuijpers (1995). "Safety and efficacy of dotarem (Gd-DOTA) versus magnevist (Gd-DTPA) in magnetic resonance imaging of the central nervous system." Invest Radiol 30(2): 75-78.

Padhani, A. R. (2003). "MRI for assessing antivascular cancer treatments." Br J Radiol 76(suppl_1): S60-80.

Padhani, A. R. M. B. B. S. M. F. and A. P. M. B. B. S. F. F. Dzik-Jurasz (2004). "Perfusion MR Imaging of Extracranial Tumor Angiogenesis." Topics in Magnetic Resonance Imaging 15(1): 41-57.

Palmowski, M., I. Schifferdecker, S. Zwick, S. Macher-Goeppinger, H. Laue, A. Haferkamp, H.-U. Kauczor, F. Kiessling and P. Hallscheidt (2009). "Tumor perfusion assessed by dynamic contrast-enhanced MRI correlates to the grading of renal cell carcinoma: Initial results." European Journal of Radiology **In Press, Corrected Proof**.

Parker, G. J., C. Roberts, A. Macdonald, G. A. Buonaccorsi, S. Cheung, D. L. Buckley, A. Jackson, Y. Watson, K. Davies and G. C. Jayson (2006). "Experimentally-derived functional form for a population-averaged high-temporal-resolution arterial input function for dynamic contrast-enhanced MRI." Magn Reson Med **56**(5): 993-1000.

Parker, G. J., J. Suckling, S. F. Tanner, A. R. Padhani, P. B. Revell, J. E. Husband and M. O. Leach (1997). "Probing tumor microvascularity by measurement, analysis and display of contrast agent uptake kinetics." J Magn Reson Imaging **7**(3): 564-574.

Patrick Therasse, S. G. A., Elizabeth A. Eisenhauer, Jantien Wanders,, L. R. Richard S. Kaplan, Jaap Verweij, Martine Van Glabbeke, Allan and M. C. C. T. van Oosterom, Steve G. Gwyther (2000). "New Guidelines to Evaluate the Response to Treatment in Solid Tumors." Journal of the National Cancer Institute **92**(3): 205 - 216.

Pavlovich, C. P. and L. S. Schmidt (2004). "Searching for the hereditary causes of renal-cell carcinoma." Nat Rev Cancer **4**(5): 381-393.

Pedrosa, I., M. Chou, L. Ngo, R. H. Baroni, E. Genega, L. Galaburda, W. DeWolf and N. Rofsky (2008). "MR classification of renal masses with pathologic correlation." European Radiology **18**(2): 365-375.

Platzek, I., S. Zastrow, P. E. Deppe, M. O. Grimm, M. Wirth, M. Laniado and C. Stroszczynski (2010). "Whole-body MRI in follow-up of patients with renal cell carcinoma." Acta Radiol **51**(5): 581-589.

Poon, R. T., S. T. Fan and J. Wong (2001). "Clinical implications of circulating angiogenic factors in cancer patients." J Clin Oncol **19**(4): 1207-1225.

Raptopoulos, V., S. Blake, K. Weisinger, M. Atkins, M. Keogan and J. Kruskal (2001). "Multiphase contrast-enhanced helical CT of liver metastases from renal cell carcinoma." European Radiology **11**(12): 2504-2509.

Raptopoulos, V. D., S. P. Blake, K. Weisinger, M. B. Atkins, M. T. Keogan and J. B. Kruskal (2001). "Multiphase contrast-enhanced helical CT of liver metastases from renal cell carcinoma." Eur Radiol **11**(12): 2504-2509.

Rini, B. I., S. Halabi, J. E. Rosenberg, W. M. Stadler, D. A. Vaena, S.-S. Ou, L. Archer, J. N. Atkins, J. Picus, P. Czaykowski, J. Dutcher and E. J. Small (2008). "Bevacizumab Plus Interferon Alfa Compared With Interferon Alfa Monotherapy in Patients With Metastatic Renal Cell Carcinoma: CALGB 90206." J Clin Oncol **26**(33): 5422-5428.

Rini, B. I., S. Halabi, J. E. Rosenberg, W. M. Stadler, D. A. Vaena, S.-S. Ou, L. Archer, J. N. Atkins, J. Picus, P. Czaykowski, J. Dutcher and E. J. Small (2008). "Bevacizumab Plus Interferon Alfa Compared With Interferon Alfa Monotherapy in Patients With Metastatic Renal Cell Carcinoma: CALGB 90206." Journal of Clinical Oncology **26**(33): 5422-5428.

Risau, W. (1997). "Mechanisms of angiogenesis." Nature **386**(6626): 671-674.
Rochlitz, C. F., S. Peter, G. Willroth, E. de Kant, H. Lobeck, D. Huhn and R. Herrmann (1992). "Mutations in the ras protooncogenes are rare events in renal cell cancer." Eur J Cancer **28**(2-3): 333-336.

Rosen, L. S. (2002). "Clinical experience with angiogenesis signaling inhibitors: focus on vascular endothelial growth factor (VEGF) blockers." Cancer Control **9**(2 Suppl): 36-44.

S. Le Moulec, P. C., B. Billemont, C. Massard, L. Vedrine, E. Gontier, G. Bonardel, A. Houlgatte (2010). Prospective evaluation of FDG-PET/CT in patients with advanced
RCC treated with antiangiogenic therapies. 2010 Genitourinary Cancers Symposium. ASCO.

Schlemmer HP, M. J., Grobholz R, Jaeger T, Michel MS, Werner A, Rabe J, van Kaick G. (2004). "Can pre-operative contrast-enhanced dynamic MR imaging for prostate cancer predict microvessel density in prostatectomy specimens?" Eur Radiol **14**(2): 309 - 317.

Schmidt, G. P., A. Baur-Melnyk, P. Herzog, R. Schmid, R. Tiling, M. Schmidt, M. F. Reiser and S. O. Schoenberg (2005). "High-resolution whole-body magnetic resonance image tumor staging with the use of parallel imaging versus dual-modality positron emission tomography-computed tomography: experience on a 32-channel system." Invest Radiol **40**(12): 743-753.

Semenza, G. L. (2003). "Targeting HIF-1 for cancer therapy." Nat Rev Cancer **3**(10): 721-732.

Sheir, K. Z., M. El-Azab, A. Mosbah, M. El-Baz and A. A. Shaaban (2005). "DIFFERENTIATION OF RENAL CELL CARCINOMA SUBTYPES BY MULTISLICE COMPUTERIZED TOMOGRAPHY." Journal of Urology, The **174**(2): 451-455.

Sidaway, P. (2016). "Kidney cancer: Response to nivolumab in RCC: RECISTing progression." Nat Rev Urol **advance online publication**.

Smith, A. D., M. L. Lieber and S. N. Shah (2010). "Assessing tumor response and detecting recurrence in metastatic renal cell carcinoma on targeted therapy: importance of size and attenuation on contrast-enhanced CT." AJR Am J Roentgenol **194**(1): 157-165.

Smith, A. D., S. N. Shah, B. I. Rini, M. L. Lieber and E. M. Remer (2010). "Morphology, Attenuation, Size, and Structure (MASS) Criteria: Assessing Response and Predicting Clinical Outcome in Metastatic Renal Cell Carcinoma on Antiangiogenic Targeted Therapy." American Journal of Roentgenology **194**(6): 1470-1478.

Sohaib, S. A., G. Cook, S. D. Allen, M. Hughes, T. Eisen and M. Gore (2009). "Comparison of whole-body MRI and bone scintigraphy in the detection of bone metastases in renal cancer." Br J Radiol **82**(980): 632-639.

Song, Y., G. Cho, J. Y. Suh, C. K. Lee, Y. R. Kim, Y. J. Kim and J. K. Kim (2013). "Dynamic contrast-enhanced MRI for monitoring antiangiogenic treatment: determination of accurate and reliable perfusion parameters in a longitudinal study of a mouse xenograft model." Korean J Radiol **14**(4): 589-596.

Sternberg, C. N., I. D. Davis, J. Mardiak, C. Szczylik, E. Lee, J. Wagstaff, C. H. Barrios, P. Salman, O. A. Gladkov, A. Kavina, J. J. Zarba, M. Chen, L. McCann, L. Pandite, D. F. Roychowdhury and R. E. Hawkins (2010). "Pazopanib in locally advanced or metastatic renal cell carcinoma: results of a randomized phase III trial." J Clin Oncol **28**(6): 1061-1068.

Sternberg, C. N., R. E. Hawkins, J. Wagstaff, P. Salman, J. Mardiak, C. H. Barrios, J. J. Zarba, O. A. Gladkov, E. Lee, C. Szczylik, L. McCann, S. D. Rubin, M. Chen and I. D. Davis (2013). "A randomised, double-blind phase III study of pazopanib in patients with advanced and/or metastatic renal cell carcinoma: final overall survival results and safety update." Eur J Cancer **49**(6): 1287-1296.

Stevenson, J. P., M. Rosen, W. Sun, M. Gallagher, D. G. Haller, D. Vaughn, B. Giantonio, R. Zimmer, W. P. Petros, M. Stratford, D. Chaplin, S. L. Young, M. Schnall and P. J. O'Dwyer (2003). "Phase I trial of the antivascular agent combretastatin A4 phosphate on a 5-day schedule to patients with cancer: magnetic resonance imaging evidence for altered tumor blood flow." J Clin Oncol **21**(23): 4428-4438.

Strimbu, K. and J. A. Tavel (2010). "What are Biomarkers?" Current opinion in HIV and AIDS **5**(6): 463-466.

Su, M. Y., Y. C. Cheung, J. P. Fruehauf, H. Yu, O. Nalcioglu, E. Mechetner, A. Kyshtoobayeva, S. C. Chen, S. Hsueh, C. E. McLaren and Y. L. Wan (2003). "Correlation of dynamic contrast enhancement MRI parameters with microvessel density and VEGF for assessment of angiogenesis in breast cancer." J Magn Reson Imaging **18**(4): 467-477.

Sun, M. R. M., L. Ngo, E. M. Genega, M. B. Atkins, M. E. Finn, N. M. Rofsky and I. Pedrosa (2009). "Renal Cell Carcinoma: Dynamic Contrast-enhanced MR Imaging for Differentiation of Tumor Subtypesâ€"Correlation with Pathologic Findings1." Radiology **250**(3): 793-802.

Tamada, T., K. Nagai, M. Iizuka, S. Imai, Y. Kajihara, S. Yamamoto, J. Kurebayashi, K. Shimozuma, H. Sonoo and M. Fukunaga (2000). "[Comparison of whole-body MR imaging and bone scintigraphy in the detection of bone metastases from breast cancer]." Nihon Igaku Hoshasen Gakkai Zasshi **60**(5): 249-254.

Tofts, P. S. (1997). "Modeling tracer kinetics in dynamic Gd-DTPA MR imaging." (1053-1807 (Print)).

Tofts, P. S., G. Brix, D. L. Buckley, J. L. Evelhoch, E. Henderson, M. V. Knopp, H. B. W. Larsson, T.-Y. Lee, N. A. Mayr, G. J. M. Parker, R. E. Port, J. Taylor and R. M. Weisskoff (1999). "Estimating kinetic parameters from dynamic contrast-enhanced t1-weighted MRI of a diffusable tracer: Standardized quantities and symbols." Journal of Magnetic Resonance Imaging **10**(3): 223-232.

Tofts, P. S. and A. G. Kermode (1991). "Measurement of the blood-brain barrier permeability and leakage space using dynamic MR imaging. 1. Fundamental concepts." Magn Reson Med **17**(2): 357-367.
Tozer, G. M., K. M. Shaffi, V. E. Prise and V. J. Cunningham (1994). "Characterisation of tumour blood flow using a 'tissue-isolated' preparation." Br J Cancer **70**(6): 1040-1046.

Turner, K. J., J. W. Moore, A. Jones, C. F. Taylor, D. Cuthbert-Heavens, C. Han, R. D. Leek, K. C. Gatter, P. H. Maxwell, P. J. Ratcliffe, D. Cranston and A. L. Harris (2002). "Expression of hypoxia-inducible factors in human renal cancer: relationship to angiogenesis and to the von Hippel-Lindau gene mutation." Cancer Res **62**(10): 2957-2961.

Ueno, D., M. Yao, U. Tateishi, R. Minamimoto, K. Makiyama, N. Hayashi, F. Sano, T. Murakami, T. Kishida, T. Miura, K. Kobayashi, S. Noguchi, I. Ikeda, Y. Ohgo, T. Inoue, Y. Kubota and N. Nakaigawa (2012). "Early Assessment by FDG-PET/CT of Patients with Advanced Renal Cell Carcinoma Treated with Tyrosine Kinase Inhibitors is Predictive of Disease Course." BMC Cancer **12**(1): 162.

van der Veldt, A. A., M. R. Meijerink, A. J. van den Eertwegh, J. B. Haanen and E. Boven (2010). "Choi response criteria for early prediction of clinical outcome in patients with metastatic renal cell cancer treated with sunitinib." Br J Cancer **102**(5): 803-809.

von Marschall, Z., A. Scholz, T. Cramer, G. Schäfer, M. Schirner, K. Öberg, B. Wiedenmann, M. Höcker and S. Rosewicz (2003). "Effects of Interferon Alpha on Vascular Endothelial Growth Factor Gene Transcription and Tumor Angiogenesis." Journal of the National Cancer Institute **95**(6): 437-448.
Wang, J. H., P. Q. Min, P. J. Wang, W. X. Cheng, X. H. Zhang, Y. Wang, X. H. Zhao and X. Q. Mao (2006). "Dynamic CT Evaluation of Tumor Vascularity in Renal Cell Carcinoma." Am. J. Roentgenol. **186**(5): 1423-1430.

Wedam, S. B., J. A. Low, S. X. Yang, C. K. Chow, P. Choyke, D. Danforth, S. M. Hewitt, A. Berman, S. M. Steinberg, D. J. Liewehr, J. Plehn, A. Doshi, D. Thomasson, N. McCarthy, H. Koeppen, M. Sherman, J. Zujewski, K. Camphausen, H. Chen and S. M. Swain (2006). "Antiangiogenic and antitumor effects of bevacizumab in patients with inflammatory and locally advanced breast cancer." J Clin Oncol **24**(5): 769-777.

Williams, R., J. M. Hudson, B. A. Lloyd, A. R. Sureshkumar, G. Lueck, L. Milot, M. Atri, G. A. Bjarnason and P. N. Burns (2011). "Dynamic Microbubble Contrast-enhanced US to Measure Tumor Response to Targeted Therapy: A Proposed Clinical Protocol with Results from Renal Cell Carcinoma Patients Receiving Antiangiogenic Therapy." Radiology **260**(2): 581-590.

Yang, J. C., L. Haworth, R. M. Sherry, P. Hwu, D. J. Schwartzentruber, S. L. Topalian, S. M. Steinberg, H. X. Chen and S. A. Rosenberg (2003). "A Randomized Trial of Bevacizumab, an Anti-Vascular Endothelial Growth Factor Antibody, for Metastatic Renal Cancer." N Engl J Med **349**(5): 427-434.

Yuasa, T., S. Urakami, S. Yamamoto, J. Yonese, K. Nakano, M. Kodaira, S. Takahashi, K. Hatake, K. Inamura, Y. Ishikwa and I. Fukui (2011). "Tumor Size Is a Potential Predictor of Response to Tyrosine Kinase Inhibitors in Renal Cell Cancer." Urology **77**(4): 831-835.

Zar, J. H. (1972). "Significance Testing of the Spearman Rank Correlation Coefficient." Journal of the American Statistical Association **67**(339): 578-580.

Zeng, F. C., M. Q. Zeng, L. Huang, Y. L. Li, B. M. Gao, J. J. Chen, R. Z. Xue and Z. Y. Tang (2016). "Downregulation of VEGFA inhibits proliferation, promotes apoptosis, and suppresses migration and invasion of renal clear cell carcinoma." Onco Targets Ther **9**: 2131-2141.

Zhang, Y. D., C. J. Wu, Q. Wang, J. Zhang, X. N. Wang, X. S. Liu and H. B. Shi (2015). "Comparison of Utility of Histogram Apparent Diffusion Coefficient and R2* for Differentiation of Low-Grade From High-Grade Clear Cell Renal Cell Carcinoma." AJR Am J Roentgenol **205**(2): W193-201.

Zhuang, S. H., L. Xiu and Y. A. Elsayed (2009). "Overall survival: a gold standard in search of a surrogate: the value of progression-free survival and time to progression as end points of drug efficacy." Cancer J **15**(5): 395-400.

Chapter 9.

Appendices

9.1. RECIST criteria

Evaluation of Target lesions

Complete Response (CR):	Disappearance of all target lesions
Partial Response (PR):	At least a 30% decrease in the sum of the LD of target lesions, taking as reference the baseline sum LD
Progressive Disease (PD):	At least a 20% increase in the sum of the LD of target lesions, taking as reference the smallest sum LD recorded since the treatment started or the appearance of one or more new lesions
Stable Disease (SD):	Neither sufficient shrinkage to qualify for PR nor sufficient increase to qualify for PD, taking as reference the smallest sum LD since the treatment started

Evaluation of non-target lesions

Complete Response (CR):	Disappearance of all non-target lesions and normalization of tumor marker level
Incomplete response / Stable Disease (SD):	Persistence of one or more non-target lesion(s) or/and maintenance of tumor marker level above the normal limits
Progressive Disease (PD):	Appearance of one or more new lesions and/or unequivocal progression of existing non-target lesions (1)

9.2.   Motzer score

Variable	Good	Poor
Performance status	0-1	>1
Histology	Clear cell	Other
LDH	<1.5 x ULN	>1.5 x ULN
Corrected calcium	Normal	>10mg/dl
Hameoglobin	Normal	<LLN
Previous nephrectomy	Yes	No

Good prognosis = 0 poor factor

Intermediate prognosis = 1-2 poor factors

Poor prognosis = >2 poor factors

9.3. ECOG performance score

Activity	Score
Fully active, able to carry out on all pre-disease performance without restriction	0
Restricted in physically strenuous activity but ambulatory and able to carry out work of a light or sedentary nature eg light house work, office work.	1
Ambulatory and capable of all self-care. Unable to carry out any work activities. Up and above more than 50% of waking hours	2
Capable of only limited self care. Confined to bed or chair more than 50% of waking hours	3
Completely disabled. Cannot carry out any self-care. Totally confined to bed or chair	4

9.4.   Cockcroft-Gault formula

Reported by Cockcroft and Gault in 1976 to estimate creatinine clearance from serum

creatinine (Cockcroft and Gault 1976)

$$eC_{cr} = \frac{(140 - age) \times Mass\ (in\ kilogram) \times Constant}{Serum\ Creatinine\ (in\ \mu mol/L)}$$

Constant = 1.23 for Male and 1.04 for female

This remains the most common formula for determining creatinine clearance, which

act as a surrogate estimate for GFR; 10-20% overestimation of GFR could happen with

creatinine clearance.

9.5. Patient information leaflet

DYNAMIC CONTRAST ENHANCED MRI (DCE-MRI) ASSESSMENT OF THE VASCULAR CHANGES INDUCED BY BEVACIZUMAB ALONE AND IN COMBINATION WITH INTERFERON –ALPHA IN PATIENTS WITH ADVANCED RENAL CELL CARCINOMA

Patient information leaflet

Version 1.2
Dated: 26th January 2009

1. Study Title

"Dynamic Contrast Enhanced MRI (DCE-MRI) assessment of the vascular changes induced with bevacizumab alone and in combination with interferon – alpha in patients with advanced renal cell carcinoma."

2. Invitation

We would like to invite you to participate in a research study. Please take time to read through the following leaflet prior to making a decision to partake in this study. It is extremely important for you to understand why the research is being done and what it will involve.

3. Purpose of the study

The combination of interferon-α and bevacizumab is proven to be active in the treatment of advanced renal cell carcinoma.

Bevacizumab acts by interfering with blood vessel growth in the tumour and has been shown to delay disease progression in advanced kidney cancers. Interferon-α is a biological therapeutic agent that has many actions including boosting immunity and also affecting the growth of new blood vessels which feed the tumour.

Previously, research has been carried out with bevacizumab alone and bevacizumab plus interferon. Both of these have been proved to be active in treatment of advanced kidney cancer. The combination of bevacizumab and interferon has been compared against interferon, which was the standard of care for this disease. This study showed that the combination treatment resulted in a significant improvement in the length of time before the cancer started growing again compared with interferon only treatment. The average time before the cancer started growing again was 10.2 months for the combination and 5.4 months for interferon only treatment.

Even though the combination of bevacizumab and interferon was found to be better than interferon alone, we are still unsure whether interferon adds significantly to the activity of bevacizumab, and if so in what way. One possibility is that the inhibitory effect on tumour blood vessels by bevacizumab is enhanced by the addition of interferon.

Bevacizumab on its own was tested previously against placebo and is found to be active against advanced kidney cancer, However it is not known if the addition of interferon to bevacizumab will increase the treatment efficacy.

This study is looking to find out whether the combination of interferon-α and bevacizumab has a greater effect on the blood vessels feeding the cancer than bevacizumab alone and also if the dose on interferon has any importance in this effect.The effect of the treatment on tumour blood vessels can be measured with a special MRI scan called Dynamic Contrast Enhanced MRI (DCE-MRI).

This trial will also be exploring markers present in blood which may correlate with the anti-blood vessel effect of these medications. We will see if any of these could predict response to treatment. These are referred to as biomarkers.

To summarise, your participation in the study will enable us to determine;
a) Whether the addition of interferon-α to bevacizumab increases the anti-tumour blood vessel effect of bevacizumab.
b) Whether the dose of interferon-α is important in this effect.
c) Whether there are biomarkers that can be used to predict response to treatment.

4. **Do I have to take part**

No, it is up to you to decide whether or not to take part. If you decide to take part, you will be given this information sheet and will be asked to sign a consent form. If you decide to take part, you are still free to withdraw at any time and without giving any reason. A decision to withdraw at any time, or a decision not to take part, will not affect the standard of care that you receive.

5. **What does the study involve**

In this research study thirty patients will be randomly allocated to one of the three arms receiving;
a) Bevacizumab alone
b) Bevacizumab + Interferon-α at 3MU
c) Bevacizumab + Interferon- α at 9MU

After 8 weeks everybody on the trial will receive both drugs as directed by their treating doctor. .

The study is "randomised" and "open-labelled". This means that once you have agreed to enter into the trial, you will be allocated to one of the three groups mentioned above. The allocation of groups is done by a computer so that each group has a similar mixture of people. Neither the doctor nor the patient can decide which group they are going to be in. This will help us to analyse the effectiveness of the treatment reliably. As the study is open-labelled, both doctor and patient will know which group they are in.

You will stay on the treatment for as long as it is benefitting you, with scans assessing response at 8 weeks and twelve weekly thereafter. If the treatment has any unacceptable side effects which cannot be simply managed, your doctor may withdraw you from the study. You can also withdraw from the study at anytime without giving any reason.

Bevacizumab is given into the vein as a drip running for 30-60 minutes. This is repeated every two weeks. Interferon-alpha is given subcutaneously (under the skin) three times each week. Many patients or family members learn to inject the interferon however a district nurse can administer the treatment if the patient wishes. Patients in group B will receive low dose interferon for the 8 weeks. Patients in group C will have low dose interferon in the first two weeks and stepped up to a higher dose for the next six weeks.

You will have two DCE-MRI scans done before treatment begins and another two once treatment has started - at week 2 and week 8. CT scans will be performed prior to the treatment, repeated at week 8 and twelve weekly thereafter.

All patients will have blood tests done prior to starting treatment and during the visits to the hospital. In addition to the normal blood tests assessing your blood counts, kidney and liver functions, additional blood test will be taken to look for biomarkers in the blood. For the purpose of biomarkers, the equivalent of five tea spoons of blood will be taken, twice before treatment and at weeks 2, 6, 8 and when treatment is discontinued. Please refer to the patient diary on *page 6* of this leaflet for more details.

You will be asked to give permission for us to gain access to any tissue samples from previous operations or biopsies. Further tests will be performed on these samples to correlate with the results obtained from the biomarker blood tests.

6. **What are the risks involved**

6.1. **Bevacizumab side effects**

Bevacizumab is routinely used to treat patients with many cancers. It has also been used worldwide in different trials for kidney cancer treatments.
Either on its own or in combination with other medications bevacizumab is tolerated very well, overall.
The most common side effects associated with bevacizumab (more than 10%) are:
a)   Fatigue.
b)   Raised blood pressure.
c)   Protein in urine.
d)   Diarrhoea.
e)   Nausea
f)   Minor bleeding as nose bleeds
g)   Difficulty in wound healing.

Less common effects (less than 10%)
a)   Bowel perforation – seen approximately in 2% of patients with bowel cancer and treated with bevacizumab and chemotherapy.
b)   Increased risk of serious bleeding from the lining of the mouth, gut and vagina. There may be bleeding into the tumour as well.
c)   An increased risk of thrombosis (blood clots) leading to heart attack, stroke or clots in lungs
d)   Allergic reaction.

Rare side effects that may be serious.
Some rare side effects will have serious consequences if not reported to the doctors and treated appropriately. It is important that you report to your doctors at anytime if you are concerned about any of the side effects you are experiencing. Rarely (<1 in 1,000 patients) patients may experience symptoms of severe headaches, blurring of vision, altered mental status with confusion or seizures, drowsiness and coma. One of these conditions is called reversible posterior leukoencephalopathy (RPLS). Another condition that occurs very rarely (<1 in 10,000 patients) is called hypertensive encephalopathy related to the rapid increase in blood pressure. If patients experience these symptoms, they should seek medical help immediately. In most cases, the blood pressure can be controlled with medications and the conditions are reversible.
Most of these serious side effects have occurred in patients receiving chemotherapy along with bevacizumab rather than bevacizumab alone.
You will be monitored closely throughout the study period for any side effects. We will offer supportive treatment as anti-sickness, anti-hypertensive medications etc or may have to stop treatment if it is necessary.

6.2.   Side effects of Interferon-α.

Interferon-α is a protein which is present naturally in our body in very small amounts. The most common side effects associated with the use of interferon-α include

a)   Flu-like symptoms

b)   Fatigue

Flu like symptoms can occur early, within a couple of hours after the injection and does not last long. The symptoms are usually more marked with the first injection and become much less of a problem with further injections.

Less common side effects are nausea and vomiting, irritation of skin at the injection site, emotional changes, and temporary reduction in the production of blood cells by the bone marrow leading to infection, anaemia or bleeding.

7. What are the benefits of participating

Bevacizumab and bevacizumab plus interferon are proven to be useful in the treatment of advanced kidney cancer. You therefore may benefit from receiving these medications. By carrying out the trial we hope to find out the mechanism by which these medications act together. This will help us to improve the way in which we combine these medications together and thus ultimately improving the treatment of kidney cancers. We also aim to find out if we can predict the response to treatment earlier with the help of MRI scans or biomarkers.

8. Alternative treatment possibilities

There will be alternate treatment options available to you. Your doctor will go through this with you in detail before enrolling on to the trial. If during the trial new information becomes available, your doctor will discuss this with you.

9. What happens after the 8 week MRI scan is completed

After the initial 8 week study period, you will receive both bevacizumab and interferon and will continue on them for as long as they benefit you. Your response will be assessed with scans twelve weekly after the study. If the treatment has any unacceptable side effects which cannot be managed with medications, your doctor may withdraw the medications. You can also withdraw from the study at anytime without giving any reason.

10. Will the participation be kept confidential

All of the information collected about you during the period of the study will be kept strictly confidential. No individual patient details will be identified while the results of the study are published.

If you agree to participate in the study, some parts of your medical records and the data collected will be reviewed by an independent safety monitor. Data may be discussed with responsible persons from Roche pharmaceuticals who are providing treatment support for the study, but no information which identifies you will be passed to them.

Your GP will be informed of your participation in the study if you agree to it. All procedures for handling, processing, storage and destruction of any data will be according to the data protection act.

11. **What if something goes wrong**

If you have concerns about any aspects of the study you should speak to the researchers who will do their best to answer your questions (please refer to contact details below). There are no special compensatory mechanisms if you are harmed by taking part in the study other than those available to all NHS patients. If you wish to complain, the normal National Health Service complaints mechanisms are available to you. Formal complaints should be addressed to:

Mr.Nick Carver, Chief Executive, Lister Hospital, Corey's Mill Lane, Stevanage SG1 4AB
(Tel: 01438 314333 extn 5112).

12. **Independent advice**

If you want to get independent advice regarding the trial or the conduct of the trial, you can contact
The Lynda Jackson Support and Information centre
Mount Vernon Hospital.
Tel: 01923844014

The patient advice and Liaison Service 'PALS' is also available for the patient to be contacted to get independent advice in each of the study sites.

13. **Organisation and funding**

The study is sponsored by the East and North Hertfordshire trust. This will be conducted in three centres
A)   Mount Vernon Hospital, Northwood, Middlesex.
B)   Royal Marsden Hospital, Sutton, Surrey.
C)   Addenbrooke's Hospital Cambridge.

The study is funded by the Roche Phamaceuticals® who manufactures the bevacizumab and will be supplying the medicines ie both bevacizumab and interferonα-2a to the patients free of cost.

14. **Contact details for the trial**

Chief Investigator: **Dr. Paul Nathan**

Consultant Medical Oncologist
Mount Vernon Hospital
Rickmansworth Road, Northwood
Middlesex HA6 2RN
Tel: +44 1923 844 966
Fax: +44 1923 844 840

Study Coordinator &

Clinical co investigator   **Dr. Anup Vinayan**

Clinical research Fellow
Mount Vernon Hospital
Rickmansworth Road, Northwood
Middlesex HA6 2RN
Tel: + 44 1923 844 637
Fax: +44 1923 844 840

Thank you for taking your time to read through this information leaflet.

9.6. Patient informed consent form

Dynamic contrast enhanced MRI (DCE-MRI) assessment of the vascular changes induced with bevacizumab alone and in combination with interferon-α in patients with advanced renal cell carcinoma

Centre no……………

Patient identification number for the trial*……………………….

(*To be completed post randomisation)

Consent form

Please initial

1	I confirm that I have read and understood the information sheet, version……. Dated………………………, regarding the above mentioned study. I have had the opportunity to consider the information, ask questions and have had these answered satisfactorily.	☐
2	I understand that the participation in this study is voluntary and that I can withdraw from it at any time, without giving any reason and without my medical care or legal rights being affected.	☐
3	I understand that the relevant sections of my medical notes and data collected during the study may be looked at by responsible individuals involved in the study and from regulatory authorities where it is relevant to my taking part in the study. I give permission for these individuals to have access to my records	☐
4	I understand that the blood samples collected are considered as a gift and will be used for laboratory research related to this trial.	☐
5	I give consent to the research team to collect the previously stored biopsy or histopathology sample of my kidney cancer for further testing	☐

6	I give permission to the research team to transfer the samples collected to designated research laboratories at oxford for further analysis.	
6	I agree that the samples collected from me and the data gathered about me can be stored for use in future research regarding kidney cancer. I understand that some of these studies may be conducted by those other than researchers involved in this study, but that all future projects will be ethically approved.	☐
7	I give my consent to take part in the above mentioned study.	☐
8	I agree to my GP being informed of my participation in the study.	☐

_____ _____ -
_____

Name of Patient   Signature   Date
(To be completed by patient)

_____ _____ -
_____

Name of Person taking consent   Signature   Date

(If different from Investigator)

_____ _____ -
_____

Name of Investigator   Signature   Date

9.7.   Sample handling manual

DCE-MRI assessment of the vascular changes induced by bevacizumab alone or in combination with IFN in patients with advanced RCC

SAMPLE HANDLING INSTRUCTIONS

A)   Blood samples for biomarker analysis

Samples

Blood sample for haematology, clinical chemistry and coagulation will be collected as per the study site's standard procedure.

SAMPLES FOR BIOMARKER ANALYSIS COLLECTED AT
   a. SCREENING – TWICE
   b. WEEK 2 on treatment
   c. WEEK 6 on treatment
   d. WEEK 8 on treatment
   e. DISCONTINUATION of treatment

Samples to be collected for biomarker analysis
      2x10ml samples in EDTA vial
      1x5ml sample in a lithium heparin vial.

Sample Handling instructions

a)   CEC,CEPC & Angiogenic marker analysis (10ml EDTA sample)

   1. 10ml of the blood to be collected in EDTA vacutainer tubes (purple top).
   2. Label the tube appropriately with the trial code, trial number of the patient and date of collection and time of collection.
   3. The sample should be transported by courier same day at room temperature to the stem cell research laboratory at John Radcliffe hospital by 4:00pm on the day of collection (transported at room temperature).
   4. Log patient details, date, time point in trial, time of collection & despatch onto lab log sheets

NOTE: 24 HR NOTICE TO BE GIVEN TO THE LABORATORY PRIOR TO SENDING SAMPLE

b)   Peripheral blood analysis for MicroRNA (10ml EDTA sample)

   1. 10 ml of blood to be collected into EDTA vacutainer tubes (purple top),
   2. Place the sample in an ice bucket immediately after drawing.

3. The sample should be centrifuged within 3 hrs of collection at 2000 G for 10 minutes in a refrigerated centrifuge (4°C).
4. The plasma is removed carefully to avoid disturbing the buffy coat and transferred to a new tube.
5. Centrifuge the plasma again at minimum of 2000 G for 10 minutes in a refrigerated centrifuge (4°C).
6. Aliquots (1 or 2) of 1.6ml plasma will be transferred to new tubes
7. Add 2ml of TRIZOL LS to the sample.
8. Samples vortexed, left for 5 minutes at room temperature,
9. Label the sample appropriately (trial code, site and trial number, date of collection)
10. Store in a freezer at -80°C.
11. Samples should be despatched in batched to the laboratory in dry ice.
12. Log patient details, time point in trial, times of collection & centrifugation in log sheet.

c) Proteomics

1. 5mls of blood will be collected in lithium heparin vacuum tubes.
2. Centrifuge the sample at 500G for 10minutes.
3. Plasma isolated should then be transferred to 1.5 – 2 ml tubes.
4. The samples are labelled appropriately (site and trial number, date of collection) and stored at -80°C.
5. The samples from an individual patient should be batched and shipped on dry ice after all time points are collected.
6. Log details – patient details, time point in study, time of collection and centrifugation onto lab log sheets.

B) Immuno-histochemistry

Archival samples requested from original path labs to be sent to sponsor site.
Samples will be anonymysed, Mark with patient initials, trialcode, site and patient number.
Samples despatched to Oxford at ambient temperature.
Please log the details in the log sheet.

C) Urine sample for proteomics

15 mls of urine sample collected once in the screening period.
Samples labelled appropriately
Store in -80°C freezer and despatched in batches to the lab with other proteomics sample in dry ice
Log details into lab log sheet.
CONTACT ADDRESS FOR SENDING SAMPLES

9.8.   Management of IMP related toxicities

Dose Modifications and Delays

The observed toxicity will be graded according to the CTCAE v3.0 guidelines. Dose modifications will be implemented according to the observed toxicity grade as specified below.

Dose Modifications for patients receiving Interferon alpha-2a

Any grade 3 toxicity attributable to interferon alpha-2a will require interferon alpha-2a to be withheld. If toxicity resolves to ≤grade 1 within 2 weeks, interferon alfa-2a may be reintroduced.

For patients receiving 9MU of IFN, if toxicity takes >2 weeks to resolve to grade 1, or, in the opinion of the investigator, if the patient would benefit from dose reduction, the following dose levels should be used:

- Highest target dose: 9 MIU of interferon alfa-2a 3x/week
- Dose Level -1: 6 MIU of interferon alfa-2a 3x/week
- Dose Level -2: 3 MIU of interferon alfa-2a 3x/week

In case of unacceptable toxicity at this lowest dose of interferon alpha-2a (as defined above), interferon alpha-2a must be discontinued. In the absence of disease progression, bevacizumab may be continued. Any patient who develop any one of the following should discontinue interferon alpha therapy

- Grade 4 toxicity
- Any Grade 3 toxicity after two dose reductions **and unsuccessful schedule modification**
- Grade 3 toxicity that does not resolve to grade 1 or less within 4 weeks

Treatment modifications in case of events attributable to bevacizumab

No dose reduction of bevacizumab is allowed.

Any patient who develop any one of the following toxicities should not receive further bevacizumab

- Gastrointestinal perforation
- Arterial thromboembolic events

- Grade 3/4 haemorrhagic events

- Symptomatic Grade 4 thrombosis

- Grade 4 hypertension (hypertensive crisis)

- Grade 4 proteinuria (nephrotic syndrome)

In case bevacizumab is discontinued, continuation of interferon alpha may be considered.

Bevacizumab-specific toxicities

Gastrointestinal Perforation

Bevacizumab should be permanently discontinued in patients who develop gastrointestinal perforation.

Surgical Procedures/Wound Healing Complications

Bevacizumab therapy should not be initiated for at least 28 days following surgery or until the surgical wound is fully healed.

Hypertension

Patients should be monitored for the development or worsening of hypertension via frequent blood pressure measurement. Blood pressure measurements should be taken after the patient has been in a resting position for ≥ 5 minutes. Repeat measurement of blood pressure for verification should be undertaken if the initial reading is ≥ 140 mmHg systolic and/or ≥ 90 mmHg diastolic blood pressure.

- Grade 1 hypertension: Asymptomatic, transient (< 24 hrs) increase by > 20 mmHg (diastolic) or to > 150/100 mmHg if previously within normal limits- No Intervention.

- Grade 2 hypertension: Recurrent or persistent (> 24 hr) or symptomatic increase by > 20 mmHg (diastolic) or to > 150/100 mmHg if previously within normal limits. Bevacizumab should be withheld. Monotherapy of anti-hypertensive is indicated as per the local policy. Once controlled to < 150/100 mmHg, patients continue bevacizumab therapy.

- Grade 3 hypertension: Requiring more than one anti-hypertensive or more intensive therapy than previously. Bevacizumab should be withheld for persistent or symptomatic hypertension and should be permanently discontinued if hypertension is not controlled.

- Grade 4 hypertension: Life threatening consequence (e.g. hypertensive crisis) Occurrence of grade 4 hypertension should lead to permanent discontinuation of bevacizumab. All doses of anti-hypertensive medicines should be recorded at all visits.

Proteinuria

All patients will have a dipstick urinalysis or 24 hour protein determination performed, prior to each bevacizumab dose. A 24 hour urine collection for protein determination is mandatory at baseline if dipstick shows ≥2+ proteinuria. All proteinuria toxicity, as determined by 24 hour urine collection, will be graded according to CTCAEv3.0 guidelines. Adjustment of bevacizumab administration for proteinuria will occur according to the following guidelines:

First occurrence of proteinuria:

- < 2+ (dipstick): Administer bevacizumab as scheduled, NO additional evaluation is required.
- 2+, 3+ and 4+ proteinuria (dipstick): Administer bevacizumab as scheduled.

Collection of 24-hour urine to determine the total protein within 3 days prior to the next scheduled dose is required:

- 24-hour proteinuria ≤ 2 g: Administer bevacizumab as scheduled. Repeat dipstick is required before each scheduled administration of bevacizumab.
- 24-hour proteinuria > 2 g: Bevacizumab treatment should be withheld pending next 24 hour total protein.

Repeat 24-hour urine protein ≤ 2 g: Administer bevacizumab as schedule. 24-hour protein should be further monitored prior to each administration of bevacizumab until it has decreased to ≤ 1 g/24 h.

Repeat 24-hour urine protein > 2 g: Bevacizumab dose should be withheld until 24-hour protein has decreased to ≤ 2 g. 24-hour protein should be further monitored prior to each administration of bevacizumab until it has decreased to ≤ 1 g/24 h.

Second and subsequent occurrence of proteinuria:

- < 3+ proteinuria (dipstick): administer bevacizumab as planned.
- ≥3+ proteinuria (dipstick): administer bevacizumab as planned and collect 24-hour urine for determination of total protein within 3 days before the next scheduled bevacizumab administration.
  - 24-hour proteinuria ≤ 2 g: Administer bevacizumab as scheduled. Repeat dipstick is required before each scheduled administration of bevacizumab.
  - 24-hour proteinuria > 2 g: Bevacizumab treatment should be withheld pending next 24 hour total protein.

Repeat 24-hour urine protein ≤ 2 g: Administer bevacizumab as schedule. 24-hour protein should be further monitored prior to each administration of bevacizumab until it has decreased to ≤ 1 g/24 h.

Repeat 24-hour urine protein > 2 g: Bevacizumab dose should be withheld until 24-hour protein has decreased to ≤ 2 g. 24-hour protein should be further monitored prior to each administration of bevacizumab until it has decreased to ≤ 1 g/24 h.

Nephrotic syndrome (Grade 4, CTCAE v3.0): Discontinue bevacizumab treatment

Thrombosis/Embolism

All toxicity will be graded according to CTCAEv3.0 guidelines. For patients who develop Grade 3 or 4 thrombosis/embolism the following action is recommended:

• Bevacizumab should be permanently discontinued in patients who develop arterial thrombo-embolic events.

• Grade 3 or 4 venous thrombosis: Hold study drug treatment for 2 weeks.

Bevacizumab may be resumed after initiation of the therapeutic dose anticoagulant therapy as soon as all of the following criteria are met:

▪ The patient must be on a stable dose of anticoagulant and, if on warfarin, have an INR within the target range (usually between 2 and 3) prior to restarting study drug treatment

▪ The patient must not have had a Grade 3 or 4 haemorrhagic event since entering the study

▪ The patient must not have had any evidence of tumour invading or abutting major blood vessels on any prior disease assessment.

• Symptomatic Grade 4 thrombosis: Discontinue the patient from the study.

Haemorrhage

All toxicity will be graded according to CTCAEv3.0 guidelines. Patients who develop Grade 3 or 4 haemorrhage should discontinue bevacizumab treatment.

Dose Adjustment of bevacizumab due to Changes in Body Weight

Body weight at baseline is to be used to calculate the required dose, and no dose modifications are foreseen unless the patient's body weight changes by more >10% from baseline.

9.9. DCE-MRI QA and QC

Version 1 Jane Taylor 3.5.13
DCE-MRI Trial QA and QC

DCE-MRI assessment of vascular changes using bevacizumab and Interferon in reanl cell carcinoma trial includes quantitative Dynamic Contrast-Enhanced MRI. This need to have specialised QA carried out to ensure their ability to produce accurate data.

This should include a dry run of the entire protocol on the Eurospin T1 phantom (T05), and then on a volunteer (minus the contrast injections). This will minimise the chance of the first patient's data being incorrect, wasting the patient's time and PSSC resources. It will also give a realistic idea of the study timings.

The primary QA needed for DCE-MRI trials is in testing the T1 quantification of the sequences to be used. Summary methodology can be found in the VIBE subsection in Q:\protocols and check sheets\analysis and QA methodology \ MR QAData acquisition_V3.doc which is expanded in this document.

VIBE sequences for measuring T1.

VIBE (Volume-interpolated breathhold examination) sequences acquire a three-dimensional block, subsequently reconstructed into thin slices. They were initially designed for rapid liver imaging, and have the option of using rapid and specialised RF pulses at low flip angles in order to select very precise blocks. These fast pulses use high RFPA voltages, and are not necessarily suitable for all patients or studies. This is mainly due to approaching the RFPA power limit or exceeding 21°. At such a point, the scanner provides a pulse of lesser flip than programmed, a fact which is only apparent on examining data after acquisition. It is therefore more useful to use RF pulses in 'normal' mode, as these do not exhibit this uncertainty and the subsequent quantification is more reliable.

To use VIBE sequences to measure T1 requires the use of a pair of images: a baseline image with very low flip angle (proton density weighted) and a T1-weighted image with much larger flip angle. More relaxation will occur with the PD, giving an image which is fully relaxed. The T1-w image will depend on how much relaxation occurs between repeats, given the flip angle, and it is possible to work out the T1 of a sample given the PD and T1w images. Optimising the T1-w flip angle for a given TR is also useful.

Analysis

This is performed using the MRIW program. There are two ways of analysing the data, one using the dedicated T1 QA function, accessed via XML files, and a simpler summary method.

Simple summary method

Open MRIW. Click File and then Import DCE-MRI…
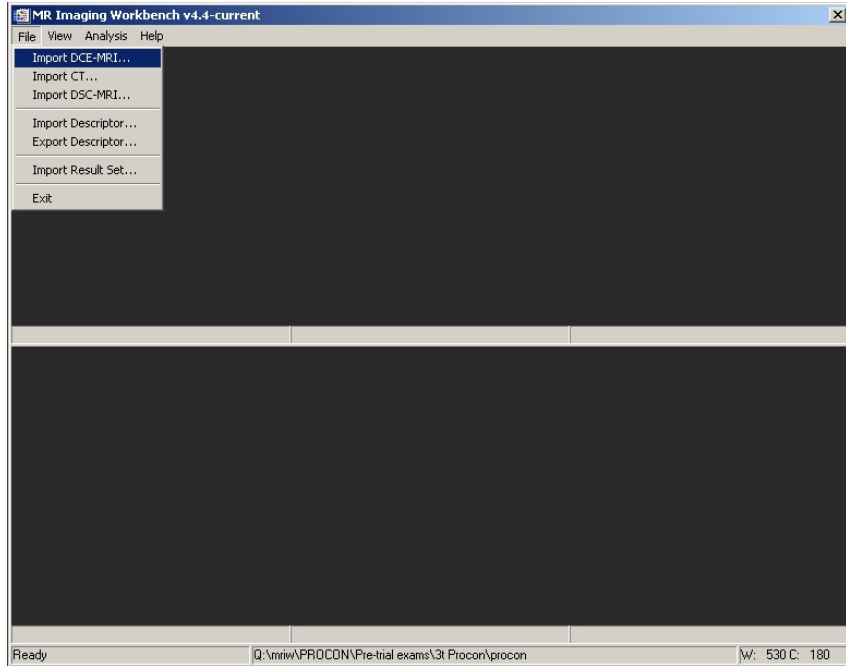
The DICOM import dialogue box will pop up. Navigate to the relevant directory and then select the pre-contrast scan (Proton-density weighted) for Reference and the contrast-enhanced scan (T1-weighted) for Dynamic.
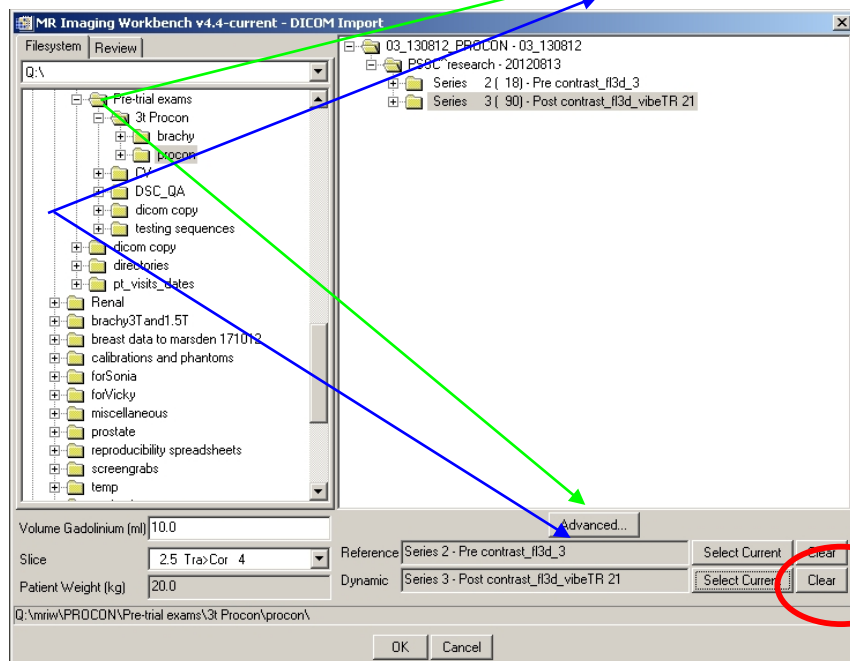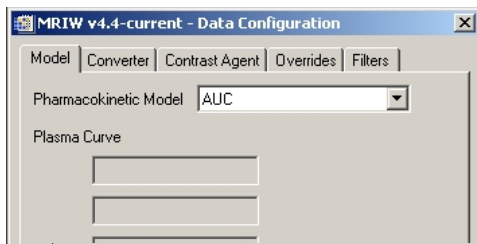
Click Advanced… and then select AUC from the drop-down menu on the Model tab. Press OK, then OK again on the DICOM import box. Data will load.
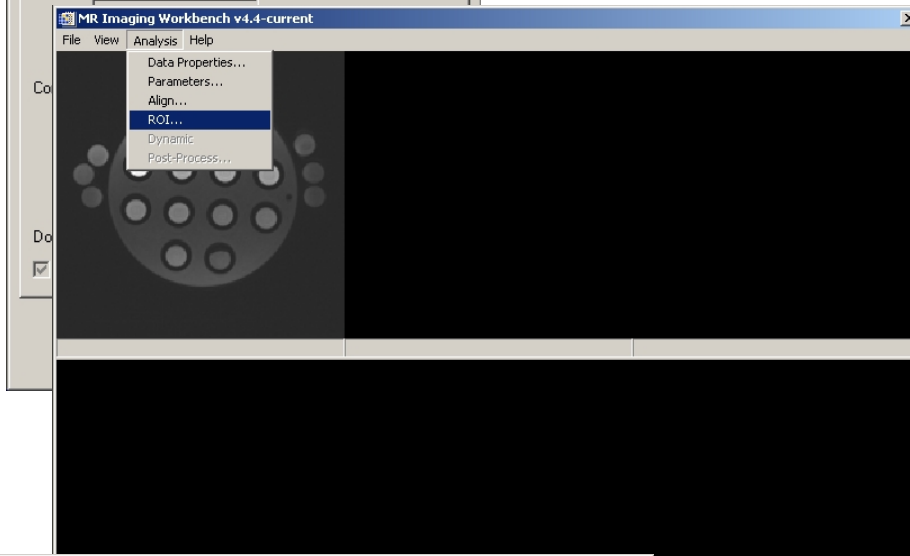
Click on the Analysis menu, and choose ROI…
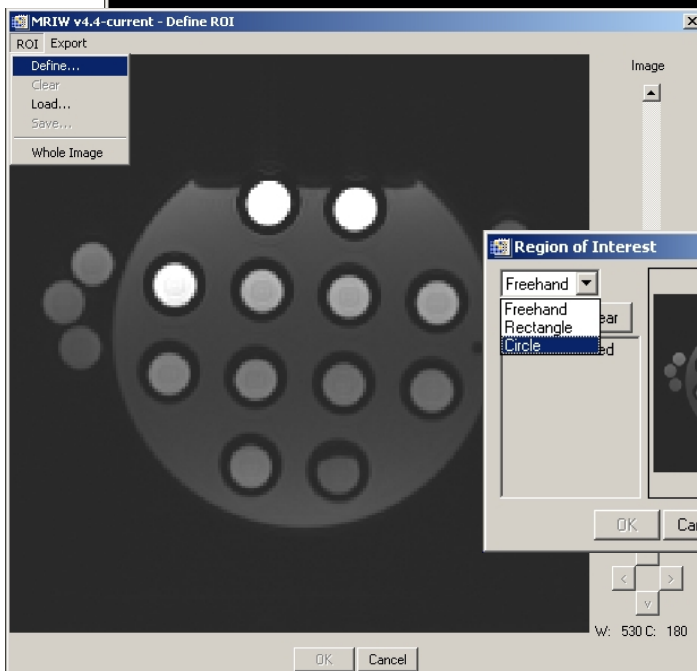
Click on the ROI menu and choose Define…

A Region of Interest box will pop up. Choose Circle from the drop-down menu.

Click the point where you wish the centre of the circle to be, and then, holding down the mouse button, drag the mouse pointer outwards. Let go of the button when the circle is the desired size.
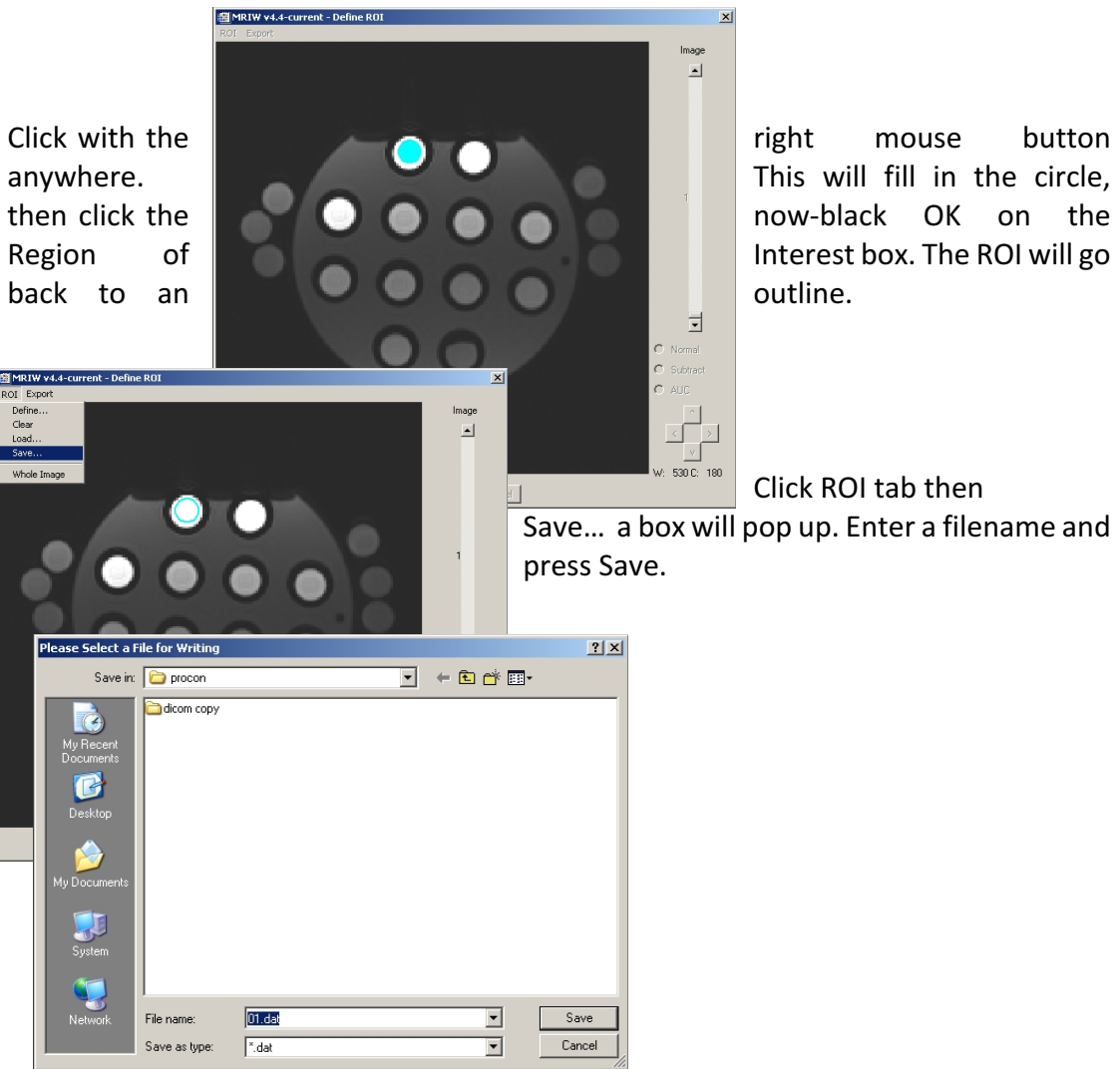
Click with the right mouse button anywhere. This will fill in the circle, then click the now-black OK on the Region of Interest box. The ROI will go back to an outline.

Click ROI tab then Save… a box will pop up. Enter a filename and press Save.

At this site, the phantom vials are conventionally placed in the cylinder as shown at right. Number the ROIs accordingly.

If in doubt, 1 is the very brightest followed by 2 and 3. Then the signal drops off rapidly, allowing the order of gels to be deduced.
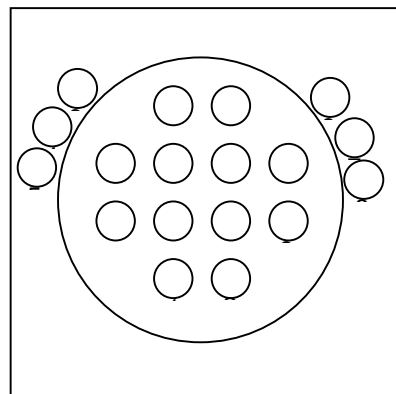
Press OK in the ROI screen to return to the main MRIW screen.

Press Analysis then Dynamic…
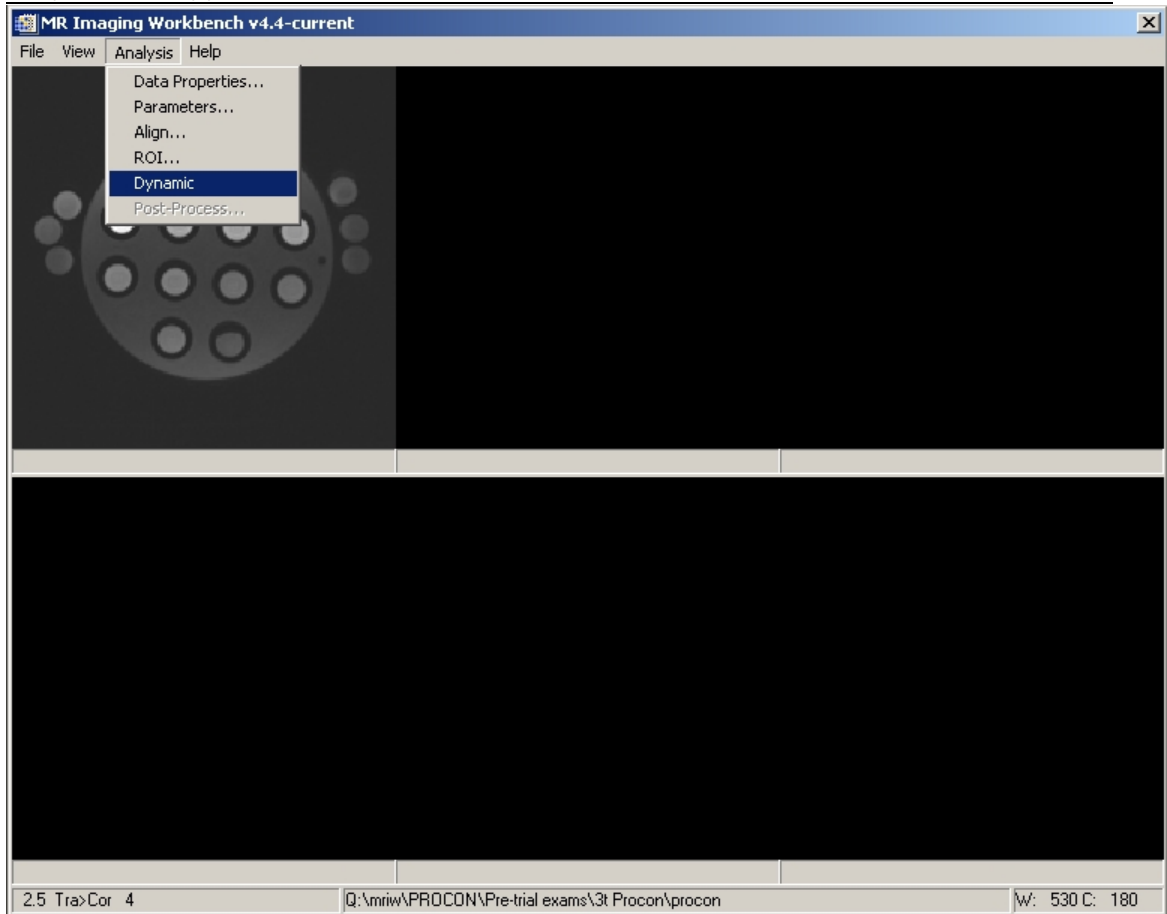
When the calculation has finished, images will pop up.

Press **Analysis** then **Post-Process…** and select **Initial T1** from the **Map** dropdown menu
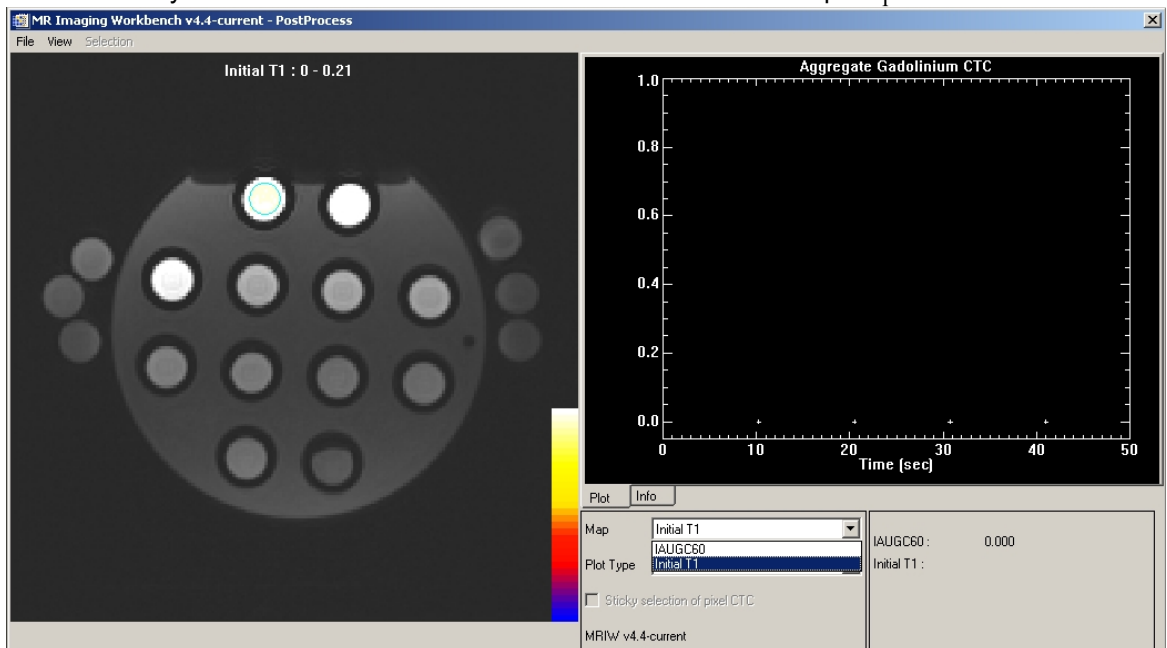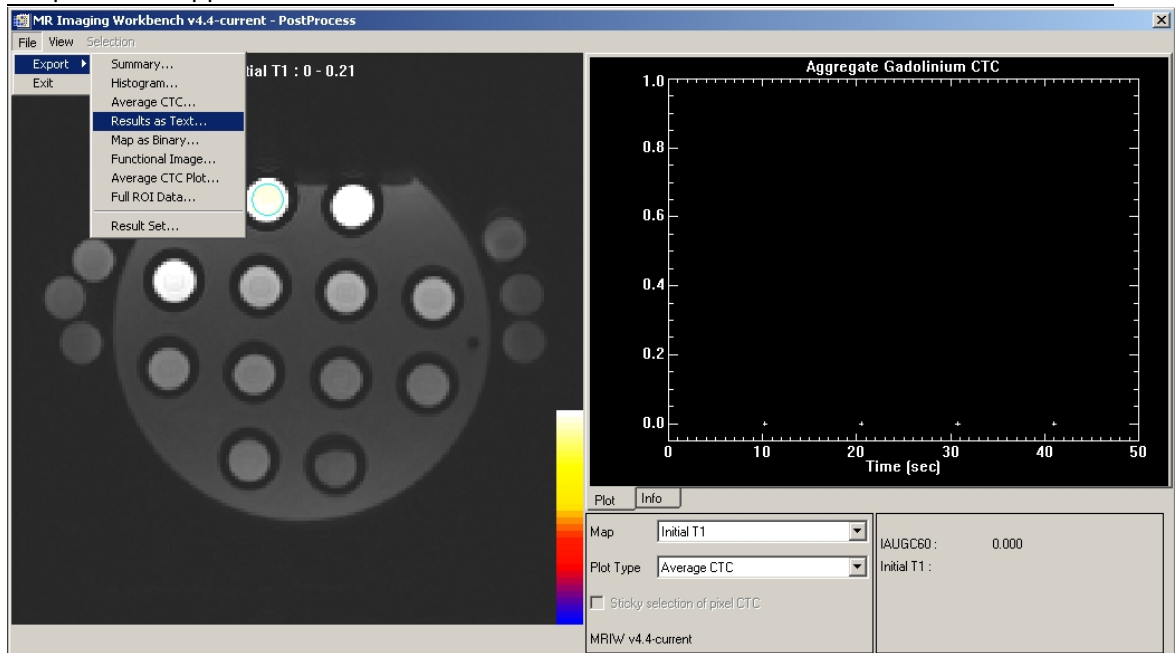
Choose File > Export > Results as Text…
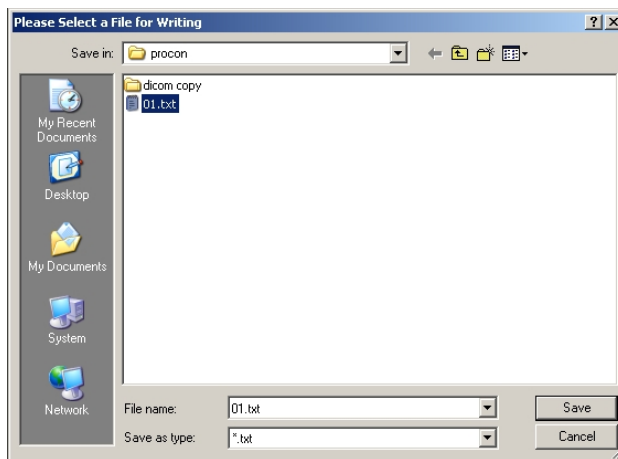
Name the output the same as the gel number.

Press Save. Close down the PostProcess box, and return to the Analysis > ROI box. Draw the next ROI around the next gel, and repeat the whole procedure until all 18 gels have been drawn and calculated.

Close MRIW.

Open MS Excel.

Open the directory with the gel results in, and then select all .txt files.
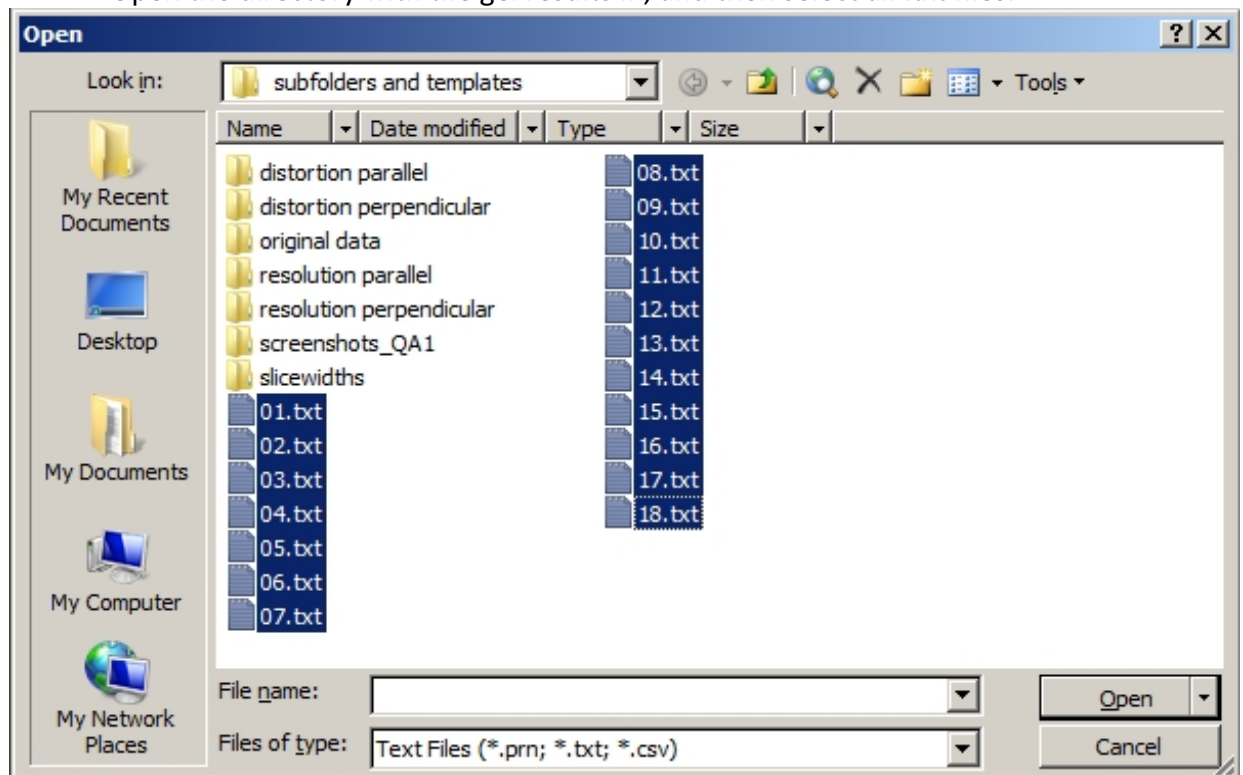
Press Open. It will open the Text Import Wizard.
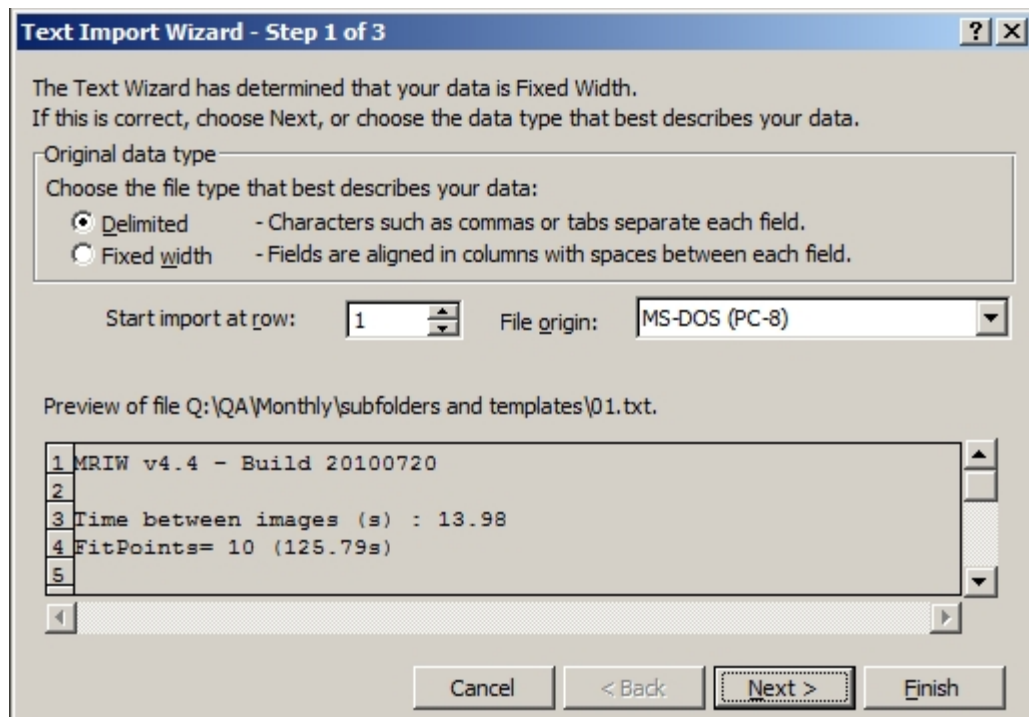
Tick Delimited, then press Next >

Tick Tab and Space then press Finish
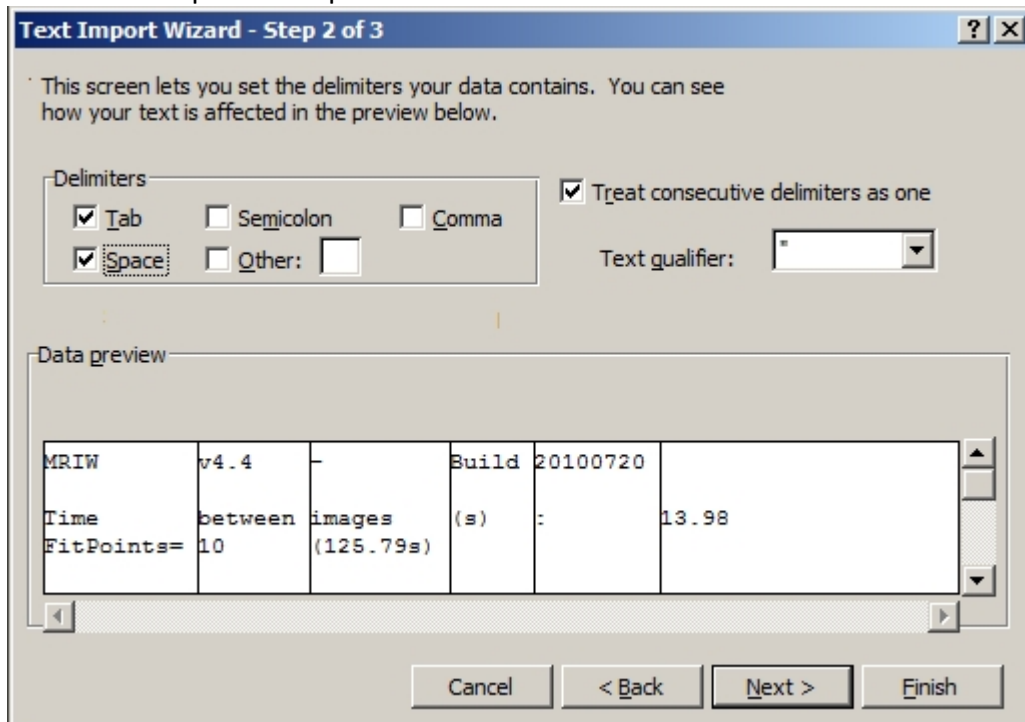
Repeat for all the gels.

In the first converted file, Scroll down to the last line of the summary (Lines 70 and 71) and select cells B72 –G72 inclusive. Copy and paste them into a new workbook. Close that text file and repeat for 02.txt – 18.txt.

	A	B	C	D	E	F	G	H	I
64		0.0001	0.0019	0.0018	0.0006	0.0004	0.0005		
65									
66	[Enhancement]								
67		Min	Max	Range	Mean	StdDev	Median		
68		0	0	0	0	0	0		
69									
70	[Initial	T1]							
71		Min	Max	Range	Mean	StdDev	Median		
72		0.1915	0.2111	0.0196	0.2002	0.0037	0.2003		
73									
74									
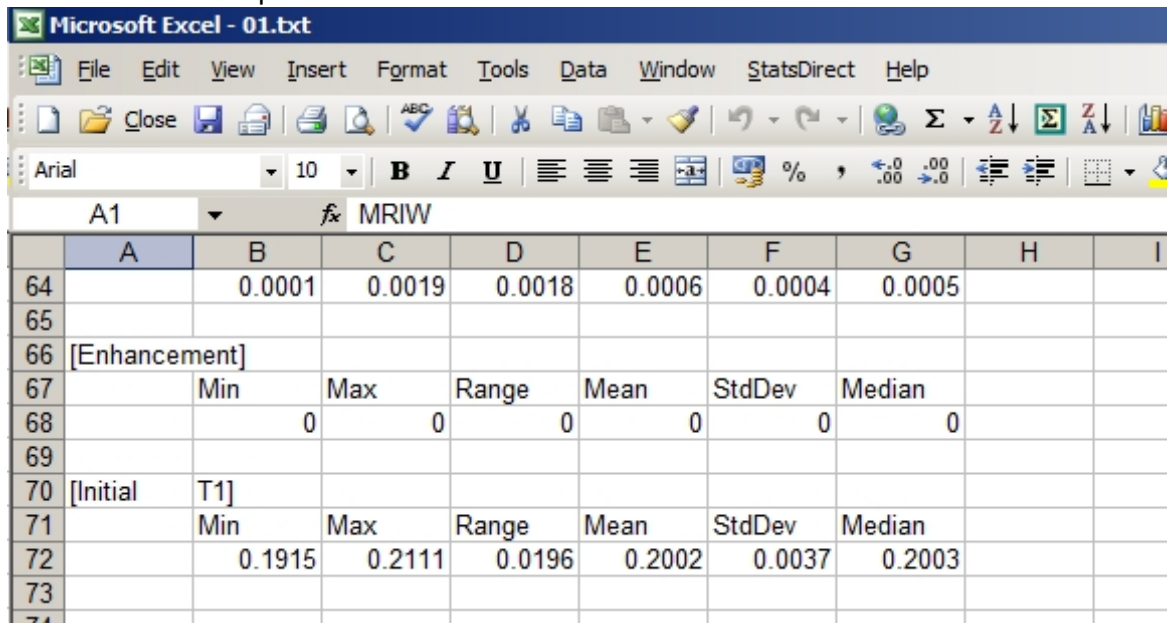
Now you will have in the summary file:

	A	B	C	D	E	F	G	H
		K16	▼	*fx*				
	A	B	C	D	E	F	G	H
1	[Initial	T1]						
2		Min	Max	Range	Mean	StdDev	Median	
3	1	0.1915	0.2111	0.0196	0.2002	0.0037	0.2003	
4	2	0.2972	0.3305	0.0333	0.3147	0.0067	0.3147	
5	3	0.3126	0.3469	0.0343	0.3254	0.0059	0.325	
6	4	0.427	0.5498	0.1228	0.4686	0.0192	0.4699	
7	5	0.4456	0.523	0.0774	0.4792	0.0165	0.4789	
8	6	0.4798	0.5248	0.045	0.5042	0.0094	0.5048	
9	7	0.6215	0.6973	0.0759	0.6518	0.017	0.6485	
10	8	0.5808	0.7065	0.1257	0.6421	0.0232	0.6421	
11	9	0.7742	1.0104	0.2362	0.8389	0.035	0.8359	
12	10	0.8849	1.0164	0.1315	0.9651	0.0246	0.9669	
13	11	0.9278	1.1628	0.235	1.0149	0.0464	1.0094	
14	12	1.7014	2.3231	0.6217	2.0251	0.1244	2.0322	
15	13	1.1269	1.4283	0.3014	1.2712	0.0658	1.2772	
16	14	1.198	1.4647	0.2666	1.345	0.0432	1.3426	
17	15	1.3071	1.6991	0.392	1.5151	0.087	1.5258	
18	16	1.3555	1.7128	0.3574	1.5302	0.0748	1.5229	
19	17	1.3248	1.7868	0.462	1.5489	0.0745	1.5497	
20	18	1.6736	2.0528	0.3793	1.8404	0.0715	1.8337	
21								

The median values need multiplying by 1000 to get their units to milliseconds, and then the reference values of T1 for the gels at the measured room temperature need to be added.

This should give

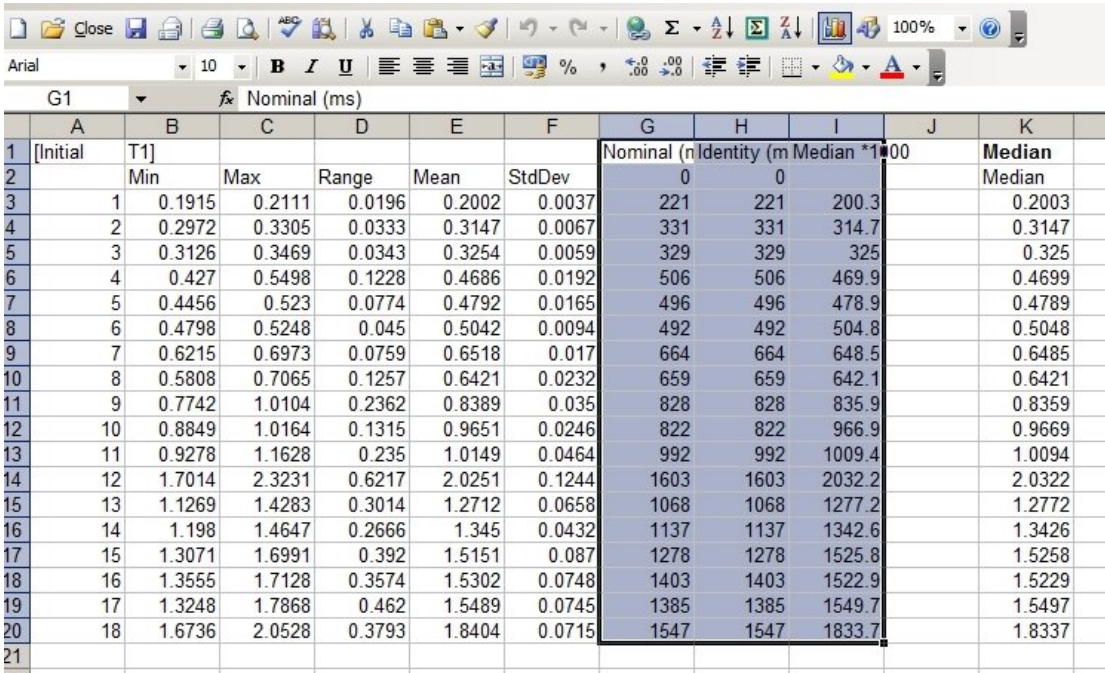|	A	B	C	D	E	F	G	H	I	J	K	L
		P20	▼	*fx*								
	A	B	C	D	E	F	G	H	I	J	K	L
1	[Initial	T1]					Nominal (n	Identity (m	Median *1000		**Median**	
2		Min	Max	Range	Mean	StdDev	0	0			Median	
3	1	0.1915	0.2111	0.0196	0.2002	0.0037	221	221	200.3		0.2003	
4	2	0.2972	0.3305	0.0333	0.3147	0.0067	331	331	314.7		0.3147	
5	3	0.3126	0.3469	0.0343	0.3254	0.0059	329	329	325		0.325	
6	4	0.427	0.5498	0.1228	0.4686	0.0192	506	506	469.9		0.4699	
7	5	0.4456	0.523	0.0774	0.4792	0.0165	496	496	478.9		0.4789	
8	6	0.4798	0.5248	0.045	0.5042	0.0094	492	492	504.8		0.5048	
9	7	0.6215	0.6973	0.0759	0.6518	0.017	664	664	648.5		0.6485	
10	8	0.5808	0.7065	0.1257	0.6421	0.0232	659	659	642.1		0.6421	
11	9	0.7742	1.0104	0.2362	0.8389	0.035	828	828	835.9		0.8359	
12	10	0.8849	1.0164	0.1315	0.9651	0.0246	822	822	966.9		0.9669	
13	11	0.9278	1.1628	0.235	1.0149	0.0464	992	992	1009.4		1.0094	
14	12	1.7014	2.3231	0.6217	2.0251	0.1244	1603	1603	2032.2		2.0322	
15	13	1.1269	1.4283	0.3014	1.2712	0.0658	1068	1068	1277.2		1.2772	
16	14	1.198	1.4647	0.2666	1.345	0.0432	1137	1137	1342.6		1.3426	
17	15	1.3071	1.6991	0.392	1.5151	0.087	1278	1278	1525.8		1.5258	
18	16	1.3555	1.7128	0.3574	1.5302	0.0748	1403	1403	1522.9		1.5229	
19	17	1.3248	1.7868	0.462	1.5489	0.0745	1385	1385	1549.7		1.5497	
20	18	1.6736	2.0528	0.3793	1.8404	0.0715	1547	1547	1833.7		1.8337	
21												

Select columns G, H and I and press the graph icon

	A	B	C	D	E	F	G	H	I	J	K
1	[Initial	T1]					Nominal (n	Identity (m	Median *1 00		**Median**
2		Min	Max	Range	Mean	StdDev	0	0			Median
3	1	0.1915	0.2111	0.0196	0.2002	0.0037	221	221	200.3		0.2003
4	2	0.2972	0.3305	0.0333	0.3147	0.0067	331	331	314.7		0.3147
5	3	0.3126	0.3469	0.0343	0.3254	0.0059	329	329	325		0.325
6	4	0.427	0.5498	0.1228	0.4686	0.0192	506	506	469.9		0.4699
7	5	0.4456	0.523	0.0774	0.4792	0.0165	496	496	478.9		0.4789
8	6	0.4798	0.5248	0.045	0.5042	0.0094	492	492	504.8		0.5048
9	7	0.6215	0.6973	0.0759	0.6518	0.017	664	664	648.5		0.6485
10	8	0.5808	0.7065	0.1257	0.6421	0.0232	659	659	642.1		0.6421
11	9	0.7742	1.0104	0.2362	0.8389	0.035	828	828	835.9		0.8359
12	10	0.8849	1.0164	0.1315	0.9651	0.0246	822	822	966.9		0.9669
13	11	0.9278	1.1628	0.235	1.0149	0.0464	992	992	1009.4		1.0094
14	12	1.7014	2.3231	0.6217	2.0251	0.1244	1603	1603	2032.2		2.0322
15	13	1.1269	1.4283	0.3014	1.2712	0.0658	1068	1068	1277.2		1.2772
16	14	1.198	1.4647	0.2666	1.345	0.0432	1137	1137	1342.6		1.3426
17	15	1.3071	1.6991	0.392	1.5151	0.087	1278	1278	1525.8		1.5258
18	16	1.3555	1.7128	0.3574	1.5302	0.0748	1403	1403	1522.9		1.5229
19	17	1.3248	1.7868	0.462	1.5489	0.0745	1385	1385	1549.7		1.5497
20	18	1.6736	2.0528	0.3793	1.8404	0.0715	1547	1547	1833.7		1.8337
21											

Choose XY (Scatter) and Finish.

Edit graph to how you want it, and fit a line to the GH columns to show the line of identity (ideal plot). This will show how the measured gel values deviate.
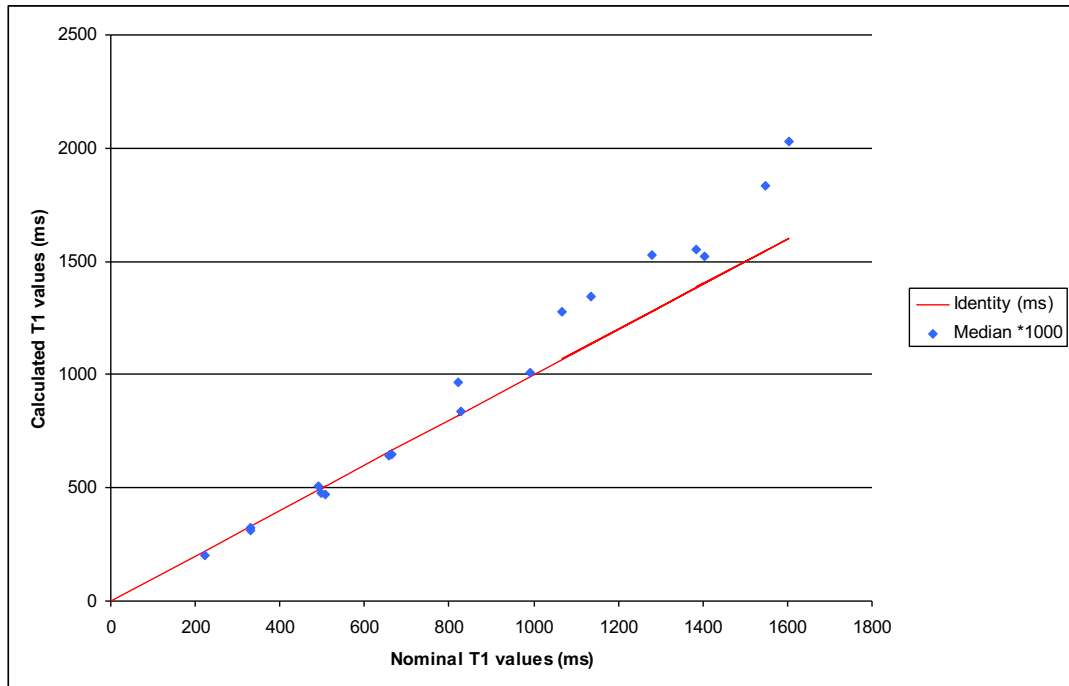
This plot shows that to about 1000ms, VIBE T1 measurements are fairly accurate, then overestimate the T1s as they get higher. This is typical of a Siemens Avanto.

9.10. Regulatory approvals

NHS

National Research Ethics Service
Charing Cross Research Ethics Committee
Room 4W/12, 4th Floor
Charing Cross Hospital
Fulham Palace Road
London, W6 8RF
Telephone: 020 8846 7283
Facsimile: 020 8846 7280

Dr Paul Nathan
Consultant Medical Oncologist
East and North Hertfordshire NHS Trust
Mount Vernon Hospital
Rickmansworth road, Northwood
Middlesex, HA6 2RN

21 January 2009

Dear Dr Nathan

Full title of study:	**Dynamic contrast enhanced MRI (DCE-MRI) assessment of the vascular changes induced with bevacizumab alone and in combination with interferon-a in patients with advanced renal cell carcinoma**
REC reference number:	**09/H0711/6**
Protocol number:	**1.1**
EudraCT number:	**2008-006414-19**

The Research Ethics Committee reviewed the above application at the meeting held on 19 January 2009. Thank you for attending to discuss the study.

Ethical opinion

The committee asked about the definition of advanced renal cell carcinoma. The researcher confirmed that this meant inoperable local spread or metastatic disease.
The committee enquired about the evidence for benefits of the treatment. The researcher explained that the latest combination therapy approximately doubled the survival of the patients.
The committee sought clarification whether the combination therapy is substantially better than monotherapy. The researcher explained that they are yet to establish the reasons for effectiveness of the combination therapy.
The committee enquired about the risk to patients' long term survival from taking part in the study, in particular receiving monotherapy. The researcher explained that the dose of Interferon has substantial side effects. The lower dose of 3MU is better tolerated and maybe antiangiogenic, thus more beneficial. The researcher pointed out the main disadvantages for the patients which are the 6 week MRI scan and the 8 week CT scan. The researcher also explained that after that the patient could switch to anything that their physician would consider appropriate.
The committee noted that there would be quite number of scans. The researcher acknowledged that the MRI scans are extra to normal patient care but explained that by doing two initial MRI scans a good baseline could be established (by assessing intra-patient variation).
The committee enquired whether the scans would be done on outpatient basis. The researcher confirmed this, and added that the patients are generally very motivated.
The committee was interested to know that if no difference were found, would progression to the next study occur. The researcher confirmed that they would progress to the next study.
The researcher explained that the present study would give information about the

This Research Ethics Committee is an advisory committee to London Strategic Health Authority
The National Research Ethics Service (NRES) represents the NRES Directorate within
the National Patient Safety Agency and Research Ethics Committees in England

mechanism of the treatment and might give some justification to a particular drug regime. The committee enquired whether patients would be still entitled to the combination therapy post study.

The researcher explained that this combination would be available for most patients although there would still be an element of "post-code prescribing" which might limit its availability.

The members of the Committee present gave a favourable ethical opinion of the above research on the basis described in the application form, protocol and supporting documentation, subject to the conditions specified below.

Conditions of the favourable opinion

The favourable opinion is subject to the following conditions being met prior to the start of the study.

Management permission or approval must be obtained from each host organisation prior to the start of the study at the site concerned.

Management permission at NHS sites ("R&D approval") should be obtained from the relevant care organisation(s) in accordance with NHS research governance arrangements. Guidance on applying for NHS permission is available in the Integrated Research Application System or at http://www.rdforum.nhs.uk.

Clinical trial authorisation must be obtained from the Medicines and Healthcare products Regulatory Agency (MHRA).

The sponsor is asked to provide the Committee with a copy of the notice from the MHRA, either confirming clinical trial authorisation or giving grounds for non-acceptance, as soon as this is available.

The committee requested the following amendments.

The patient information sheet:
- The following sentence "there will therefore be no disadvantage to receiving treatment in any of the above-mentioned groups" should be removed
- Should specify the extent of benefits of the combination therapy
- Should indicate that it is uncertain whether monotherapy (i.e.bevacizumab without interferon) is inferior to the combination therapy in terms of efficacy, and whether the dose of interferon can also affect the outcome.

Approved documents

The documents reviewed and approved at the meeting were:

Document	Version	Date
Student CV		23 December 2008
Flow Chart of Protocol		17 December 2008
Participant Consent Form	1.1	17 December 2008
Participant Information Sheet	1.1	17 December 2008
GP/Consultant Information Sheets	1.1	17 December 2008
Sample Diary/Patient Card	1.1	17 December 2008
Peer Review		04 November 2008
Letter from Sponsor		10 November 2008
Protocol	1.1	17 December 2008
Investigator CV		23 December 2008
Application		23 December 2008

Membership of the Committee

The members of the Ethics Committee who were present at the meeting are listed on the attached sheet.

Statement of compliance

This Committee is recognised by the United Kingdom Ethics Committee Authority under the Medicines for Human Use (Clinical Trials) Regulations 2004, and is authorised to carry out the ethical review of clinical trials of investigational medicinal products.

The Committee is fully compliant with the Regulations as they relate to ethics committees and the conditions and principles of good clinical practice.

The Committee is constituted in accordance with the Governance Arrangements for Research Ethics Committees (July 2001) and complies fully with the Standard Operating Procedures for Research Ethics Committees in the UK.

After ethical review

Now that you have completed the application process please visit the National Research Ethics Website > After Review

You are invited to give your view of the service that you have received from the National Research Ethics Service and the application procedure. If you wish to make your views known please use the feedback form available on the website.

The attached document "After ethical review – guidance for researchers" gives detailed guidance on reporting requirements for studies with a favourable opinion, including:

- Notifying substantial amendments
- Progress and safety reports
- Notifying the end of the study

The NRES website also provides guidance on these topics, which is updated in the light of changes in reporting requirements or procedures.

This Research Ethics Committee is an advisory committee to London Strategic Health Authority
The National Research Ethics Service (NRES) represents the NRES Directorate within
the National Patient Safety Agency and Research Ethics Committees in England

We would also like to inform you that we consult regularly with stakeholders to improve our service. If you would like to join our Reference Group please email referencegroup@nres.npsa.nhs.uk.
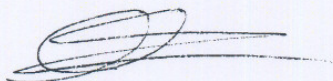
09/H0711/6	Please quote this number on all correspondence

With the Committee's best wishes for the success of this project

Yours sincerely

pp

Dr Charles Mackworth-Young
Chair

Email: carli.sager@imperial.nhs.uk

Enclosures: *List of names and professions of members who were present at the meeting and those who submitted written comments*
"After ethical review – guidance for researchers" SL-AR1 for CTIMPs

Copy to: *Ms Fiona Smith*

Charing Cross Research Ethics Committee

Attendance at Committee meeting on 19 January 2009

Committee Members:

Name	Profession	Present	Notes
Mrs Peg Belson	Lay Member	No	
Dr Alison Crombie	Anthropologist Nurse	Yes	
Dr Amod Dalvin	Psychiatrist	No	
Dr David Evans	General Practitioner	Yes	
Dr Kanagasabai Ganeshaguru	Scientist	Yes	
The Rev'd Nigel Griffin	Hospital Chaplain	Yes	
Dr Shaun Griffin	Member	Yes	
Dr Akil Jackson	HIV Physician	Yes	
Mr David Leonard	Pharmacist	No	
Miss Katie Macdonald	Clinical Trials Manager	Yes	
Dr Charles Mackworth-Young	Consultant Physician	Yes	
Dr Colin Michie	Consultant Paediatrician	No	
Dr Frank Miskelly	Consultant Physician	Yes	
Dr Mark Palazzo	Consultant Anaesthetist	Yes	
Lady Alexandra Roche	Lay Member	Yes	

Also in attendance:

Name	Position (or reason for attending)
Miss Carli Sager	Committee Co-ordinator

This Research Ethics Committee is an advisory committee to London Strategic Health Authority
The National Research Ethics Service (NRES) represents the NRES Directorate within
the National Patient Safety Agency and Research Ethics Committees in England

NHS

National Research Ethics Service
Charing Cross Research Ethics Committee

Room 4W/12, 4th Floor
Charing Cross Hospital
Fulham Palace Road
London, W6 8RF
Tel: 020 8846 7283
Fax: 020 8846 7280

Dr Paul Nathan
Consultant Medical Oncologist
Mount Vernon Hospital
Rickmansworth road, Northwood
Middlesex
HA6 2RN

24 February 2009

Dear Dr Nathan

Study title:	**Dynamic contrast enhanced MRI (DCE-MRI) assessment of the vascular changes induced with bevacizumab alone and in combination with interferon-a in patients with advanced renal cell carcinoma**
REC reference:	**09/H0711/6**
Protocol number:	**1.1**
EudraCT number:	**2008-006414-19**
Amendment number:	**1**
Amendment date:	**10 February 2009**

The above amendment was reviewed at the meeting of the Sub-Committee of the REC held on 17 February 2009.

Ethical opinion

The members of the Committee present gave a favourable ethical opinion of the amendment on the basis described in the notice of amendment form and supporting documentation.

Approved documents

The documents reviewed and approved at the meeting were:

Document	Version	Date
Participant Information Sheet	1.2	26 January 2009
Participant Information Sheet	1.2	26 January 2009
Covering Letter		02 February 2009
Annex 2 Notification of Amendment (CTIMPs)	1	10 February 2009

Membership of the Committee

The members of the Committee who were present at the meeting are listed on the attached sheet.

R&D approval

All investigators and research collaborators in the NHS should notify the R&D office for the relevant NHS care organisation of this amendment and check whether it affects R&D approval of the research.

Statement of compliance

This Committee is recognised by the United Kingdom Ethics Committee Authority under the Medicines for Human Use (Clinical Trials) Regulations 2004, and is authorised to carry out the ethical review of clinical trials of investigational medicinal products.
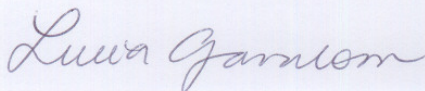
The Committee is fully compliant with the Regulations as they relate to ethics committees and the conditions and principles of good clinical practice.

The Committee is constituted in accordance with the Governance Arrangements for Research Ethics Committees (July 2001) and complies fully with the Standard Operating Procedures for Research Ethics Committees in the UK.

09/H0711/6:	Please quote this number on all correspondence

Yours sincerely

[signature]

Miss Lucia Gavalova
Committee Co-ordinator

E-mail: Lucia.Gavalova@imperial.nhs.uk

Enclosures	List of names and professions of members who were present at the meeting and those who submitted written comments
Copy to:	*Ms Fiona Smith,*

Safeguarding public health

MHRA

Dr P Nathan
MOUNT VERNON HOSPITAL
DEPARTMENT OF MEDICAL ONCOLOGY
MOUNT VERNON CENTRE FOR CANCER TREATMENT
NORTHWOOD
MIDDLESEX
HA6 2RN
UNITED KINGDOM

27/04/2009

Dear Dr P Nathan

THE MEDICINES FOR HUMAN USE (CLINICAL TRIALS) REGULATIONS 2004 S.I. 2004/1031

Our Reference: 31057/0002/001-0001
Eudract Number: 2008-006414-19
Product: Avastin
Protocol number: RD 2007-114

NOTICE OF ACCEPTANCE OF AMENDED REQUEST

I am writing to inform you that the Licensing Authority accepts your amended request for a clinical trial authorisation (CTA), received on 22/04/2009.

The authorisation is effective from the date of this letter although your trial may be suspended or terminated at any time by the Licensing Authority in accordance with regulation 31. You must notify the Licensing Authority within 90 days of the trial ending.

Finally, you are reminded that a favourable opinion from the Ethics Committee is also required before this trial can proceed; changes made as part of your amended request may need to be notified to the Ethics Committee.

Yours sincerely,

Clinical Trials Unit
MHRA

9.11. Publications

Nathan.PD, A.Vinayan; "Imaging techniques as predictive and prognostic biomarkers in renal cell carcinoma"; <u>Ther Adv Med Oncol.</u> 2013 Mar;5(2):119-31.

P.Nathan, A.Vinayan, D.Stott, J.Juttla, V.Goh; " CT response assessment combining reduction in both size and arterial phase density correlates with time to progression in metastatic renal cancer patients treated with targeted therapies" Cancer Biology & Therapy 9(1); 15-19; January, 2010; © 2010 Landes Bioscience.

V.Goh, B.Ganeshan, P.Nathan, A.Vinayan, K.Miles "Assessment of response to tyrosine kinase inhibitors in metastatic renal cell cancer: CT texture as a predictive biomarker" Radiology: 2011 Oct;26(1): 165-71

Imaging techniques as predictive and prognostic biomarkers in renal cell carcinoma

Paul Nathan and **Anup Vinayan**

Abstract: A number of imaging modalities are showing promise as predictive and prognostic biomarkers in advanced renal cell carcinoma. This review discusses progress to date in this exciting area and identifies areas of future promise.

Keywords: biomarkers, imaging, prediction, prognosis, renal cell carcinoma

Introduction

Therapeutic options for patients with advanced renal cell carcinoma (RCC) have dramatically improved over the last few years with the advent of a number of novel agents targeting both tumour vasculature and tumour growth. Sunitinib [Motzer *et al*. 2007b], bevacizumab in combination with interferon [Escudier *et al*. 2007b], temsirolimus [Motzer *et al*. 2007a], sorafenib and everolimus [Motzer *et al*. 2008] have all become standard agents for the treatment of this disease.

There is a clinical need to identify which patients are likely to derive most and least benefit from targeted therapies early in the course of treatment, that is, to predict response, and to identify which patients have aggressive or indolent disease, that is, to determine prognosis.

RCC is highly vascular, driven at least in part by the frequent overexpression of vascular endothelial growth factor (VEGF) [Nicol *et al*. 1997]. As all of the new therapeutic agents appear to have at least some effect upon tumour vasculature, imaging modalities that provide a quantitative assessment of the change in vascularity may have a particular role in this disease.

This review discusses imaging modalities that have shown promise as either predictive or prognostic tests in advanced RCC and identifies areas of future opportunity.

Predictive biomarkers

Validated tools, which could predict clinical benefit from a therapy, would lead to significant improvements in clinical management. Early identification of responders, nonresponders or subpopulations of patients at risk for side effects would help to identify patients who have greatest or least benefit from a specific intervention. Predictive biomarkers would therefore help to avoid exposing patients to the risk of unnecessary side effects from treatments from which they would be destined to derive little or no benefit.

There are now a significant number of new therapies which have proven to be clinically effective, but which have not succeeded in passing health–economic assessments by reimbursement authorities. The cost-effectiveness analyses that bodies such as the National Institute for Health and Clinical Excellence perform would be significantly impacted upon if it were possible to identify subpopulations of patients who would derive most benefit from the drugs. This would lead to a greater possibility that new therapies would be available for patients once efficacy had been demonstrated.

Imaging-defined response evaluation criteria in solid tumours (RECIST) [Therasse *et al*. 2000] have been the basis of treatment response assessment in oncology since their introduction. The criteria were developed and validated to assess

Correspondence to:
Paul Nathan, PhD, FRCP
Mount Vernon Cancer
Centre – Medical Oncology,
Rickmansworth Road,
Northwood, Middlesex HA6
2RN, UK
nathan.pd@gmail.com

Anup Vinayan, MRCP
Mount Vernon Cancer
Centre – Medical
Oncology, Northwood ,
Middlesex, UK

responses to conventional therapies such as chemotherapy and radiotherapy rather than the new generation of targeted agents. RECIST criteria are based upon change in size of target lesions. However, antivascular agents appear to be frequently clinically active without inducing the significant size change required for a RECIST-defined response. No imaging modality has yet been validated that can predict the treatment response of RCC treated with targeted therapies.

Primary RCC and its metastases are noted to be highly vascular and are associated with an upregulation of VEGF. Most sporadic and familial clear cell RCCs have an inactive VHL gene product either because of bi-allelic alterations in the gene or post-transcriptional modification. Lack of functional VHL gene product results in stabilization of hypoxia inducible factor (HIF) 1, 2 and increased transcription of factors such as VEGF and platelet-derived growth factor. Activation of multiple pathways driven by these and other factors results in increased angiogenesis in these tumours. This is thought to underpin the significant clinical activity of antiangiogenic targeted therapies in RCC. Imaging techniques that can assess vascularity and changes in vascularity of these tumours may therefore have potential to be useful as predictive biomarkers.

Assessment of changes in vascularity

The gold standard for assessing vascularity and angiogenesis in a tumour is by measuring the mean vascular density, which is performed by counting vascular structures directly with histology. This technique has limitations as it is invasive and cannot be performed repeatedly to assess treatment response in humans. Also, as it does not explore the whole treatment volume, there is an increased chance of sampling error due to tumour heterogeneity [Lebret *et al.* 2007; Renshaw *et al.* 1997].

A number of clinically applicable functional imaging techniques are capable of quantitatively assessing the vascularity of tumours *in vivo* pre and post treatment. These techniques include dynamic contrast-enhanced magnetic resonance imaging (DCE-MRI), dynamic contrast-enhanced computed tomography (DCE-CT), dynamic contrast-enhanced ultrasound (DCE-US), diffusion-weighted MRI (DW-MRI), arterial spin label MRI (ASL-MRI) and positron emission tomography (PET) with oxygen-labelled water. Each of these techniques provides quantitative or semiquantitative data related to blood flow and some can also provide information on blood volume, cellularity or vessel permeability. DCE imaging techniques such as DCE-MRI, DCE-CT and DCE-US use exogenous contrast agents to differentiate vascular characteristics, while other MRI techniques as ASL-MRI and DW-MRI use the inherent changes in magnetic resonance between tissues without the use of an external contrast agent. The latter group has a potential advantage as 20–30% of patients with RCC have impaired renal function, which increasingly precludes the use of exogenous contrast agents.

Dynamic contrast-enhanced imaging techniques. Dynamic functional imaging using exogenous contrast media centres on quantitative analysis of biodistribution of contrast media in tissues. These techniques use the difference in pharmacokinetics of the contrast agent between tissues and tumour to provide tumour-specific and tissue-specific information [Marcus *et al.* 2009].

DCE-MRI as a biomarker of angiogenesis has been tested and validated over the last decade in a variety of tumours. The gold standard correlation was with immunohistochemical microvessel density measurements. Investigators have attempted to correlate imaging with tissue expression of proangiogenic growth factors including VEGF (broad correlations in some studies and no correlations in others) [Padhani and Dzik-Jurasz, 2004; Schlemmer *et al.* 2004].

The relationship between contrast concentration and signal intensity is complex and nonlinear in DCE-MRI [Kiessling *et al.* 2007]. Along with the concentration, it also depends on the imaging sequence used, machine setup, inherent heterogeneity of the tumour and native relaxation rate of the tissues [Padhani, 2003].

The rate of delivery and washout of contrast media into the tumour vasculature bed depends on several physiological characteristics of the tumour vascular microenvironment. Depending on the techniques used, parameters such as K_{trans} (transfer constant, related to the influx of contrast agents from plasma to the tumour interstitial space), Kep (efflux of agents back to the vasculature), Ve (effective volume of distribution), rBF (relative blood flow), rBV (relative blood volume), IAUGC (initial area under gadolinium curve) can be obtained. The values are then fitted with statistical models for analysis.

In 2008, Flaherty and colleagues published a pilot study, which used DCE-MRI assessment in patients with metastatic RCC treated with sorafenib. This study showed that inhibition of tumour vascular permeability by sorafenib, demonstrated by a reduction in K_{trans}, was associated with improved progression free survival (PFS) ($p = 0.01$). Elevated baseline K_{trans} was a statistically significant predictive marker for favourable response to treatment ($p < 0.02$) [Flaherty et al. 2008]. A prospective randomized phase II study again with sorafenib in RCC by Stadler and colleagues also showed a good correlation of high baseline K_{trans} with improved PFS ($p < 0.027$). In this study, however, change in K_{trans} or $IAUGC_{90}$ were not significantly related to PFS [Hahn et al. 2008]. Further trials are underway to evaluate the use of DCE-MRI in RCC.

Most modern MRI scanners have the ability to perform these image acquisitions but there are several limitations to widespread use. Imaging protocols need to be optimized according to the area to be scanned and the type of tumour being analysed. The appropriate software needs to be available and there also remain issues regarding quantification, tumour heterogeneity and motion artefact. Low molecular weight gadolinium, which is used as standard, has a limitation as these small agents rapidly leak out of the highly permeable vasculature in the tumour. This in turn affects the data acquisition in dynamic imaging as this is defined by vascular permeability and tumour perfusion. Gadolinium in higher molecular weight conjugates could be used to overcome this problem, as these are less sensitive to vascular permeability.

Lamuraglia and colleagues used DCE-US along with a new perfusion software as a predictive tool in metastatic RCC [Lamuraglia et al. 2006]. Thirty patients who were enrolled in a randomized clinical trial comparing sorafenib with placebo were recruited. DCE-US examination was performed at baseline, week 3 and week 6. The good responders were defined by a combination of a decrease in contrast uptake greater than 10% and a stable or decrease in tumour size. The responders identified at week 3 had a statistically significant improvement in PFS ($p < 0.0004$) and overall survival (OS) ($p < 0.0004$) over the nonresponders.

A recent prospective multicentre study by Lassau and colleagues investigated the use of DCE-US as a predictive biomarker in patients treated with antiangiogenic agents. A total of 539 patients with different tumour types including 157 patients with RCC were recruited from 19 centres in France. Perfusion parameters were collected from these patients with DCE-US at baseline, on day 7, day 14, day 30, day 60 and 2 monthly thereafter. This was correlated to the RECIST assessment performed 2 monthly. They showed that a decrease in area under the curve (AUC) by more than 40% at 1 month was predictive of response for time to progression (TTP) ($p < 0.01$) and OS ($p < 0.04$) [Lassau et al. 2012].

A simultaneous study with DCE-US from Toronto by Williams and colleagues in 17 patients with metastatic RCC treated with sunitinib showed a decrease in median tumour fractional blood volume by 73.2% after 2 weeks of treatment with a disruption-replenishment infusion method of microbubble and a significant decrease in bolus peak with the bolus method. In this study no definite correlation was noted with best response as assessed by RECIST [Williams et al. 2011].

US is a widely available and inexpensive technique. Therefore performing frequent and serial examinations at short intervals is possible when using this technique. However, the main problem with US is the limited ability to penetrate through large areas of tissue when trying to image deeply located tumours, and more specifically, the inability to penetrate through air or bone. Because RCC frequently metastasizes to the lung and mediastinum, the use of DCE-US in large cohorts of patients is unknown. A potential advantage of DCE-US is the fact that the microbubbles are intravascular and therefore, in theory, the quantification of tumour perfusion should not be affected by vessel permeability. However, the technique tends to be more operator dependent and those with the relevant skills are not available in all locations.

To date, no studies have been published using DCE-CT as a tool for treatment response prediction in RCC. This technique does hold promise as the concentration kinetics of the contrast are related directly and linearly to enhancement and analysis is therefore relatively straight forward [Miles, 2002]. However, there is little general agreement about the techniques to use for modelling and further quantitative analysis. Evidence from rectal carcinoma showed that baseline blood flow and blood volume were significantly lower in nonresponders compared with responders treated with chemoradiotherapy [Bellomi et al. 2007].

The study also showed a significant decrease in blood flow, blood volume and permeability surface area product post treatment. CT scanning is the commonest tool used at present to monitor treatment response, therefore it would be a practical and easy option to incorporate DCE-CT protocols in almost all centres once a general agreement is obtained and the technique is validated further.

Imaging techniques that use no external contrast agent. A number of MRI techniques which do not resort to an external contrast agent have been developed and are being assessed as biomarkers of treatment response. Between 20% and 30% of patients with RCC are unable to have external contrast due to renal impairment and techniques that do not resort to external contrast are thus valuable[Nathan *et al.* 2010]. These techniques use the magnetic field to modify the magnetic properties of the tissue including the tumour.

ASL-MRI uses the inherent nuclear spin of endogenous water protons to label arterial blood. Quantitative images of blood flow to the tissue can be generated by differential labelling inside and outside the tissue of interest. The technique has potential to be used as a quantitative marker for response assessment to antivascular treatment. The feasibility of this technique to monitor response to antiangiogenic therapy in RCC metastases was demonstrated by de Bazelaire and colleagues [de Bazelaire *et al.* 2005]. In a phase II trial of 10 patients, ASL-MRI and DCE-MRI were used to assess the treatment response in patients with metastatic RCC treated with an antiangiogenic agent (PTK787/ZK222584). The study showed that changes in blood flow detected by ASL-MRI at 1 month correlated with the change in tumour size measured at 4 months or at disease progression ($p < 0.01$) [de Bazelaire *et al.* 2008]. If validated in larger studies, ASL-MRI thus might prove to be an important biomarker in early assessment of treatment response.

Techniques such as blood oxygen level dependent MRI (BOLD-MRI) and DW-MRI which use no external contrast are other methods with potential to predict treatment response. BOLD-MRI uses the difference in magnetic properties of oxy-haemoglobin and deoxyhaemoglobin and hence BOLD signals are related to tumour hypoxia. DW-MRI evaluates the property of water diffusion depending on the Brownian motion of the water molecules in tissues. Desar and colleagues noted that sunitinib-induced antiangiogenic effects in RCC can be reliably measured with DW-MRI as early as 3–10 days after starting the treatment [Desar *et al.* 2011]. This needs further evaluation before it can be reliably used as a predictive biomarker. There are as yet no published data with either of these techniques to predict responses in RCC to targeted therapies.

Assessment of change in metabolic activity

Fluorodeoxyglucose (FDG)-PET/CT scan is a valuable tool, which has already established its role in the assessment and management of many tumour types. By combining a short-lived radioactive tracer with a biologically active molecule, PET scan provides a functional map of the disease investigated. The most common biological molecule used in oncology is FDG. This glucose analogue is rapidly and preferentially taken up by the rapidly growing malignant cells, thus leading to intense radiolabelling of that tissue. A combined CT and PET scan provides a combination of metabolic activity with anatomical localization of tissues. The use of FDG-PET/CT in treatment response assessment, that is, as a predictive marker in RCC, looks promising but has not been fully evaluated. A recent study by Powles and colleagues looked at the use of sequential FDG-PET scanning as a correlative marker of OS in patients with RCC treated with sunitinib [Powles *et al.* 2010]. A total of 44 patients were enrolled in this phase II study. Patients had three FDG-PET scans: before treatment, at 4 and 16 weeks. Reduction in maximum standardized uptake value (SUVmax) by 20% was considered a response and was correlated with OS. The study showed that high baseline SUVmax suggested a trend towards low OS [hazard ratio (HR) 3.30; 95% confidence interval (CI) 1.36–8.45]. Metabolic response was noted on the PET scan after 4 weeks. However, disease progression according to the 16-week scan correlated with a decreased OS (HR –5.96; 95% CI –2.43 to +19.02).

Similar results were noted in smaller trials of 12 patients and 14 patients by Minamimoto and Revheim and colleagues respectively [Minamimoto *et al.* 2010; Revheim *et al.* 2011]. Using a 20% reduction in FDG-PET uptake, Minamimoto and colleagues were able to separate good responders with a mean PFS of 233.8 days and poor responders with a PFS of 75 days.

A pharmacodynamic study using serial 3deoxy3' fluorothymidine PET (FLT-PET) scans on patients at baseline, during treatment with sunitinib and after withdrawal of drug within cycle 1 showed an increase in cellular proliferation during sunitinib withdrawal [Liu *et al.* 2011]. This is noted to associate with VEGF ligand levels and early exploratory analysis suggests that the extent of flare could predict poorer clinical benefit from the drug.

New criteria for response assessment

RECIST criteria depend upon the change in sum of the unidimensional measurements of target lesions. However, the clinical benefit does not always correlate with change in size alone in tumours treated with targeted therapies. Emerging evidence shows that some patients continue to derive clinical benefit from continuation of sunitinib after documented disease progression based on RECIST criteria [Teo *et al.* 2012]. This retrospective analysis of 39 patients treated with sunitinib showed that such use of a tyrosine kinase inhibitor (TKI) beyond progression gives prolonged disease control and is safe. The use of RECIST alone as a measure of treatment response is therefore arguable.

Choi criteria. Choi proposed an alternative set of criteria for the assessment of gastrointestinal stromal tumours (GIST) treated with the targeted agent imatinib [Choi, 2008; Choi *et al.* 2007]. The Choi criteria require either a change in size or a change in density (contrast enhancement) to predict a response. They have been found to be more reliable than RECIST in monitoring GIST responses to treatment using PET-CT as a gold standard. It has been suggested that the Choi criteria could be suitable for assessment of targeted therapies in other cancers, but this has not yet been extensively evaluated.

In renal cancer, van der Veldt and colleagues have analysed the use of Choi criteria in treatment response assessment in RCC and found them to correlate better to TTP than RECIST [van der Veldt *et al.* 2010]. A total of 55 patients with metastatic RCC treated with sunitinib were analysed retrospectively. The pretreatment and first evaluation post-treatment scan were analysed with RECIST and Choi criteria separately and correlated with PFS and OS. At first evaluation, according to the RECIST criteria, seven patients had a response, 38 had stable disease and 10 had

progressive disease. According to the Choi criteria, these numbers were 36, 6 and 13 respectively. In patients having a partial response, the Choi criteria had a significantly better predictive value for PFS and OS ($p < 0.001$ for both) than RECIST ($p = 0.689$ and 0.191 respectively). The predictive value of RECIST increased to a statistically significant level only when best response during treatment was taken into account.

The Choi criteria and RECIST were again compared with a smaller cohort of 22 patients treated with sorafenib reported by Hittinger and colleagues [Hittinger *et al.* 2011]. Even though the Choi criteria defined more patients as responders, they did not differentiate between patients who did and those who did not have therapeutic improvements in PFS or OS.

'Modified' Choi criteria. We proposed a modification of the Choi criteria in the assessment of treatment response to targeted therapy in metastatic RCC in which both a change in size and density are required [Nathan *et al.* 2010]. The standard Choi criteria require a decrease in size by 10% or a decrease in CT contrast enhancement by 15% for a response. We suggested a modification of the Choi criteria in which both a minimum 10% size decrease and a 15% reduction in enhancement are required to define a response. We performed a retrospective study of 32 patients with metastatic RCC treated with TKIs. Twelve patients were excluded as they did not have contrast-enhanced scans due to renal dysfunction. Both baseline and 12-week post-treatment contrast-enhanced scans were collected and analysed. According to the response obtained on the 12-week scan, patients were assigned to progressive disease, stable disease or partial response using RECIST, Choi and modified Choi criteria, correlated with TTP. Patients who had a partial response according to the modified Choi criteria had a statistically significant longer TTP than those who were deemed to have stable disease (mean 448 *versus* 89 days, $p = 0.002$). Neither RECIST nor Choi criteria defined partial responders went on to have a significant improvement in TTP compared with those who had stable disease. Further larger trials are planned to validate these results. CT enhancement was measured in the arterial phase rather than in the more usual portovenous phase in this study. This may be relevant as renal tumours are highly vascular and enhance well in the arterial phase [Lee *et al.* 2005; Raptopoulos *et al.* 2001].

Size and attenuation CT criteria/morphology, attenuation, size and structure criteria. Another study exploring the use of a combination of change in size and CT attenuation to predict treatment response in metastatic RCC was published by Smith and colleagues [Smith *et al.* 2010a]. Contrast-enhanced CT scans of 53 patients with metastatic RCC treated with either sunitinib or sorafenib were analysed. In calculating the attenuation data, Smith and colleagues used volumetric mean attenuation of target lesions in place of mean attenuation in the most representative axial image. They proposed new imaging criteria, size and attenuation CT (SACT) criteria. The criteria defined favourable response as any of the following: a decrease in tumour size of at least 20%; a decrease in tumour size of at least 10% and at least half of nonlung target lesions with decreased mean attenuation of at least 20 Hounsefield units (HU); or one or more lung lesions with decreased mean attenuation by at least 40 HU. Unfavourable response was defined as any of the following: an increase in tumour size of at least 20%; new metastasis; marked central fill in of a target lesion; or new enhancement in a homogenously hypoattenuating nonenhancing mass. A comparison was made between the SACT criteria, RECIST criteria and a modification of the Choi criteria (with volumetric attenuation data of the whole tumour rather than mean attenuation in an axial slice) in predicting a PFS greater than 250 days in this patient population. The favourable response defined by the SACT criteria had a sensitivity of 75% and a specificity of 100% in identifying patients with PFS greater than 250 days. These values were 16% and 100%, and 93% and 44% for the RECIST criteria and volumetric modified Choi criteria, respectively.

The same group attempted to improve on the SACT criteria by including specific morphologic or structural changes (e.g. necrosis) and eliminating the need for volumetric three-dimensional analysis in their new criteria [referred to as morphology, attenuation, size and structure (MASS) criteria] [Smith *et al.* 2010b]. According to the MASS criteria, favourable response was defined as no new lesion and any of the following: a decrease in tumour size of at least 20%; one or more predominantly solid enhancing lesions with marked central necrosis or marked decreased attenuation (≥40 HU). An unfavourable response was defined as an increase in tumour size of at least 20% in the absence of marked necrosis or marked decreased attenuation; and new metastasis, marked central fill-in, or new increased enhancement. Other changes, which did not fit in with these criteria were classified as an indeterminate response. The MASS criteria showed an increased sensitivity of 86% and specificity of 100% in recognizing good responders (TTP and improved disease specific survival $p < 0.0001$).

The group further recommended that the combination of memorial sloan kettering cancer centre (MSKCC) criteria and MASS criteria together could give a high overall accuracy in identifying patients with PFS less than 1 year or at least 1 year [Smith *et al.* 2011].

Tumour burden and growth rate. Basappa and colleagues investigated the effect of tumour burden (TB) with treatment with VEGF-targeted therapy. Sixty-nine patients were retrospectively analysed. Median TB and site of metastasis were examined. With multivariate analysis, at baseline, the total number of metastases (<10) and the TB above the diaphragm (<6.5 cm) were independent positive predictors of OS [Basappa *et al.* 2011]. TB ($p = 0.003$) and total metastases (≤12) were noted as predictors of OS at TTP.

Initial tumour size and the rate of size reduction in response to targeted therapy were predictive markers reported by Yuasa and colleagues[Yuasa *et al.* 2011]. In this 139-patient retrospective analysis, a linear, moderate to strong association was noted between the pretreatment tumour size and reduction in growth rate on therapy (correlation coefficient −0.441, $p < 0.001$). When a threshold value of 23.9 mm was applied, it was noted that the smaller tumours showed a better rate of shrinkage ($p < 0.001$).

Use of tumour growth rate (TGR) was retrospectively analysed by Ferte and colleagues [Ferte *et al.* 2012]. Images from patients recruited to large phase III trials with sorafenib (TARGET) and everolimus (RECORD) were assessed ($n = 902$). TGR was defined as the value obtained by dividing tumour shrinkage by time between two evaluations. All treatment periods, including before, under treatment (at first cycle), at progression and after treatment interruption, were noted. The results showed that the TGR under treatment was significantly decreased with both sorafenib and everolimus. High TGR under treatment was associated with poor PFS (HR 2.6) and OS (HR 2.3) in patients treated with sorafenib and poor OS (HR 1.2) in the smaller everolimus cohort. TGR after interruption was significantly

higher in both sorafenib and everolimus cohorts than TGR at progression (14.6 *versus* 31 and 17.9 *versus* 32.1, respectively). The inclusion of TGR thus allows the practitioner to evaluate the tumour response more carefully.

The threshold of tumour response as change in sum of longest diameter (ΔSLD) to mammalian target of rapamycin inhibitor everolimus was investigated by Oudard and colleagues [Oudard *et al.* 2012]. The data from the phase III RECORD-1 trial were analysed and a series of arbitrary thresholds were identified to attempt to distinguish responders from nonresponders. With response defined by the optimal threshold of −5%ΔSLD, the median PFS was 8.4 months for the responders and 5.0 months for the nonresponders (HR 2.4).

Prognostic biomarkers

Imaging biomarkers that provide an insight into the natural course of the disease are of potential use in identifying patients who are most or least likely to benefit from treatment as well as in interpreting clinical trials. The prognosis of any malignancy could be related to a variety of factors. RCC is a heterogeneous group of diseases. There are a number of histological subtypes and within each subtype there is a widely varying natural history between patients. Some tumours are very aggressive while others remaining indolent. Some patients experience stable metastatic disease for a significant period of time that does not require systemic treatment until progression is seen.

Several clinicopathological prognostic models are designed to assess survival in the postnephrectomy [Leibovich score, University of California, Los Angeles (UCLA) score] [Leibovich *et al.* 2005; Zisman *et al.* 2001] and metastatic setting (Motzer score, UCLA score) [Motzer *et al.* 1999]. These prognostic models use histological features, including Fuhrman grade and necrosis, performance status and a variety of biochemical markers for categorization into prognostic groups.

The MSKCC (Motzer) criteria classified patients into good, intermediate and poor prognostic groups depending on five factors: primary tumour remaining *in situ*, Eastern Cooperative Oncology Group performance status, anaemia, lactate dehydrogenase level and hypercalcaemia. Median survival in patients with zero risk factors was 20 months but median survival in the intermediate-risk group (one or two risk factors) and the poor prognostic group (more than two risk factors) were 10 months and 4 months respectively [Motzer *et al.* 1999]. The MSKCC criteria have been widely used in many phase III trials of RCC evaluating antiangiogenic agents either to stratify patients in trial analysis [Escudier *et al.* 2007b; Motzer *et al.* 2007b, 2008] or to define entry criteria in other trials [Escudier *et al.* 2007a; Hudes *et al.* 2007].

Evidence from these trials showed that the beneficial effects of these drugs were maintained across prognostic groups but were significantly greater in good and intermediate prognostic groups. Hence prognostic grouping of RCC has an important role in selection of treatment and also in determining the time of introduction of systemic treatment. Imaging techniques can potentially act as noninvasive tools in identifying these prognostic factors. These include assessment of histological subtype, nuclear grading and in the accurate staging of disease.

Assessment of histological subtypes

There has been debate as to whether prognosis of RCC varies significantly with histological subtype. Studies have in part been hampered by small numbers of the rarer subtypes and associated lack of control for other prognostic factors. RCC can be subclassified according to histology as clear cell, papillary type I and II, chromophobe, sarcomatoid, collecting duct and a variety of very rare and unclassified subtypes(World Health Organization classification) [Ebele *et al.* 2004; Kovacs *et al.* 1997]. The clear cell (conventional) subtype is the most common and accounts for approximately 70% of cases. The papillary subtype accounts for around 15–20% of cases. The type II papillary and other subtypes are less common. There is good evidence that tumours with sarcomatoid elements have a poorer prognosis than the majority of tumours without [Cangiano *et al.* 1999].

With the emerging possibility that treatment decisions may be influenced by histological subtype, together with the fact that core biopsy is associated with diagnostic inaccuracy [Lebret *et al.* 2007] a noninvasive technique to assess histological subtype would be of potential clinical value. A number of different imaging modalities have been assessed for this purpose. These include multislice CT, DW-MRI and DCE-MRI.

Sheir and colleagues attempted to use multislice CT to differentiate histological subtypes. They reviewed 87 CT images of patients with RCC retrospectively and compared them with histopathology. Biphasic CT scans of the kidneys were performed using unenhanced, corticomedullary phase (CMP) and excretory phase (EP) (30 and 300 s after contrast injection respectively) protocols. It was noted that the degree of enhancement in the CMP and EP was the most valuable parameter in attempting to differentiate between histological subtypes ($p < 0.001$). Mean CT attenuation (+2 standard deviations) in the CMP was 138.2 ± 38.0 HU for clear cell, 89.2 ± 31.4 HU for papillary and 55.17 ± 24.0 HU for chromophobe tumours. In the excretory phase, clear cell tumours showed an enhancement of 73.0 ± 17.6 HU while papillary and chromophobe had an enhancement of 70.0 ± 10.4 and 33.9 ± 12.1 HU respectively. The difference between subtypes in both the CMP and EP was statistically significant ($p < 0.001$). The cutoff value for highest accuracy for diagnosis of clear cell carcinoma was 83.5 HU for CMP and 64.5 HU for EP. Other factors such as presence or absence of cystic degeneration, tumour vascularity and pattern of enhancement also supplemented this differentiation [Sheir *et al.* 2005].

Pedrosa and colleagues attempted evaluation of malignant renal tumours with the help of noncontrast-enhanced and contrast-enhanced MRI and correlated this with histology. The study cohort consisted of 76 patients who had both MRI and histological confirmation [Pedrosa *et al.* 2008]. Renal masses were analysed for size, location, necrosis, haemorrhage, signal intensity and uniformity of signal intensity, type and extent of fat and contrast enhancement, peri-renal fat invasion and renal vein thrombosis. They were then assigned to one of eight different groups defined according to MRI appearance. The results were compared with the histological analysis and the sensitivity and specificity of these MRI groups were calculated to predict the histological diagnosis and nuclear grade. The MRI classification had a sensitivity of 93% and specificity of 75% for the diagnosis of clear cell subtype, using the presence of solid enhancing mass with or without necrosis. Retroperitoneal collaterals, intravoxel fat signal and necrosis all correlated directly with clear cell subtype. MRI features such as hemorrhagic cyst with peripheral enhancing growth in the wall and solid hypo-enhancing homogeneous masses with low SI on T2-weighted images were predictors of

the papillary subtype with good sensitivity (80%) and specificity (94%).

Sun and colleagues explored the use of DCE-MRI as a tool in predicting the histopathological subtype of RCC. They compared the difference in enhancement pattern in CMP and nephrographic phase images with histopathology. In both the CMP and nephrographic phase, clear cell tumours showed maximum signal intensity change and papillary tumours the least. Signal intensity change in the CMP was the most effective parameter differentiating clear cell and papillary subtypes with a sensitivity of 93% and a specificity of 96% [Sun *et al.* 2009]. DCE-MRI was also useful in predicting the nuclear grade of the tumour as reported by Palmowski and colleagues. Twenty-one patients were analysed with DCE-MRI presurgically; tumour perfusion and tissue–blood ratio were noted for the entire tumour and also for the most highly vascularized area in the tumour. Higher grade tumours had significantly higher perfusion values ($p < 0.05$) in the most vascular area [2.14 ± 0.89 *versus* 1.40 ± 0.49 ml/g/min] and the entire tumour (1.59 ± 0.44 *versus* 1.08 ± 0.38 ml/g/min) [Palmowski *et al.* 2009].

These imaging techniques are of interest, however their use in clinical practice will require much more robust validation and they are unlikely to replace the use of histological diagnosis in the near future.

Staging of renal cell carcinoma
Accurate staging of RCC is an important factor influencing the prognosis. While CT, MRI, PET and bone scans all are used routinely in staging a variety of different cancers, there is debate regarding the usefulness of some of these techniques in RCC.

Assessment of skeletal metastasis. Nuclear medicine (NM) bone scans with Tc99 provide limited anatomical detail and only provide information about tumour deposits where an osteoblastic reaction has occurred. RCC bony metastases are predominantly osteoclastic, resulting in a low sensitivity of conventional bone scans. Staudenherz and colleagues showed that the sensitivity of bone scintigraphy varied from 10% to 60% in RCC [Staudenherz *et al.* 1999].

MRI has been suggested as a more sensitive tool in the assessment of skeletal metastasis than NM

bone scan. A recent study by Sohaib and colleagues compared the efficacy of whole body MRI scan and NM bone scan in the assessment of bony RCC metastasis. This prospective study of 47 patients showed that even though both bone scan and MRI were highly specific (94% *versus* 97%), the sensitivity of whole body MRI scan was much superior (94%) to bone scan (62%) in the detection of renal metastasis to bone ($p = 0.007$). MRI also had the advantage of assessment of soft tissue disease simultaneously [Sohaib *et al.* 2009].

Assessment of visceral disease. For assessment of lymph node and visceral disease, FDG-PET scan has been found to be extremely sensitive in characterizing metastases from a variety of tumour types. However, there is a significant incidence of false-positive results, which is perhaps not surprising given that FDG is not a cancer-specific tracer [Antoch *et al.* 2003; Schmidt *et al.* 2006]. Small lesions in the lung and liver may remain FDG occult due to smearing of the signal as a result of organ motion. Use of PET-CT is also inferior to whole body MRI in cancers with a frequent metastatic spread to the bone, liver and central nervous system [Antoch *et al.* 2003; Schmidt *et al.* 2005]. Poor uptake of FDG has also been noted in tumour types such as RCC, prostatic malignancy and low-grade soft tissue malignancies [Schmidt *et al.* 2006].

The value of FDG PET scans in RCC diagnosis is debated with multiple small studies showing sensitivity ranging from 32% to 100% for initial diagnosis and staging of primary RCC [Montravers *et al.* 2000; Nakatani *et al.* 2011]. The largest of these series, published by Kang and colleagues, included 66 patients with RCC and showed a sensitivity of 60% [Kang *et al.* 2004]. Nakatani and colleagues suggested a higher FDG sensitivity for RCC metastasis but this has not yet been validated [Nakatani *et al.* 2011]. Larger series of studies are required to validate the use of FDG-PET scan in RCC but as the specificity of this technique was higher than conventional imaging in previous studies, its use would be limited at present as a tool to help resolve dilemmas in selected cases with equivocal conventional imaging but high suspicion.

In a retrospective study by Le Moulec and colleagues, 21 patients with metastatic RCC who received FDG-PET/CT study at baseline and after 2 months were evaluated [Le Moulec *et al.* 2010]. The study noted that patients with a negative PET/CT had a better outcome (overall median survival not reached *versus* 23 months, $p = 0.05$). Patients with a median value of SUVmax greater than 5.7 had a short PFS and OS (3 months *versus* 9 months, $p = 0.03$) and (23.3 months *versus* 9.1 months). Another observation in the study was that in eight patients the early PET/CT findings were consistent with the later CT results.

A recent as yet unpublished study from Japan by Nakaigawa and colleagues examined whether SUVmax from the pretreatment FDG-PET scan could be used as a prognostic marker for survival [Nakaigawa *et al.* 2012]. In 67 patients enrolled and monitored in this study, the researchers noted that the SUVmax varied widely in RCC tumours from an undetectable level increasing to 16.6 (mean 7.6 ± 3.6) with an increasing trend towards poorer prognosis ($p < 0.001$, HR −1.289). The results were further analysed with SUVmax results stratified as less than 7.0, between 7.0 and 12 and greater than 12.0. Median OS for patients was 1229 ± 991 days, 446 ± 202 days and 95 ± 43 days respectively.

In a separate study of 35 patients, this group suggested that an FDG-PET scan 1 month after treatment initiation could be used as a predictive marker for therapeutic response to TKIs based on whether the tumour size had increased and SUVmax had decreased by less than 20% or by at least 20% [Ueno *et al.* 2012].

Assessment of mechanism of drug action and role in drug development. Imaging biomarkers have an increasing role in early phase drug development. The phase I trial end points have now moved away from the traditional end points of maximum tolerated dose and toxicity assessment to also incorporate pharmacodynamic end points which evaluate the mechanism of drug action and also to aid evaluation of the therapeutic window of these targeted agents.

With a view to streamlining the drug development process, the US Food and Drug Administration has approved performing exploratory investigator new drug (IND) studies (termed as phase 0 trials). The purpose of these early studies is to assist in the go *versus* no-go decision for a product using human models than relying on inconsistent animal data. Functional imaging has an important role in this setting as it can provide evidence of drug activity as well as help in selection of the functional dose of the drug.

Discussion

RCC appears to be more sensitive to treatment with antiangiogenic drugs than many other tumours due to the high vascularity of the tumour and its dependence on the VHL pathway in pathogenesis. With an increasing number of therapeutic agents in development, the need for biomarkers is more critical than ever for analysing efficacy and potentially improving the cost–benefit ratio of treatment. There are now emerging data about how these newer techniques could fit into the paradigm of RCC management, starting from initial diagnosis and staging to therapeutic response assessment. These early data need extensive and robust validation. Functional imaging with DCE-MRI and DCE-CT holds promise as predictive and prognostic biomarkers in treatment response in patients with RCC. DW-MRI can give insight into histological subtypes and in the diagnosis of skeletal metastasis, which is appealing and may have utility in clinical practice. Evidence needs to be generated about the use of other techniques in RCC, such as ASL-MRI and MR spectroscopy.

In conclusion, in an area in which biomarker development is the focus of international research activity, imaging as a biomarker in RCC holds most promise in making an impact upon the clinical management of this disease.

Funding

Conflict of interest statement

The authors declare no conflict of interest in preparing this article.

References

Antoch, G., Vogt, F., Freudenberg, L., Nazaradeh, F., Goehde, S., Barkhausen, J. *et al.* (2003) Whole-body dual-modality PET/CT and whole-body MRI for tumor staging in oncology. *JAMA* 290: 3199–3206.

Basappa, N., Elson, P., Golshayan, A., Wood, L., Garcia, J., Dreicer, R. *et al.* (2011) The impact of tumor burden characteristics in patients with metastatic renal cell carcinoma treated with sunitinib. *Cancer* 117: 1183–1189.

Bellomi, M., Petralia, G., Sonzogni, A., Zampino, M. G., and Rocca, A. (2007) CT perfusion for the monitoring of neoadjuvant chemotherapy and radiation therapy in rectal carcinoma: initial experience. *Radiology* 244(2): 486–493.

Cangiano, T., Liao, J., Naitoh, J., Dorey, F., Figlin, R. and Belldegrun, A. (1999) Sarcomatoid renal cell carcinoma: biologic behavior, prognosis, and response to combined surgical resection and immunotherapy. *J Clin Oncol* 17: 523–528.

Choi, H. (2008) Response evaluation of gastrointestinal stromal tumors. *Oncologist* 13 (Suppl. 2): 4–7.

Choi, H., Charnsangavej, C., Faria, S., Macapinlac, H., Burgess, M., Patel, S. *et al.* (2007) Correlation of computed tomography and positron emission tomography in patients with metastatic gastrointestinal stromal tumor treated at a single institution with imatinib mesylate: proposal of new computed tomography response criteria. *J Clin Oncol* 25: 1753–1759.

De Bazelaire, C., Alsop, D., George, D., Pedrosa, I., Wang, Y., Michaelson, M. *et al.* (2008) Magnetic resonance imaging measured blood flow change after antiangiogenic therapy with PTK787/ZK 222584 correlates with clinical outcome in metastatic renal cell carcinoma. *Clin Cancer Res* 14: 5548–5554.

De Bazelaire, C., Rofsky, N., Duhamel, G., Michaelson, M., George, D. and Alsop, D. (2005) Arterial spin labeling blood flow magnetic resonance imaging for the characterization of metastatic renal cell carcinoma1. *Acad Radiol* 12: 347–357.

Desar, I., ter Voert, E., Hambrock, T., van Asten, J., van Spronsen, D., Mulders, P. *et al.* (2011) Functional MRI techniques demonstrate early vascular changes in renal cell cancer patients treated with sunitinib: a pilot study. *Cancer Imaging* 11: 259–265.

Ebele, J., Sauter, G., Epstein, J. and Sesterhenn, I. (eds) (2004) *World Health Organization Classification of Tumours. Pathology and Genetics of Tumours of the Urinary System and Male Genital Organs*. Lyon: IARC.

Escudier, B., Eisen, T., Stadler, W., Szczylik, C., Oudard, S., Siebels, M. *et al.* (2007a) Sorafenib in advanced clear-cell renal-cell carcinoma. *N Engl J Med* 356: 125–134.

Escudier, B., Pluzanska, A., Koralewski, P., Ravaud, A., Bracarda, S., Szczylik, C. *et al.* (2007b) Bevacizumab plus interferon alfa-2a for treatment of metastatic renal cell carcinoma: a randomised, double-blind phase III trial. *Lancet* 370: 2103–2111.

Ferte, C., Albiges, L., Soria, J., Loriot, Y., Fizazi, K. and Escudier, B. (2012) The use of tumor growth rate (TGR) in evaluating sorafenib and everolimus treatment in mRCC patients: an integrated analysis of the TARGET and RECORD phase III trials data. *J Clin Oncol* 30(Suppl.): abstract 4540.

Flaherty, K., Rosen, M., Heitjan, D., Gallagher, M., Schwartz, B., Schnall, M. *et al.* (2008) Pilot study of DCE-MRI to predict progression-free survival with sorafenib therapy in renal cell carcinoma. *Cancer Biol Ther* 7: 496–501.

Hahn, O., Yang, C., Medved, M., Karczmar, G., Kistner, E., Karrison, T. *et al.* (2008) Dynamic contrast-enhanced magnetic resonance imaging pharmacodynamic biomarker study of sorafenib in metastatic renal carcinoma. *J Clin Oncol* 26: 4572–4578.

Hittinger, M., Staehler, M., Schramm, N., Übleis, C., Becker, C., Reiser, M. *et al.* (2011) Course of size and density of metastatic renal cell carcinoma lesions in the early follow-up of molecular targeted therapy. *Urol Oncol* 23 August (Epub ahead of print).

Hudes, G., Carducci, M., Tomczak, P., Dutcher, J., Figlin, R., Kapoor, A. *et al.* (2007) Temsirolimus, interferon alfa, or both for advanced renal-cell carcinoma. *N Engl J Med* 356: 2271–2281.

Kang, D., White, R., Jr, Zuger, J., Sasser, H. and Teigland, C. (2004) Clinical use of fluorodeoxyglucose F 18 positron emission tomography for detection of renal cell carcinoma. *J Urol* 171: 1806–1809.

Kiessling, F., Jugold, M., Woenne, E. and Brix, G. (2007) Non-invasive assessment of vessel morphology and function in tumors by magnetic resonance imaging. *Eur Radiol* 17: 2136–2148.

Kovacs, G., Akhtar, M., Beckwith, B., Bugert, P., Cooper, C., Delahunt, B. *et al.* (1997) The Heidelberg classification of renal cell tumours. *J Pathol* 183: 131–133.

Lamuraglia, M., Escudier, B., Chami, L., Schwartz, B., Leclère, J., Roche, A. *et al.* (2006) To predict progression-free survival and overall survival in metastatic renal cancer treated with sorafenib: pilot study using dynamic contrast-enhanced Doppler ultrasound. *Eur J Cancer* 42: 2472–2479.

Lassau, N., Vilgrain, V., Taieb, S., Lacroix, J., Aziza, R., Cuinet, M. *et al.* (2012) Evaluation with DCE-US of antiangiogenic treatments in 539 patients allowing the selection of one surrogate marker correlated to overall survival. *J Clin Oncol* 30(Suppl.): abstract 4618.

Lebret, T., Poulain, J., Molinie, V., Herve, J., Denoux, Y., Guth, A. *et al.* (2007) Percutaneous core biopsy for renal masses: indications, accuracy and results. *J Urol* 178: 1184–1188.

Lee, E., Heiken, J., Huettner, P. and Na-Chiangmai, W. (2005) Renal cell carcinoma visible only during the corticomedullary phase of enhancement. *AJR Am J Roentgenol* 184(3 Suppl.): S104–S106.

Leibovich, B., Cheville, J., Lohse, C., Zincke, H., Frank, I., Kwon, E. *et al.* (2005) A scoring

algorithm to predict survival for patients with metastatic clear cell renal cell carcinoma: a stratification tool for prospective clinical trials. *J Urol* 174: 1759–1763.

Le Moulec, S., Carassou, P., Billemont, B., Massard, C., Vedrine, L., Gontier, E.. (2010) Prospective evaluation of FDG-PET/CT in patients with advanced RCC treated with antiangiogenic therapies. *2010 Genitourinary Cancers Symposium*. 5–7 March, San Francisco, ASCO.

Liu, G., Jeraj, R., Vanderhoek, M., Perlman, S., Kolesar, J., Harrison, M. *et al.* (2011) Pharmacodynamic study using FLT PET/CT in patients with renal cell cancer and other solid malignancies treated with sunitinib malate. *Clin Cancer Res* 17: 7634–7644.

Marcus, C., Ladam-Marcus, V., Cucu, C., Bouché, O., Lucas, L. and Hoeffel, C. (2009) Imaging techniques to evaluate the response to treatment in oncology: current standards and perspectives. *Crit Rev Oncol Hematol* 72: 217–238.

Miles, K. (2002) Functional computed tomography in oncology. *Eur J Cancer* 38: 2079–2084.

Minamimoto, R., Nakaigawa, N., Tateishi, U., Suzuki, A., Shizukuishi, K., Kishida, T. *et al.* (2010) Evaluation of response to multikinase inhibitor in metastatic renal cell carcinoma by FDG PET/contrast-enhanced CT. *Clin Nucl Med* 35: 918–923.

Montravers, F., Grahek, D., Kerrou, K., Younsi, N., Doublet, J., Gattegno, B. *et al.* (2000) Evaluation of FDG uptake by renal malignancies (primary tumor or metastases) using a coincidence detection {gamma} camera. *J Nucl Med* 41: 78–84.

Motzer, R., Escudier, B., Oudard, S., Hutson, T., Porta, C., Bracarda, S. *et al.* (2008) Efficacy of everolimus in advanced renal cell carcinoma: a double-blind, randomised, placebo-controlled phase III trial. *Lancet* 372: 449–456.

Motzer, R., Hudes, G., Curti, B., McDermott, D., Escudier, B., Negrier, S. *et al.* (2007a) Phase I/II trial of temsirolimus combined with interferon alfa for advanced renal cell carcinoma. *J Clin Oncol* 25: 3958–3964.

Motzer, R., Hutson, T., Tomczak, P., Michaelson, M., Bukowski, R., Rixe, O. *et al.* (2007b) Sunitinib versus interferon alfa in metastatic renal-cell carcinoma. *N Engl J Med* 356: 115–124.

Motzer, R., Mazumdar, M., Bacik, J., Berg, W., Amsterdam, A. and Ferrara, J. (1999) Survival and prognostic stratification of 670 patients with advanced renal cell carcinoma. *J Clin Oncol* 17: 2530–2540.

Nakaigawa, N., Yao, M., Tateishi, U., Minamimoto, R., Uemura, H., Inoue, T. *et al.* (2012) Impact of

maximum standardized uptake value (SUVmax) evaluated by 18-fluoro-2-deoxy-dglucose positron emission tomography/computed tomography (FDG PET/CT) on survival for patients with advanced renal cell carcinoma. *J Clin Oncol* 30(Suppl.): abstract 4626.

Nakatani, K., Nakamoto, Y., Saga, T., Higashi, T. and Togashi, K. (2011) The potential clinical value of FDG-PET for recurrent renal cell carcinoma. *Eur J Radiol* 79: 29–35.

Nathan, P., Vinayan, A., Stott, D., Juttla, J. and Goh, V. (2010) CT response assessment combining reduction in both size and arterial phase density correlates with time to progression in metastatic renal cancer patients treated with targeted therapies. *Cancer Biol Ther* 9: 15–19.

Nicol, D., Hii, S., Walsh, M., Teh, B., Thompson, L., Kennett, C. *et al.* (1997) Vascular endothelial growth factor expression is increased in renal cell carcinoma. *J Urol* 157: 1482–1486.

Oudard, S., Thiam, R., Fournier, L., Medioni, J., Lamuraglia, M., Scotte, F. *et al.* (2012) Optimisation of the tumour response threshold in patients treated with everolimus for metastatic renal cell carcinoma: analysis of response and progression-free survival in the RECORD-1 study. *Eur J Cancer* 48: 1512–1518.

Padhani, A. (2003) MRI for assessing antivascular cancer treatments. *Br J Radiol* 76(Suppl. 1): S60–S80.

Padhani, A. and Dzik-Jurasz, A. (2004) Perfusion MR imaging of extracranial tumor angiogenesis. *Top Magn Reson Imaging* 15: 41–57.

Palmowski, M., Schifferdecker, I., Zwick, S., Macher-Goeppinger, S., Laue, H., Haferkamp, A. *et al.* (2009) Tumor perfusion assessed by dynamic contrast-enhanced MRI correlates to the grading of renal cell carcinoma: initial results. *Eur J Radiol* 74: e176–e180.

Pedrosa, I., Chou, M., Ngo, L., Baroni, R., Genega, E., Galaburda, L. *et al.* (2008) MR classification of renal masses with pathologic correlation. *Eur Radiol* 18: 365–375.

Powles, T., Kayani, I., Blank, C., Chowdhury, S., Horenblas, S., Sarwar, N. *et al.* (2010) The safety and efficacy of sunitinib prior to planned nephrectomy in metastatic clear cell renal cancer. *J Clin Oncol* 28(15 Suppl.): abstract 4603.

Raptopoulos, V., Blake, S., Weisinger, K., Atkins, M., Keogan, M. and Kruskal, J. (2001) Multiphase contrast-enhanced helical CT of liver metastases from renal cell carcinoma. *Eur Radiol* 11: 2504–2509.

Renshaw, A., Lee, K., Madge, R. and Granter, S. (1997) Accuracy of fine needle aspiration in distinguishing subtypes of renal cell carcinoma. *Acta Cytol* 41: 987–994.

Revheim, M., Winge-Main, A., Hagen, G., Fjeld, J., Fosså, S. and Lilleby, W. (2011) Combined positron emission tomography/computed tomography in sunitinib therapy assessment of patients with metastatic renal cell carcinoma. *Clin Oncol* 23: 339–343.

Schlemmer, H., Merkle, J., Grobholz, R., Jaeger, T., Michel, M., Werner, A. *et al.* (2004) Can pre-operative contrast-enhanced dynamic MR imaging for prostate cancer predict microvessel density in prostatectomy specimens? *Eur Radiol* 14: 309–317.

Schmidt, G., Baur-Melnyk, A., Herzog, P., Schmid, R., Tiling, R., Schmidt, M. *et al.* (2005) High-resolution whole-body magnetic resonance image tumor staging with the use of parallel imaging versus dual-modality positron emission tomography-computed tomography: experience on a 32-channel system. *Invest Radiol* 40: 743–753.

Schmidt, G., Haug, A., Schoenberg, S. and Reiser, M. (2006) Whole-body MRI and PET-CT in the management of cancer patients. *Eur Radiol* 16: 1216–1225.

Sheir, K., El-Azab, M., Mosbah, A., El-Baz, M. and Shaaban, A.A. (2005) Differentiation of renal cell carcinoma subtypes by multislice computerized tomography. *J Urol* 174: 451–455.

Smith, A., Lieber, M. and Shah, S. (2010a) Assessing tumor response and detecting recurrence in metastatic renal cell carcinoma on targeted therapy: importance of size and attenuation on contrast-enhanced CT. *AJR Am J Roentgenol* 194: 157–165.

Smith, A., Shah, S., Rini, B., Lieber, M. and Remer, E. (2010b) Morphology, Attenuation, Size, and Structure (MASS)criteria: assessing response and predicting clinical outcome in metastatic renal cell carcinoma on antiangiogenic targeted therapy. *Am J Roentgenol* 194: 1470–1478.

Smith, A., Shah, S., Rini, B., Lieber, M. and Remer, E. (2011) Utilizing pre-therapy clinical schema and initial CT changes to predict progression-free survival in patients with metastatic renal cell carcinoma on VEGF-targeted therapy: a preliminary analysis. *Urol Oncol* 26 September (Epub ahead of print).

Sohaib, S., Cook, G., Allen, S., Hughes, M., Eisen, T. and Gore, M. (2009) Comparison of whole-body MRI and bone scintigraphy in the detection of bone metastases in renal cancer. *Br J Radiol* 82: 632–639.

Staudenherz, A., Steiner, B., Puig, S., Kainberger, F., and Leitha, T. (1999) Is there a diagnostic role for bone scanning of patients with a high pretest probability for metastatic renal cell carcinoma? *Cancer* 85(1): 153–155.

Sun, M., Ngo, L., Genega, E., Atkins, M., Finn, M., Rofsky, N. *et al.* (2009) Renal cell

carcinoma: dynamic contrast-enhanced MR imaging for differentiation of tumor subtypes correlation with pathologic findings. *Radiology* 250: 793–802.

Teo, M. and McDermott, R.; Department of Medical Oncology, Adelaide and Meath Hospital, incorporating the National Children's Hospital, Dublin, Ireland (2012) Does RECIST-defined progression correlate with lack of further sunitinib (SU) benefit in advanced renal cell carcinoma (aRCC)? *J Clin Oncol* 30(Suppl.): abstract e15093.

Therasse, P., Arbuck, S., Eisenhauer, E., Wanders, J., Kaplan, R., Rubinstein, L. *et al.* (2000) New guidelines to evaluate the response to treatment in solid tumors. *J Natl Cancer Inst* 92: 205–216.

Ueno, D., Yao, M., Tateishi, U., Minamimoto, R., Makiyama, K., Hayashi, N. *et al.* (2012) Early assessment by FDG-PET/CT of patients with advanced renal cell carcinoma treated with tyrosine kinase inhibitors is predictive of disease course. *BMC Cancer* 12: 162.

van der Veldt, A., Meijerink, M., van den Eertwegh, A., Haanen, J. and Boven, E. (2010) Choi response criteria for early prediction of clinical outcome in patients with metastatic renal cell cancer treated with sunitinib. *Br J Cancer* 102: 803–809.

Williams, R., Hudson, J., Lloyd, B., Sureshkumar, A., Lueck, G., Milot, L. *et al.* (2011) Dynamic microbubble contrast-enhanced US to measure tumor response to targeted therapy: a proposed clinical protocol with results from renal cell carcinoma patients receiving antiangiogenic therapy. *Radiology* 260: 581–590.

Yuasa, T., Urakami, S., Yamamoto, S., Yonese, J., Nakano, K., Kodaira, M. *et al.* (2011) Tumor size is a potential predictor of response to tyrosine kinase inhibitors in renal cell cancer. *Urology* 77: 831–835.

Zisman, A., Pantuck, A., Dorey, F., Said, J., Shvarts, O., Quintana, D. *et al.* (2001) Improved prognostication of renal cell carcinoma using an integrated staging system. *J Clin Oncol* 19: 1649–1657.

Visit SAGE journals online
http://tam.sagepub.com

SAGE journals

CT response assessment combining reduction in both size and arterial phase density correlates with time to progression in metastatic renal cancer patients treated with targeted therapies

P.D. Nathan,[1],* A. Vinayan,[1] D. Stott,[2] J. Juttla[3] and V. Goh[3]

[1]Mount Vernon Cancer Centre; Northwood, Middlesex UK; [2]University of Hertfordshire; Hatfield, UK; [3]Paul Strickland Scanner Centre; Northwood, UK

Background: Response assessment is critical in evaluating effectiveness of anticancer treatment. Tyrosine kinase inhibitors (TKIs) in renal cell carcinoma (RCC) are associated with significant clinical benefit but may not result in significant tumour size reduction. Thus standard size-based response assessment with RECIST is insensitive, resulting in low response rates which do not reflect disease control measured by time to progression. We compared the use of combined size and density response criteria with standard size based criteria in metastatic RCC patients treated with TKI's.

Results: Partial response (PR) and stable disease (SD) defined by modified criteria successfully identified patients with a long TTP (448 days) or short TTP (89 days) respectively (p = 0.002). Neither RECIST nor standard Choi criteria successfully discriminated between patients having a short or long clinical benefit.

Patients and methods: CT scans from 32 patients with metastatic RCC treated with either sunitinib (18) or cediranib (14) were assessed. 12 patients were excluded from the analysis as 10 had non-contrast enhanced scans due to renal impairment and 2 stopped treatment due to toxicity. Scans from 20 evaluable patients at baseline and 12 weeks on treatment were assessed using RECIST, Choi and modified criteria in which both a 10% decrease in size and 15% decrease in density were required to define a partial response (PR). Response assessment performed using each of the three methods was compared with time to disease progression (TTP) defined by RECIST using Kaplan-Meier statistics and Log-rank test with significance at 5%.

Conclusion: A combined reduction in both size and arterial phase density of RCC metastases treated with TKIs correlates with TTP. RECIST and standard Choi criteria appear inferior.

Introduction

Imaging defined response assessment underpins evaluation of therapeutic effectiveness of many anti-cancer treatments in both routine clinical practice and drug development. Response Evaluation Criteria of Solid Tumors (RECIST) have been the standard method of treatment evaluation for solid tumors since their introduction in 2000. RECIST defined response depends on the size change in the sum of uni-dimensional measurements of the tumor target lesions performed with an imaging modality.[1] While RECIST is clinically relevant for conventional chemotherapeutic agents, this appears not to be the case for a new generation of targeted anti-cancer agents. Many targeted agents have profound anti-tumor effects with resulting clinical benefit but low RECIST defined response rates. With sunitinib,[2] sorafenib[3] and avastin + interferon,[4] the treatment of renal cell

carcinoma (RCC) has been transformed. Progression free survival has doubled compared to either standard treatments or placebo. Yet, RECIST defined response rates are relatively low (Sunitinib 31%,[2] Sorafenib 10%[3] and Avastin + interferon 30%[4]). Many patients who derive significant clinical benefit from these drugs never attain a RECIST defined response. Response criteria that correlate with clinical benefit are needed both in routine clinical practice and in clinical trials of novel targeted agents. This would allow early identification of non-responders which in turn would enable an early change in therapy and avoidance of unnecessary treatment-related side effects.

The first targeted therapy to demonstrate significant clinical benefit was imatinib, a potent c-kit antagonist, which has profound activity against gastro-intestinal stromal tumors (GIST).[5] GIST tumors treated with imatinib usually shrink slowly with treatment but frequently develop a necrotic centre thus RECIST

Table 1. Response classification according to RECIST, choi and modified choi criteria and association with time to progression (TTP)

Classification	Partial response (PR)		Stable disease (SD)		Log rank
	No. of patients	TTP days median (95% CI)	No. of patients	TTP days median (95% CI)	Test *sign.*
RECIST	5	168 (50–286)	15	428 (129–726)	0.643
Choi	19	399 (85–713)	1	*	*
Modified criteria	13	448 (99–797)	7	89 (79–99)	0.002

Patients who had a partial response according to modified Choi criteria had a statistically significant longer time to progression than those who were deemed to have stable disease (mean 448 vs. 89 days, p = 0.002); Neither RECIST nor Choi criteria defined partial responders went on to have a significant improvement in TTP compared to those who had stable disease.

criteria are poor at predicting clinical benefit. Choi et al.[5,6] developed a set of criteria for GIST tumors which incorporated a change in target lesion size of >10% *or* a change in density of >15%. These criteria have been shown to be better predictors of clinical response to imatinib than RECIST defined response and have been advocated as a more appropriate response assessment tool in this disease.[5]

It has been suggested that the Choi criteria may be suitable for targeted therapy assessment in other cancers[6] but these criteria have not been extensively evaluated. A pilot study in soft tissue sarcoma showed that the Choi criteria were superior to RECIST in assessing treatment response of soft tissue sarcoma treated with chemotherapy and radiotherapy.[7]

In this study, we compare RECIST, Choi and "modified" Choi response criteria in which changes in *both* size and density of target lesions are required to define a response in RCC patients treated with the multi-targeted tyrosine kinase inhibitors sunitinib or cediranib, and their effect on time to progression and survival.

Results

Of the 32 patients, 18 had treatment with sunitinib and 14 had treatment with cediranib. 10 patients were excluded from the analysis as contrast enhanced scans were not performed due to impaired renal function and 2 patients ceased treatment due to toxicity rather than disease progression. Of the 20 evaluable patients, 11 were treated with sunitinib and 9 with cediranib.

Fourteen of 20 patients progressed on treatment with a median time to progression of 260 days. The remaining 6 evaluable patients remain on treatment and all have >1 year follow up (median: 483 days).

The number of patients having a partial response (PR) or stable disease (SD) defined by each of the three response criteria are shown in **Table 1** together with the median time to progression (median TTP). No patients were seen to have progressive disease at the three month time point using any of the response criteria. The modified Choi criteria provided the greatest segregation of median TTP (95% CI) for the partial response (PR) and stable disease (SD) groups: 448 (99–797) days (PR) versus 89 (79–99) days (SD). On evaluation with RECIST criteria, median TTP (95% CI) was 168 (50–286) days in the PR and 428 (129–726) days in the SD group. Using Choi criteria, median TTP of the PR group was 399 (85–713) days. Only one patient had Choi criteria defined stable disease.

Kaplan-Meier analyses are shown in **Figure 1**. Using the modified Choi criteria which combined reductions in size and density, there is a statistically significant difference in median time to progression between the PR and SD groups (Log Rank test p = 0.002). Kaplan-Meier curves for SD & PR groups defined by RECIST criteria showed no significant difference in median TTP (Log Rank test: p values of 0.643). As only a single patient had Choi criteria defined SD no statistical analysis was performed on this group.

A scatter plot (**Fig. 2**) demonstrates change in target lesion size and density for all patients between baseline scan and 3 month scan and identifies whether disease progressed in <100 days, 100–199 days, 200–399 days or >400 days. It may be possible to identify thresholds other than 10% for size and 15% for density that give even greater separation between patients having long and short term benefit from TKIs although a larger population of prospectively acquired data would be required for this.

Discussion

Imaging defined response assessment is the cornerstone of modern oncological practice. For therapies which result in significant tumor shrinkage, imaging response criteria which are based solely upon change in tumor size may be entirely appropriate. A number of targeted treatments have been proven to be clinically active in advanced RCC and some have become standard of care. In large phase III trials it was observed that overall RECIST defined response rates were low (10–31%)[2-4,11] but that (a) many patients had a degree of tumor shrinkage but less than a RECIST defined response and (b) RECIST responders were not the only patients who experienced clinical benefit with significant prolongation of progression free survival. The implication is that RECIST defined responses do not successfully identify groups of patients who either do or do not derive significant clinical benefit from targeted therapies.

RCC is a very vascular tumor and is therefore highly suitable for arterial based imaging. This is particularly so given that anti-angiogenic targeted therapies are significantly active in the treatment of advanced RCC. Arterial based imaging is therefore likely to be a sensitive method to detect clinically relevant anti-angiogenic drug induced changes in this disease.

A number of modalities can be used clinically to assess changes in arterial blood supply. Both Dynamic Contrast Enhanced (DCE) MRI and DCE-Ultrasound have been demonstrated to be predictive of responses to sorafenib, a multi-targeted TKI,
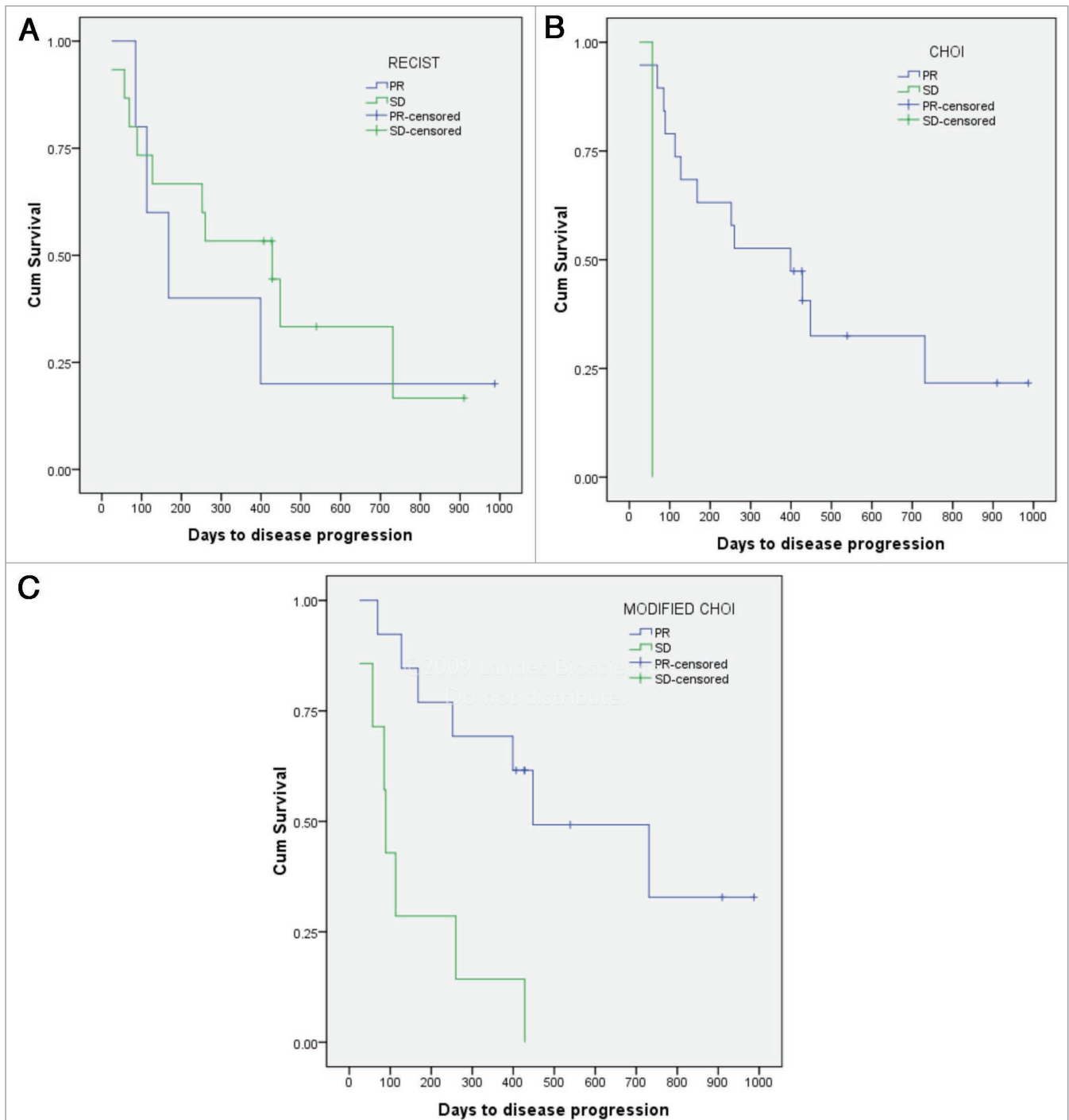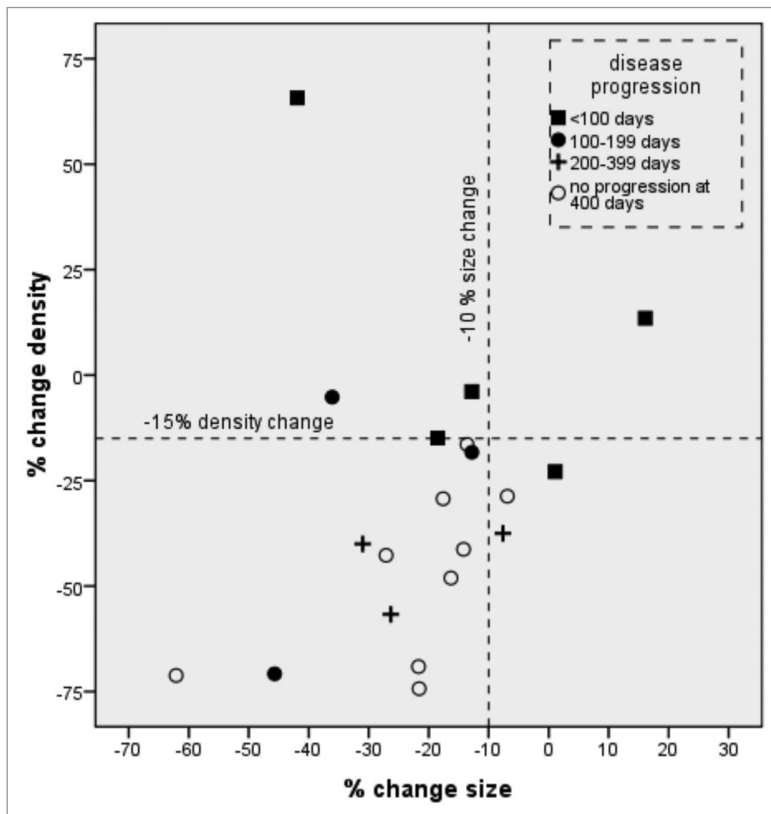
Figure I. Kaplan-Meier curve for time to disease progression: Ia)RECIST estimated median TTP 168 and 428 days for PR and SD group with log rank P value 0.643. Ib) with Choi criteria estimated median TTP was 399 for the PR group. As only 1 patient had Choi defined SD, no statistical analysis was performed. Ic) Modified choi criteria showing a TTP 448 and 95 days for PR and SD groups with a significance of p=0.002 with log rank p test.

in patients with advanced RCC. In two small studies DCE-MRI defined baseline Ktrans was predictive of PFS.[12,13] DCE-ultrasound defined responses in which a 10% reduction in enhancement were included in response criteria also correlated with PFS.[14] We have used arterial-phase contrast enhanced CT scans to evaluate standard RECIST, Choi, and modified criteria.

The Choi criteria, developed for response evaluation of imatinib treated GIST tumors, define a partial response by either a 10% reduction in size or a 15% reduction in density during the portal venous phase of contrast.

In this study we compared RECIST, Choi and "modified" Choi criteria in which both a minimum of a 10% reduction in

Figure 2. Scatter plot of change in density and change in size for all patients. TTP is indicated.

ROI analysis remains a topic of debate, but there is preliminary evidence to suggest that the most reproducible method is to delineate the ROI around the tumor outline,[16] as performed in this study.

This small study requires validation on a larger dataset, ideally with images taken from a variety of scanning centres to demonstrate the broader applicability of this technique.

It remains to be seen whether these modified response criteria are suitable for contrast enhanced CT studies that are acquired at a single phase, most commonly the portal-venous phase. It is likely, from clinical experience, that reduction in enhancement of tumors will be less marked in this contrast phase.

There is significant clinical need to be able to identify which patients are likely to derive most benefit from targeted agents early in treatment. This would allow an early change in therapeutic option for patients who are unlikely to benefit and avoidance of unnecessary toxicities.

In conclusion, we have observed that response criteria that account for changes in both size and enhancement of arterial perfusion in advanced renal cell carcinoma better predict for outcome with TKI based treatment than standard RECIST or Choi criteria and may be more appropriate.

Patients and Methods

size and a 15% reduction in density were required to define a response in metastatic RCC patients receiving either sunitinib or cediranib. The ability of each criteria defined response to correlate with RECIST defined time to progression was assessed.

Neither RECIST nor conventional Choi criteria defined responses correlated with time to progression. However "modified" Choi criteria defined responses successfully identified a group of patients with extended TTP (median 448 days) with non-responders having a significantly shorter TTP (median 89 days). Thus the Choi criteria may not be applicable to renal cell carcinoma directly, but require tumor specific adaptation to account for differences in both tumor physiology and drug action. Arterial phase imaging is particularly appropriate for functional evaluation of RCC.

Arterial phase contrast enhanced CT imaging has a number of advantages over other methods evaluating arterial vascular changes in response to drug therapy such as DCE-MRI and DCE-US.[13-15] The wide availability of CT scanners with fast scanning speeds enables arterial phase imaging at most centres. DCE-MRI is not available at most centres and not all tumor deposits are at anatomical sites assessable by DCE-US. All target lesions that are currently assessed by RECIST criteria should be amenable to assessment by our modified criteria. Nevertheless there are some issues with evaluation of tumor density using region of interest (ROI) analysis, that apply not just to CT but also to other imaging modalities. The best method to perform

32 patients with metastatic clear cell renal cell carcinoma, who started treatment with the multi-targeted tyrosine kinase inhibitors (TKI's) sunitinib or cediranib at Mount Vernon Cancer Centre between November 2005 and February 2008 comprised the study group. Patients receiving cediranib were enrolled on a phase II clinical trial (Eudract 2006-002455-33), patients receiving sunitinib were enrolled on an expanded access study (Eudract 2005-002097-30). All patients were receiving first line treatment for metastatic clear cell renal cell carcinoma, all had a baseline CT scan performed within 4 weeks of starting treatment and all had a second CT scan at twelve weeks to assess response to treatment. At least one year of follow up data was available for each patient. Of the 32 patients, 10 were excluded from the analysis as impaired renal function precluded a contrast enhanced CT. A further two patients were excluded from the analysis as treatment was stopped due to toxicities rather than disease progression, leaving 20 evaluable patients.

All patients with no contraindications to intravenous contrast underwent contrast enhanced multidetector CT (Siemens Sensation 16, Siemens Medical Solutions, Forccheim, Germany). Following injection of 100 mL of 350 mg/mL iodinated contrast agent (Optiray, Covidien Healthcare, Mansfield, MA, USA) at 4 mL/sec via a pump injector and saline chaser, the thorax and upper abdomen (from the supraclavicular fossa to the iliac crest) was imaged in the arterial phase of enhancement (25 sec delay). The abdomen and pelvis (from the dome of the diaphragm to the pubis) was imaged in the portal venous phase of enhancement

(70 sec delay). This is the standard protocol of our institution as evidence shows that highly vascular tumors such as renal cell carcinoma exhibit an early hyper-enhancement on multiphase CT.[8,9]

All CTs (baseline and 12 week scan) were analysed by an experienced oncological radiologist. This was a retrospective study. The radiologist was unaware of the time to progression of any of the patients in this study. Target lesions were selected in each patient. Target lesion size (cm) and Hounsfield unit (HU) density value at the arterial phase of enhancement were recorded in each patient. The HU density value was obtained by delineating a freehand region-of-interest (ROI) within the boundaries of the tumor outline, taking care to ensure this included the entire tumor visible. Patients were assigned to progressive disease (PD), stable disease (SD) or partial response (PR) using each criterion separately: RECIST, Choi and modified Choi criteria (**Table 1**). RECIST criteria[1,10] mandates a 30% decrease in the size of sum of longest diameters of the target lesions for a partial response (PR) and a 20% increase in size of sum of longest diameters of the target lesions for progressive disease (PD). Changes less than

a 30% reduction in size or a 20% increase in size are assigned as stable disease (SD). Choi criteria require either a 10% reduction in size or a 15% decrease in the density of target tumors for a PR.[5] The modified criteria required both a decrease of 10% in size *and* a 15% reduction in enhancement in the arterial phase for a partial response (PR).

The time to disease progression (TTP) from the start of the treatment for individual patient was calculated from the follow up visit records. TTP was defined as the number of days from the start of therapy to the day in which progression was confirmed by standard RECIST radiological criteria. Patients were assigned to either the SD or PR groups defined by each of the three response criteria and an assessment of correlation with TTP performed.

Median time to disease progression (median TTP) with 95% confidence intervals were calculated from the Kaplan-Meier curves, and correlated with SD and PR classifications for the three response assessment criteria. The Log rank test was used to assess the significance of differences obtained in the analysis.

References

1. RECIST guidelines. National Cancer Institute of the United States of America 2000.
2. Motzer RJ, Hutson TE, Tomczak P, Michaelson MD, Bukowski RM, Rixe O, et al. Sunitinib versus Interferon Alfa in Metastatic Renal-Cell Carcinoma. N Engl J Med 2007; 356:115-24.
3. Escudier B, Eisen T, Stadler WM, Szczylik C, Oudard S, Siebels M, et al. Sorafenib in advanced clear-cell renal-cell carcinoma. N Engl J Med 2007; 356:125-34.
4. Escudier B, Pluzanska A, Koralewski P, Ravaud A, Bracarda S, Szczylik C, et al. Bevacizumab plus interferon alfa-2a for treatment of metastatic renal cell carcinoma: a randomised, double-blind phase III trial. The Lancet 370:2103-11.
5. Choi H. Response Evaluation of Gastrointestinal Stromal Tumors. Oncologist 2008; 13:4-7.
6. Choi H, Charnsangavej C, Faria SC, Macapinlac HA, Burgess MA, Patel SR, et al. Correlation of Computed Tomography and Positron Emission Tomography in Patients With Metastatic Gastrointestinal Stromal Tumor Treated at a Single Institution With Imatinib Mesylate: Proposal of New Computed Tomography Response Criteria. J Clin Oncol 2007; 25:1753-9.
7. Stacchiotti S, Collini P, Messina A, Morosi C, Barisella M, Bertulli R, et al. High-Grade Soft-Tissue Sarcomas: Tumor Response Assessment—Pilot Study to Assess the Correlation between Radiologic and Pathologic Response by Using RECIST and Choi Criteria. Radiology 2009; 2512081403.
8. Raptopoulos V, Blake S, Weisinger K, Atkins M, Keogan M, Kruskal J. Multiphase contrast-enhanced helical CT of liver metastases from renal cell carcinoma. European Radiology 2001; 11:2504-9.
9. Lee EY, Heiken JP, Huettner PC, Na-ChiangMai W. Renal Cell Carcinoma Visible Only During the Corticomedullary Phase of Enhancement. Am J Roentgenol 2005; 184:104-6.
10. Patrick Therasse SGA, Elizabeth A. Eisenhauer, Jantien Wanders, Richard S, Kaplan LR, Jaap Verweij, et al. New Guidelines to Evaluate the Response to Treatment in Solid Tumors. J Natl Cancer Inst 2000; 92:205-16.
11. Ratain MJ, Eisen T, Stadler WM, Flaherty KT, Kaye SB, Rosner GL, et al. Phase II Placebo-Controlled Randomized Discontinuation Trial of Sorafenib in Patients With Metastatic Renal Cell Carcinoma. J Clin Oncol 2006; 24:2505-12.
12. Flaherty KT, Rosen MA, Heitjan DF, Gallagher ML, Schwartz B, Schnall MD, O'Dwyer PJ. Pilot study of DCE-MRI to predict progression-free survival with sorafenib therapy in renal cell carcinoma. Cancer Biol Ther 2008; 7:496-501.
13. Hahn OM, Yang C, Medved M, Karczmar G, Kistner E, Karrison T, et al. Dynamic Contrast-Enhanced Magnetic Resonance Imaging Pharmacodynamic Biomarker Study of Sorafenib in Metastatic Renal Carcinoma. J Clin Oncol 2008; 26:4572-8.
14. Lamuraglia M, Escudier B, Chami L, Schwartz B, Leclère J, Roche A, Lassau N. To predict progression-free survival and overall survival in metastatic renal cancer treated with sorafenib: Pilot study using dynamic contrast-enhanced Doppler ultrasound. Eur J Cancer 2006; 42:2472-9.
15. Rosen MA, Schnall MD. Dynamic Contrast-Enhanced Magnetic Resonance Imaging for Assessing Tumor Vascularity and Vascular Effects of Targeted Therapies in Renal Cell Carcinoma. Clin Cancer Res 2007; 13:770-6.
16. Goh V, Halligan S, Gharpuray A, Wellsted D, Sundin J, Bartram CI. Quantitative assessment of colorectal cancer tumor vascular parameters by using perfusion CT: influence of tumor region of interest. Radiology 2008; 247:726-32.

Assessment of Response to Tyrosine Kinase Inhibitors in Metastatic Renal Cell Cancer: CT Texture as a Predictive Biomarker[1]

Vicky Goh, MD, FRCR
Balaji Ganeshan, PhD
Paul Nathan, FRCP
Jaspal K. Juttla, FRCR
Anup Vinayan, FRCR
Kenneth A. Miles, MD, FRCR

Purpose: To assess changes in tumor computed tomographic (CT) texture after two cycles of treatment with tyrosine kinase inhibitors (TKIs) and to determine if tumor texture correlates with measured time to progression in patients with metastatic renal cell cancer who received TKIs.

Materials and Methods: A waiver of institutional review board approval was obtained for this retrospective analysis. Contrast material–enhanced CT texture parameters were assessed in 39 patients with metastatic renal cell cancer who received a TKI. A total of 87 metastases were analyzed at baseline and after two treatment cycles. Changes in tumor entropy and uniformity were derived with a software algorithm that selectively filters and extracts texture at different scales (fine to coarse detail: 1.0–2.5) and were recorded. Response assessment was also obtained by using response evaluation criteria in solid tumors (RECIST), as well as Choi and modified Choi criteria. The correlation of texture parameters and standard criteria with measured time to progression was assessed by using Kaplan-Meier analysis and a Cox regression model. Statistical significance was set at 5%.

Results: Tumor entropy decreased by 3%–45% and uniformity increased by 5%–21% for the different scale values after administration of a TKI. With a threshold change of −2% or less for uniformity at a coarse scale value of 2.5, Kaplan-Meier curves of the proportion of patients without disease progression were significantly different and better than those for standard response assessment ($P = .008$ vs $P = .267$, $P = .053$, and $P = .042$ for RECIST, Choi, and modified Choi criteria, respectively). Cox regression analysis showed that texture uniformity was an independent predictor of time to progression (odds ratio, 4.02; 95% confidence interval: 1.52, 10.65; $P = .005$).

Conclusion: CT texture analysis reflecting tumor heterogeneity is an independent factor associated with time to progression and has potential as a predictive imaging biomarker of response of metastatic renal cancer to targeted therapy.

© RSNA, 2011

Supplemental material: *http://radiology.rsna.org/lookup/suppl/doi:10.1148/radiol.11110264/-/DC1*

Radiology

The introduction of multitargeted tyrosine kinase inhibitors (TKIs), including sunitinib, sorafenib, and pazopanib, into clinical practice has doubled the duration of progression-free survival in patients with renal cell cancer when compared with standard treatment or administration of a placebo (1–3). Assessment of treatment response to TKIs remains a challenge. It is now well established that conventional response evaluation criteria in solid tumors (RECIST)-defined response rates are far lower than the proportion of patients who derive clinically useful disease control (4). Substantial tumor necrosis may occur as a consequence of the antivascular effect, resulting in a change in tumor attenuation but little overall size change (5–8). This heterogeneity in tumor morphology is not taken into account by RECIST criteria, and a better method with which to assess and predict response is still needed.

Alternative response criteria incorporating size and enhancement change (9,10) have been validated in patients with gastrointestinal stromal tumors that were treated with a targeted agent (imatinib) and applied to renal cell cancer treated with TKIs (11–14). Recent studies have shown a correlation between various size and enhancement

criteria and clinical outcome in patients with renal cell cancer ([a] Choi criteria, partial response defined by 10% reduction in size or 15% reduction in enhancement [11]; [b] modified Choi criteria, partial response defined by both a 10% reduction in size and a 15% reduction in enhancement [12]; [c] size and attenuation computed tomography [CT] criteria, favorable response defined by >20% reduction in size or >10% reduction in size and >50% of nonlung target lesions with >20 HU reduction in mean attenuation or one or more target lesions with >40 HU reduction in mean attenuation [13]; and [d] morphology, attenuation, size, and structure criteria, favorable response defined by a ≥20% decrease in tumor size or one or more predominantly solid enhancing lesions with marked central necrosis or marked decreased attenuation [≥40 HU] [14]).

Heterogeneity, such as heterogeneity of the tumor blood supply, is a well-recognized feature of malignancy. CT texture analysis is an image processing algorithm that can be used to quantify this heterogeneity by assessing the distribution of texture coarseness and irregularity within a lesion. Much of the heterogeneity visible at CT represents photon noise, which can mask any underlying biologic heterogeneity. By using filters that select for image features at larger scales, CT texture analysis can be used to reduce the effect of photon noise while enhancing biologic heterogeneity. Heterogeneity at relevant scales can then be quantified by using a range of parameters, including entropy and uniformity. Entropy is a measure of texture irregularity, while uniformity reflects the distribution of gray levels within the tumor: higher entropy and lower uniformity represent increased tumor heterogeneity. Previous computer simulation studies have shown that CT texture analysis may reflect the underlying

vasculature (15), and exploratory studies have suggested that image brightness and coarseness may yield predictive and prognostic information in patients with non–small cell lung cancer (16) and colorectal cancer (17–21). To our knowledge, the potential of CT texture analysis has not been explored in this context in patients with renal cell cancer.

The aim of this study was to assess changes in tumor CT texture after two cycles of TKIs and to determine if tumor texture correlates with measured time to progression in patients with metastatic renal cell cancer treated with TKIs.

Materials and Methods

One author (B.G.) is the scientific director of TexRAD (University of Sussex, Falmer, Sussex, England), which provided the software used for analysis in this study. Another author (K.A.M.) is the clinical director of TexRAD. All other authors had control of the data and information submitted for publication.

Patients

Institutional review board waiver was obtained for this retrospective analysis. Patients with metastatic renal cell cancer who underwent treatment with TKIs at our institution (Mount Vernon Hospital, Northwood, England) between 2005 and 2009 were identified in a prospectively recorded institutional renal cancer

Advances in Knowledge

- CT texture analysis can reveal changes in tumor heterogeneity after treatment of metastatic renal cell carcinoma with tyrosine kinase inhibitors (TKIs): tumor entropy decreases and uniformity increases.
- Change in tumor heterogeneity after two cycles of TKI therapy for metastatic renal cancer correlates with measured time to progression; by using a threshold change of −2% or less for uniformity at a coarse scale value of 2.5, Kaplan-Meier curves of the proportion of patients without disease progression were significantly different and better than those for standard response assessment after two cycles of TKI therapy ($P = .008$).

Implication for Patient Care

- The addition of texture analysis to standard response assessment may improve the prediction of response to TKIs in patients with metastatic renal cell carcinoma.

Table 1

RECIST, Choi, and Modified Choi Criteria for Categorization of Response

Response Criteria	Partial Response	Stable Disease	Progressive Disease
RECIST	>30% size reduction	<30% size reduction and <10% size increase	>20% size increase and new disease
Choi	>10% size reduction or >15% enhancement reduction	<10% size reduction or <15% enhancement reduction	>10% size increase, enhancement criteria not fulfilled, and new disease
Modified Choi	>10% size reduction and >15% enhancement reduction	<10% size reduction and <15% enhancement reduction	>10% size increase, enhancement criteria not fulfilled, and new disease

Figure 1
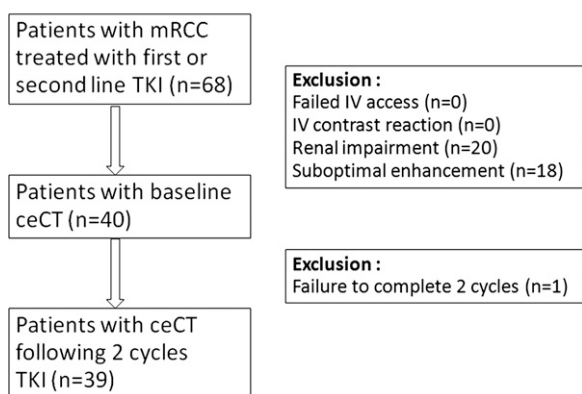
Figure 1: Flowchart of study population and exclusion criteria. *ceCT* = contrast-enhanced CT, *IV* = intravenous, *mRCC* = metastatic renal cell carcinoma.

database (A.V., P.N.). Inclusion criteria were as follows: *(a)* Patients were TKI naïve and were receiving the drug as a first- or second-line treatment for metastatic renal cell carcinoma. *(b)* Baseline contrast material–enhanced CT was performed within 4 weeks before treatment commencement. *(c)* Contrast-enhanced CT was performed after treatment to assess response. Exclusion criteria were as follows: *(a)* Patients had contraindications to contrast-enhanced CT (previous iodinated contrast material hypersensitivity reaction, renal impairment with serum creatinine level >120 μmol/L, or estimated glomerular filtration rate <60 mL/min). *(b)* Intravenous cannulation failed. *(c)* Contrast enhancement was suboptimal (aortic enhancement <200 HU at 25 seconds). A total of 68 patients were identified in the institution database. Of these, 29 were excluded, leaving 39 patients for analysis (23 men, 16 women; mean age, 61.43 years; age range, 38.6–75.8 years) (Fig 1).

CT Examination

All patients underwent contrast-enhanced multidetector CT (Somatom Definition or Sensation 16; Siemens Healthcare, Forchheim, Germany) after injection of 100 mL of an iodinated contrast agent (350 mg of iodine per milliliter, Optiray 350; Covidien Healthcare, Mansfield, Mass) and a 50-mL saline chaser at a rate of 4 mL/sec via a pump injector. The thorax and upper abdomen (from the supraclavicular fossa to the iliac crest) were imaged in the arterial phase of enhancement (25-second delay), and the abdomen and pelvis (from the dome of the diaphragm to the pubis) were imaged in the portal venous phase of enhancement (70-second delay), as per the standard practice in our institution, with the following acquisition parameters: 120 kV; effective tube current, 150 mAs (thorax) or 200 mAs (abdomen and pelvis) with dose modulation; pitch, 1.2; detector configuration, 24.0 × 1.2 mm; section collimation, 3 mm; field of view, 300–450 mm; matrix, 512 mm. Target lesions were defined as per RECIST, version 1.1 (five target lesions, maximum of two lesions per organ) (4). Initial response after two cycles of treatment was categorized, as per RECIST. Tumor attenuation was measured with

automated volume of interest analysis (syngoCT Oncology; Siemens Healthcare) encompassing the entire tumor (mean volume, 111 cm^3; range, 2–947 cm^3), and response was further classified according to Choi (9) and modified Choi (12) criteria (Table 1) by two radiologists working in consensus (V.G., J.K.J.; >12 and 7 years experience in CT imaging, respectively).

Textural Analysis

Arterial phase images underwent texture analysis performed with TexRAD, a proprietary software algorithm developed by Ganeshan et al (16) (Appendix E1 [online]). This was performed by an observer (B.G., 5 years of experience with texture analysis of CT images) who was blinded to the clinical outcome. The technique comprised an initial filtration step in which we used a Laplacian of Gaussian spatial band-pass filter to selectively extract features of different size and intensity variations. This resulted in a series of derived images that displayed features at different spatial scales from fine to coarse within a region of interest (ROI) drawn around the renal metastasis (Fig 2). The scale was selected by tuning the filter parameter between 1.0 and 2.5, where 1.0 indicates fine texture (features of approximately 4 pixels in width); 1.5, 1.8, and 2.0 indicate varying degrees of medium texture (features of approximately 6, 8, and 10 pixels in width, respectively); and 2.5 indicates coarse texture (features of approximately 12 pixels in width). After filtration, any pixels with negative values were assigned a value of zero.

ROIs were delineated around the tumor outline. The ROI was further refined by excluding areas of air with a

Radiology

thresholding procedure that enabled us to remove from analysis any pixels with attenuation below -50 HU. Mean ROI size was 2791 pixels (range, 72–17442 pixels). Heterogeneity within this ROI was quantified with and without image filtration by calculating entropy (irregularity, e) and uniformity (distribution of gray level, u) with the following equations:

$$e = -\sum_{I=1}^{k} [P(I)] \log_2 [P(I)] \qquad (1)$$

and

$$u = \sum_{I=1}^{k} [P(I)]^2, \qquad (2)$$

where I is the pixel value (between $I = 1$ to k [where k is the highest pixel value]) in the ROI and $P(I)$ is the probability of the occurrence of that pixel value. Higher entropy and lower uniformity represent increased heterogeneity (18).
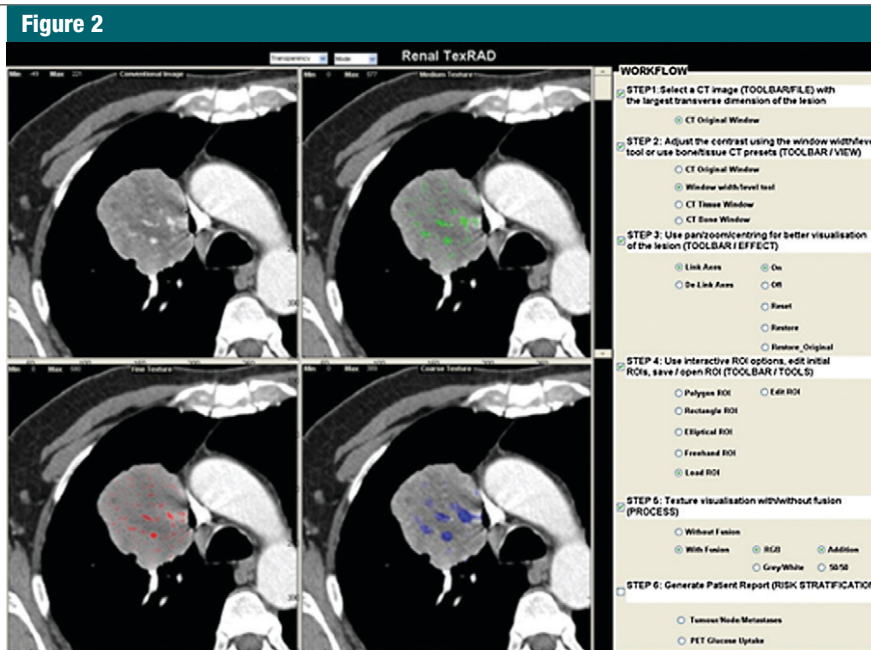
Entropy and uniformity were recorded for absolute scale values for each patient's tumor on baseline CT images and CT images acquired after two cycles of treatment. The percentage change in image entropy and uniformity was also recorded.

Follow-up

This was defined by the clinical drug trial protocol. The minimum length of follow-up was 18 months after baseline CT or until disease progression if sooner. Disease progression during follow-up was defined with RECIST criteria and was confirmed with subsequent imaging and clinical follow-up.

Statistical Analysis

For each patient, average texture measures from all metastases at baseline CT and at CT after two cycles of treatment and the percentage change from the baseline value were used for statistical analyses. Statistical analyses were performed by using software (MedCalc for Windows, version 9.2.0.0; Medcalc, Mariakerke, Belgium). The relationship of texture parameters and RECIST, Choi, and modified Choi response criteria after two cycles of treatment and

measured time to progression were assessed by using Kaplan-Meier analysis. The threshold values for texture parameters used in the Kaplan-Meier analysis were established with receiver operating characteristic (ROC) analysis, which tested the ability of each parameter to help identify time to disease progression. The point on the ROC curve furthest from the line of no discrimination was considered the optimum threshold for predicting a shorter time to progression. Time to progression was defined as the time from the date of baseline CT to the date of disease progression (defined by RECIST criteria). Kaplan-Meier curves for patients with values above and below each threshold were constructed to display the proportion of patients with-

out disease progression at any given time. Differences between Kaplan-Meier curves for texture and RECIST, Choi, and modified Choi criteria were evaluated by using a nonparametric log-rank test, with a P value of less than .05 considered to indicate a significant difference. After this, Cox regression analysis was performed to determine if any significant parameters (texture and RECIST, Choi, or modified Choi response criteria after two cycles of treatment) were independent predictors of time to progression.

Results

All 39 patients had clear cell carcinomas, with the exception of two patients with papillary and sarcomatoid cancers. Patients

Figure 2

Figure 2: Left and middle: Conventional CT image of a right upper lobe lung metastasis (upper left) and corresponding CT images selectively displaying fine (upper middle), medium (lower left), and coarse (lower middle) texture obtained with filter values of 1.0 (width, 4 pixels), 1.5 (width, 6 pixels), and 2.5 (width, 12 pixels). Right: Chart shows software processing steps undertaken to generate the data displayed.

Table 2

Response Categorization of Patients after Two Treatment Cycles

Response Criteria	Partial Response	Stable Disease	Progressive Disease
RECIST	6 (15)	32 (82)	1 (3)
Choi	33 (84)	3 (8)	3 (8)
Modified Choi	22 (56)	14 (36)	3 (8)

Note.—Data are numbers of patients. Data in parentheses are percentages.

Table 3

Mean Value and Percentage Change for Entropy and Uniformity for Absolute Scale Values at Baseline and after Two Treatment Cycles

Filter Scale Value	Entropy			Uniformity		
	Baseline	After Two Treatment Cycles	Change (%)	Baseline	After Two Treatment Cycles	Change (%)
No filtration	6.95 ± 0.37	6.73 ± 0.43	−3.08 ± 4.34	0.010 ± 0.002	0.012 ± 0.004	+21.00 ± 28.36
1.0	3.06 ± 0.55	2.60 ± 0.84	−15.20 ± 23.35	0.47 ± 0.07	0.53 ± 0.13	+14.72 ± 20.80
1.5	2.31 ± 0.72	1.81 ± 0.92	−21.73 ± 39.66	0.59 ± 0.11	0.67 ± 0.16	+14.91 ± 20.21
1.8	1.89 ± 0.81	1.53 ± 0.92	−16.96 ± 50.40	0.66 ± 0.13	0.72 ± 0.16	+10.61 ± 19.48
2.0	1.62 ± 0.85	1.35 ± 0.88	−9.51 ± 133.76	0.71 ± 0.15	0.76 ± 0.15	+8.15 ± 17.99
2.5	1.23 ± 0.81	1.08 ± 0.77	−45.77 ± 139.91	0.78 ± 0.14	0.80 ± 0.13	+4.96 ± 17.26

Note.—Data are means ± standard deviations.

Table 4

ROC and Kaplan-Meier Analysis for Entropy and Uniformity at Different Scale Values

Filter Scale Value	Entropy		Uniformity	
	ROC Threshold	P Value	ROC Threshold	P Value
Baseline				
Without filtration	>6.33	.28	≤0.01	.54
1.0	>2.48	.10	≤0.52	.21
1.5	>1.46	.09	>0.40	.17
1.8	>1.07	.09	>0.48	.02
2.0	≤2.65	.07	>0.48	.02
2.5	≤2.33	.02	>0.55	.02
Percentage change				
Without filtration	≤-5.26	.19	>13.95	.13
1.0	>-6.66	.11	≤2.58	.02
1.5	>-7.80	.15	≤3.14	.07
1.8	>-13.11	.05	≤5.23	.07
2.0	>-5.35	.03	≤0.49	.02
2.5	>4.02	.11	≤-2.00	.0008

Note.—P values were obtained with Kaplan-Meier analysis.

Figure 3

Figure 3: ROC curve shows percentage change in uniformity. Area under the ROC curve (0.71; 95% confidence interval: 0.53, 0.85) was significant (*P* = .016).
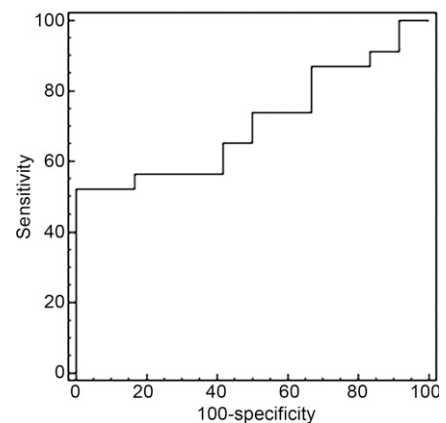
received sunitinib (*n* = 26), cedirinib (*n* = 6), pazopanib (*n* = 4), and regorafenib (*n* = 3). A total of 87 target lesions were analyzed. The initial treatment responses, as categorized with RECIST, Choi, and modified Choi criteria, are summarized in Table 2. Subsequently, follow-up imaging showed that 26 of 39 patients had progressed with treatment during the study period. Median time to progression was 336 days (range, 57–1364 days).

The mean values for entropy and uniformity for absolute scale values at baseline and after two treatment cycles are summarized in Table 3.

Our ability to use entropy and uniformity at different scale values to predict time to progression is summarized in Table 4. With coarse texture (filter value, 2.5; approximately 12 pixels in width), both baseline entropy and baseline uniformity, as well as percentage change in uniformity, were significantly correlated with time to progression (Table 4). With a threshold change of −2% or less in uniformity at a scale value of 2.5, the area under the ROC curve was significant (0.71; 95% confidence interval: 0.53, 0.85; *P* = .016) (Fig 3). Kaplan-Meier curves of the proportion of patients without disease progression were significantly different for percentage change in uniformity and were better than those for RECIST-, Choi-, and modified Choi–defined response after two cycles of TKI therapy (*P* = .008

vs *P* = .267, *P* = .053, and *P* = .042, respectively) (Fig 4).

Cox regression analysis indicated that the percentage change in coarse uniformity was an independent predictor (odds ratio, 4.02; 95% confidence interval: 1.52, 10.65; *P* = .0053), while modified Choi criteria were not significant (odds ratio, 1.07; 95% confidence interval: 0.38, 3.00; *P* = .8911), indicating no interaction between texture uniformity and enhancement and size change (assessed with the criteria).

Discussion

Imaging-defined response assessment (RECIST) is a cornerstone of modern oncologic practice; however, it is limited in a number of targeted therapies, including treatment with TKIs. Administration

Radiology
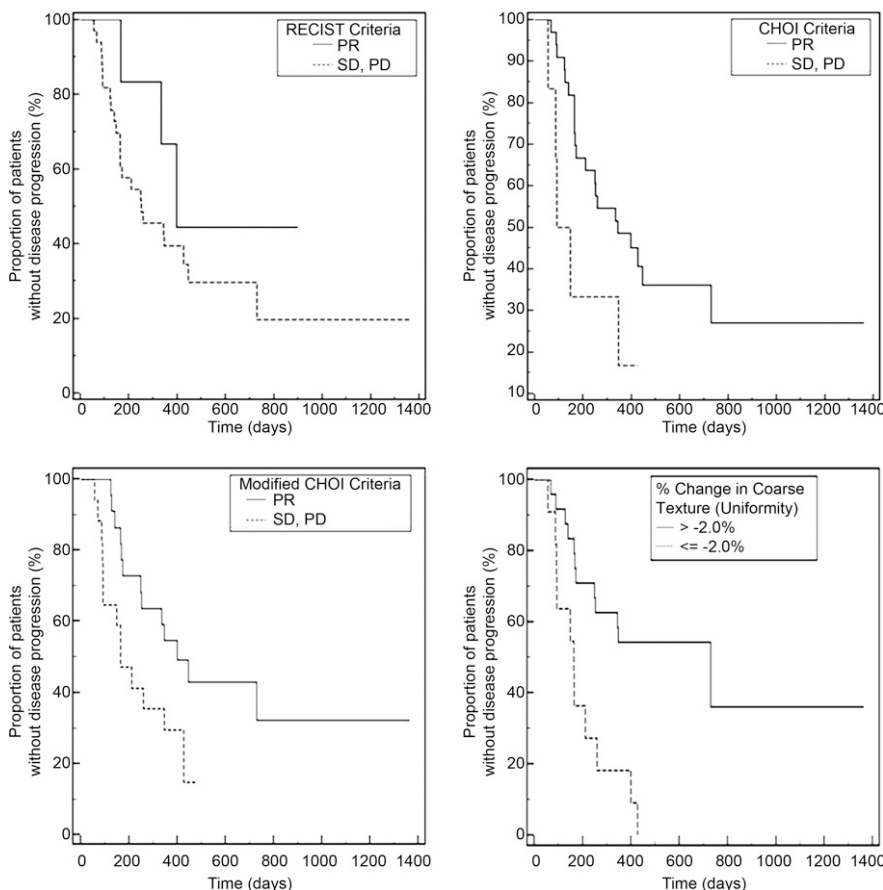
Figure 4

Figure 4: Kaplan-Meier curves show proportion of patients without disease progression for RECIST, Choi, and modified Choi criteria and percentage change in uniformity.

of TKIs is now standard in patients with first-line metastatic renal cell carcinoma. In large phase III trials, overall RECIST-defined response rates were low (10%–31%); however, many patients had a degree of tumor shrinkage, although this was less than a RECIST-defined response. Patients who did not have a RECIST response also experienced clinical benefits, with a substantial prolongation of progression-free survival.

Early identification of patients who will not derive a clinical benefit from treatment has a number of advantages. Patients could be saved from drug toxicity, they could be switched to an alternative treatment earlier, and there are potential cost savings if drugs are used in only those patients who will benefit from them. There has been at an estimated cost of $18 611 per progression-free year gained, $67 215 per life-year gained, and $52 593 per quality-adjusted life-year gained for sunitinib versus interferon (21). Cost-effectiveness would improve if we were able to identify nonresponding patients earlier.

The addition of tumor attenuation change to size criteria may improve response assessment (11–14); however, such analysis does not necessarily best reflect changes in tumor heterogeneity. Heterogeneity is a well-recognized feature of malignancy. Heterogeneity of the tumor blood supply is associated with oxidative stress, promotion of survival factors, and genomic instability (22). A heterogeneous blood supply will also affect treatment response due to poor delivery of chemotherapeutic agents to areas of low vascularity. Much of the heterogeneity visible at CT represents photon noise,

which can mask any underlying biologic heterogeneity. By using filters that select for image features at larger scales, CT texture analysis can reduce the effect of photon noise while enhancing biologic heterogeneity. Heterogeneity at relevant scales can then be quantified by using a range of parameters, including coarseness (entropy) and irregularity (uniformity).

In our study, we found that CT texture changed after two cycles of therapy: entropy—reflecting texture irregularity—decreased, while uniformity increased (tumor heterogeneity was reduced after two cycles of therapy). This would be consistent with a decrease in vascularization and the development of necrosis. This is supported by the findings of previous computer simulations and human studies, which have suggested that texture reflects underlying vascularization (15): texture has been correlated with hepatic blood flow (hepatic perfusion index) in patients with colorectal cancer.

Change in uniformity after two cycles of treatment also appeared to best reflect time to progression. In comparison to the standard RECIST criteria and the combined size and enhancement response criteria (Choi and modified Choi criteria) used to assess initial TKI therapy effect after two cycles of treatment (partial response, stable disease, or progressive disease), the percentage change in texture uniformity (above the 2.0 value, which enhances the contribution from underlying vessels) was an independent predictor of time to progression. By using a threshold change of −2% or less for uniformity at a coarse scale (filter value, 2.5; 12 pixels in width), Kaplan-Meier curves of the proportion of patients without disease progression were significantly different from and better than those for RECIST, Choi, and modified Choi partial response criteria. This indicates that uniformity yields information in addition to enhancement and size change, and thus enables complementary assessment. Kaplan-Meier curves for percentage change in entropy at a coarse scale were not significantly different, indicating that these measures were not identical but that they reflected different aspects of heterogeneity.

We also found that baseline entropy (≤2.33) and uniformity (>0.55) at a

Radiology

coarse scale correlated with time to progression, suggesting that baseline heterogeneity may also yield predictive information. An advantage of texture analysis is that it imposes no additional burden on a patient, as it is an additional postprocessing step of standard CT images that were obtained for standard response assessment.

There were limitations to this study. First, renal impairment may preclude the use of intravenous iodinated contrast material in patients with renal disease. In this retrospective study, the use of intravenous iodinated contrast material was precluded by renal impairment in 29% of the patients. Nevertheless, texture analysis still may yield useful information on underlying tumor heterogeneity without the use of intravenous contrast material, as has been shown in patients with other cancers (16,17). Second, texture parameters may be affected by the phase (arterial or portal venous) of acquisition. To our knowledge, there are no published data that enable one to confirm or refute this supposition for filtered texture data. Third, one must consider the possibility that acquisition parameters (tube voltage or tube current) may affect texture parameters. A previous water phantom study in which researchers used varying tube current (100–250 mAs) at 80 and 120 kV and then varying tube voltage at a fixed tube current of 150 mAs suggests this has less of an effect on uniformity (17). Fourth, to date, texture analysis has been performed for a limited tumor area and not the whole tumor; however, texture analysis still shows promise as a predictive biomarker. This is likely to change in the future, as software improvements will enable whole-tumor segmentation and analysis.

In conclusion, CT entropy decreases and uniformity increases with multitargeted TKIs. CT texture has potential as a predictive biomarker, and it may better reflect time to progression than standard response criteria based on size change, enhancement change, or both.

References

1. Motzer RJ, Hutson TE, Tomczak P, et al. Sunitinib versus interferon alfa in metastatic renal-cell carcinoma. N Engl J Med 2007; 356(2):115–124.
2. Escudier B, Eisen T, Stadler WM, et al. Sorafenib in advanced clear-cell renal-cell carcinoma. N Engl J Med 2007;356(2):125–134.
3. Sternberg CN, Davis ID, Mardiak J, et al. Pazopanib in locally advanced or metastatic renal cell carcinoma: results of a randomized phase III trial. J Clin Oncol 2010;28(6):1061–1068.
4. Eisenhauer EA, Therasse P, Bogaerts J, et al. New response evaluation criteria in solid tumours: revised RECIST guideline (version 1.1). Eur J Cancer 2009;45(2):228–247.
5. Motzer RJ, Michaelson MD, Redman BG, et al. Activity of SU11248, a multitargeted inhibitor of vascular endothelial growth factor receptor and platelet-derived growth factor receptor, in patients with metastatic renal cell carcinoma. J Clin Oncol 2006;24(1):16–24.
6. Baccala A Jr, Hedgepeth R, Kaouk J, Magi-Galluzzi C, Gilligan T, Fergany A. Pathological evidence of necrosis in recurrent renal mass following treatment with sunitinib. Int J Urol 2007;14(12):1095–1097; discussion 1097.
7. Griffin N, Gore ME, Sohaib SA. Imaging in metastatic renal cell carcinoma. AJR Am J Roentgenol 2007;189(2):360–370.
8. Faivre SJ, Bouattour M, Dreyer C, Raymond E. Sunitinib in hepatocellular carcinoma: redefining appropriate dosing, schedule, and activity end points. J Clin Oncol 2009;27(35): e248–e250; author reply e251–e252.
9. Choi H, Charnsangavej C, Faria SC, et al. Correlation of computed tomography and positron emission tomography in patients with metastatic gastrointestinal stromal tumor treated at a single institution with imatinib mesylate: proposal of new computed tomography response criteria. J Clin Oncol 2007;25(13):1753–1759.
10. Benjamin RS, Choi H, Macapinlac HA, et al. We should desist using RECIST, at least in GIST. J Clin Oncol 2007;25(13):1760–1764.
11. van der Veldt AA, Meijerink MR, van den Eertwegh AJ, Haanen JB, Boven E. Choi response criteria for early prediction of clinical outcome in patients with metastatic renal cell cancer treated with sunitinib. Br J Cancer 2010;102(5):803–809.
12. Nathan PD, Vinayan A, Stott D, Juttla J, Goh V. CT response assessment combining reduction in both size and arterial phase density correlates with time to progression in metastatic renal cancer patients treated with targeted therapies. Cancer Biol Ther 2010;9(1):15–19.
13. Smith AD, Lieber ML, Shah SN. Assessing tumor response and detecting recurrence in metastatic renal cell carcinoma on targeted therapy: importance of size and attenuation on contrast-enhanced CT. AJR Am J Roentgenol 2010;194(1):157–165.
14. Smith AD, Shah SN, Rini BI, Lieber ML, Remer EM. Morphology, Attenuation, Size, and Structure (MASS) criteria: assessing response and predicting clinical outcome in metastatic renal cell carcinoma on antiangiogenic targeted therapy. AJR Am J Roentgenol 2010;194(6):1470–1478.
15. Bézy-Wendling J, Kretowski M, Rolland Y, Le Bidon W. Toward a better understanding of texture in vascular CT scan simulated images. IEEE Trans Biomed Eng 2001;48(1): 120–124.
16. Ganeshan B, Abaleke SC, Young RC, Chatwin CR, Miles KA. Texture analysis of non-small cell lung cancer on unenhanced computed tomography: initial evidence for a relationship with tumour glucose metabolism and stage. Cancer Imaging 2010;10:137–143.
17. Miles KA, Ganeshan B, Griffiths MR, Young RC, Chatwin CR. Colorectal cancer: texture analysis of portal phase hepatic CT images as a potential marker of survival. Radiology 2009; 250(2):444–452.
18. Ganeshan B, Miles KA, Young RC, Chatwin CR. Hepatic entropy and uniformity: additional parameters that can potentially increase the effectiveness of contrast enhancement during abdominal CT. Clin Radiol 2007;62(8): 761–768.
19. Ganeshan B, Miles KA, Young RC, Chatwin CR. Hepatic enhancement in colorectal cancer: texture analysis correlates with hepatic hemodynamics and patient survival. Acad Radiol 2007;14(12):1520–1530.
20. Ganeshan B, Miles KA, Young RC, Chatwin CR. In search of biologic correlates for liver texture on portal-phase CT. Acad Radiol 2007; 14(9):1058–1068.
21. Remák E, Charbonneau C, Négrier S, Kim ST, Motzer RJ. Economic evaluation of sunitinib malate for the first-line treatment of metastatic renal cell carcinoma. J Clin Oncol 2008; 26(24):3995–4000.
22. Nelson DA, Tan TT, Rabson AB, Anderson D, Degenhardt K, White E. Hypoxia and defective apoptosis drive genomic instability and tumorigenesis. Genes Dev 2004;18(17): 2095–2107.